Analysis of the role of RXRα in monocyte-macrophage differentiation and function using U937 monoblastoid cells.

Timothy James Stonehouse

A thesis submitted for the degree of
Doctor of Philosophy

1998
University College
University of London

ProQuest Number: U642393

All rights reserved

INFORMATION TO ALL USERS
The quality of this reproduction is dependent upon the quality of the copy submitted.

In the unlikely event that the author did not send a complete manuscript
and there are missing pages, these will be noted. Also, if material had to be removed,
a note will indicate the deletion.

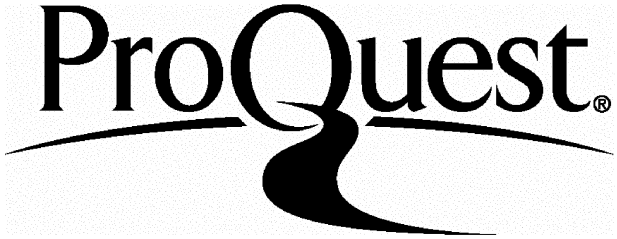

ProQuest U642393

Published by ProQuest LLC(2015). Copyright of the Dissertation is held by the Author.

All rights reserved.
This work is protected against unauthorized copying under Title 17, United States Code.
Microform Edition © ProQuest LLC.

ProQuest LLC
789 East Eisenhower Parkway
P.O. Box 1346
Ann Arbor, MI 48106-1346

ABSTRACT

In this thesis the U937 monoblast cell line has been used as a model for investigation of the immunobiology of the mononuclear phagocyte system, both in terms of differentiation, and in terms of functional properties, such as phagocytosis and accessory cell activity.

Retinoid X receptor-α (RXRα), a member of the nuclear receptor superfamily, was shown to be expressed in primary human monocytes, and its expression was increased upon differentiation in response to human serum. Expression of RXR dimeric partners, RARα and RARβ, was not induced in the same way. Expression of these proteins was also assessed in previously derived novel U937 transfectants that hyper-expressed (αG2S cells), or hypo-expressed (αB5A cells), RXRα. Retinoic acid (RA) activation of αG2S cells led to an altered pattern of expression of surface antigens which suggested a more mature phenotype, when compared to αB5A cells and an empty vector control cell line (MEP). RA-treated αG2S cells were also more efficient at phagocytosing opsonised-SRBC. This immunophagocytic process was inhibited in all three cell lines by prior addition of CD13, CD16 and CD18 mAbs. The increase in efficiency of phagocytosis correlated with a more intense and altered phosphotyrosine response during phagocytosis. Phagocytosis induced activation of members of the MAPK family of kinases in all three cell lines, and phosphoproteins from the U937 transfectants interacted differentially with a panel of SH2 domain fusion proteins. RA-treated αG2S cells were also resistant to ionising radiation-induced cell death. This phenomena was RA-dependent, as vitamin D treatment did not have the same effect.

To examine accessory cell function of both the U937 parent cell line and the U937 transfectants, a model U937-T-cell interaction assay was

developed, where the cell line provides a co-stimulatory signal for CD3-mediated T-cell activation, independent of CD80/CD86/CD28 interaction. A β2-integrin (CD11a/18)/ICAM-1 (CD54) interaction was implicated, and there was evidence to suggest the dominant response was in cells with a CD8+ phenotype. This implied a reduced requirement for CD28-mediated signalling by CD8+ T-cells, and this was confirmed since proliferation of the CD4+ T-cell population increased significantly in response to an added CD28 mAb. CD11a/18 mAbs inhibited U937/T-cell cluster formation as well as proliferation. CD45 mAbs increased the size of the U937/T cell clusters formed, suggesting that ligation of CD45 may be important in the targeting of T-cells towards antigen presenting cells. MAbs to CD53, CD98 and CD147 inhibited U937 dependent T-cell proliferation. CD53 mAbs were not inhibitory when pre-pulsed on to U937 cells, suggesting an effect at the T-cell level. CD98 and CD147 mAbs were inhibitory in pre-pulsing, but also inhibited an accessory cell independent proliferation assay, suggesting these molecules play a role both at the accessory cell level and at the level of the T-cell. The observation that most inhibitory antibodies induce tyrosine phosphorylation in both U937 and T-cells was consistent with this finding. Finally, αG2S cells induced greater T-cell proliferation when used as an accessory cell, than MEP cells, which itself was more efficient than αB5A cells. Previous exposure to opsonised-SRBC had no effect on the accessory cell capabilities of these cells, demonstrating that phagocytic and accessory cell functions are not mutually exclusive.

Table of Contents.

List of Tables.

List of Figures.

Acknowledgements.

The supervision, advice and guidance received over the past three years from Prof. David Katz, Prof. Paul Brickell and Prof. Benny Chain, has been very much appreciated. I would particularly like to thank Prof. David Katz for his constant enthusiasm and willingness to talk over problems. I would like to thank all other members of the Dept. of Immunology for all their help, but in particular Patrick, Ness, Tom, Debbie, Louise, Charles and Pete, who made the a lab such a great place to work in, and who have become excellent friends and eaters of curry. I was "helped" during this project by various summer and BSc students, thanks to Paul Herridge for testing some of the adhesion panel of mAbs in the U937/CD3 T-cell assay, Joel Branch, for doing FACS analysis on the U937 transfectants, Ben Kendrick, for doing the mAb-phosphotyrosine studies on U937 and T-cells, and (the incomparable) Hutan Ashrafian, who did some of the FACS analysis of U937 and T-cells. I also grudgingly acknowledge "Captain Rhodesia", the miserable bar manager, for serving vast amounts of flat lager and completely undrinkable bitter. Thanks also to Dr. Darrin Smith for the GST-SH2 fusion proteins, various antibodies and for originally giving me a job in Cambridge which got me into science.

On a home note, I would like to thank Mike and Jo for being top housemates, putting up with me, and making living in London a great experience. Of course, many thanks to Caroline for all her love, support and determination that I should get this thing finished in three years!!

This thesis is dedicated to my Mum and Dad, without who's guidance and support, even when thousands of miles away, nothing would have been possible.

Chapter 1

Introduction

1.1. The myeloid cell lineage.

This section will give a brief introduction to the myeloid cell lineage, and the monoblastoid U937 cell line.

1.1.1. Myelopoiesis: Development of myeloid cells.

Haemopoietic stem cells, which are located in the bone marrow of adults, are the precursors of erythroid, megakaryocytoid, lymphoid and myeloid cell lineages. The eventual fate of each stem cell is determined by factors such as interleukins (IL), colony stimulating factors (CSF), and certain hormones which induce clonal proliferation and differentiation of stem cells. Figure 1.1.1A. shows the progression of differentiation towards the monocyte/macrophage lineage. This process, from stem cell to a mature monocyte, takes six days in the bone marrow (Groopman and Golde, 1981). In bone marrow, IL-1, IL-3, and IL-6 induce heteromitosis of stem cells, which gives rise to one new stem cell and to a pluripotent granulocyte-erythrocyte-megakaryocyte-macrophage colony forming unit (GEMM-CFU). From this stage, the further presence of IL-1 and IL-3 commits these cells to become a common precursor of both granulocyte and monocyte/macrophage lineages, hence known as a granulocyte-macrophage colony forming unit (GM-CFU).

These GM-CFU precursors can then be differentiated sequentially to a macrophage colony forming unit (M-CFU), to a monoblast, to a pro-monocyte, and then to a mature monocyte. This differentiation is controlled by IL-3, granulocyte-macrophage CSF (GM-CSF), and macrophage CSF (M-CSF). IL-3 and GM-CSF are thought to be involved in proliferation of the immature cells, and M-CSF involved in proliferation and differentiation towards the monocyte/macrophage

lineage (reviewed by Ogawa, 1993). All the above processes occur in the bone marrow. Following these events, mature monocytes enter the blood stream. Monocytes are generally smaller than their immediate precursors, and have well developed lysosomes and an enhanced phagocytic abilities. From the bloodstream, monocytes enter body tissues. Once present in tissues monocytes differentiate to macrophages under the influence of factors that include M-CSF, GM-CSF, IL-1, IL-3, and tumour necrosis factor α (TNFα). Figure 1.1.1B. shows an example of this representing the differentiation of a monoblastic cell line U937, to become monocytes, and the factors that have been used to stimulate differentiation of these cells.

Figure 1.1.1A.

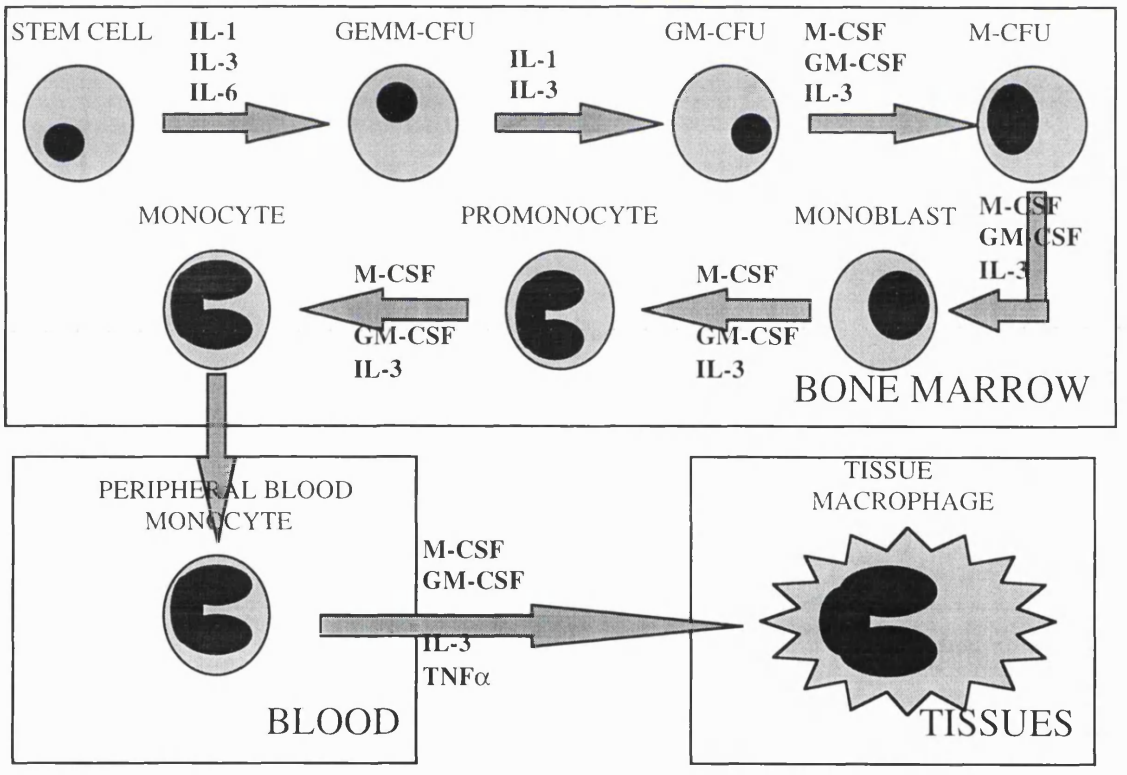

Figure 1.1.1A. Schematic representation of monocyte/macrophage development, and the factors that determine this process.

Figure 1.1.1B.

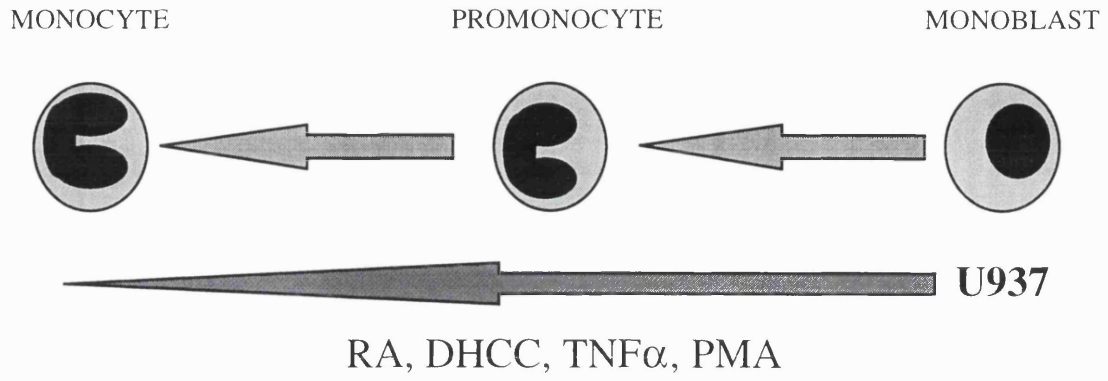

Figure 1.1.1B. Schematic representation of the relative position of the human leukaemic U937 cell line in monocyte/macrophage development, and factors that have been shown to differentiate this cell line to become monocytes.

Human monocytes have a half life of three days in the blood stream. These cells bind to endothelium either randomly or during recruitment to areas of inflammation. A variety of adhesion molecules are involved in the interaction of monocytes with endothelium, including selectins, and integrins (reviewed by Springer, 1990). The monocytes will extravasate through the endothelium and migrate into the surrounding tissue, where they differentiate into tissue macrophages. The exact phenotype of these mature cells is dependent on the tissue that they have entered and the context of that tissue at the time of maturation. Dendritic cells, which are the most potent known antigen presenting cells (APC) and act as "sentinels" of the immune system; microglia, which develop in brain tissue; osteoclasts, which develop in bone; Kupffer cells, which develop in liver; and Langerhans cells; which develop in skin, are all of the monocyte/macrophage lineage and these examples demonstrate the versatility and importance of the lineage. Tissue macrophages can differentiate further to form both epitheloid cells and multi-nucleated

giant cells, which are features of granulomatous inflammatory diseases such as tuberculosis (Weinberg et al., 1984).

1.1.2. Molecular mechanisms that regulate myeloid cell differentiation.

In recent studies, some of the molecular mechanisms behind myelopoiesis have been unravelled by the investigation of transcription factors implicated in myeloid cell development, and of the genes which these factors control (as reviewed by Valledor et al., 1998). Figure 1.1.2. gives a schematic representation of transcription factors involved in monocyte/macrophage development. Survival and proliferation of stem cells is regulated by a number of transcription factors. These include GATA 2 and PLZF, both members of the zinc finger family, SCL, which is a member of the basic helix loop helix (bHLH) family, and the homeobox proteins, HOXB3 and HOXB4. The transcription factors GATA 1, GATA 2, SCL and Myc are implicated in regulating differentiation to GEMM-CFU and expression of PLZF, HOXB3 and HOXB4 is down regulated during this step. However, for cells to progress beyond GEMM-CFU, expression of GATA 1, GATA 2, SCL and c-myc must be repressed. For example, over-expression of SCL leads to repression of essential monocyte proteins, such as CD11b and lysozyme, and the lack of inhibition of proliferation associated with mature monocytes.

Myb has been shown to control the survival and proliferation of GM-CFU, and the commitment of these cells to M-CFU. Myb is also able to activate expression of monocyte-specific proteins such as Mim-1 and lysozyme. Survival and proliferation of M-CFU cells is dependent on M-CSF, and expression of M-CSF receptor is controlled by PU.1, a member of the Ets family, and a myeloid-specific transcription factor. Recently, liganded M-CSF receptor has been shown to interact with and directly activate phospholipase C-γ2 (PLC-γ2), in a process that also involves

phosphatidylinositol 3-kinase (PI3-K). When this interaction was blocked, M-CSF-induced differentiation was abrogated (Bourette et al., 1997), thus showing the importance of signalling via the M-CSF receptor, and PU.1. Furthermore, PU.1 in co-operation with other factors, activates transcription of GM-CSF receptors. During subsequent maturation of M-CFU, PU.1 is essential for the transactivation of genes involved in the functional properties of macrophages. These include CD11b, CD18, CD14, the high and low affinity receptors for IgG (FcγRI and FcγRIII respectively), and the scavenger receptors I and II. CCAAT enhancer-binding protein β (C/EBPβ) is also thought to play a role in transactivation of functionally important macrophage genes. The characteristic reduction in cell proliferation associated with a mature monocyte phenotype required two mechanisms. Firstly, Myc and Myb, are down-regulated as over-expression of either proteins at this stage will block monoblast differentiation. Secondly, interferon regulatory factor-1 (IRF-1) is induced in monocytes, this transactivates the transcription of interferon α and β (IFNα and β), which act as autocrine signals that promote inhibition of proliferation.

Other factors implicated in the maturation of monocytes to macrophages are EGR1 (a member of the zinc finger family), HOXB7, and NF-Y. Expression of EGR1 is restricted to monocytes and macrophages, although EGR1 null mutant mice still develop macrophages, questioning the importance of this factor in development of this lineage. NF-Y has been implicated in the expression of ferritin, a protein involved in iron metabolism, which controls the expression of MHC class II, thus allowing the mature macrophage to act as an iron storage compartment and as an APC respectively.

Figure 1.1.2.

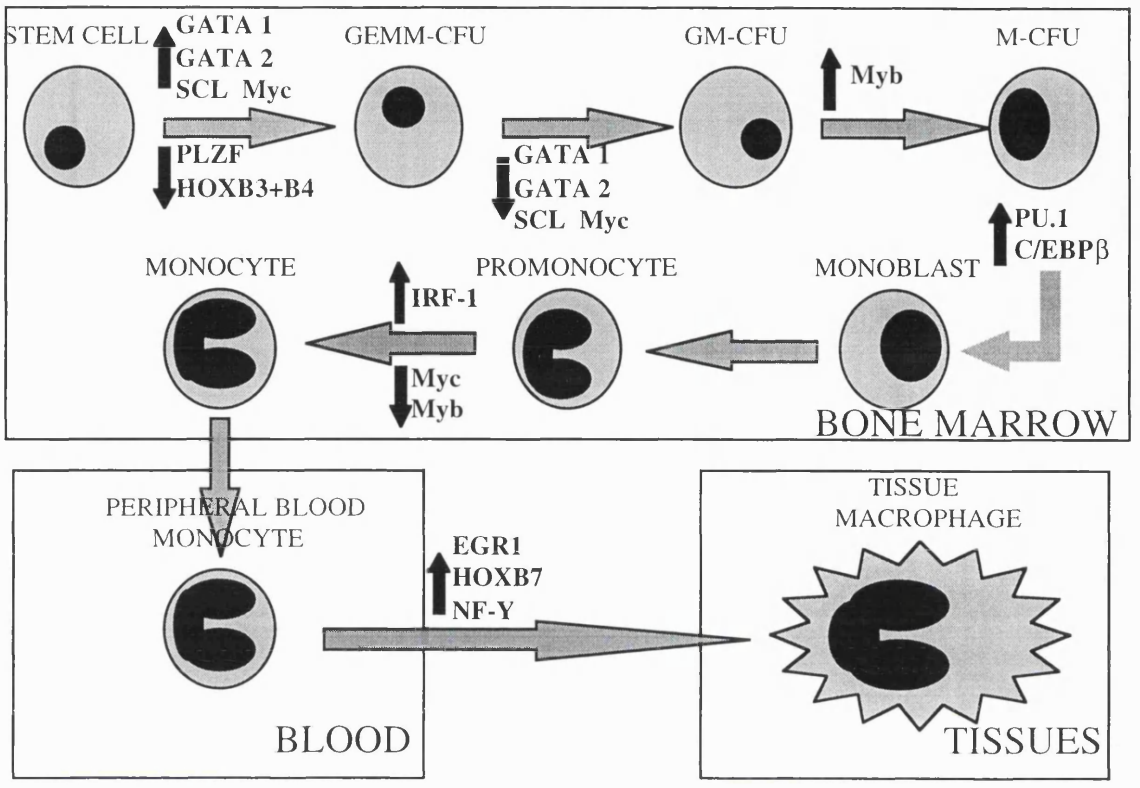

Figure 1.1.2. Schematic representation of transcription factors involved in monocyte/macrophage development, black upward arrows indicates factors expressed at that point, black downward arrows indicates factors down-regulated at that point.

1.1.3. Functions of monocytes/macrophages.

Once the cells have matured into tissue macrophages, there is a further potential developmental step, which involves the conversion of resting macrophages to an activated state. This activation is mediated by inflammatory mediators such as IFNγ (Black et al., 1987), GM-CSF (Reed et al., 1987), and TNFα (De Titto et al., 1986) which are secreted by cells surrounding the resting macrophage, or as a direct response to bacterial products, such as lipo-polysaccheride (LPS). This reflects the principal function of activated macrophages in host defence against a range of pathogens. It is these macrophages that have the ability to phagocytose and then present antigen to T-cells, and also to recruit other branches of the

immune system by secreting inflammatory factors such as TNFα, IL-1, IFNα and β, and reactive oxygen species (as reviewed by Johnston, 1988).

Monocytes and macrophages, along with neutrophils, are professional phagocytes. Phagocytosis is mediated by several receptors expressed on both monocytes and macrophages. The mannose receptor is an example of a protein that is involved in phagocytosis via the recognition of biochemical features of pathogens. This receptor will interact with terminal mannose or fucose saccharides on the capsule of invading bacteria. Fcγ receptors and complement receptors CR1, CR3, and CR4 are examples of proteins that are involved in phagocytosis via interaction with host proteins that have previously bound to the pathogen, in a process known as opsonisation. Fcγ receptors recognise IgG coated particles, whilst CR1, CR3, and CR4 recognise particles coated with components of the complement pathway. There are three classes of Fcγ receptors expressed on monocytes and macrophage. These are FcγRI (CD64), the high affinity IgG receptor, FcγRII (CD32), a low affinity IgG receptor, and FcγRIII (CD16), a second low affinity IgG receptor. Phagocytosis induces monocytes and macrophages to secrete pro-inflammatory factors, induces the respiratory burst, and also induces antibody dependent cellular cytotoxicity (ADCC) activity. Phagocytosis mediated by monocytes and macrophages is discussed in detail in section 1.2. of this chapter.

Another key property of monocytes and macrophages is their ability to adhere to lymphatic and vascular endothelium, and to extracellular matrix proteins such as laminin and fibronectin (Pawlowski et al., 1985; Pawlowski et al., 1988). Adhesion is also necessary for many of the monocyte/macrophage functions previously mentioned, such as phagocytosis, cytotoxicity, and the production of inflammatory factors. There are three families of cell surface proteins that mediate adhesion. These are integrins, selectins, and the immunoglobulin superfamily members (reviewed by Springer, 1990). The integrins are large

heterodimeric glycoproteins responsible for cell-cell and cell-matrix interactions. Integrins are classified into sub-families according to the β chain involved, β1 integrins comprise a CD29 β chain and a series of possible α chains (CD49a, b, c, d, e, or f). These β1 integrins are also known as very late antigens, or VLA-1 to VLA-6. β2 integrins comprise a CD18 β chain with either CD11a (LFA-1), CD11b (Mac-1), or CD11c (p150/95) α chains. There are also other integrins such as the β3 (cytoadhesins) and β7 subfamilies. β1 and β3 subfamilies bind mainly to matrix proteins such as collagen, laminin, fibronectin and vitronectin, whereas the β2 subfamily interact with cellular proteins. For example, LFA-1 interacts with immunoglobulin family adhesion molecules such as ICAM-1 (CD54), ICAM-2 (CD102), and ICAM-3 (CD50). The selectins, comprising of L-selectin (CD62L), P-selectin (CD62P) and E-selectin (CD62E), are involved in leukocyte-endothelium interactions, and ~~has~~ have been shown to be vital in leukocyte rolling along vascular endothelium, which is the first stage of leukocyte extravasation. Selectins bind to oligosaccharides such as CD15 (Le^x) and CD15s (sialyl Le^x) (Prieto et al., 1994).

1.1.4. The U937 cell line.

The U937 cell line was first isolated from a patient with diffuse histiocytic lymphoma and has proven to be a useful model for the studies of the monocyte/macrophage lineage (Sundstrom and Nillson, 1976). The cell line is already committed to the monocyte lineage. Figure 1.1.1B. shows how U937 can be induced to differentiate from its "normal" monoblastoid state, in sequential steps (see figure 1.1.1A.), to become a monocyte. Differentiation can be induced with agents such as phorbol 12-myristate 13-acetate (PMA) (Forsbeck et al., 1985), IFNγ and TNFα (Harris et al., 1985), retinoic acid (RA) (Olsson and Breitman, 1982), and the active vitamin D metabolite 1,25-dihydroxycholecalciferol (DHCC) (Amento et al., 1984). In this way, U937 cells have been used as model to study

differentiation of monocytes/macrophages, as well as monocyte/ macrophage functions.

U937 cells proliferate in suspension culture in the presence of growth factors supplied by foetal calf serum. Undifferentiated U937 cells have a doubling time of between 20 and 48 hours, and express few Fc, C3 or chemotactic peptide receptors (Sundstrom and Nillson, 1976). The enormous amount of literature about U937 cells reflects the extensive use of this cell line as model system, and also the stability of the cell line over the twenty years of its existence.

1.1.4.1. Molecular events involved in growth arrest of U937 cells.

Following differentiation towards a monocyte phenotype, induced by a variety of factors, U937 cells shift to a non-proliferative state indicative of a monocyte phenotype. Many proteins have been implicated in this switch to a non-proliferative state.

Myc has been shown to dimerise with Max, and this heterodimer binds to response elements and activates transcription of specific genes. Max may also dimerise with Mad, and in this case act as a repressor of transcription (reviewed by Marcu et al., 1992). After PMA treatment of U937 cells, Myc expression is reduced, whilst Mad levels increase. Furthermore, the ratio of Myc-Max dimers to Mad-Max is changed in favour of the latter, to the extent that no Mad-Max dimers are found in untreated U937 cells, and no Myc-Max dimers are found in differentiated U937 cells (Ayer and Eisenman, 1993). These changes correlate with the switch from proliferation to non-proliferation.

Another important group of proteins involved in the cell cycle are the cyclin dependent kinases (cdk). After PMA treatment, cdk2 is dephosphorylated, which reduces its activity. Furthermore, this decrease in activity of cdk2 is associated with a decrease in cyclin A levels, and

cdk2 is complexed with cyclin E (Asiedu et al., 1997). Other evidence for the involvement of cdk in U937 cell growth arrest is that levels of a cdk inhibitor, known as p21, WAF1, or CIP1, is increased upon differentiation induced by both RA and DHCC, and that this increase is mediated by RA and Vitamin D response elements in the p21 promoter (Liu et al., 1996a; Liu et al., 1996b).

GTA is a tyrosine kinase that has been associated with the cell cycle, having a sequence similar to the cell cycle control gene, cdc2. PMA treatment of U937 cells induced increases in GTA levels and activity. GTA is thought to act by controlling the phosphorylation, and activity, of β-1,4-galactosyltransferase, an enzyme found in the golgi that has been implicated in cell cycle control (Kraft et al., 1992).

Interferon regulatory factor 1 (IRF1) is a transcription factor first found to respond to interferons (IFN) and regulate the cell cycle. Growth arrest induced by all-*trans* RA treatment of U937 cells has been correlated with increased expression of IRF1, and this response is not mediated by signal transducers and activator of transcription (STAT) molecules, which are normally associated with IFN signalling, suggesting that the IRF1 gene promoter contains an RA response element (Matikainen et al., 1996).

EGR1 has been shown to be restricted to the monocyte lineage, and has been shown to be expressed in PMA-treated U937 cells. HL-60 cells are equivalent to GM-CFU cells (see figure 1.1.1A.) that can be induced to differentiate along either a monocyte or granulocyte lineage. HL-60 cells that were induced to become granulocytes did not express EGR1. In fact HL-60 cells transfected to constitutively express EGR1 could only be induced to differentiate to the monocyte lineage (Nguyen et al., 1993). Both U937 and HL-60 cells, when treated with antisense oligonucleotides for EGR-1, could not differentiate to monocytes (Liebermann and Hoffman, 1994). However, in more recent experiments, EGR1 knockout

mice had normal numbers of functional macrophages (Lee et al., 1996), questioning the importance of this molecule in monocyte development, and suggesting that *in vivo* other molecules can replace it.

1.1.4.2. U937 cells as a model for monoblastic differentiation.

Although the U937 cell line is regarded as a monoblast, expression of adhesion molecules by the cell line resembles that of peripheral blood monocytes (Prieto et al., 1994). When U937 cells are induced to differentiate with PMA, they acquire several other macrophage phenotypic properties, such as adherence, expression of Fc receptors, the ability to phagocytose, ADCC, and the ability to produce lysozyme and alkaline phosphatase (Harris and Ralph, 1985). These properties demonstrate how useful U937 cells have been as an *in vitro* model of monocyte/macrophage differentiation and function.

1.1.5. Differentiation of U937 cells.

Although many substances have been shown to induce terminal differentiation of U937 cells, in the interests of being concise, this section concentrates on the actions of PMA, RA and DHCC, as these substances are used in this project, and have been used previously in the laboratory for the study of U937 cells (Brown et al., 1997).

1.1.5.1. Differentiation of U937 cells induced by PMA.

PMA activates protein kinase C (PKC), and this activation has many downstream signalling effects. PKC activation leads to phosphorylation of IκB, a regulatory protein of the NFκB transcription factor. This leads to dissociation of NFκB from IκB, allowing NFκB to translocate to the nucleus and activate transcription of target genes (Baeuerle and Baltimore, 1988). PKC also activates the AP-1 binding proteins Fos and Jun. The transcriptional activity of Jun has been shown to be regulated by being phosphorylated by a member of the mitogen activated protein kinase (MAPK) family (Pulverer et al., 1993). MAPK are themselves

regulated by phosphorylation, and PKC activates this pathway by activating upstream Raf-1. PMA has also been shown to down-regulate expression of phospholipase Cγ-1 (PLCγ-1), but to leave levels of PLCγ-2 unchanged during differentiation of U937 cells (Lee Y.H. et al., 1995), and to induce the activation of STAT5 (Woldman et al., 1997). This STAT response involves a specific STAT5 isoform, with STAT5a, but not STAT5b being activated (Meinke et al., 1996).

Other important effects of PMA-induced differentiation include the synthesis of cytokines such as IL-1α, TNFα, CSF-1, and IFNα+β (Indoh et al., 1996; Knudsen et al., 1986; Liu and Wu, 1992), adherence to plastic, increased expression of CD18 and CD54 (ICAM-1), increased expression of cyclo-oxygenase; and production of lysozyme and oxygen free radicals (reviewed by Harris and Ralph, 1985).

1.1.5.2. Differentiation of U937 cells induced by RA and DHCC.

All-*trans* RA or 9-*cis* RA, induce partial growth arrest and differentiation of U937 cells. RA is necessary for LPS-stimulated induction of IL-1β and TNFα synthesis (Taimi et al., 1993), and has been shown to be involved in the down-regulation of expression of both forms of the TNF receptor (p60 and p80) in U937 cells (Totpal et al., 1995). Addition of RA has been shown to induce an increase in expression of CD18 and CD11b, which is consistent with monocyte differentiation, but RA is not capable of inducing CD14 expression (James et al., 1997b; Sellmayer et al., 1994). This suggests that RA is not capable of inducing a full monocyte phenotype, but does differentiate the cells to an intermediate stage. The addition of DHCC to U937 cells induces a more profound level of growth arrest and differentiation than RA, but RA synergises with DHCC, as measured by expression of CD11b, CD18 and CD14; and an increase in the level of phagocytosis (James et al., 1997b).

Another aspect of the role of RA in U937 cell biology is that PMA-induced differentiation of U937 cells induce increased expression of two members of a class of retinoic acid receptor, the retinoid X receptors (RXR), known as RXRα and RXRβ (Brown et al., 1997). DHCC also induces expression of RXRα protein (Defacque et al., 1997). Both PMA and DHCC treatment also induce increased expression of vitamin D receptors (VDR) (Hewison et al., 1989). However, in another report, addition of RA to U937 cells led to a decrease in transcription of the RXRα gene, and this was antagonised by addition of DHCC (Nakajima et al., 1996). Research in our laboratory has produced a U937-derived cell line that expresses reduced levels of VDR. A major property of these cells is that they are prone to apoptosis, suggesting that VDR expression may act as a protective mechanism against programmed cell death (Hewison et al., 1996).

The synergistic differentiating effects of DHCC with other agents such as TGFβ and GM-CSF on U937 cells has been established (James et al., 1997a; Testa et al., 1993; Zuckerman et al., 1988). RA and DHCC will synergise in inducing cytokine secretion to the same level as addition of DHCC and LPS (Taimi et al., 1993). As previously described, DHCC, but not RA, induces expression of CD14 in U937 cells. The reason for this is that ~~the~~ there is a vitamin D responsive element (although not a consensus vitamin D response element, see section 1.5), present in the promoter region of the gene coding for CD14 (Zhang et al., 1994). In one report, DHCC and RA had antagonistic effects on the expression of CD14 and the low affinity Fc receptor for IgE (CD23) in U937 cells. PMA- and RA-induced expression of CD23, whilst PMA- and DHCC-induced CD14 expression. Furthermore, this report found that all-*trans* RA inhibited the PMA- or DHCC-induced expression of CD14, and DHCC inhibited the PMA- or RA-induced expression of CD23 (Oberg et al., 1993). However, in another more recent report, addition of 9-*cis* RA co-operatively induced an increase in expression of CD14 in DHCC-treated U937 cells

(Nakajima et al., 1996). With the use of specific retinoic acid receptor (RAR) or RXR agonists and antagonists, the synergism between RA and DHCC activity was shown to be mediated by both RAR and RXR (Defacque et al., 1997).

The antagonistic roles of DHCC and RA are reflected in the differential effects that these factors have on the HL-60 cell line. DHCC induces HL-60 cells to differentiate to become monocytes, whilst RA induces these cells to become granulocytes. This RA-induced differentiation of HL-60 cells requires RARα (Collins et al., 1990). The antagonistic effects of RA and DHCC have parallels in animal models. These include studies using chick yolk sac macrophages. When these cells are grown in primary culture they are able to differentiate into multi-nucleated giant cells (MNGC), and then, sequentially, into osteoclasts. DHCC promotes the formation of the MNGCs, whilst RA promotes the proliferation of the macrophages, thus inhibiting the formation of DHCC-induced MNGC (Woods et al., 1995).

In summary, the formation of heterogeneous populations of monocytes and macrophages throughout the body is dependent on numerous factors, that include RA, DHCC, bacterial products such as LPS, free radicals and cytokines. The precise control of differentiation is regulated by the concentration of the factor and the point in development where the cell comes into contact with any factor. The studies described represent a selection of many hundreds of studies where the U937 cell line has been used as a model for monocyte/macrophage differentiation and activation. As this model is so well-established, the U937 cell line was chosen as the model for investigation in this thesis.

1.2. Phagocytosis by monocytes and macrophages.

Phagocytosis is the process of recognition and engulfment of pathogenic organisms and cell debris that accumulate during infection, inflammation or wound repair.

Phagocytosis is carried out mainly by professional phagocytes, which include monocytes, macrophages and neutrophils. The process is mediated by proteins expressed on phagocytes that recognise either common pathogenic structural motifs, such as bacterial cap components, or host components that have already bound to pathogens, such as IgG or complement. The phagocytic process is a critical element in eliminating pathogenic organisms, and is also important for induction of specific immunity. The process of engulfing pathogens ensures that potentially destructive processes used to kill the pathogen, such as lysozyme release, generation of reactive oxygen species, and generation of nitric oxide (NO), are focused into internal compartments of the phagocytes, thus limiting the damage that can be inflicted on invaded tissues. Phagocytosis mediated by any of the receptors mentioned involves an interaction between receptor and ligand, which leads to signal transduction and, in turn, to cytoskeletal rearrangement and engulfment. The signals that precede, and are associated with, engulfment are limited to the area around the ligand-receptor complex, which is therefore associated with a localised cytoskeletal rearrangement within the cell.

In this section, the emphasis will be on phagocytosis by cells of the monocyte/macrophage lineage. Phagocytosis by neutrophils will not be discussed, although these cells do express some of the same receptors involved in phagocytosis, and others present on neutrophils, such as FcεRI, have analogous signalling cascades to the FcγR receptors.

1.2.1. Receptors that mediate phagocytosis on monocytes and macrophages.

Cells of the monocyte/macrophage lineage express several proteins that are able to mediate phagocytosis. These include the Fcγ Receptors, which are proteins that recognise IgG, complement receptor 1 (CR1), CR3 and CR4, which are receptors that recognise components of the complement pathways, and mannose receptors that recognise terminal mannose or fucose residues (reviewed by Brown E.J., 1995).

1.2.1.1. Structure of Fcγ receptors.

Fcγ receptors are members of the immunoglobulin superfamily. These proteins recognise IgG-coated particles. There are three classes of Fcγ receptors expressed on monocytes and macrophages. These are FcγRI (CD64) the high affinity IgG receptor which recognise monomeric IgG, FcγRII (CD32) and FcγRIII (CD16), which are low affinity IgG receptors that recognise immune complexes. Several genes encode the FcγRs. Three genes (known as A, B, and C) exist for both FcγRI, and FcγRII. Two genes (known as A and B) exist for FcγRIII (Ravetch and Kinet, 1991).

Figure 1.2.1.1. shows the domain structure of the FcγRs that are expressed on monocytes or macrophages. All three FcγRs have highly homologous extracellular portions containing binding domains that recognise the Fc portion of IgG. The most divergent parts of each receptor are the transmembrane and intracellular portions, suggesting that the response to IgG will depend on which FcγR it interacts with, as each receptor may signal through different signalling pathways. In order to transduce the phagocytic signal some forms of FcγR interact with dimers of homologous disulphide-linked γ or ζ chains. These subunits were first identified as part of the signalling mechanisms of FcεRI, and the T-cell receptor (TCR), respectively (Brooks and Ravetch, 1994). Different FcγRs show no preference for IgG subclasses, and all mediate

phagocytosis in a similar way, using similar signal transduction pathways (Indik et al., 1995).

Figure 1.2.1.1.
FcγR

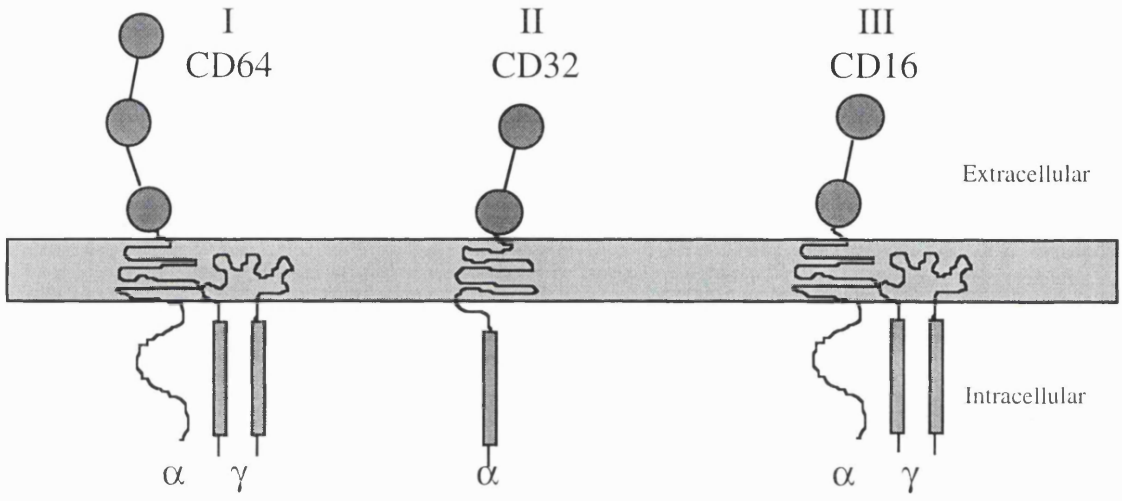

Figure 1.2.1.1. Schematic representation of the structures of Fcγ receptors. Circles designate regions of Ig-like homology, whilst oblong boxes designate ITAM regions.

FcγRI is a 72kD sialoglycoprotein. It has three extracellular Ig-like domains, which are responsible for the high affinity for IgG. All three of its subtypes (A, B and C) are expressed on monocytes and macrophages. FcγRI is associated with a γ chain that is important for the expression of the receptor at the cell surface and for signal transduction (Indik et al., 1991a). FcγRII is a 40kD sialoglycoprotein. It has only two extracellular Ig-like domains, and the presence of two (rather than three) domains probably accounts for the relative low affinity of this receptor for IgG. Only two subtypes, A and C, are expressed on monocytes and macrophages, as subtype B is expressed on lymphocytes. FcγRII is not associated with a γ chain, and this protein mediates signal transduction without an additional factor (Indik et al., 1991b). FcγRIII is a

sialoglycoprotein of between 50-70kD. This receptor also has only two extracellular Ig-like domains, and so is another low affinity receptor for IgG. Only subtype A of this protein is expressed on monocytes and macrophages. Subtype B, which is a glycosylphosphatidylinositol (GPI)-linked form of the receptor, and therefore has no cytoplasmic tail, is expressed exclusively on neutrophils. FcγRIII is associated with a γ chain, which mediates signal transduction. In the same study, FcγRIII also mediated phagocytosis when associated with a ζ chain which is usually expressed in lymphocytes, and is part of the TCR signal transduction mechanism (Park et al., 1993a; Park et al., 1993b).

The intracellular portions of the FcγRs, or the associated γ or ζ chains, contain motifs that mediate phagocytic signal transduction. These motifs contain tyrosine residues, which are phosphorylated in response to cross linking of FcγRs with IgG (Reth, 1989). These motifs are known as immunoreceptor tyrosine-based activation motifs (ITAM) (Isakov, 1997). ITAMs consist of two pairs of tyrosines and leucines in a consensus sequence of: D/E-X_7-D/E-X-X-Y-X-X-L-X_7-Y-X-X-L (where D = aspartic acid, E = glutamic acid, Y = tyrosine, L = leucine, and X = any residue). The specificity of signalling is determined by the actual sequence of the ITAM and in particular the sequence between the tyrosine and the leucine residues (eg. Y-X-X-L) (Indik et al., 1991a; Mitchell et al., 1994).

1.2.1.2. Signal transduction by Fcγ receptors.

Figure 1.2.1.2. shows a model for the early events of FcγR-mediated signal transduction. The first step in mediating the phagocytic stimulus is the cross-linking of two or more FcγRs by the binding of an IgG-opsonised particle. Artificial cross-linking FcγRs with antibodies will also induce phagocytic signalling (Metzger and Kinet, 1988). After this cross linking, tyrosines in the ITAMs of the FcγRs or associated γ chains become phosphorylated (Santana C. et al., 1996). The exact mechanism of

this tyrosine phosphorylation following FcγR cross linking is poorly understood.

Figure 1.2.1.2.

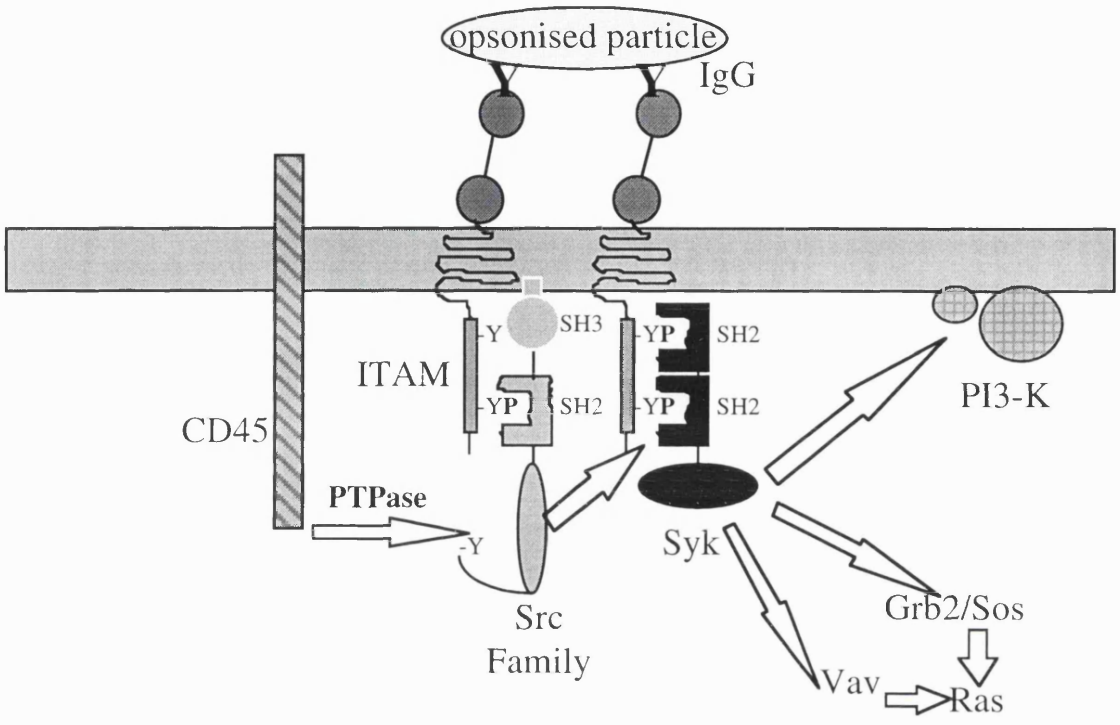

Figure 1.2.1.2. Schematic representation of the probable signal transduction mechanisms involved following FcγR cross linking. See text for details.

In phagocytes, members of the Src family of kinases associate with inactive FcγRs; Src, Fyn, Fgr, Hck, and Lyn have all been identified as associating with inactive FcγRs, depending on what cell type is being investigated (Bolen, 1991; Santana C. et al., 1996). These kinases are attached to the plasma membrane by myristoylation at their amino terminal end. The kinases have three main functional domains, a Src homology 3 (SH3), and Src homolgy 2 (SH2) domains, and a catalytic domain which is followed by a short carboxy terminal tail (see section 1.3. for an overview on Src family protein kinases). This tail region has a tyrosine residue which when phosphorylated interacts with its own SH2

domain and inhibits catalytic activity (Cooper and Howell, 1993). Cross linking of FcγRs leads to dephosphorylation of the C terminal tyrosine of Src family kinases, possibly by the leukocyte specific protein tyrosine phosphatase (PTPase) CD45 (Adamczewski et al., 1995), thus freeing the catalytic domain and activating the kinase activity. This dephosphorylation also frees the SH2 domain of the Src family kinase which binds phosphorylated tyrosines in the ITAM of FcγRs (Ghazizadeh et al., 1994).

Syk is a member of the ZAP-70 family of kinases and has been implicated in FcγR signalling. Syk is an exclusively cytoplasmic protein. Syk has been found to co-immunoprecipitate with γ chain of FcγRI and FcγRIIIA in macrophages (Darby et al., 1994). On cross-linking of FcγRs in macrophages and monocytes, Syk has been shown to be phosphorylated, and its kinase activity increased (Agarwal et al., 1993). COS-1 cells (a monkey kidney fibroblast cell line) transfected with FcγRI or FcγRIIIA and γ chain can be induced to phagocytose IgG-opsonised particles at low efficiency. However, co-transfection of Syk with the same components greatly increases the efficiency of phagocytosis (Indik et al., 1995). Syk activity is also vital to ITAM dependent activation of actin assembly (Cox et al., 1996). Both these observations demonstrate the importance of Syk in FcγR-mediated phagocytosis. Furthermore, both Y-X-X-L sequences in the ITAM of the γ chain are necessary for Syk activity, suggesting that Syk binds the ITAM via its two SH2 domains, and catalytic activity is stimulated by these phosphotyrosine residues on the ITAM (Indik et al., 1995).

Proteins activated downstream of Syk are not clearly defined. However, a number of phosphorylated proteins have been identified after FcγR induction of phagocytosis. Phospholipase Cγ1 (PLCγ1) and PLCγ2 have been shown to be phosphorylated during phagocytosis (Azzoni et al., 1992; Ting et al., 1992). The PLC family of proteins are responsible for production of inositol triphosphate (IP3) and diacylglycerol (DAG)

second messengers, which themselves induce activation of protein kinase C (PKC). Phosphatidylinositol-3 kinase (PI3-kinase) has been shown to play an important role in phagocytic signal transduction, as a specific inhibitor of PI3-kinase, wortmannin, inhibits phagocytosis (Ninomiya et al., 1994). Other phosphorylated proteins involved in signal transduction that have been detected are p95 Vav and p62/GAP-associated proteins (Darby et al., 1994). p21 Ras has also been shown to be phosphorylated, and this activation is associated with interactions with guanine nucleotide exchange factors via adaptor proteins such as Shc and Grb2 (Galandrini et al., 1996). Downstream of p21 Ras, members of the mitogen-activated protein kinase (MAPK) family have also been found to be phosphorylated in response to FcεRI ligation, mediated via SOS and Grb2 (Hirasawa et al., 1995; Jabril Cuenod et al., 1996). An unknown protein of 115kD has also been shown to be phosphorylated, associated with an SH2 domain of PI3-kinase (Ninomiya et al., 1994).

An area of dispute in phagocytic signalling is the role played by Ca^{2+} ions. One of the first biochemical changes recognised after FcγR ligation was a rise in cytosolic Ca^{2+} concentration. Release of Ca^{2+} ions from intracellular stores is normally mediated by second messengers such as IP3, which as we have already seen, is induced during FcγR-mediated phagocytosis. Ca^{2+} release was always considered relevant as all FcγRs induced an increase in intracellular Ca^{2+}, which was concentrated around the phagosome (Sawyer et al., 1985). However, it has been shown that FcγR-mediated phagocytosis can proceed in a Ca^{2+}-dependent or independent manner depending on the activation state of the phagocyte (Rosales and Brown, 1991). Subsequently it was discovered, using transfected mutants of FcγRIIA, that Ca^{2+}-independent phagocytosis is a function of utilisation of γ chains, suggesting that Ca^{2+}-independent phagocytosis is important for signalling via FcγRI and FcγRIII, but not FcγRII (Edberg et al., 1995). However, Ca^{2+} release may have a regulatory role in FcγR-mediated phagocytosis, as the cytoplasmic tail of

FcγRI, whilst not containing an ITAM, has been shown to mediate Ca^{2+} release on receptor ligation (Indik et al., 1992).

One end point of the signal transduction induced by FcγR ligation is the activation of "functional" proteins, and the polymerisation of actin that will perform the process of engulfment. Several putative functional proteins have been identified as being phosphorylated upon FcγR ligation. These include, paxillin, a protein associated with the cytoskeleton and found with F-actin in phagosomes (Greenberg et al., 1994), and L-plastin, which is also associated with F-actin (Jones and Brown, 1996). L-plastin has also been suggested as a mediator of Ca^{2+} release in phagocytosis (Rosales et al., 1994). Other proteins phosphorylated on FcγR ligation are p47 and p67 phox, which are components of NADPH oxidase, a complex that produces superoxide, a precursor of microbicidal oxidants (Roos et al., 1996; Sumimoto et al., 1996).

1.2.1.3. Role of complement receptors (CR) in phagocytosis.

There are three classes of CR expressed on monocytes and macrophages. These are CR1 (CD35), CR3 (CD11b/18), and CR4 (CD11c/18). CR1, a member of the regulators of complement activation gene family, binds the complement component C3b. CR3 and CR4 are both members of the β2 integrin superfamily, and bind the complement component iC3b, as well as the extracellular matrix protein fibrinogen (reviewed by Brown E.J., 1995). It was shown many years ago that complement opsonisation of a particle enhances the efficiency of IgG-mediated phagocytosis (Ehlenberger and Nussenzweig, 1977), and that patients with a genetic deficiency of CD18 do not phagocytose IgG-coated particles (Arnaout et al., 1983). When integrins are activated, they are known to signal cytoskeletal rearrangement, which is consistent with the role of these receptors in regulating phagocytosis.

The receptor that has been studied in most detail is CR3 (CD11b/18, also known as Mac-1). Studies with monoclonal antibodies (mAbs) against specific integrins indicated that this receptor is required for efficient FcγR mediated phagocytosis (Gresham et al., 1991). CR3 and FcγRIII have been shown to co-cap and this close association is inhibited by N-acetylglucosamine, suggesting that CR3 and FcγRIII are physically connected via a carbohydrate-lectin link (Zhou et al., 1993). Aggregated IgG can inhibit binding of CR3 mAbs on cells that do not express FcγRIII, suggesting that CR3 is also closely associated with other FcγRs (Brown et al., 1988). Absence of a signal via CR3 during FcγR-mediated phagocytosis leads to a lack of phosphorylation of paxillin, a protein that associates with F-actin (Graham et al., 1994). This suggests that CR3 acts to optimise phagocytosis by regulating cytoskeletal rearrangement, and also demonstrates that the signalling events described as being mediated by FcγRs may actually be effects of proteins closely associated to FcγRs.

1.2.1.4. Other functional properties of monocytes and macrophages induced on phagocytosis.

Phagocytosis induces other functional properties of monocytes and macrophages, including the release of inflammatory mediators which recruit other parts of the immune response, and antibody-dependent cellular cytotoxicity (ADCC). ADCC is mainly carried out by natural killer (NK)-cells, mediated by FcγRIIIA, but macrophages also have the same potential. In NK cells, ADCC is mediated by similar FcγR-mediated signalling events to those involved in phagocytosis, except that Src family kinases are not involved in the initial activation of Syk (Zoller et al., 1997). After FcγR ligation, ADCC by both NK and macrophages is mediated by the release of cytolytic granules which attack the bound opsonised particle.

1.2.2. Role of FcγRs in monocyte and macrophage differentiation and activation.

The act of undergoing phagocytosis has profound effects on monocytes and macrophages. Exposure of U937 cells to IgG molecules leads to growth arrest, increased expression of CD11b, and increased secretion of TGF-β, that are characteristic of monocyte/macrophage differentiation. This IgG-mediated effect was specific for IgG1 and IgG2b subclasses, as IgG2a and IgM did not effect the U937 cells. Furthermore, these IgG-mediated effects could be blocked by pre-pulsing U937 cells with antibodies to FcγRII (Micouin et al., 1997). This suggests that the presence of opsonised particles during myelopoiesis may act as factors in cell differentiation and maturation. This could be analogous to events which occur during development of T lymphocytes, as signalling through the T-cell receptor (TCR), which involves ITAMs and analogous signalling cascades to FcγR-mediated signalling, plays a vital role in T-cell negative and positive selection (van Oers et al., 1996b).

1.3. Signalling mechanisms.

Mechanisms of signal transduction have been important subjects of research in the recent past, and several of these mechanisms have been investigated in this thesis. Therefore, to give a greater understanding of these mechanisms, this section will briefly describe the structure and functions of the Src family; the ras/MAPK pathways, including the adaptor proteins Shc, Grb-2 and Grb-10; the PI3-K system; and the PLCγ system; as activation of these systems have been implicated in either phagocytosis or in T-cell activation.

1.3.1. Src family of protein-tyrosine kinases.

There are currently nine known members of the Src family of kinases. They are expressed in a wide range of tissues, and have been shown to be important in the transduction of various signals. The Src family kinases can be placed into two groups on the basis of their expression pattern, those that are ubiquitously expressed (Src, Yes, Yrk and Fyn) and those that are expressed exclusively in haemopoietic cell lineages (Fgr, Blk, Lck, Hck and Lyn). Of particular relevance to this project, the activity of Src, Fyn, Fgr, Hck, and Lyn, has been shown strongly associated with FcγR mediated phagocytosis (see section 1.2.-in particular Figure 1.2.1.2.), while, Lck and Fyn, have been shown to be strongly associated with T-cell receptor (TCR) signal transduction (see section 1.4.).

1.3.1.1. Structural features.

Members of the Src kinase family have three functional domains that share approximately 60-70% sequence similarity between the members of the family. The first functional domain, situated at the C-terminal end, is the catalytic domain that acts as a tyrosine kinase. This domain is capable of phosphorylating tyrosine residues on other proteins as well as auto-phosphorylating its own tyrosine residues (as reviewed by Erpel and Courtneidge, 1995). This domain consists of sub-domains denoted I to XI,

which perform the catalytic functions and are common to all tyrosine kinases.

Each member of the Src family has two highly conserved tyrosine residues, one in the catalytic domain, and the other situated in the C-terminal domain. The C-terminal tyrosine is highly phosphorylated *in vivo* and is involved in the regulation of kinase activity. Mutation of this regulatory tyrosine residue from Lck, Src or Fyn gives rise to proteins with increased kinase activity and cell transforming ability (as reviewed by Erpel and Courtneidge, 1995). A second tyrosine situated in the catalytic domain of all Src family kinases is a target for autophosphorylation. Phosphorylation of this tyrosine regulates the kinase activity of Lck (Buss et al., 1986), but not of Src (Piwnica Worms et al., 1987), suggesting that tyrosine phosphorylation at this site has differential effects on members of the Src family.

The second functional region of these proteins is the Src homology 2 domain (SH2), which has found to be conserved in several other proteins involved in signal transduction. These domains specifically bind to phosphopeptide motifs composed of a phosphotyrosine (p-Tyr) residue, followed by three to five residues situated C-terminal of p-Tyr. The context of the p-Tyr determines SH2 domain binding specificity and therefore, which signal transduction mechanisms can be activated. This explains how functionally related SH2 domains from different signalling proteins specifically bind appropriate phosphotyrosine residues. Although SH2 domains of various signalling proteins may have as little as 25% sequence similarity, crystal structures of various SH2 domains reveal that they have similar structures. This conserved structure consists of a hemi-sphere, the flat surface of which contains a deep pocket in which the phosphotyrosine residue will fit (Waksman et al., 1992). As well as specifically binding phosphotyrosine residues from other proteins, the Src SH2 domain also binds its own C-terminal phosphotyrosine residue which

is important in regulation of its kinase activity (Cooper and Howell, 1993).

The third functional region of the Src family is the Src homology 3 domain (SH3), which again is highly conserved and present in many other signal transducing proteins. SH3 domains interact with proline rich regions of other proteins, allowing protein-protein interactions. SH3 domains have been shown to consist of conserved aromatic residues that act as ligand binding sites, and variable loops that confer ligand specificity (Booker et al., 1993; Koyama et al., 1993). SH3-ligand interaction does not result in conformational change of the SH3 domain, the SH3 domain acting as a preformed template (Yu et al., 1994). The consensus sequence of SH3 binding peptides has been defined as X-P-Φ-P-P-X-P (where X = any residue; P = proline; Φ = a hydrophobic residue). The proline residues are involved in binding the SH3 domain, whilst the non-proline residues confer specificity of binding (Yu et al., 1994). Src also exhibits intramolecular SH3-binding, with a region of its C-terminal domain, and this is also important in the regulation of kinase activity (Pawson, 1997).

The fourth structural domain are unique to each member of the Src family at the N-terminal end of the protein. The only conserved feature of this region is a glycine residue at position 2 (G-2). This glycine is responsible for the attachment of Src family kinases to the inner surface of the cell membrane. This is achieved by the post-translational covalent attachment of myristate, a 14 carbon saturated fatty acid, to G-2 (reviewed by Resh, 1994). Mutation of G-2 does not interfere with the kinase activity of Src family kinases, but the proteins do not translocate to the cell membrane (Buss et al., 1986; Kamps et al., 1985). The unique N-terminal domains have also been shown to be important in the localisation of some members of the Src family. For example, two cysteine residues of this region in Lck, interact and localise Lck to the cytoplasmic tail of

the T-cell co-receptors CD4 and CD8 (Shaw et al., 1989; Turner J.M. et al., 1990).

1.3.1.2. Regulation of kinase activity.

Src family kinases are regulated by phosphorylation and dephosphorylation of their own tyrosine residues. In an inactive state the C-terminal tyrosine is phosphorylated, this phosphorylation promotes the interaction of the C-terminal phosphotyrosine with the SH2 domain of the same protein, thus hindering the ability of the SH2 domain to bind any other phosphotyrosine residue, and masking the catalytic kinase domain.

Activation of Src family kinases is associated with dephosphorylation of the C-terminal tyrosine residue, thus freeing the SH2 domain and unmasking the kinase domain. This dephosphorylation is performed by protein tyrosine-phosphatases (PTPase), for example, the PTPase CD45 is associated with the dephosphorylation of Src in FcγR-mediated phagocytosis (Adamczewski et al., 1995), and dephosphorylation of Lck and Fyn in TCR mediated signalling (Wange and Samelson, 1996) (see sections 1.2 and 1.4 respectively). Phosphorylation of the second tyrosine, residing in the kinase domain of Src family kinases, is associated with an activated state and appears to be involved in stabilising the active conformation (Buss et al., 1986).

Down-regulation of Src family kinase activity is associated with the phosphorylation of the C-terminal tyrosine residue by another family of tyrosine kinases. These proteins, known as Csk kinases, contain a tyrosine kinase domain that specifically phosphorylates the C-terminal tyrosine residue of Src family kinases (Bergman et al., 1992; Nada et al., 1991). The importance of Csk was demonstrated in a murine T-cell line, where the over-expression of Csk lead to a decreased amount of TCR-induced tyrosine phosphorylation, and therefore, a down regulation of T-cell activation (Chow et al., 1993).

1.3.1.3. Signal transduction mechanisms involving Src family kinases.
Src kinases are involved in the transducing of many signals through their ability to interact with surface receptors. Src family kinases have been shown to be involved in signalling via the PDGF receptor, the EGF receptor, and via β1 and β2 integrins (all reviewed by Parsons and Parsons, 1997).

Some other processes that Src family protein-tyrosine kinases are thought to be important in, include FcγR-mediated signalling (many members of the Src family have been implicated), signalling via the TCR (Fyn and Lck), and B cell receptor (BCR) signalling (Blk, Fyn and Lyn) (reviewed by Weiss and Littman, 1994). Src family kinases transduce these signals by respectively interacting with phosphotyrosine residues contained within the ITAM of FcγR or γ chain in phagocytic cells, CD3 or ζ chain in T-cells, or Igβ in B cells. These catalytically active Src kinases are thought to interact with and activate members of the ZAP-70 family, which then themselves transduce a signal downstream (Agarwal et al., 1993; Iwashima et al., 1994) (see section 1.2 and 1.4). Lyn has also been shown to interact and activate PI3-K in B cells following BCR ligation (Yamanashi et al., 1992). In monocytes, Lyn, Fgr and Hck have all been shown to be activated by ligation of the LPS receptor (CD14), although only Lyn interacted directly with CD14 (Stefanova et al., 1993).

1.3.2. The Ras/MAPK signal transduction pathway.

Nearly all cell surface receptors utilise one or more of the mitogen-activated protein kinase (MAPK) cascades in their repertoire of signal transduction mechanisms. This section will deal with this transduction, from cell surface receptor, to initiation of transcription.

1.3.2.1. Adaptor molecules that interact with cell surface receptors.

As previously described, cell surface receptor protein tyrosine kinases, or protein tyrosine kinases associated with cell surface receptors (such as CD3), once activated have the ability to auto-phosphorylate on tyrosine residues. This process can recruit adaptor molecules to the receptor which act as scaffolding for further signal transduction. These adaptor molecules have no catalytic activity themselves, but contain domains that recognise p-Tyr residues, and motifs which allow downstream signalling molecules to dock and transduce signals. Many adaptor molecules have been identified, amongst these Shc, Grb-2 and Grb-10, have been implicated in mediating signals to many pathways including the Ras/MAPK pathway.

Shc is an adaptor molecule that consists of two functional domains, a C-terminal SH2 domain that recognises p-Tyr residues, and a N-terminal p-Tyr-binding (PTB) domain that also binds to p-Tyr residues. PTB domains recognise phosphopeptide motifs ~~that~~ in which the p-Tyr residue is preceded by residues that that form a β turn. The specificity of binding of PTB domains is determined by hydrophobic residues located 5 to 8 residues N-terminal of the p-Tyr residue. PTB domains like SH2 domains, can be found as components of docking proteins that recruit additional signalling proteins to the vicinity of the activated receptor. There is also evidence that PTB domains, unlike SH2 domains, can bind non-phosphorylated peptide motifs, suggesting that PTB domains are primarily involved in peptide recognition. Thus, Shc binds to a broad range of activated receptors, and contains two Y-X-N-X motifs (where Y = tyrosine, N = Asparagine, and X = any amino acid), which can be phosphorylated by the kinase activity of the bound receptor, or by an additional kinase (reviewed by Pawson and Scott, 1997).

Grb-2 and the related molecule Grb-10, are adaptor molecules that consist of two SH3 domains flanking a SH2 domain. Grb-2 can bind the p-Tyr residues of receptor protein tyrosine kinases or associated proteins,

including Shc, via its SH2 domain. Grb-2 physically associates with the Ras-guanine nucleotide exchange factor (Ras-GEF), Sos, via a SH3 domain, in many tissues, but can also be associated with other proteins in a tissue specific manner. For example, in T-cells following TCR ligation, Grb-2 associates with both Sos and SLP-76, a protein important in the mediation of the increase in IL-2 production (reviewed by Pawson and Scott, 1997). Grb-10 has similar functions as an adaptor protein, but with differing binding specificities.

1.3.2.2. Ras activation, regulation and effector functions.

Ras, also known as p21 Ras proteins, are highly evolutionary conserved proteins that have been shown to be involved in the transduction of signals from many cell surface receptors. Ras proteins and the Ras sub-family function as binary switches by cycling between the active GTP-bound conformation (Ras-GTP), and the inactive GDP-bound conformation (Ras-GDP). Two main classes of regulatory protein regulate the activation state of Ras proteins. The guanine nucleotide exchange factors (GEF), promote the transition from the inactive GDP-bound, to the active Ras-GTP state. Whilst the GTPase-activating proteins (GAP), stimulate conversion to the inactive Ras-GDP state. (as reviewed by Marshall, 1996). See figure 1.3.2.2.

Two regions of Ras differ in conformation between the GDP-bound and GTP-bound states. These are referred to as SwitchI and SwitchII regions. The SwitchI region is composed of residues 30-38. Within this motif residues 32-38 are conserved amongst all members of the Ras sub-family, so specificity of interactions for each Ras species is determined by residues outside this area. Mutation of residues within and around this region has shown that certain residues are vital for the signalling capacity of Ras, but not for GTP-binding. These mutations are known as effector mutations. The SwitchII region is composed of residues 60-76, is highly mobile and can exist in multiple conformations. Mutation of residues

within or around the SwitchII region compromises some Ras functions such as the binding of PI3-K. Amongst the proteins shown to interact with Ras-GTP, no obvious consensus sequence exists, suggesting that the flexibility of the SwitchII region is important in Ras-protein interactions (reviewed by Marshall, 1996).

The Grb-2-activated Ras-GEF, Sos, promotes the formation of active Ras-GTP. p120 RasGAP and neurofibromin have both been shown to be GAP proteins, which preferentially bind Ras-GTP and stimulate its GTPase activity, thus promoting Ras-GDP formation. The first proteins that Ras-GTP was shown to activate were members of the Raf family of tyrosine kinases, Raf-1, A-Raf and B-Raf. These proteins are involved in signalling to the extracellular signal regulated kinase (ERK) branch of the MAPK pathway. The equivalent protein in the c-jun N-terminal kinase (Jnk) branch of the MAPK pathway, MEKK-1, has also been shown to be activated by Ras-GTP. These proteins have been shown to interact with residues in and around the SwitchI region of Ras-GTP. The p110 sub-unit of PI3-K has been shown to interact with the SwitchII region of Ras-GTP, and this interaction enhances the catalytic activity of PI3-K. Ras-GTP has also been shown to activate phospholipase D (PLC-D), via an interaction with Ral-GDS, a protein first characterised as a GEF for the Ras related protein p27Ral. Some reports have also shown that Ras-GTP can bind and activate protein kinase C-ζ (PKC-ζ) (as reviewed by Marshall, 1996). In T-cells, a functional link between the Ras-GTPase and the Rac-GTPase family has been shown, with Rac1 playing a critical role in Ras-GTP signalling that couples TCR ligation to NFAT induced gene transcription. The interaction between Rac and Ras is believed to be due to direct interactions between Ras-and Rac-GEFs, or Ras-and Rac-GAPs (as reviewed by Reif and Cantrell, 1998). Figure 1.3.2.2. shows a schematic representation of the mechanisms involved in Ras activation.

Rac is a member of an alternative family of Ras-like GTPases, which consists of Rac, Rho, and Cdc-42. These proteins are activated by a similar GDP-GTP shuttle. Activation of this class of GTPase is stimulated by a wide range of stimuli, and are able to transduce signals to a wide variety of downstream pathways. One of the most important functions of these Ras like proteins is in signalling cytoskeletal rearrangements (as reviewed by Reif and Cantrell, 1998). Rac and Cdc-42 have both been shown to interact and induce activation of MEKK 1-3, which lie upstream of the Jnk and p38 protein kinase pathways (reviewed by Robinson and Cobb, 1997).

Figure 1.3.2.2.

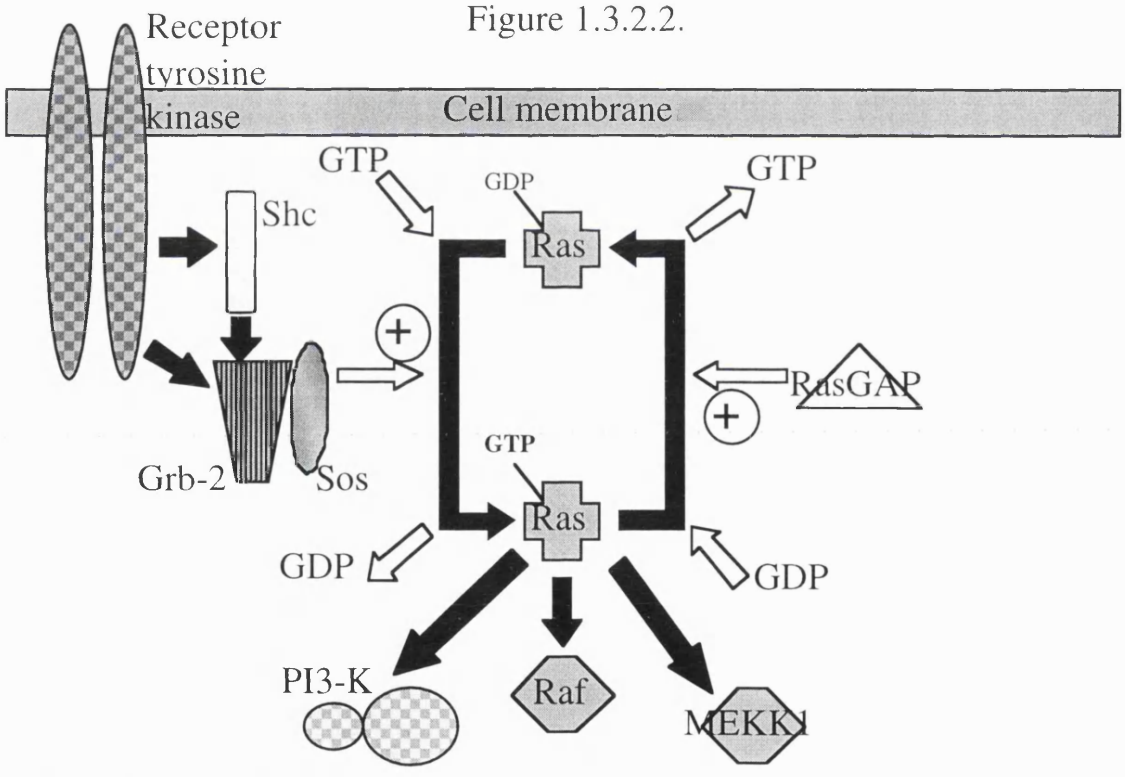

Figure 1.3.2.2. Schematic representation of the probable mechanisms involved in the formation of active Ras-GTP, and proteins that Ras-GTP has been reported to be involved in activating. See text for details.

1.3.2.3. The MAPK signalling cascades.

The MAPK family is split into three main independent cascades, one which involves the phosphorylation of ERK1 and ERK2, and two others

which are termed as the stress MAPK cascades. One of these involves the phosphorylation of Jnk, and the other which involves phosphorylation of p38. These signalling pathways are also highly conserved in evolution, with MAPK cascades existing in organisms such as yeast, as well in vertebrates. Recently, other MAPK cascades have been identified, but these are not well defined, and so this section will concentrate on the better defined cascades described above. See figure 1.3.2.3. for a schematic representation the MAPK pathways.

The generalised hierarchy of MAPK cascade activation is that an upstream protein (such as Ras-GTP), will induce phosphorylation of a MAPK/ERK kinase kinase (MEKK), which in turn induces phosphorylation of a MAPK/ERK kinase (MEK), which itself phosphorylates a MAPK protein. Phosphorylated MAPK is the final effector in this pathway, interacting with nuclear factors that regulate gene transcription. The MAPK proteins need to be phosphorylated on both a threonine and a tyrosine residue to be activated. In Yeast, Ste5 acts as a scaffold on which the components of the MAPK pathway are situated. Although no equivalent protein has been discovered in mammals, it seems likely that such a protein does exist (reviewed by Robinson and Cobb, 1997).

The ERK1 and ERK2 pathway proceeds downstream from Ras-GTP formation. The first MEKKs discovered were the Raf family members, which are activated by interacting with Ras-GTP. This interaction leads to a conformational change in Raf that unmasks the kinase domain. This active conformation can also be stabilised by phosphorylation of Raf tyrosine residues, by Src family kinases (reviewed by Morrison and Cutler, 1997). Raf proteins themselves phosphorylate and activate only MEK1/2. MEK1/2 proteins in turn activate ERK1/2, which are the final effector proteins of this cascade.

The Jnk kinase pathway is activated by the addition of stressful stimuli to cells. This leads to the formation of the active GTP bound forms of Rac and Cdc42. These proteins are members of the Rho family of Ras like GTPases. Rac-GTP and Cdc42-GTP interact and activate another family of kinases, the p21 activated protein kinases (PAKs). PAKs subsequently activate MEKK1-3, and these proteins in turn activate MEK4, which itself activates the final effector protein Jnk. MEKK1-3 proteins are also able to activate other branches of the MAPK system, and these proteins act on MEK1/2 of the ERK pathway, and MEK3 and MEK6 of the p38 pathway (as reviewed by Robinson and Cobb, 1997).

Figure 1.3.2.3.

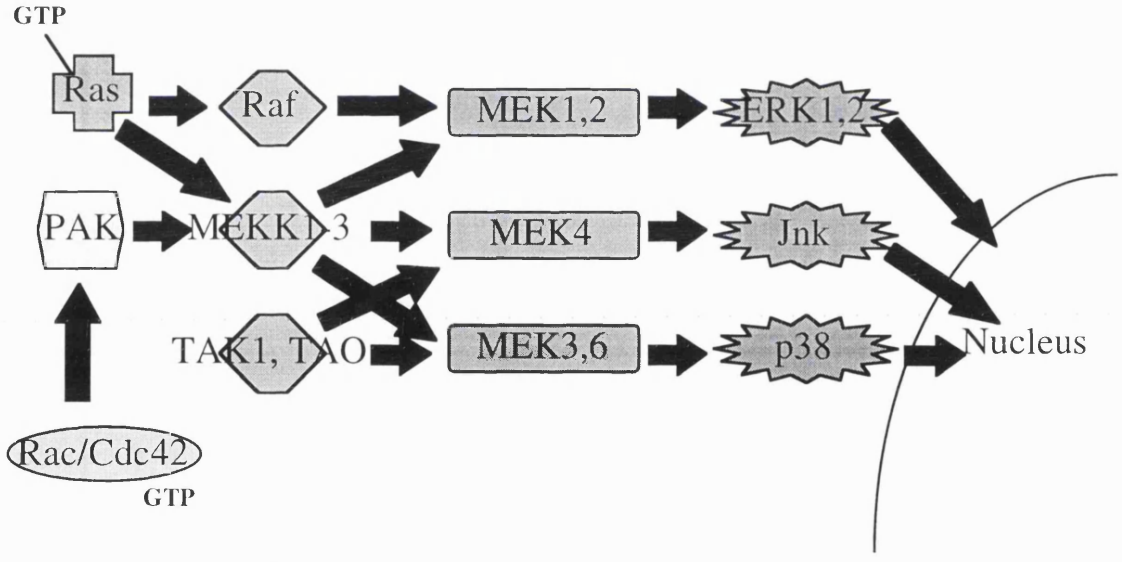

Figure 1.3.2.3. Schematic representation of the probable interactions involved in transduction of signals through the MAPK pathway. See text for details.

The p38 pathway is not as well defined as the cascades already described, but it is known that p38 activation is also induced upon addition of stressful stimuli. One MEKK for this pathway is the TGF-β-activated kinase 1 (TAK1), and another is the thousand and one amino acid kinase

(TAO). Both of these kinases act on MEK3 and MEK6, which themselves act on p38, which acts as the final effector protein of this pathway. TAK1 and TAO are also able to act on MEK4, which is a component in Jnk activation (as reviewed by Robinson and Cobb, 1997).

1.3.2.4. Transcription factors activated by MAPKs.

Once MAPK proteins have been activated by upstream signalling proteins they migrate to the nucleus and regulate the activity of transcription factors by phosphorylation of serine or threonine residues. Factors that have been identified as targets for MAPK phosphorylation include: Elk1, which has multiple phosphorylation sites acted upon by ERK1/2, and Jnk; Ets-1 and Ets-2, which are acted upon by ERK2; the related proteins Jun, which is acted upon by Jnk, and Fos, which is acted upon by ERK1/2; ATF-2 which is activated by both Jnk and p38. It is likely that many more substrates of MAPK proteins remain to be discovered (as reviewed by Treisman, 1996).

1.3.2.5. Effects of MAPK activation.

In all mammalian ERK1/2 cells are activated by mitogens, and prolonged translocation of ERKs to the nucleus increases expression of cyclin D1, thus inducing cells to enter the cell cycle. In fact a constitutively active ERK proteins lead to cell transformation. In some cell lines, ERK activation has been associated with differentiation. High levels of ERK proteins are expressed in all cells, and half of all ERK in activated cells is associated with the cytoskeleton, suggesting that ERKs have a role in cytoskeletal organisation.

Jnk has also been shown to be activated after some mitogenic stimuli, although this effect could also be due to an anti-apoptotic effect of Jnk activation in some cells. In contrast p38 activation is thought to inhibit cell proliferation, as p38 activation leads to an inhibition of cyclin D1

expression. Jnk activation has been associated with hepatic regeneration and T-cell activation.

As their name implies, the stress MAPKs, Jnk and p38, are activated in response to stresses on the cell such as heat shock, osmotic shock, cytokines, antioxidants, UV light and DNA-damaging agents. The consequence of this activation appears to be growth arrest, and in some cases apoptosis, although it is thought that Jnk/p38 activation in isolation is not sufficient to induce apoptosis (as reviewed by Robinson and Cobb, 1997).

1.3.3. Phosphoinositide 3-kinase (PI3-K).

PI3-K phosphorylates the D-3 position of the inositol ring of phosphatidylinositol (PtdIns). This produces PtdIns 3-P (where P = a phosphate group), from PtdIns; PtdIns 3,4-P_2, from PtdIns 4-P; and PtdIns 3,4,5- P_3, from PtdIns 4,5- P_2. The most important of these products is PtdIns 3,4,5- P_3. More than one form of PI3-K has been identified, but the best defined kinase consists of a dimer of a p85 regulatory sub-unit, and a p110 catalytic sub-unit. The p85 sub-unit consists of a single SH3 and two SH2 domains. The p110 sub-unit consists of a p85 binding domain, a Ras binding domain, a lipid kinase unique domain, and a catalytic domain (reviewed by Carpenter and Cantley, 1996). Activation of PI3-K has been associated with FcγR-mediated phagocytosis (reviewed by Sanchez Mejorada and Rosales, 1998), as well as being central to TCR mediated signalling (Qian and Weiss, 1997).

1.3.3.1. Regulation of PI3-K activity.

The levels of the lipids that act as substrates for PI3-K are tightly regulated in cells. A further level of regulation is that the catalytic activity of PI3-K can be inactivated by phosphorylation of serine and threonine residues in the p85 regulatory domain. This protein kinase activity is intrinsic within the p110 sub-unit, being located within the lipid kinase

domain. The SH2 and SH3 domains of the p85 sub-unit have been shown to interact with specific domains of receptor tyrosine kinases such as the receptors for platelet derived growth factor (PDGF) and epidermal growth factor (EGF) (as reviewed by Carpenter and Cantley, 1996).

1.3.3.2. Functions of PI3-K metabolites.

Studies using PI3-K inhibitors, such as wortmannin, dominant-negative forms of PI3-K and constitutively active forms of PI3-K, have revealed four distinct functions of PI3-K products. These four functions (outlined below), result from the interaction of the PtdIns products of PI3-K with motifs such as Pleckstrin homology (PH) domains. These domains specifically bind phospholipids, and are important in activation of protein kinases, and in positioning of signalling proteins to the cell membrane.

PI3-K has been shown to play an important role in mitogenesis. Inhibition of catalysis by the p110 sub-unit blocked the DNA synthesis that is normally induced by PDGF and EGF. As described previously PI3-K, is able to interact with Ras-GTP via its p110 sub-unit. It has been shown that increased levels of activated Ras-GTP lead to an increased concentration of PI3-K-derived products, suggesting that PI3-K is downstream of Ras. However, addition of constitutively active PI3-K leads to an increased concentration of active Ras-GTP, suggesting that PI3-K is upstream of Ras. This implies that the Ras-PI3-K interaction is complex.

PI3-K activity has been shown to have an anti-apoptotic effect, which was demonstrated on serum starved PC12 cells which spontaneously apoptose. This apoptosis is inhibited by transfection of constitutively active wild type PDGF receptor, but not by a mutant PDGF receptor that lacked a PI3-K binding site.

PI3-K has been shown to be important in vesicle trafficking and secretion. Addition of wortmannin inhibits Golgi-to-lysosome trafficking of cathepsin D, and cells accumulate large prelysosomal vesicles. Mutant PDGF receptors, that lack a PI3-K binding site, inhibit PDGF dependent lysosomal degradation of the receptor. Wortmannin has also been shown to inhibit insulin dependent secretion, and secretion by basophils.

PI3-K products have also been shown to have effects on the cytoskeleton. PtdIns 4,5-P_2 promotes actin filament growth, and actin uncapping. Both Rac and Rho activation were shown to increase PtdIns 4,5-P_2 levels in these experiments, suggesting that PI3-K can also interact with these cytoskeletal associated GTPases. Mutant PDGF receptors that lack a PI3-K binding site, and wortmannin, inhibit PDGF dependent cell membrane ruffling in response to PDGF. Finally some evidence exists for PI3-K playing a role in integrin signalling (all reviewed by Carpenter and Cantley, 1996).

1.3.4. Phospholipase C (PLC).

The phosphoinositide-specific PLCs hydrolyses PtdIns 4,5-P_2 to generate inositol 1,4,5-P_3 (IP3) and diacylglycerol (DAG). IP3 causes the release of calcium from intracellular stores, whilst DAG leads to activation of protein kinase C. In these ways PLCs are important regulators of intracellular calcium levels. There are three forms of PLC: β, γ and δ, and isozymes of each type also exist (eg PLC-γ1 etc). All three forms contain two regions of high homology designated X and Y, preceded by a PH domain. PLCγ also has two SH2 and one SH3 domains (reviewed by Spiegel et al., 1996; Toker, 1998). Activation of PLCγ has been associated with some forms of phagocytosis, as has the regulation of intracellular calcium levels (reviewed by Sanchez Mejorada and Rosales, 1998).

1.3.4.1. Regulation of PLC activity.

Two mechanisms of PLC activation have been described. PLC-β is activated via heterotrimeric G proteins, whereas PLC-γ binds to receptor protein-tyrosine kinases or receptor-associated protein-tyrosine kinases via its SH2 domains, and is activated by phosphorylation of a single tyrosine residue. Sites that bind PLC-γ are found on PDGF receptors, EGF receptors, nerve growth factor (NGF) receptors and fibroblast growth factor (FGF) receptors (reviewed by Toker, 1998).

1.3.4.2. Effects of DAG.

PKC is the only clearly defined target for DAG. PKC are a series of isozymes that share a common requirement for phospholipid in order to be activated. DAG or its analog PMA activate most PKC isozymes. Calcium and some other lipid products act as co-factors in DAG activation of PKC. PKCα has been shown to phosphorylate Raf-1, to activate the MAPK cascade; other isozymes phosphorylate MARCKS, a protein involved in cytoskeletal rearrangement; myogenin and P-glycoprotein (reviewed by Toker, 1998).

1.4. T-cell activation.

The activation of T-cells in response to antigen (Ag) requires at least two types of signals to be provided by an antigen presenting cell (APC) (Schwartz, 1992). The first of these is mediated via the interaction of the antigen specific T-cell receptor (TCR) with peptide that is associated with major histocompatibilty complex (MHC) molecules on the surface of the APC (Schwartz, 1985). As a result of this interaction, the TCR associated CD3 complex mediates intracellular signals that are necessary but not sufficient for T lymphocyte clonal proliferation (Barber et al., 1989; Weiss and Littman, 1994). In fact, if MHC-TCR interaction occurs without any second signal then the T-cell will go into an unresponsive state known as anergy (Jenkins et al., 1991a).

The second critical or co-stimulatory signal is mediated either by proteins on the T-cells that interact with co-stimulatory molecules on the surface of the APC (Jenkins et al., 1991b; Linsley et al., 1991a) or by soluble cytokines produced by APC acting on the T-cell. Unlike TCR mediated signals, these co-stimulatory signals are not Ag specific. The type of co-stimulatory signal that is delivered is dependent on several factors, including not only the type and activation status of the APC (Thomas et al., 1993), but also the type of T-cell (CD4+ or CD8+), and whether the T-cells are of naive or memory phenotype (Byrne et al., 1988).

1.4.1. MHC-TCR interaction.

MHC are associated with antigenic peptides on the surface of APC, and a primary component for T-cell activation is the interaction of this complex with its specific T-cell receptor, in a process known as antigen-specific MHC-restricted T-cell recognition.

1.4.1.1. MHC - peptide complex

MHC class I (MHC-I) or class II (MHC-II) glycoproteins are tightly complexed to antigenic or self peptide fragments generated from the

degradation of proteins which are (in basic terms) either synthesised by the same cell (for MHC-I), or ingested through an endocytic pathway (for MHC-II). MHC-I are expressed on all cells, and by "collecting" self-peptides they act as monitors of the internal cellular environment. MHC-I interact with TCRs of T-cells that also express the co-receptor CD8. MHC-II are expressed only on specialist APC, and act as monitors of the external environment. MHC-II interact with TCRs of T-cells that express the co-receptor CD4 (as reviewed by Germain and Margulies, 1993).

1.4.1.2. TCR and TCR mediated signalling.

The TCR is a complex of several proteins that can be separated into two functional units, the ligand binding domain that recognises the MHC-peptide complex, and a domain that mediates signal transduction. The ligand binding domain consists of a clonal specific αβ dimer, for most T-cells, although a small percentage of T-cells have a ligand binding domain consisting of a γδ dimer. The αβ dimer must bind to both the specific peptide and the MHC determinant. αβ dimers are di-sulphide linked and both have two Ig like domains extracellularly, and have very short, non signal transducing, intracellular portions. The signal transduction domain consists of at least six non-polymorphic sub-units, including a CD3γ-CD3ε dimer, a CD3ε-CD3δ dimer, and a TCR ζ-ζ homodimer. Each CD3 molecule has an extracellular Ig like domain, and one ITAM intracellularly. Each ζ chain has only a small extracellular portion and three ITAM intracellularly (as reviewed by Wange and Samelson, 1996).

On ligand binding, signal transduction through the TCR is analogous to that of FcγR signalling (see section 1.2.). The first event on ligand binding is the phosphorylation of tyrosines on the ITAMs of CD3 and ζ chains. Lck and Fyn are critical to this phosphorylation, and these proteins have been shown to phosphorylate tyrosines in the ITAMs (as reviewed by Wange and Samelson, 1996). Recently, it has been shown that Lck is the most important regulator of ITAM phosphorylation (van Oers et al.,

1996a). Two proteins are known to regulate the activity of Lck and Fyn in T-cells. Csk, is a tyrosine kinase which phosphorylates the C terminal tyrosine of these proteins and thus maintains them in an inactive state; CD45 is a PTPase which acts antagonistically to dephosphorylate the same tyrosine, thus freeing the SH2 and catalytic domains, and activating Lck and Fyn (as reviewed by Weiss and Littman, 1994).

ZAP-70 (ζ associated protein-70), which is in the same family as Syk, plays an essential role in signalling. ZAP-70 bind phosphorylated ITAMs and is subsequently itself phosphorylated and activated by Lck or Fyn (Iwashima et al., 1994). ZAP-70 is phosphorylated on three tyrosine residues, and these residues act as docking sites for other proteins involved in signal transduction, or for proteins involved in down-regulating the TCR response (Kong et al., 1996). Phosphorylated ZAP-70, as well as binding phosphorylated ITAMs, has been shown to bind Lck, Abl, Cbl, ras-GAP, Vav, and the PTPase SHP-1 (SH2 containing tyrosine phosphatase-1). SHP-1 and Cbl are thought to reduce ZAP-70 activity, whilst Abl, ras-GAP, and Vav are thought to mediate downstream signalling events. Several common downstream pathways are utilised in TCR signal transduction, and these include the production of IP3 and DAG, Ca^{2+} ion mobilisation, the activation of the ras/MAPK pathway, and the activation of Rac and Rho family proteins (as reviewed by Qian and Weiss, 1997).

1.4.2. Co-stimulation of T-cells.

Although the MHC-TCR signal is vital for T-cell activation, proliferation will not occur without a second co-stimulatory signal. Several cell surface co-stimulatory interactions have been implicated in T-cell activation. The most thoroughly investigated is that between CD80 (B7.1)/CD86 (B7.2) on the APC, and CD28/CTLA-4 on the T-cells (Jenkins et al., 1991b; Linsley et al., 1991a; Linsley et al., 1991b; Norton et al., 1992). Other interactions implicated are between CD2 and CD58, CD59 or CD48

(Liversidge et al., 1996; Menu et al., 1994; van der Merwe et al., 1994), between CD70 and CD27 (Brown G.R. et al., 1995; Hintzen et al., 1995), and between the β2 integrins, especially LFA-1 (CD11a/18) and the intercellular adhesion molecules (Damle et al., 1992a; Van Seventer et al., 1990). However, there have been several suggestions that there may well be other additional co-stimulatory molecules.

1.4.2.1. Interaction between CD28 or CTLA-4 and its ligands B7.1 (CD80) or B7.2 (CD86).

CD28 is a co-stimulatory receptor expressed on T-cells, and interaction with B7.1 or B7.2, along with successful MHC-TCR interaction, leads to optimal T-cell activation. CD28 occupancy leads to increased IL-2 production (Linsley et al., 1991a), an increase in expression of the anti-apoptotic protein BCL-$_{XL}$ (Lin et al., 1997; Noel et al., 1996), and enhanced cell-cell interactions (Turcovski Corrales et al., 1995). In humans, B7.1 is expressed mainly on dendritic cells. Other resting APCs express little B7.1. B7.2 is expressed at low levels on all APC (Hathcock et al., 1994). Expression of both B7 molecules is induced on activation, B7.2 is rapidly induced, whilst B7.1 is induced slower, with increased expression not occurring until 48 hours after stimulation (Lenschow et al., 1994). Furthermore, expression studies of B7.1 and B7.2 in human lymph nodes showed gradients of expression of B7.1, B7.2 and CD28 across the lymph node and in germinal centres in particular, suggesting that where B7 is expressed is as important as when it is expressed (Vyth Dreese et al., 1995).

CD28 and CTLA-4 are related glycoproteins of the immunoglobulin superfamily. The extracellular domains of each protein contains a conserved region that acts as the binding site for B7 (Peach et al., 1994). CTLA-4 has a ten times greater binding affinity for B7 than CD28, and the binding of both have very fast kinetics (Van der Merwe et al., 1997). Furthermore, CTLA-4 binds B7.2 with a lower affinity and faster off rate

than B7.1, which has important functional implications (Linsley et al., 1994). Intracellularly, both CD28 and CTLA-4 have several highly conserved SH2 and SH3 binding domains, important in signal transduction. CD28 is expressed at constant levels on the surface of most T-cells. In contrast to this CTLA-4 is expressed at undetectable levels on the surface of T-cells prior to T-cell activation (Walunas et al., 1994), MHC-TCR engagement, CD28 ligation and IL-2 all cause an increase in CTLA-4 expression (Green et al., 1994). Although expression of CTLA-4 is increased upon T-cell activation, there is a level of basal expression, and this protein is stored in perinuclear golgi vesicles (Leung et al., 1995), which are transported to the surface of the T-cell, specifically the site of TCR engagement, upon activation (Linsley et al., 1996).

The generation of CD28 null mice has shown that many T-cell responses are inhibited by the absence of CD28. After immunisation these mice do not form germinal centres (Ferguson et al., 1996), and it appears as though CD28 null T-cells can initiate, but not sustain proliferative responses (Lucas et al., 1995). The data at present suggests that CD28 is critically important in sustaining immune responses.

The first reports of the function of CTLA-4 suggested that activation synergised with CD28. These studies were carried using mAbs to CTLA-4, which induced stronger T-cell activation (Linsley et al., 1991b). However, it is now clear that these results were induced through the blocking of the inhibitory pathway that is mediated by the interaction between CTLA-4 and B7. This was demonstrated in CTLA-4 cross linking experiments, using secondary antibodies, which inhibited T-cell proliferation induced by CD3 and CD28 mAbs (Krummel and Allison, 1995). This decrease was due to an inhibition of cell division, rather than an increase in the level of apoptosis (Krummel and Allison, 1996). In CTLA-4 null mice, the absence of CTLA-4 leads to huge T-cell lymphoproliferation, which leads to death between three to four weeks of

age (Tivol et al., 1995). Therefore, the data suggests that CTLA-4 transduces an inhibitory signal that modulates TCR and CD28 signalling.

The signalling cascade induced upon ligation of CD28 or CTLA-4 by B7 is not clear. CD28 is thought to integrate, and amplify TCR mediated signals, and has been shown to activate JNK (Su et al., 1994), and to interact with PI3-kinase (Hutchcroft and Bierer, 1996), and the protein kinase Itk (August et al., 1994). CTLA-4 signal transduction is thought to be linked to a protein phosphatase activity, as CTLA-4 null T-cells have hyper phosphorylated ζ chain, ZAP-70, Shc, Fyn, and Lck. In the same study CTLA-4 was shown to be associated with the tyrosine phosphatase SHP-2 (PTP-1D, or SYP) (Marengere et al., 1996). One important effect of CD28 ligation is in the amplification of signalling through Ras, Rac and Rho. CD28 ligation leads to an increase in the stability of TCR induced Vav phosphorylation, activated Vav acts as a Rac and Rho GEF, thus promoting the formation of the active Rac-GTP and Rho-GTP states. Furthermore, CD28 ligation induces phosphorylation of $p62^{dok}$, a protein that when phosphorylated complexes with both p120 RasGAP and p190 RhoGAP, thus sequestering these negative regulators of Ras and Rho functions away from their respective targets (as reviewed by Reif and Cantrell, 1998).

The current model of CD28/CTLA-4 - B7 interaction, and how this determines immune induction, is dependent on the activation state of the APC. If the APC is activated and has high amounts of Ag/MHC complex, and is expressing high amounts of B7, when the APC interacts with its specific TCR, the high amounts of Ag will stimulate a large "GO" signal, via the TCR; along side this the high numbers of B7 will interact with CD28 sending the second necessary "GO" signal, thus inducing T-cell activation. However, if the APC is unactivated, has low amounts of Ag/MHC complex, and is expressing low B7, now when the APC interacts with its specific TCR, the low amounts of Ag will give a small "GO"

signal, via the TCR, but along side this the low amounts of B7 will interact preferentially with the low levels of CTLA-4 expressed on resting T-cells rather than CD28 (as CTLA-4 has a ten times greater affinity for B7 than CD28), thus sending a "STOP" signal and inhibiting immune induction. Following T-cell activation, CTLA-4 is thought to play a role in regulating T-cell activation. As described previously expression of both CTLA-4 and B7.1 are increased after 48 hours of activation of either T-cells or APC. CTLA-4 has a greater affinity for B7.1 than for B7.2, which is the B7 molecule increased early after activation of APC. Thus the simultaneous increased expression of both CTLA-4 and B7.1 may limit T-cell activation.

1.4.2.2. Interaction between CD2 and its ligands CD58, CD59, or CD48.

CD2 is constitutively expressed on T-cells, and has been implicated in adhesive reactions, and in signal transduction that may play a role in co-stimulation. CD2 is a member of the immunoglobulin superfamily, that has two extracellular Ig like domains, and a long cytoplasmic tail that contains several sequences that are putative SH3 binding motifs (as reviewed by Davis and van der Merwe, 1996).

There are three known possible ligands for CD2, the primary ligand in humans is CD58 (LFA-3) molecule, which like CD2 is a member of the Ig-superfamily. In mice, CD48 is found to be a ligand for CD2, and some evidence exists that this is also a ligand in humans, but that this is a weak interaction. Both CD58 and CD48 are closely related to each other and to CD2, and are expressed widely on a number of cells. Two groups have independently shown that CD2 will bind CD59, which is an unrelated protein that is involved in cellular protection from complement lysis. However other groups have been unable to confirm this interaction (as reviewed by Davis and van der Merwe, 1996).

The main function of CD2 is to mediate transient adhesion of T-cells to antigen-presenting cells and target cells. To achieve this CD2 has low binding affinities for its ligands, and very fast dissociation rates. Specific blocking of the CD58-CD2 interaction with mutant CD58 has been shown to inhibit T-cell proliferation, suggesting that this interaction is important in regulation of T-cell activation (Miller et al., 1993). In another study CD58 was also implicated in activation of T-cell responses, and an interaction between CD59 and CD2 increased this CD58 dependent activation (Menu et al., 1994).

The cytoplasmic tail of CD2 has been shown to interact with Fyn, Lck, and PI3-kinase (Carmo et al., 1993) proteins which have been shown to be important in mediating TCR signal transduction. CD2 has been shown to interact with TCR/CD3, CD4, CD5, CD8, and CD45, (Beyers et al., 1992). These interactions may explain the co-stimulatory capacity of CD2.

1.4.2.3. Interaction between CD27 and its ligand CD70.

CD27 is a lymphocyte-specific member of the TNF receptor family and binds to a type II transmembrane molecule belonging to the TNF gene family, CD70. CD70 is expressed on APC and on activated lymphocytes (Brown G.R. et al., 1995).

Specific interaction of CD27 and CD70 has been shown to provide a potent signal for cytokine production, and proliferation of unprimed CD45RA+ peripheral blood T-cells (Hintzen et al., 1995). In a further study CD27 mAbs, induced substantial proliferation of CD45RA+ peripheral blood T-cells in the presence of a suboptimal dose of PMA, anti-CD2, or anti-CD3 together with a second Ab to cross-link the CD27 molecule (Kobata et al., 1994). These data demonstrate that this interaction is important in the stimulation of resting naive T-cells, and less important in induction memory T-cell responses.

Furthermore, an increase in intracellular Ca^{2+} ions was observed in PMA-treated T-cells when the CD27 molecule was cross-linked. CD27 ligation also induced protein tyrosine phosphorylation of ZAP-70. This response is blocked by protein kinase inhibitors and PKC inhibitors, showing that the activation of protein tyrosine kinases and protein kinase C is required for CD27-mediated T-cell co-stimulation (Kobata et al., 1994).

1.4.2.4. Interaction between β2 integrins and ICAM molecules.

β2 integrins as described before, are adhesion/signalling molecules expressed specifically on leukocytes. Of particular importance in co-stimulation of T-cell responses is LFA-1 (a dimer of CD11a and CD18), which is expressed on lymphocytes and APCs. LFA-1 will bind with ICAM-1 (CD54), ICAM-2 (CD102) (as reviewed by Springer, 1990), or ICAM-3 (CD50) (de Fougerolles and Springer, 1992). ICAM molecules are members of the immunoglobulin superfamily, and each ICAM has a different number of Ig-like extracellular domains.

Induction of ICAM molecule expression in a number of cell types in inflammation is vital for leukocyte migration, and this adhesive property is mediated by ICAM-LFA-1 interactions (as reviewed by Springer, 1990). Expression of ICAM molecules is also induced in APC upon activation, and the interaction of ICAM molecules, the most important being ICAM-1, on APC with LFA-1 on T-cells has been implicated in co-stimulation of T-cell activation (Damle et al., 1992a; Teunissen et al., 1995; Van Seventer et al., 1990).

ICAM-1-LFA-1 interactions have been shown to mediate a number of signalling events in T-cells during T-cell activation. In a model using a CD3 mAb as a mimic for TCR ligation, ICAM-1-LFA-1 interaction leads to prolonged phospholipase C activation, and a sustained increase in intracellular levels of free Ca^{++} (Van Seventer et al., 1992). Cytohesin-1,

a cytoplasmic protein, upon interaction with CD18 increases the binding affinity of LFA-1 for ICAM-1 in lymphoid cells (Kolanus et al., 1996), demonstrating a way that adhesion and co-stimulation may be modulated by intracellular T-cell proteins.

Integrin ligation has been shown to induce signal transduction via many cascades. Rho, a small GTPase, has been shown to interact with activated β1 and β2 integrins in lymphoid cells (Laudanna et al., 1996). Activated integrins form focal adhesions which act as anchoring points for the actin cytoskeleton. Focal adhesions are important in mediation of signalling, with focal adhesion kinase (FAK) interacting with Src family kinases and activation of the ras/MAPK pathway via Grb-2 and SOS (reviewed by Howe et al., 1998).

1.4.3. U937 cells as accessory cells for T-cell activation.

Jenkins *et al* demonstrated that the monoblastoid U937 cell can act as an accessory cell providing co-stimulatory signals for T-cell activation induced by a CD3 mAb (Johnson and Jenkins, 1994). This co-stimulatory activity was independent of the CD80/CD86 - CD28 pathway, as U937 cells do not express CD80, and express very low levels of CD86 (Johnson and Jenkins, 1994). Antibodies against CD11a/18 were not able to substitute for U937 cells in this model, suggesting that the β2 integrin/ICAM interaction also did not provide the essential second signal in this model.

In another more recent study, the specifics of U937 cell co-stimulation were investigated. This study showed that stimulating CD4+ naive peripheral blood T-cells with a CD3 mAb, and using U937 as accessory cells, lead to the exclusive generation of Th1-like T-cells. Furthermore, U937 cells transfected to express B7.1 (CD80) had the ability to co-stimulate the proliferation of both Th-1 and Th-2 cells (Palmer and van Seventer, 1997).

1.5. Retinoid X receptor.

Retinoid X receptors (RXRs) are members of the steroid/thyroid hormone nuclear receptor superfamily, which act as ligand-dependent *trans*-acting transcription factors. Nuclear receptors can be sub-divided into two groups. The first contains the steroid oestrogen receptors (ER), and glucocorticoid receptors (GR). These receptors bind their respective ligands, homodimerise, and bind response elements in promoter regions of genes to activate or inhibit gene transcription (Evans, 1988). The mechanism of activation and DNA binding of these receptors differs from that of the second class of nuclear receptors, which will be the focus of this introduction. This second class of nuclear receptors contain RXRs, retinoic acid receptors (RAR), farsenoid X activated receptors (FXR), vitamin D receptors (VDR), thyroid hormone receptors (TR), and the peroxisome proliferator activated factor receptors (PPAR). There are also many orphan receptors that belong to this second class of nuclear receptor but whose ligands are unknown. All known members of this second class of nuclear receptors bind directly to small lipophilic ligands. In this way nuclear receptors are able to control gene transcription directly. The second class of nuclear receptors also need to form dimers in order to bind response elements on DNA and affect transcription. These receptors form heterodimers, most commonly with RXRs, which therefore act as regulators of nuclear receptor activity. RXRs are also able to homodimerise in the presence of their high affinity ligand, 9-*cis* RA. This section will describe the structure and function of RXRs, and how these functions relate to the monocyte/macrophage lineage, which led to our initial interest in the role of RXRs in monoblast differentiation.

1.5.1. Isolation of retinoic acid responsive nuclear receptors.

Vitamin A (retinol), from which other retinoids are derived, has long been associated with photoreceptors in the retina, as lack of retinol leads to night blindness. Retinol deficient mouse embryos have also been shown to develop congenital malformations of heart and eyes, in a condition

known as VAD syndrome (as reviewed by Blomhoff, 1994). This suggested that retinol derivatives play a role in foetal development. In particular, one retinol derivative, retinoic acid (RA) was shown to have profound effects on differentiation and development. This suggested the presence of a specific receptor for this small lipophilic molecule, as had been identified for steroid and thyroid hormones.

The first retinoic acid receptor was isolated in 1987, and was designated RARα (Giguere et al., 1987; Petkovich et al., 1987). Subsequently, two more RAR proteins, RARβ, and RARγ were isolated. These proteins have ligand-and DNA-binding domains that indicate that these proteins belong to the nuclear receptor superfamily.

The first human retinoid X receptor (RXRα) was isolated in 1990, using low stringency hybridisation screening of a liver and kidney cDNA library with a RARα probe (Mangelsdorf et al., 1990). RXRβ and RXRγ isoforms have since been isolated (Leid et al., 1992; Mangelsdorf et al., 1992; Yu et al., 1991). Based on sequence and structure, the RXRs represent a distinct gene family from RARs, but both families of receptors bind RA, despite having only 27% sequence similarity in their ligand binding domains (Mangelsdorf et al., 1990). Up until that time it had been thought that the only active form of RA was all-*trans* RA, but it was then demonstrated that RARs bind 9-*cis* RA, as well as all-*trans* RA with high affinity (Levin et al., 1992). Furthermore, 9-*cis* RA was also found to be the high affinity ligand for the RXRs, which do not bind all-*trans* RA (Heyman et al., 1992). In 1995, a further high affinity receptor for 9-*cis* RA was isolated, and this was designated LXR. Unlike the ubiquitous expression of both RAR and RXR, LXR expression is limited to liver and gut tissues. RAR/RXR heterodimers or RXR/RXR homodimers are not able substitute for LXR/RXR-mediated retinoid responses, suggesting that LXRs mediate unique retinoid responses specific to liver and gut tissues (Willy et al., 1995).

The ability of RXR to act as a heterodimeric partner for RAR, LXR and many other nuclear receptors, was thought to imply that RXR acted as an accessory "silent" partner. However, it has recently been shown that 9-*cis* RA-binding to RXR directly potentiates transcription mediated by RAR-RXR heterodimers (Chen et al., 1996; Minucci et al., 1997). Similar results have also been shown with VDR-RXR heterodimers, where 9-*cis* RA bound RXR potentiates DHCC-induced expression (Zou et al., 1997). These results demonstrate the flexibility of RXR and the importance of 9-*cis* RA in the regulation of nuclear receptor function.

1.5.2. Retinoid metabolism.

Retinol is obtained from plant carotenoids and animal retinyl esters in the diet, and is stored predominantly as retinyl esters in liver stellate cells (as reviewed by (Rowe and Brickell, 1993). Retinol is mobilised to the tissues in complexes with retinol-binding proteins. Once inside target cells retinol binds to cellular retinol binding protein (CRBP). Retinol can then be metabolised to all-*trans* RA, by cytochrome P-450 oxidases, and this in turn can be metabolised by isomerases to produce 9-*cis* RA. RA is bound inside cells by cellular retinoic acid binding proteins (CRABP). There are two forms of CRABP, -I, and -II, that are expressed in a tissue specific manner, and their main functions are thought to be to regulate cellular RA concentration (Boylan and Gudas, 1991).

1.5.3. Structure and function of RXR.

The structure of RXRs resembles that of RARs and other members of the nuclear receptor superfamily. Nuclear receptors contain five structural domains that are associated with functional properties, Figure 1.5.3. shows a schematic representation of an RXR. These structural domains are labelled A to F, and include a DNA binding domain (C), a ligand binding domain (E), dimerisation interfaces, and regions involved in gene transcription (AF-1 and AF-2 regions) (Evans, 1988).

Figure 1.5.3.

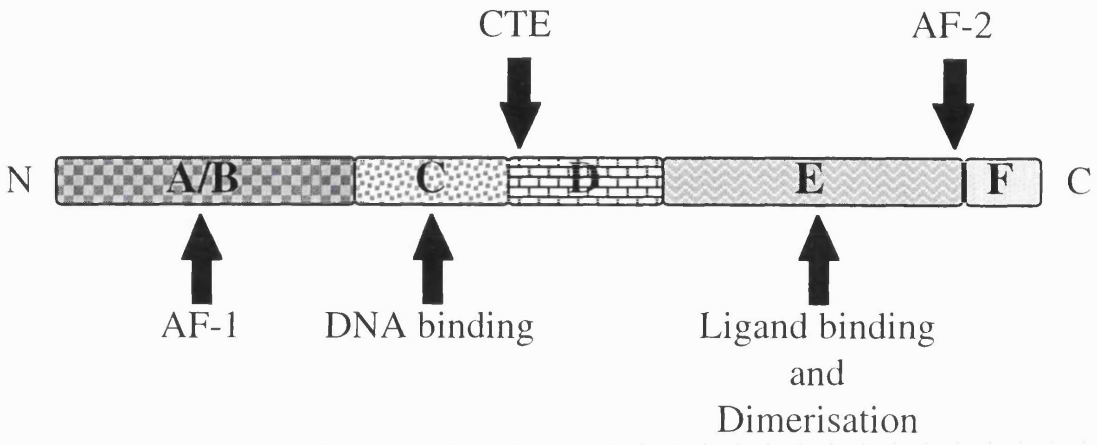

Figure 1.5.3. General structure of RXRα, and where domains involved in functional activity are located.

1.5.3.1. DNA binding domain (DBD).

A nuclear receptor as a ligand dependent transcription factor, must bind ligand and dimerise with another nuclear receptor before it can bind DNA. It is necessary that the ligand be bound for subsequent transactivation of transcription by the dimer. The DBD of RXR spans a core of 66 amino acid residues comprising two zinc finger modules and two perpendicular α helices. RXRs have a further functional part of the DBD, this is the carboxy terminal extension (CTE), which contains a third α helix that is found immediately after the two core consensus α helices, this increases the size of the whole DBD to 94 amino acid residues (see Figure 1.5.3.1.). The first α helix of the core region (the recognition helix), binds to DNA via the major groove, whilst the CTE helix makes extensive contacts with the minor groove (Rastinejad et al., 1995). The cumulative effect of this interaction is to bring basic amino acids into close proximity with DNA, which make contact with both base pairs and phosphate backbone, and so facilitate a strong protein-DNA interaction. The CTE helix also plays a role in RXR homodimer formation, with the

CTE helix of the upstream RXR DBD interacting with the second zinc finger of the downstream RXR DBD, hence serving as a dimerisation interface (Lee et al., 1993).

The DNA response element to which nuclear receptors bind consist of two half sites of the consensus sequence 5'-AGGTCA-3'. The half sites are arranged as either direct, inverted, or palindromic repeats. The response elements of ER and GR, which form homodimers, bind to palindromic repeats, whilst receptors that dimerise with RXR bind to direct repeats that are spaced by 1 to 6bp. The distance between the half sites determines the specificity of the response element. Generally, retinoic acid response elements (RARE), the response elements that bind RAR-RXR heterodimers, comprise a direct repeat (DR) spaced by 5bp (DR5), or 2bp (DR2). VDRE are DR3 elements, whilst TRE and LXRE are DR4 elements (Leid et al., 1992; Umesono et al., 1991). In the presence of 9-*cis* RA, RXR homodimers will bind DR1 elements (Zhang et al., 1992). Table 1.5.3.1. shows a summary of RXR heterodimeric partners and their respective response elements. In addition to the spacing of the half sites, the actual sequence of the half sites and the 5' extension of the RE is also important in nuclear receptor activity (Vivanco Ruiz et al., 1991; Willy et al., 1995). The importance of the sequence of the spacer region of the RE has also been demonstrated by the observation that alterations of the DR4 spacer of a TRE could in some cases abolish transactivation, and in other cases enhance it (Katz et al., 1995). Other unique response elements have been shown to exist, for instance, a RXR-RAR heterodimer has been shown to bind a unique DR9 RE (Cao et al., 1996). Heterodimeric partners have also been shown to bind RE that should be for other nuclear receptors, for instance RAR-RXR heterodimers have been shown to bind to a classical DR3 VDRE (Zou et al., 1997).

The crystal structure of the DBD of RXR-TR heterodimer on its RE (Rastinejad et al., 1995), has helped to visualise how the spacing between

DR are able to determine the specificity of nuclear receptor binding. This paper demonstrates that a change of one nucleotide in spacer length requires the RXR partner to rotate around the double helix by 36° in order for both receptors to be in the correct orientation in the major groove. Therefore, it is the dimerisation interfaces of RXR and its partners that determine the specificity of what particular RE that heterodimers bind.

Figure 1.5.3.1.

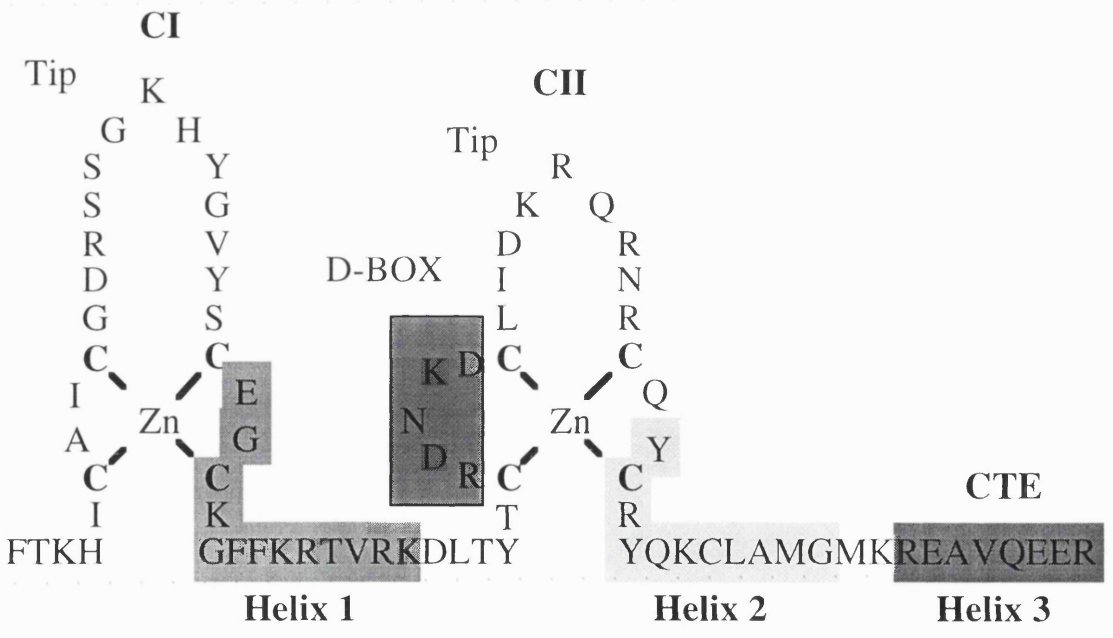

Figure 1.5.3.1. Schematic representation of the RXRα DNA binding domain. Helix regions and D-box are shown as shaded regions. CI and CII represent zinc finger motifs.

Nuclear receptors which heterodimerise with RXR and bind to RE that are direct repeats have a "head to tail" organisation, and so RXR heterodimers have a polarity. In studies using TR-RXR, LXR-RXR and RAR-RXR heterodimers, bound to DR4, DR4 or DR5 RE, respectively, it was shown that RXR occupies the 5' half site (Kurokawa et al., 1993; Willy and Mangelsdorf, 1997; Zechel et al., 1994b). However, RAR-RXR

heterodimers can bind DR1 elements and silence ligand dependent transcription at this site. This interaction occurs with the RAR occupying the 5' half site (Forman et al., 1995). This demonstrates the importance of nuclear receptor dimer polarity. PPAR-RXR heterodimers also bind to DR1 elements, with a similar orientation to that of RAR-RXR binding to DR1, with PPAR occupying the 5' half site (Ijpenberg et al., 1997).

The signal mediated by nuclear receptor dimers is dependent on available ligand and RE. RAR-RXR heterodimers can activate transcription via DR2, or DR5 RE, when activated by all-*trans* RA. However, 9-*cis* RA will have the same effects on DR2 and DR5 RE, and will additionally promote formation of RXR-RXR homodimers, thus activating DR1, DR2, and DR5 RE in a more efficient manner (Zhang et al., 1992). Emphasising this difference in the effects of RA isomers is the fact that RAR-RXR heterodimers also bind to DR1 RE and inhibit transcription at this site (Kurokawa et al., 1994). An additional complication of nuclear receptor functions is that TR and VDR have been shown to able to homodimerise and activate transcription, VDR-VDR homodimers acting via DR6 RE, and TR-TR homodimers acting via DR4 RE, in the presence of their respective ligands (Brent et al., 1992; Carlberg et al., 1993). Furthermore, VDR-TR heterodimers have also been observed. These receptors are capable of interaction on addition of either ligand. In the presence of DHCC (the ligand for VDR), VDR-TR dimers bind to DR4 RE, with the VDR binding to the upstream 5' half site; whilst in the presence of T_3 (the ligand for TR), VDR-TR dimers will bind DR3 RE, with the TR binding to the upstream 5' half site (Schrader et al., 1994). It is probable that formation of liganded VDR and TR homodimers, and VDR-TR heterodimers is rare as TR-VDR dimers are formed in the absence of RXR (Schrader et al., 1994; Yen et al., 1996), and liganded VDR can be displaced from VDR homodimers by RXR, to form RXR-VDR dimers.

Table 1.5.3.1.

RXR dimeric partner	Ligand	Possible response elements
RXRα,β,γ	9-*cis* RA	DR1
PPARα,β	Fatty acids	DR1
PPARγ	PG-J2	DR1
VDR	DHCC	DR3
TRα,β	Thyroid hormone	DR4, IR0, ER6, ER8
RARα,β,γ	RA	DR1, DR2, DR5, IR0
LXR	RA	DR4
FXR	farsenoids	IR1

Table 1.5.3.1. Dimeric partners of RXR, ligands needed to induce formation of dimers with RXR, and response elements that specific dimer pairs bind. See text for details. DRN= direct repeat of consensus half site sequences, separated by N base pairs. IR= inverted repeat of half sites. ER= everted repeat of half sites. PG-J2= prostaglandin-J2.

1.5.3.2. Ligand binding domain (LBD).

The LBD comprises of a 225 amino acid residue carboxy terminal region, that is capable of autonomous ligand binding (Evans, 1988). In addition to functioning as an LBD, this region also includes homo- and hetero-dimerisation interfaces, and transactivation interfaces. The LBD contains many hydrophobic amino acid residues which are involved in the formation of pockets into which 9-*cis* RA fits (Evans, 1988). RXRα, RXRβ, and RXRγ all bind 9-*cis* RA with dissociation constants (Kd) of 15.7, 18.3, and 14.1 nM, respectively (Allenby et al., 1993). The LBDs of RAR and RXR show little sequence homology, although both will bind 9-*cis* RA (RARs Kd are between 0.2 and 0.7 nM). RARs, but not RXRs, will also bind all-*trans* RA with similar affinities (Allenby et al., 1993).

Using X-ray crystallography, the structure of the unliganded RXRα LBD has been determined (Bourguet et al., 1995). Approximately 65% of the LBD is made up of a unique nuclear receptor motif consisting of 11 α-helices (H1 to H11), These helices are organised in a three layer structure, with helices H4, H5, H8, H9 and the N terminal part of H11 sandwiched

between H1, H2 and H3 on one side and H6, H7 and H10 on the other. This structure forms two 9-*cis* RA binding pockets. Pocket A is formed by H1, H3, H5 and H11, and pocket B by H5 and H7. Evidence from this study and previous data suggests that pocket B is the actual binding site for 9-*cis* RA (Forman and Samuels, 1990). The AF-2 transactivation function associated with the RXRα LBD was shown to reside in the C terminal part of H11, and this region was shown to extend away from the core of the LBD at an angle of 45°. This external exposure of the AF-2 allows it to interact with proteins involved in transcription initiation, as well as contributing to the sequence specificity of the receptor.

Unliganded nuclear receptors are often associated with nuclear receptor co-repressors (N-CoR) (see section 1.5.4.). The binding of ligand leads to a conformational change in the structure of the α-helices in the LBD, which allows proteins that mediate transcription (see section 1.5.4.) to bind nuclear receptors (Wurtz et al., 1996). It has been demonstrated that the integrity of the N terminal H1 helix is important in repression of transcriptional functions by nuclear receptors, whereas the integrity and positioning of the C terminal helix, which contains the AF-2 motif, is vital for transcriptional activation (Wurtz et al., 1996). These data suggest a model whereby N-CoRs interact with H1 in unliganded receptors, leading to silencing of transcription. Upon ligand binding the surface of H1 is hidden or changed by conformational change, which allows co-activator proteins to bind and initiate nuclear receptor transcription (Perlmann and Evans, 1997). Evidence for the change in conformation of the LBD on ligand binding was provided by a panel of mAbs specific for the LBD of RARγ. Some members of this panel bound to unliganded RARγ only, whilst others only bound liganded RARγ (Driscoll et al., 1996), demonstrating a gross shift in 3-D structure of the LBD.

1.5.3.3. Receptor dimerisation.

Nuclear receptors contain two independent dimerisation motifs, one contained in the C terminal of the LBD, and the other contained in the DBD. The dimerisation motif contained in the LBD consists of 20 amino acid residues. Mutation of these residues in RAR, VDR and TR results in the loss of the ability to dimerise with RXR. However, the mutation of these residues in RXR did not effect its ability to dimerise with wild type RAR, VDR and TR (Rosen et al., 1993). This LBD dimerisation interface does not mediate dimer specificity, but rather acts to stabilise the complex (Mader et al., 1993).

The second dimerisation interface in RXR is located in the core or CTE regions of the DBD. As described previously the CTE region of the upstream RXR has been shown to mediate homodimerisation on a DR1 RE, this region interacting with the second zinc finger region (CII) of the downstream RXR (Lee et al., 1993). The interface of RAR-RXR heterodimerisation has been shown to be mediated by the CII zinc finger of the upstream RXR, and the CTE of the downstream RAR on a DR2 RE (Zechel et al., 1994a). Heterodimerisation of RXR-TR on a DR4 RE, and RXR-RAR on a DR5 RE, demonstrated that the D-box of the CII zinc finger region of the upstream RXR interacts with the tip of the RAR CI zinc finger, or with 7 amino acid residues on the N terminal side of the CI zinc finger region of TR (Zechel et al., 1994b). It is this DBD interaction that determines the specificity of homo- or hetero-dimerisation, with respect to which DR elements the nuclear receptor dimers will bind (Zechel et al., 1994b).

1.5.3.4. AF-1 and AF-2 transactivating regions.

Transactivation by steroid receptors such as ER is modulated by two regions in the receptor, named the autonomous transactivation functions (AF-1 and AF-2) (as reviewed by Gronemeyer, 1991). In RXRs, AF-1 is situated in the A/B domain, whilst AF-2 is situated at the C terminus of

the LBD (on H11) (see figure 1.5.3.) (Nagpal et al., 1993; Nagpal et al., 1992). In these same studies, modulation by AF-1 conferred promoter specificity of ligand-inducible AF-2 transactivation. (Nagpal et al., 1993). This was demonstrated by the fact that a chimeric RARα1 (regions A, B and C)-RARγ1 (regions D, E and F), protein activated RAREs normally associated with RARα1 function, and vice versa (Nagpal et al., 1992).

1.5.4. Initiation of transcription by RXR dimers.

Unliganded RXR homo- and hetero-dimers have been shown to bind to response elements but not activate transcription, showing how vital the conformational change of the LBD upon ligand binding, and subsequent dissociation of co-repressor proteins and interaction with co-activating proteins, is for functional activity. In recent years many researchers have concentrated on the identity and function of co-activator and co-repressor proteins. Furthermore, other studies have suggested that dimers involving RXR can act in a totally ligand-independent manner.

1.5.4.1. Ligand-independent transactivation.

A notable exception to the rule that unliganded dimers do not induce transcription, was provided when it was shown that VDR-RXR heterodimers, RAR-RXR heterodimers, or RXR homodimers (but not those involving RXRγ) are capable of inducing transcription in a ligand-independent manner. This occurred upon the addition of okadaic acid, a compound that inhibits the activity of protein phosphatases 1 and 2a (Lefebvre et al., 1995; Matkovits and Christakos, 1995), suggesting that phosphorylation of RAR, RXR or VDR may be important in regulation of activity. This is similar to data with ER and GR, the activity of which has been demonstrated to be regulated by phosphorylation (Bodwell et al., 1998; Castano et al., 1998), suggesting that phosphorylation may be a common means of regulation for all nuclear receptors.

1.5.4.2. Repressors of nuclear receptor transactivation.

As previously described, unliganded nuclear receptors are associated with repressors of transcriptional activity. Two putative repressor proteins, silencing mediator for RAR and TR (SMRT) and nuclear receptor co-repressor (N-CoR), have been shown to bind unliganded RAR and TR (Chen and Evans, 1995; Horlein et al., 1995). The binding of these repressors requires the structural integrity of helix 1 (H1) of the LBD of RAR and TR. These repressors form complexes with SIN3 and histone deacetylases (Alland et al., 1997; Nagy et al., 1997), suggesting that chromatin remodelling and histone deacetylation is involved in nuclear receptor mediated repression (Pazin and Kadonaga, 1997; Wolffe, 1997). Further evidence for the role of histone acetylation in the control of repression is that RAR-RXR heterodimers are only able to bind a DR5 RE associated with nucleosomal histone proteins, following hyper acetylation of these histones (Lefebvre et al., 1998). Another means of repressing transcription is through competition for RE. As shown previously, although RAR-RXR, RXR-RXR and PPAR-RXR dimers all bind to DR1 RE, RAR-RXR heterodimers will silence transcription at this site, whilst the other dimers will activate transcription. Therefore, the relative amounts of each receptor and their respective ligands leads to competition for both the DR1 RE, and RXR as a binding partner (DiRenzo et al., 1997). The orphan nuclear receptor TR4, has recently been shown to bind specifically as a monomer to half sites of DR1 or DR5 RARE, with a higher affinity than RAR-RXR heterodimers, thus inhibiting RA-dependent transcription (Lee Y.F. et al., 1998).

RAR and RXR can act as repressors of transcription, through direct interaction with other transcription factors. RARα, RARβ and RXRα have been shown to interact with and sequester Fos/Jun dimers, which comprise the AP-1 transcription factor, thus repressing AP-1 transcription by preventing DNA binding (Salbert et al., 1993; Schule et al., 1991). Further studies have shown that RA treatment leads to

decreased transcription of the c-*fos* gene. This repression was shown to be mediated by both RAR and RXR (Lee H.Y. et al., 1998). The antagonistic interactions of retinoids and AP-1 is not surprising as retinoids are generally associated with growth arrest, whilst AP-1 is activated by the MAPK family, leading to mitogenic/growth responses.

1.5.4.3. Co-activators of nuclear receptor mediated transcription.

Putative co-activator proteins include TIF1α, Trip1, receptor interacting protein 140 (RIP140), steroid receptor co-activator 1 (SRC-1), TIF2, receptor associated co-activator 3 (RAC-3), ACTR, CREB-binding protein (CBP) and NCoA-62 (Baudino et al., 1998; Cavailles et al., 1995; Kalkhoven et al., 1998; LeDouarin et al., 1995; Lee J.W. et al., 1995; Li et al., 1997; Onate et al., 1995; Voegel et al., 1998). Recently, a protein has been discovered that has both co-repressing and co-activating functions, in binding to both liganded and unliganded LBD of numerous nuclear receptors (Huang et al., 1998). Co-activators bind to various members of the nuclear receptor superfamily, and it seems likely that specific interactions between receptors and co-activators in part define specificity of the transcriptional response. All co-activators discovered, bind to the LBD of ligand-activated nuclear receptors, and require the integrity of the AF-2 core region for co-activating activity (Glass et al., 1997). Some of these factors have intrinsic histone acetyltransferase (HAT) activity, and can interact with protein complexes that contains a HAT enzyme, p/CAF (Bannister and Kouzarides, 1996; Chen H. et al., 1997; Ogryzko et al., 1996). These data reinforce the suggestion that chromatin rearrangement via histone acetylation is involved in transcriptional activation by nuclear receptors.

Both co-activator proteins and nuclear receptors have been shown to interact with basal transcriptional machinery. It has been shown that RXR-RAR heterodimers initiate transcription via interaction with the TATA box-associated ubiquitous transcription factor TFIID. The

interaction is between RAR and TFIID, and is bridged by a further protein, which was shown to have activity analogous to E1A (Berkenstam et al., 1992). A direct interaction between unliganded VDR and TFIIB has also been demonstrated (MacDonald et al., 1995). Further studies using ligand-bound VDR implicated SP-1, AP-1 and Oct-1 transcription factors in VDR transactivation (Liu and Freedman, 1994). Interestingly, in the same study when a VDRE controlling a reporter gene was duplicated, much stronger transactivation was observed, suggesting that numbers of RE may important in regulating VDR mediated transcription. The co-activator, CBP, has been shown to interact with RNA helicase A, which in turn forms a complex with RNA polymerase II (Nakajima et al., 1997), confirming a further link between nuclear receptor, co-activator and transcriptional machinery.

1.5.5. Expression of RXRs in foetal and adult tissue.

The effects of retinoic acid in vertebrate embryonic development have been well documented. RA has been shown to play a key role in limb morphogenesis, formation of the nervous system, and craniofacial development. RXR, and its developmental functions, are evolutionary very old, as the homologue of RXR in *Drosophila*, *usp*, which dimerises with the ecdysone receptor (EcR), is involved in the process of insect metamorphosis (Yao et al., 1993).

The expression of both RAR and RXR has been extensively studied in mouse and chick embryos. Excess amounts of RA given to mouse embryos, leads to abnormalities of development, particularly craniofacial malformation and digit deletion in the limbs (Kochar, 1973). Furthermore, local application of RA to the anterior region of the developing chick limb bud leads to mirror image duplication of the wing (Tickle et al., 1982). Study of murine embryonal RXR expression showed that RXRα and RXRβ are expressed in a wide variety of tissues, including liver, skin, intestine and face. RXRγ was shown to have more restricted

expression, being expressed only in discrete areas of nervous tissue and muscle (Dolle et al., 1994; Mangelsdorf et al., 1992). In recent years, knockout mouse technology has been used to generate RXR and RAR null (-/-) mice. RXRα null mice had thinned myocardium and a defect of the ventricular septum arising from early differentiation of myocytes, and also extensive eye defects, including thickened cornea, and ventral rotation of the lens and a shortened ventral retina (Kastner et al., 1994; Sucov et al., 1994). Double knockouts of RXRα, RARα or RARγ, increased the severity of the eye and heart abnormalities (Kastner et al., 1994). Subsequent studies utilising dominant negative RARs and RXRs on myoblast cell lines, have shown that both RAR-RXR and RXR-RXR dimers are capable of inducing myoblast differentiation, and that RXR-RXR dimers are more efficient at inducing this process (Alric et al., 1997). The defects occurring due to lack of RAR and RXR match some of those found in VAD syndrome, which is caused by a lack of retinol during embryogenesis. Thus, these genetic studies provide further evidence that dietary retinol is the source of RXR and RAR ligand. In other studies, expression of a dominant negative form of RAR in mice inhibited development of skin, by blocking the switch of keratin expression from immature K1 and K14, to mature K10 and K5, thus inhibiting the development of the outer layers of the skin (Saitou et al., 1995).

In adult murine tissues, expression of RXRα is limited to the liver, skin and kidney, expression of RXRγ is limited to muscle and heart tissues, whilst expression of RXRβ is widespread (Mangelsdorf et al., 1992).

1.5.6. Expression of RXR in haemopoietic cells.

RA treatment of myeloid leukaemias, and the subsequent remission of disease, strongly suggests a role of retinoid receptors in overcoming the differentiation block in these cells. As previously described, RA is able to induce differentiation of leukaemic U937 and HL-60 cells (see section

1.1.). However, treatment with RA does not represent a cure as recurrence of the leukaemia will occur up to six months following RA treatment (Warrell et al., 1993). It has been shown that mutant HL-60 cells that are resistant to the differentiation inducing effects of RA, express mutant forms of RARα (Li et al., 1994), and that granulocytic differentiation of wild type HL-60 cells is mediated by RARα (Collins et al., 1990). Transfection of a dominant negative RARα into multipotent haemopoietic progenitors, FDCP mix A4, inhibited the normal differentiation of these cells to a neutrophilic phenotype, and mast cells and basophils were produced (Tsai et al., 1992). The use of retinoid analogues specific for RAR and RXR, has shown that HL-60 neutrophilic differentiation is mediated by RXR-RAR heterodimers, and that only an RAR-specific ligand (TTNPB), and not a RXR-specific ligand (SR11217), was capable of inducing neutrophilic differentiation of HL-60 cells (Dawson et al., 1994).

The majority of acute promyelocytic leukaemias (APL) occur due to a chromosomal translocation of chromosome 15 to 17, t(15;17) (as reviewed by Grignani et al., 1994). This translocation results in a fusion of RARα and PML, which are the genes located at the chromosomal break points. The PML protein is normally situated in distinct areas of the nucleus, known as PML oncogenic domains (POD). PML has been implicated in regulation of transcription (Dyck et al., 1994; Kakizuka et al., 1991). In APL, PML staining is dispersed throughout the nucleus, having formed heterodimers with the PML-RAR fusion protein. After treatment with RA, the PODs are reformed and cells differentiate (Dyck et al., 1994; Weis et al., 1994). Other work has shown that RXR can also heterodimerise with PML-RAR, that RXR PML-RAR dimers repressed transcription from a VDRE, and that RXR PML-RAR dimer could not be detected following RA-treatment (Perez et al., 1993; Weis et al., 1994). These data suggest that APL caused by this translocation is due to the

PML-RAR dimer acting as a dominant negative RAR, and a dominant negative PML.

9-*cis* RA has been shown to inhibit erythroid cell development, by completely inhibiting the formation of burst forming unit-erythroid (BFU-E) in the presence of cytokines which normally lead to erythroid cell development. This inhibition was mediated by both RAR-RXR and RAR-RXR dimers (Rusten et al., 1996).

In contrast to the induction of neutrophilic differentiation of HL-60 cells by RA, DHCC will induce monocytic differentiation of the same cells (see section 1.1.). However, RA potentiates the monocytic differentiation of HL-60, U937 and THP-1 cells induced by DHCC. By using specific ligands, it was shown that this potentiation of differentiation by RA was mediated by RARα-RXR, RXR-RXR and VDR-RXR heterodimers (Defacque et al., 1997). Furthermore, in a recent study, neutrophilic differentiation of HL-60 cells induced by RA resulted in decreased expression of VDR, whilst monocytic differentiation induced by DHCC resulted in decreased expression of RAR, but not RXR (McTernan et al., 1998). The potentiation of DHCC-induced monocytic differentiation by RA could also be due to the fact that, in mice, RXR specific ligands have been shown to induce expression of 24-hydroxylase which acts on 25-hydroxyvitamin D3, to generate DHCC (Zou et al., 1997).

Following six days treatment with 9-*cis* RA, differentiated HL-60 cells will apoptose. Using specific ligands for RAR and RXR, it has been shown that TTNPB (RAR specific), which induces RAR-RXR heterodimerisation mediates differentiation; and that LGD1069, which induces RXR-RXR heterodimerisation mediates apoptosis (Nagy et al., 1995). In HL-60 cells RA has also been shown to up-regulate expression of transglutaminase, a protein that accumulates in nuclei prior to apoptosis (Chiocca et al., 1989). BCL-2 is a protein which has been associated with suppression of

apoptosis, and RARγ has been shown to inhibit expression of BCL-2, thus making cells more prone to apoptosis. Furthermore, BAG-1, another anti-apoptotic protein, has been shown to bind directly to RAR but not to RXR, and to suppress binding of RAR-RXR dimers to RE. This interaction inhibited the RA-induced decrease in BCL-2 expression (Liu et al., 1998).

RAR and RXR have been shown to play a role in T-cell-apoptosis, and it has been suggested that RA may play a crucial role in negative and positive selection of T-cells in the thymus. Activation-induced apoptosis (negative selection) requires the interaction of Fas with Fas-ligand. Treatment with 9-*cis* RA inhibits activation-induced T-cell hybridoma apoptosis by repressing expression of Fas-ligand, via a RE in the Fas-ligand promoter (Brunner et al., 1995). In a more recent study, treatment of mouse CD4+CD8+ thymocytes with 9-*cis* RA or all-*trans* RA induced apoptosis, with 9-*cis* RA being 50 times more effective than all-*trans* RA. Induction of apoptosis was mediated by RARγ, and antagonised by RARα. Addition of RXR-specific ligands induced apoptosis, neutralising the anti-apoptotic effects of RARα, and so it was suggested that *in vivo* formation of 9-*cis* RA may play a role in the default cell death pathway of thymocytes (Szondy et al., 1997).

1.6. U937 derived RXRα transfectants.

The previous sections (1.1. and 1.5.) have summarised the role of RXR as an important regulator of differentiation and development of many foetal and adult tissues, and have examined the mechanisms of how this role is mediated. The importance of RXR in development of haemopoietic cell lineages has been shown by studies of APL and leukaemic cell lines such as HL-60 and U937. The capacity of RXR ligands to induce differentiation of APL cells (see section 1.5.6.), the demonstration that RA is capable of inducing differentiation of HL-60 cells to a neutrophilic lineage (Collins et al., 1990), the potentiation of DHCC induced differentiation of HL-60 cells by RA to a monocytic lineage (Brown et al., 1994), and the ability of DHCC and RA to differentiate U937 cells (James et al., 1997b), prompted further investigation in our laboratory of the role of RXR in monocytic differentiation. This issue was addressed by the transfection of plasmid expression vectors containing human RXRα cDNA, in both sense and antisense orientations, into the human monoblastic U937 cell line. Two clones were derived. These were αG2S, which hyperexpresses RXRα, and αB5A, which hypoexpressed RXRα.

1.6.1. Production of U937-derived RXRα transfectants.

In summary the full length RXRα cDNA (a gift from David Mangelsdorf, Southwestern Medical Centre, Dallas, USA), was cloned into the expression vector pMEP4 (Groger et al., 1989), in either orientation. This yielded two constructs, one with the RXRα cDNA in a sense orientation, and one in an antisense orientation, with respect to the inducible human metallothionein IIa (hMTIIa) promoter (Brown et al., 1997; Brown T.R.P., 1995). These constructs were transfected into U937 cells by electroporation, transfected cells were selected by the addition of 300μg/ml hygromycin B, as the pMEP4 vector encodes a hygromycin B resistance gene, and individual clones obtained by limiting dilution. Of the individual clones isolated, two were selected for further detailed study. The sense clone was designated αG2S and the antisense clone designated

αB5A (Brown et al., 1997; Brown T.R.P., 1995). Another U937-derived cell line, that had been transfected with pMEP4 lacking any insert, was used in these studies as an empty vector control cell line. This cell line, named MEP, had been shown not to differ significantly from the parental U937 cell line, with respect to its growth characteristics, differentiation and expression of cell surface antigens (Hewison et al., 1994).

1.6.2. Characterisation of RXRα expression in selected clones.

Expression of RXRα mRNA in the two chosen clones was assessed by northern hybridisation with a double-stranded DNA probe (Brown et al., 1997; Brown T.R.P., 1995). This showed that expression of RXRα mRNA was increased in sense αG2S cells, compared to both αB5A and MEP cells. Induction of the hMTIIa promoter with cadmium ions, increased levels of RXRα mRNA further in αG2S cells. The expression of functional RXRα protein was assessed by the transient transfection of a construct comprising a luciferase reporter gene, under the control of a DR5 RARE response element, into αG2S, αB5A and MEP cells (Brown et al., 1997; Brown T.R.P., 1995) Addition of 9-*cis* RA to αG2S cells induced a 25-fold increase in luciferase activity, which increased to 80-fold when cadmium ions were added, demonstrating high levels of functional RXRα in αG2S. Addition of 9-*cis* RA to MEP cells induced a small amount of luciferase activity, which represents the basal level of RXR and RAR levels in this cell line, this induction was unaffected by further addition of cadmium. Addition of 9-*cis* RA in isolation or with cadmium to αB5A cells induced similar levels of luciferase activity to those for MEP cells, but this was not surprising as U937 cells also express RXRβ, which can activate the DR5 RARE. Levels of RXRα protein in the transfectants were not directly determined in the thesis by Brown (Brown T.R.P., 1995), and this is the subject of Chapter 3.1.2.

1.6.3. Functional responses of the U937 transfectants to differentiating stimuli.

As shown in section 1.1, differentiation of U937 cells induces a characteristic growth arrest response. Therefore, growth arrest of U937 transfectants mediated by agents known to induce U937 differentiation was assessed (Brown et al., 1997; Brown T.R.P., 1995). The αG2S cell line showed increased sensitivity to growth arrest induced by both all-*trans* RA or 9-*cis* RA, that could not be accounted for by cell death, whilst αB5A cells had complete resistance to the growth arresting properties of all-*trans* RA, 9-*cis* RA and DHCC. However, αB5A cells did cease to proliferate upon the combined addition of DHCC and 9-*cis* RA. TNF-α and PMA inhibited transfectant proliferation approximately equally.

The expression of cell surface antigens on the U937 transfectants that are indicative of a differentiated monocytic phenotype was assessed, both before and after 9-*cis* RA treatment (Brown et al., 1997; Brown T.R.P., 1995). The β2 integrin chains CD11a, CD11b, CD11c and CD18 were all expressed, and an increase in the percentage of all three transfectant cell lines that express CD11b and CD11c was observed upon 9-*cis* RA treatment. There was also an increase in the density of CD11b on 9-*cis* RA-treated αG2S cells. All three transfectant cell lines also expressed the Fcγ receptors CD16, CD32 and CD64, at equal levels both before and after 9-*cis* RA treatment.

1.6.4. Discussion of these findings.

In these experiments, 9-*cis* RA was much more potent at inducing growth arrest in αG2S and MEP cells than all-*trans* RA, confirming the greater potency of 9-*cis* RA, with its ability to activate both RAR and RXR, to induce myeloid differentiation (Sakashita et al., 1993). It is not clear from these data whether the growth arrest was induced by RAR-RXR or RXR-RXR dimers, although HL-60 differentiation has been shown to be mediated by RAR-RXR dimers (Nagy et al., 1995). The ability of 9-*cis*

RA to induce more profound growth arrest than all-*trans* RA is indicative of the importance of ligand binding by RXR in this process, as presumably all-*trans* RA-liganded RAR-RXR heterodimers bind the same response elements as 9-*cis* RA-liganded RAR-RXR but have less effect. However, αG2S cells did not show an increased sensitivity to the growth inhibitory effects of DHCC, possibly because levels of VDR expressed in the cells may be limiting.

In contrast, the αB5A cell line has a much reduced sensitivity to the growth arresting properties of 9-*cis* RA, all-*trans* RA and DHCC. This suggests that the growth inhibitory effects of these agents were mediated by RXRα, which signals via RXRα-RXR, RAR-RXRα and RXRα-VDR dimers respectively. These data suggest that RXRβ, which is expressed in these cells, does not participate in signalling growth arrest. However, αB5A did respond to the anti-proliferative effects of combined 9-*cis* RA and DHCC treatment, suggesting that RXRβ that has bound its ligand, can interact with liganded VDR to induce growth arrest. Another possibility is that the combined addition of RA and DHCC induced increased the expression of RXRα in U937 cells (Defacque et al., 1994), and that the RXRα antisense mRNA expressed in αB5A cells is insufficient to inhibit this increase in RXRα mRNA.

All three transfectant cell lines responded equally to the growth inhibitory effects of PMA and TNF-α, indicating that growth arrest mediated by these agents is RXRα independent.

The β2 integrin chains, CD11b and CD11c, were expressed on a higher percentage of all three cell lines upon 9-*cis* RA treatment, and with an increased density of CD11b on αG2S cells. This shows that increase in levels of these β2 integrin chains is RXR dependent and, as this increase is not inhibited in αB5A cells, that the response can be mediated by RXRα or RXRβ.

In summary, the generation of U937 transfectants that differentially express RXRα, has provided a useful model for investigating monoblast differentiation, especially regarding the role of RXRα in this process.

1.7. Aims.

The experimental aims of this thesis fall into two parts. In the first part, the role of RXRα in normal monocyte development was confirmed, by assessing expression of RXRα and some of its dimeric nuclear receptor partners in peripheral blood monocytes after addition of differentiating stimuli (Chapter 3). The level of expression of RXRα was characterised, as well as that of some of its dimeric partners, in the U937 transfectants (Chapter 3). Extensive phenotyping of cell surface antigen expression was also assessed on 9-*cis* RA-treated U937 transfectants (Chapter 3). Finally the ability of the U937 transfectants to immunophagocytose opsonised-SRBC was examined (Chapter 3), and the phosphotyrosine signalling responses of the U937 transfectants to immunophagocytosis was investigated (Chapters 3 and 4).

The aims of the second part of the thesis were to examine the role of the U937 cell line as an accessory cell in T-cell co-stimulation in a CD3 mAb dependent T-cell proliferation assay (Chapter 5). To test CD11a/18 and CD54 mAbs, and extensive panels of mAbs from the 6th Human Leukocyte Differentiation Workshop (6th HLDA) for effects on T-cell proliferation in this assay, in an attempt to identify novel co-stimulatory molecules (Chapter 5), and to investigate the mechanism of action of any novel co-stimulatory molecules identified (Chapter 5). To examine which T-cell subsets are co-stimulated by U937 cells (Chapter 5). These studies formed the basis for an investigation of the capability of the RXRα U937 transfectants to co-stimulate T-cells in the same assay (Chapter 6).

Chapter 2

Materials and Methods

2.1. Isolation, culture, and differentiation of human peripheral blood monocytes.

Peripheral blood (60 or 120 mls) was obtained by venesection from normal, healthy volunteers using a 19/21g butterfly into a heparinised (100U/ml) syringe. Blood was diluted 1:3 into phosphate buffered saline (PBS) containing 2.2mM EDTA. 30ml of diluted blood were layered over 17.5ml Lymphoprep 1077 density medium (Nycomed, Oslo, Norway) and centrifuged for 30 mins at 600 g (brake off) at room temperature to separate leukocytes from erythrocytes. The interface over the Lymphoprep was harvested and diluted 1:2 with Hanks buffered saline solution (HBSS). Cells were washed three times in HBSS. Monocytes were obtained by a 2 hour plastic adherence step. Following this the plate was agitated gently and the supernatant removed and replaced with 3ml of RPMI 1640 complete medium (CM) (Gibco, Paisley, UK), comprising of RPMI 1640 supplemented with 10% fetal calf serum, 2mM L-glutamine, 100 U penicillin/streptomycin and 20 μM β-mercaptoethanol.

To further purify the monocyte population, lymphocytes were immunomagnetically depleted, using CD3 (UCHT 1, final concentration 2μg/ml), CD2 (final concentration 2μg/ml) and CD19 (BU12, supernatant dilution 1:10) monoclonal antibodies (mAbs) were added to deplete T- (CD3 and CD2) and B-cells (CD19). Cells were incubated in the presence of these mAbs for 45 mins on ice, with occasional agitation. After 45 mins cells were washed twice in ice cold HBSS and then resuspended in 2ml ice cold complete medium. 10μl of immunomagnetic beads (Dynal M-450 sheep anti-mouse Ig coated beads, Dynal, Olso, Norway) were added per 1 x 10^6 cells to be depleted. Beads and cells were incubated

together for 45 mins at 4°C on a rotator to allowing binding of beads to antibody coated cells. Beads were removed by placing on a magnetic depeletor for 10 mins, supernatant was then transferred to a fresh tube and placed on the magnet for 10 mins. The final supernatant contained purified monocytes.

Monocytes were treated in serum free conditions with either 10^7 M 1,25-dihydroxycholecalciferol (DHCC), for 1 or 7 days, or with 2% human AB sera. Monocytes were also treated in 10% FCS with 300ng human recombinant granulocyte monocyte-colony stimulating factor (GM-CSF, Schering Plough, France), 150ng human recombinant interleukin-4 (IL-4, Schering Plough, France) and 150ng human recombinant tumour necrosis factor-α (TNF-α, Schering Plough, France) for one or seven days. Treated cells were spun and lysed in 500µl of a 1% (v/v) NP40 lysis buffer, comprising 150mM NaCl, 1% NP40, 50mM Tris-HCl pH8.0, 1mM sodium orthovanadate, 2mM hydrogen peroxide, 1mM PMSF, 10µg/ml Aprotinin (all from Sigma, Poole, UK.).

2.2. Culture of cell lines.

Stably transfected U937 transfectant cell lines αG2S, αB5A, and MEP were grown in CM with the addition of 15µg/ml Hygromycin B (Calbiochem, Nottingham, UK). Cells were kept in continuous culture and split 1 in 5 with fresh CM twice weekly. For experiments cells were split 1 in 3 with fresh CM, allowed to grow for 48 hours and then cultured in the presence of 1µM 9 cis RA, or 500nM DHCC for a further 24 hours. If expression of the transfected gene was required 20µM $CdCl_2$ was added for 24 hours.

2.3 Preparation of U937 transfectant cell lysates.

Cells were counted and $5x10^6$ cells spun at 1500rpm for 7 minutes. Cell pellets were then dried and lysed in 200µl of a 1% (v/v) NP40 lysis buffer, comprising 150mM NaCl, 1% NP40, 50mM Tris-HCl pH8.0,

1mM sodium orthovanadate, 2mM hydrogen peroxide, 1mM PMSF, 10μg/ml Aprotinin (all from Sigma, Poole, UK.). Lysates were left on ice for 20 minutes, and then either processed immediately for immunoblotting, or stored at -80°C. Cell lysates were clarified by being spun at 15,000 rpm for 10 minutes at 4°C. In some experiments cells were lysed in 200μl of 2X SDS denaturing loading buffer consisting of 2% (w/v) SDS lysis buffer, comprising, 50mM Tris pH 6.8, 20% (v/v) glycerol, 10% (w/v) SDS, 10% (v/v) β-mercaptoethanol, 0.05% (w/v) bromophenol blue (all Sigma, Poole, UK.), which lyses the whole cell including the nucleus.

2.4. Immunoblotting.

Aliquots of the clarified cell lysate were boiled in 2X SDS denaturing loading buffer, for 4-5 minutes. Boiled lysates were electrophoresed on 10% (w/v) or 15% (w/v) polyacrylamide gels (Protogel, National Diagnostics, Georgia, USA.), and separated proteins were electro-blotted on to nitrocellulose filters (Hybond-ECL, Amersham Int, U.K) overnight (40mA), or for three hours (250mA). Filters were blocked with PBS containing 3% (w/v) BSA (Sigma, Poole, U.K.) for 2-3 hours, and then probed with a primary antibody (Ab) for 1 to 16 hours, depending on the Ab used (see Table 2.4), in PBS containing 3% (w/v) BSA and 0.1% (v/v) Tween 20 (Sigma, Poole, U.K.). The filters were washed three times in PBS containing 3% (w/v) BSA and 0.1% (v/v) Tween 20, and a 1 in 2000 dilution of either an HRP conjugated rabbit anti-mouse or a swine anti-rabbit secondary Ab (both DAKO, Dakopatts, High Wycombe, UK.) was added for 1 hour, in PBS containing 3% (w/v) BSA and 0.1% (v/v) Tween 20. Three final washes were performed with PBS containing 0.1% (v/v) Tween 20. Results were obtained by incubating the filters with Enhanced Chemiluminescence (ECL) fluid (Amersham Int, U.K) for 1 minute, as per manufacturers instructions, and visualising the bands on X ray film (Kodak X-OMAT-AR, Amersham Int, U.K.)

Table 2.4. Antibodies used in immunoblotting.

Ab name or catalogue #	Specificity	Dilution	Time hours	Species	Originator
	Actin	0.5µg/ml	1	Mouse	
D-20	RXRα	0.4µg/ml	2	Rabbit	Santa Cruz (Insight, London, U.K.)
C-20	RARα	0.4µg/ml	2	Rabbit	Santa Cruz (Insight, London, U.K.)
C-19	RARβ	0.4µg/ml	2	Rabbit	Santa Cruz (Insight, London, U.K.)
4G10	p-Tyr	0.25µg/ml	1	Mouse	UBI (TCS, Botolph Claydon, U.K.)
9105S	ERK 1/ERK 2	1/2000	1	Mouse	NEB (Hitchin, U.K.)
C-17-G	jnk	1/2000	1	Rabbit	Santa Cruz (Insight, London, U.K.)
G-7	phospho-jnk	1/2000	16	mouse	Santa Cruz (Insight, London, U.K.)
9211	p38	1/2000	3	Rabbit	NEB (Hitchin, U.K.)
9211S	phospho-p38	1/2000	3	Rabbit	NEB (Hitchin, U.K.)
P13520	paxillin	1/5000	3	Mouse	Transduction labs (Lexington USA)
	p47-phox	1/2000	2	Rabbit	Prof A. Segal. (UCL, London, U.K.)
	p67-phox	1/2000	2	Rabbit	Prof A. Segal. (UCL, London, U.K.)
S14620	shc	1/5000	2	Mouse	Transduction labs (Lexington USA)

Abs were stripped from the filters with stripping buffer (62.5mM Tris-HCl pH 6.7, 2% (w/v) SDS and 0.7% 2-mercaptoethanol, all from Sigma, Poole, U.K.) at 56°C for 30 minutes. Filters were washed thoroughly five times in PBS containing 0.1% (v/v) Tween 20. The filters were then incubated in an identical way with an actin mAb (DAKO, Dakopatts, High Wycombe, UK.), as a control for protein loading in each lane.

2.5. Phenotypic analysis.

Flow cytometry was carried out to analyse cell surface protein expression. 10^5 cells in 100µl of CM were plated out in round-bottomed 96 well plates (NUNC, Roskilde, Denmark), and spun at 1500 rpm, for 5 minutes at 4 °C. The supernatant was removed, and cells resuspended in 50µl 10% (v/v) normal rabbit serum (10% NRS) in Hanks balanced salt solution (HBSS), (Gibco, Paisley, UK). After 15 minutes on ice, the primary mAb was added and cells left on ice for 45 minutes (see appendix I for all mAbs used in this study). Cells were spun as before and washed 3 times in 100µl 10% NRS in HBSS. 50µl of a 1/20 dilution of FITC-conjugated rabbit anti-mouse IgG secondary antibody (DAKO, Dakopatts, High Wycombe UK.) in 10% NRS in HBSS was added for 45 minutes. Cells were then washed 3 times in 10% NRS in HBSS, before cells were fixed in 50µl of 3.7% paraformaldehyde in PBS, and 100µl of HBSS added. Plates were stored at 4°C in the dark for up to a week and then examined by FACS (Becton Dickinson, U.K.), and the results analysed using WinMDI software (Hewlett Packard).

2.6. Preparation of opsonised Sheep Red Blood Cells (op-SRBC).

2ml of SRBC (TCS, Botolph Claydon. U.K.) were washed twice with ice-cold HBSS (Gibco, Paisley, UK) to remove lysed cells, counted and diluted to 10^9 SRBC in 1ml HBSS. A 1/200 dilution of rabbit anti-SRBC polyclonal Ab (Cappell, ICN, High Wycombe, UK.) was added for 1 hour

at 37°C. The op-SRBC were then washed three times with ice cold HBSS to remove excess Ab, and the final pellet resuspended in 1ml HBSS.

2.7. Radiolabelling of op-SRBC.

The same procedure that produced op-SRBC (section 2.6.) was used, but with 50μCi (25μl) of sodium ^{51}chromate (ICN, High Wycombe, UK) added in addition to the anti-SRBC Ab. Incubation was performed in a shaking water bath for 2 hours at 37°C. ^{51}Chromate labelled op-SRBC (^{51}Cr-op-SRBC) were then washed three times with ice cold HBSS to remove excess Ab and radioactivity, and the final pellet resuspended in 1ml HBSS. For control experiments, unopsonised SRBC were labelled with sodium ^{51}chromate only, in the same way.

2.8. Assessment of immunophagocytosis.

Immunophagocytosis by the U937 transfectants was assessed by **(i)** the size of the complexes formed between these and the op-SRBC as observed by microscopy (X40 magnification) after 2 hours of culture; and **(ii)** the amount of radioisotope taken up when ^{51}Cr-op-SRBC were used in the phagocytosis assay. In the latter experiments, $2x10^6$ cells, in 2ml CM, in triplicate wells were cultured with 40μl of the pre-prepared op-SRBC to give a ratio of 1 transfectant cell : 20 op-SRBC for 2 hours. Cells were washed once in ice-cold HBSS, non-immunophagocytosed ^{51}Cr-op-SRBC were lysed with 500μl of water, and pellets washed twice more in ice cold HBSS to remove any unincorporated radioactivity. Radioactivity in the cell pellets was measured using a gamma counter.

2.9. Morphological analysis of immunophagocytosis.

U937 transfectants were counted and diluted to $2x10^6$ cells per 2ml of CM. 40μl of the pre-prepared op-SRBC ($4x10^7$ cells) were added and cultured for two hours. The effect of immunophagocytosis on cell morphology was assessed by staining the cells for actin. Cells exposed to op-SRBC were fixed and stained by incubating in 3.7% formaldehyde,

100µg/ml lysophosphatidylcholine (Sigma, Poole, UK), and 5µg/ml TRITC-labelled phalloidin (Sigma, Poole, UK) in PBS for 15 minutes on ice. Cell pellets were washed and mounted on poly-L-lysine (Sigma, Poole, UK.)-coated cover slips. Results were monitored by confocal fluorescence microscopy (BIO RAD, UK.).

2.10. Regulation of immunophagocytosis by cell surface molecules.

To investigate molecules involved in immunophagocytosis, 10^7 U937 transfectants were incubated with saturating levels, dilutions of 1/50, of a range of mAbs for 1 hour at 4°C (see appendix II). Cells were washed twice to remove unbound mAb. The ability of these antibody-bound cells to immunophagocytose ^{51}Cr-op-SRBC was assessed in an identical fashion using the quantitative assay described previously in section 2.8.

2.11. Phosphotyrosine assays.

U937 transfectants were counted and diluted to $2x10^6$ cells per 2ml of CM. 40µl of pre-prepared op-SRBC ($4x10^7$ cells) were added to each to give a ratio of 1 transfectant cell:20 op-SRBC. The transfectants and op-SRBC were co-cultured for a wide range of time points varying from 1 minute to 2 hours. These cells washed once in ice cold HBSS containing 1mM sodium orthovanadate (Sigma, Poole, U.K.) and 2mM hydrogen peroxide (Sigma, Poole, U.K.) as phosphatase inhibitors. Unbound op-SRBC were lysed by the addition of 500µl of ice cold water to the pellet. The pellet was washed once more in ice-cold HBSS containing phosphatase inhibitors. Pellets were dried thoroughly and lysed in 100µl of a 1% NP40 lysis buffer (see section 2.3.). Lysates were left on ice for 20 minutes, and then either processed immediately for immunoblotting, or stored at -80°C. Cell lysates were clarified by being spun at 15,000 rpm for 10 minutes at 4 °C.

2.12. Effects of binding inhibitory mAbs to the phosphotyrosine response to op-SRBC.

$5x10^6$ transfected U937 cells were incubated with saturating levels, dilutions of 1/50, of CD13, CD16, CD18, CD32, and CD64 mAbs for 1 hour at 4°C. Cells were washed twice to remove unbound mAb. Following this phosphotyrosine assays as described in section 2.11. were carried out.

2.13. Immunoprecipitations (IP).

$6x10^6$ transfected U937 cells in 2ml CM were co-cultured with 100µl of op-SRBC for 0 or 10 minutes. Cells were washed once in ice-cold HBSS, containing 1mM sodium orthovanadate (Sigma, Poole, U.K.), and 2mM hydrogen peroxide (Sigma, Poole, U.K.) as phosphatase inhibitors. Unbound op-SRBC were lysed by the addition of 1ml of ice cold water to the pellet. The pellet was washed once more in ice cold
HBSS containing phosphatase inhibitors. Pellets were dried thoroughly and lysed in 200µl of a 1% NP40 lysis buffer (see 2.3.) containing 5% glycerol (Sigma, Poole, U.K.). Lysates were left on ice for 20 minutes, and spun at 15,000 rpm for 10 minutes at 4°C. 150µl of each supernatant were incubated with 6µg of 4G10 anti-phosphotyrosine mAb for 2-3 hours at 4°C on a rotator, and then with 50µl of Protein A sepharose (Sigma, Poole, U.K.) for a further 2 hours at 4°C on a rotator. The beads were washed 5 times in ice cold lysis buffer, 50µl of 2X SDS denaturing loading buffer added, and samples boiled for 4-5 minutes before being electrophoresed.

2.14. Isolation of glutathione-SH2 fusion proteins.

XL2 bacteria were transformed with plasmids encoding GST-SH2 fusion proteins (kind gifts of Dr D Smith, University of Cambridge), by a standard heat shock protocol (Sambrook, 1989), and stored as glycerol stocks at -80°C. 15 ml cultures of the bacteria were set up overnight, and transferred to 300ml of 2XTY media the next morning. The cells were allowed to grow to an OD_{600} of 0.6 - 0.8, the end of log phase growth, and

fusion protein production induced by the addition of 1mM IPTG (Sigma, Poole, U.K.). The cultures were allowed to grow for 4 hours. To isolate fusion proteins cells were lysed by sonication and the supernatant incubated with 150µl of glutathione bound agarose (Sigma, Poole, U.K.) for 1 hour. The agarose pellet was washed 5 times with lysis buffer, and fusion protein concentration assessed visually by Coomasie blue R250 (Sigma, Poole, U.K.) staining of electrophoresed isolated GST-SH2 proteins. Figure 2.14 shows an example of fusion proteins ran alongside lysates from induced transformed XL2 bacteria.

2.15. Glutathione-SH2 fusion protein assays.

Cell lysates for incubation with glutathione fusion protein constructs were prepared in the same way as for immunoprecipitation, except samples were lysed in a 1% Triton X-100 buffer, comprising 50mM Hepes pH 7.5, 150mM NaCl, 10% (v/v) glycerol, 1% (v/v) Triton X-100, 1.5mM magnesium chloride, 1mM EGTA, 100mM sodium fluoride, 10mM sodium pyrophosphate, 1mM sodium orthovanadate, 1mM PMSF, 1mM benzamidine, 10µg/ml Aprotinin (all from Sigma, Poole, U.K.). 50µl of each lysate were incubated with 20µl of GST-SH2 fusion-protein loaded glutathione-bound agarose (10-20µg) (see section 2.13.) for 2 hours at 4°C. The agarose pellet was then washed four times in lysis buffer, 20µl of 2X SDS denaturing loading buffer added, and samples boiled for 4-5 minutes. 10µl of each sample were run on a 10% polyacrylamide gel, and anti-phosphotyrosine immunoblotting performed as before.

Figure 2.14.

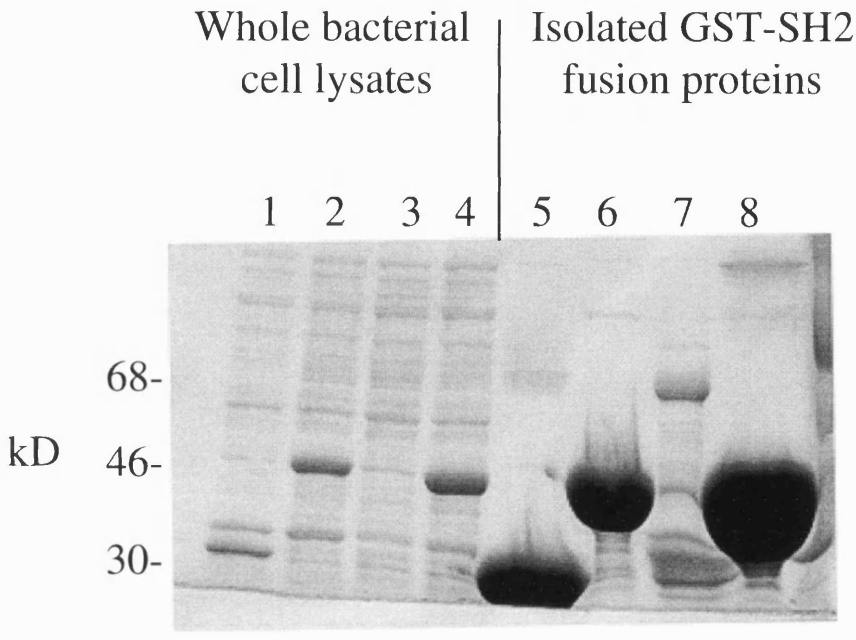

Figure 2.14. Expression of GST-SH2 fusion proteins in XL2 blue cells.
Transformed XL2 blue bacteria were grown from fresh stocks, production of fusion protein induced by the addition of IPTG, and bacteria allowed to grow for 4 hours. Bacteria were then harvested and lysed by sonication. Lanes 1-4 on the gel show these lysates. Fusion proteins were isolated from lysates by addition of glutathione bound agarose, lanes 5-8 on the gel show these isolated GST-SH2 fusion proteins (see section 2.14.). Lanes 1 and 5 show expression and isolation of GST empty vector fusion protein; lanes 2 and 6, GST-Shc-SH2 fusion protein; lanes 3 and 7, GST-Shc-PTB fusion protein; and lanes 4 and 8, GST-Src-SH2 fusion protein.

2.16. Isolation of T-cells.

Human tonsils (from routine tonsillectomies, Royal National Throat Nose and Ear Hospital, London, U.K.) were used as a source of T-cells. Tonsils were cut into small pieces with a scalpel, digested with 1mg/ml collagenase (Sigma, Poole, UK.) for 90 minutes at 37°C and then pushed through a 125mm pore size nylon mesh (Cadisch, London, UK.) to separate lymphomedullary cells from surrounding connective tissue. The remaining cells were separated by centrifugation through a five step iso-osmolar Percoll gradient (Pharmacia, Milton Keynes, UK) at 600 x g for 30 minutes. The high density cell populations (50-70% Percoll) were further depleted of monocytes by the removal of adherent cells, and depleted of B cells by immunomagnetic beads (anti-mouse IgG Dynabeads, Dynal, Norway) using CD19 (BU12) and MHC class II (L243) (both gifts of D. Hardie, University of Birmingham, Birmingham, U.K.) as primary reagents. To further purify the T-cells into CD8+ and CD4+ sub populations, either a CD4 mAb (QS4120) or a CD8 mAb (UCHT4) (both gifts of Dr Diana Wallace, ICRF Human Tumour Immunology Unit, London, U.K.) was added before the immunomagnetic bead depletion step.

2.17. U937/CD3 - T-cell proliferation assay.

X-irradiated U937 cells, T-cells, and CD3 mAb (UCHT1, Harlan-Sera Lab, Loughborough UK.) at various concentrations; were plated in triplicate in flat-bottomed 96 well plates (NUNC, Roskilde, Denmark.). After 48 hours of culture, U937/T-cell cluster formation was assessed by microscopy (X40 magnification), and T-cell proliferation was assessed by measuring incorporation of radiolabelled thymidine (^{3}H Thymidine) (ICN Biomedical, High Wycombe UK.) over 16 hours. The labelled cells were harvested on to filters and counted on a scintillation counter (Wallac U.K.).

2.18. Addition of mAbs to the U937/CD3-T-cell proliferation assay.

Dilutions of test mAbs (see appendix III) were added to 10^4 irradiated U937 cells, $2x10^5$ tonsillar T-cells, and 0.1µg/ml of CD3 mAb (UCHT1) in triplicate wells of a 96 well plate. T-cell proliferation was assessed between 48 and 64 hours of culture by the incorporation of ^3H Thymidine (ICN Biomedical, High Wycombe, UK.). The labelled cells were harvested on to filters and counted on a scintillation counter (Wallac, Milton Keynes, U.K.).

2.19. Cell viability studies.

For cell viability studies the assay was set up in an identical way to the co-stimulation assay (see section 2.22.), but in duplicate. Cells were harvested at 24 hours of culture without isotope and viability assessed by trypan blue dye exclusion (Gibco, Paisley, UK). Viable cells were counted using a haemocytometer. Any mAb which caused a large decrease in cell number compared to a no mAb control was considered to have a potential cytotoxic effect on the assay.

2.20. Pre-incubation of U937 cells with inhibitory antibodies.

To examine the role of any inhibitory mAb further, $2x10^5$ irradiated U937 cells were pre-plated in a U-bottomed 96 well plate, mAbs added and cells incubated for 1 hour at 37°C. The cells were then washed in complete media twice to remove excess mAb. Cell numbers were counted and 10^4 irradiated, mAb-coated U937 cells were included in the same assay system as before. As an internal control, proliferation of the irradiated, mAb-coated U937 cells was assessed by tritiated thymidine incorporation.

2.21. Activation of T-cells with PMA and ionomycin.

An alternative accessory cell CD3 independent T-cell proliferation assay was set up using a combination of phorbol 12-myristate 13- acetate

(PMA) and ionomycin to initiate T-cell activation. 25ng/ml of PMA and 4μg/ml of ionomycin were added to $2x10^5$ isolated T-cells per well of a 96 well plate, and dilutions of inhibitory mAbs added to triplicate wells. T-cell proliferation was assessed as previously by measuring incorporation of radiolabelled thymidine (^3H Thymidine) (ICN Biomedical, High Wycombe UK.) into the cells between 48 and 64 hours of culture.

2.22. Phosphotyrosine studies on the effects of inhibitory mAbs on U937 and T-cells.

1/100 dilutions of selected mAbs were cultured with $2x10^6$ U937 cells, or $4x10^6$ purified T-cells for 10 or 60 minutes in CM at 37°C. Cells were washed once in ice-cold HBSS and lysed in 1% NP40 lysis buffer (see section 2.3.) on ice for 20 minutes, and then either processed immediately for immunoblotting, or stored at -80°C. Cell lysates were clarified by being spun at 15,000 rpm for 10 minutes at 4 °C. Anti-phosphotyrosine immunoblotting was then performed on these lysates (see section 2.4.).

2.23. Proliferation assays with irradiated U937 transfectants.

10^7 transfected U937 cells in 20ml HBSS were exposed to **(i)** various amounts of radiation from an X-ray generator (General Electric, Ohio, USA.), or **(ii)** differing amounts of ultra violet (UV) light from a UV lamp (UVP, California, USA.). Post - irradiated viable cells were separated from non - viable cells over Ficoll-Hypaque (Sigma, Poole, U.K.) (density 1.077). Cells were washed twice in HBSS and counted, $2x10^4$ cells were cultured in 200μl of CM, and proliferation assessed between 48 and 64 hours of culture by the incorporation of ^3H Thymidine (ICN Biomedical, High Wycombe UK.). The assay was harvested on to filters and counted on a scintillation counter (Wallac, Milton Keynes, U.K.).

2.24. Apoptosis of irradiated U937 transfectants.

10^7 transfected U937 cells in 20ml HBSS were exposed to 4000 rads from an X-ray generator (General Electric, Ohio, USA). The post-X-irradiated viable cells were separated from non-viable cells over Ficoll-Hypaque (Sigma, Poole, U.K.) (density 1.077). Cells were recultured in 10ml CM for a further 24 hours. $3x10^6$ cells from each sample were fixed in freshly prepared 4% paraformaldehyde (w/v) for 20 minutes at RT, followed by three washes with PBS. Fixed cells were permeabilised in 0.1% Triton X100 in a 0.1% sodium citrate solution on ice for 2 minutes. The cells were then attached to poly-l-lysine coated cover slips and incubated with TdT-mediated dUTP nick end labelling (TUNEL) reaction mixture (Boehringer Mannheim, Germany), for 60 mins at 37 °C. Coverslips were then washed 3 times in PBS, 50µg/ml of propidium iodide solution added and cells viewed on a confocal microscope (BIO-RAD, UK).

2.25. Cell cycle analysis of irradiated U937 transfectants.

10^7 transfected U937 cells in 20ml HBSS were exposed to 4000 rads from an X-ray generator (General Electric, Ohio, USA). The post-irradiated viable cells were separated from non-viable cells over Ficoll-Hypaque (Sigma, Poole, U.K.) (density 1.077). Cells were recultured in 10ml CM for a further 24 hours. $5x10^6$ cells from each sample were fixed in ice cold 100% ethanol for 30 minutes on ice, then washed twice in ice cold HBSS. Fixed cells were then treated with 0.2µg/ml of RNase 1 (Sigma, Poole, U.K.) for 30 minutes at 37 °C. 50µg/ml of propidium iodide solution were added one minute prior to FACS analysis (Becton Dickinson), and results were analysed using WinMDI software (Hewlett Packard).

2.26. U937 transfectant CD3-dependent T-cell proliferation assays.

Transfected U937 cells, were counted and 10µg of mitomycin C (Sigma, Poole, U.K.) per 10^6 cells were added and cells left overnight. In some

experiments, immunophagocytosis was performed prior to the addition of mitomycin C. For this, cells were diluted to $1x10^7$ in 10ml of CM. The culture was split in two and op-SRBC added to only half of the culture for two hours. Excess op-SRBC were removed in the same way as previously shown, and cells recultured in 5ml of new CM. Cells were counted again and then mitomycin C added and cells left overnight. The next morning cells were washed 5 times in HBSS. To 10^4 of each cell line, were added, $2x10^5$ tonsillar T-cells and 0.1μg/ml of a CD3 mAb (UCHT1, Harlan Sera Lab, Loughborough, UK). T-cell proliferation was assessed between 48 and 64 hours of culture by the incorporation of ^3H Thymidine (ICN Biomedical, High Wycombe UK.). The cells were harvested on to filters and counted on a scintillation counter (Wallac, Milton Keynes, U.K.).

Chapter 3

3.1. Results.

The role of RXRα in U937 differentiation and activation; effects of differential expression of RXRα in U937 derived cell lines on the efficiency of immunophagocytosis.

As discussed in Chapter 1., the U937 cell line is a monoblastic leukaemia cell line that is committed to monocyte differentiation and has proved a valuable *in vitro* tool for studying aspects of this differentiation step (Sundstrom and Nillson, 1976). Treatment of U937 with agents such as RA, DHCC, tumour necrosis factor-α (TNF-α), and phorbol 12-myristate 13-acetate (PMA) induces the appearance of characteristics consistent with a mature monocyte/macrophage (Harris and Ralph, 1985; Sellmayer et al., 1994; Testa et al., 1993). These characteristics include growth arrest, up-regulated expression of cell surface adhesion receptors, production of lysozyme and superoxide radicals, and the potential to phagocytose.

Previously in our laboratory (Brown et al., 1997; Brown T.R.P., 1995), it has been demonstrated that induction of U937 cell differentiation by treatment with PMA for twenty four hours led to an increase in RXRα mRNA production, suggesting a role for RXRα in U937 differentiation. U937 stable cell transfectants were then generated, in which expression of sense RXRα RNA or antisense RXRα mRNA was placed under the control of an inducible metallothionein IIa gene promoter (Brown et al., 1997; Brown T.R.P., 1995). The sense (αG2S) cell line was shown to overexpress RXRα mRNA, and to have higher levels of functional RXRα protein as measured by the increased ability of αG2S cells to activate a transiently transfected luciferase reporter gene controlled by a DR-5 retinoic acid response element. The αG2S cell line had increased sensitivity to both all-*trans* RA and 9-*cis* RA, as demonstrated by growth

inhibition. The antisense (αB5A) cell line had decreased levels of functional RXRα protein, as measured by the reporter gene assay, had reduced sensitivity to both all-*trans* RA and 9-*cis* RA and did not respond to DHCC, as demonstrated by a lack of growth inhibition. In addition, αG2S cells exhibited increased expression of the integrin CD11b. These results indicated that RXRα has a role in mediating growth inhibition and cell adhesion during myelomonocytic differentiation, and suggested that different species of RXRα heterodimers may control different features of mature monocyte/macrophage function.

In the first part of this study, the objective was to examine the levels of RXRα protein, and some of its dimerisation partners, in monocytes and macrophages separated from peripheral blood, both before and after treatment with various differentiating stimuli.

In parallel, the phenotype of the stably transfected U937 transfectants was confirmed by investigating more directly the level of expression of RXRα protein in the αG2S, αB5A and MEP empty vector control cell lines, both before and after induction of the metallothionein promoter by addition of cadmium ions. The expression of RARα and RARβ was also assessed in these cells.

The phenotype of U937 transfectants was investigated by FACS analysis of cell surface markers, using mAbs from the myeloid panel of the 6th Human Leukocyte Differentiation Workshop (6th HLDA), as well as other mAbs directed against other myeloid markers.

To further investigate these cell lines, immunophagocytosis, a primary function of monocyte/macrophages, was investigated in the U937 transfectants. Furthermore, immunophagocytosis was correlated with analysis of expression of p47-phox, a protein involved in the production of superoxide radicals (Roos et al., 1996), and with any differences in

pattern and intensity of the phosphotyrosine response to immunophagocytic stimulus. Finally, the nature of the cell surface molecules involved in immunophagocytosis in these cell lines was investigated.

3.1.1. Expression of RXRα, RARα, and RARβ, in peripheral blood monocytes during differentiation.

Monocytes were purified from peripheral blood from the same person on two separate occasions and cells treated with differentiation-inducing stimuli for either one or seven days. Cells were lysed and levels of protein expression determined by immunoblotting. Figure 3.1.1. shows the levels of RXRα, RARα, RARβ and actin (which acted as a control for relative amounts of protein in each sample) found in these monocytes from two separate experiments. These results show that RXRα was expressed in peripheral monocytes (lanes 1 and 8), and that expression of RXRα was increased upon treatment of human AB serum in both experiments for 1 (lanes 3 and 11), and 7 days (lanes 6 and 12). The addition of IL-4, GM-CSF and TNFα for 1 or 7 days did not induce increased expression of RXRα, but the protein was still expressed (1 day-lanes 4 and 10; 7 days-lanes 5 and 13). Interestingly, the level of expression of RXRα was reduced, in three of four samples, following addition of DHCC for 1 or 7 days (1 day-lanes 2 and 9; 7 days-lanes 7 and 14). RARα was expressed in monocytes and upon differentiation of these cells, but the levels of expression were not influenced by any of the agents tested. RARβ was also expressed at a much lower level, and its expression was not influenced by any of the agents tested. In some lanes more than one band was seen, suggesting different protein conformations, or perhaps the presence of multiple protein species. Table 3.1.1. shows the relative amounts of protein expressed in each lane, normalised for the amount of protein loaded in each lane, as measured by the level of actin in each lane (see bottom panel of Figure 3.1.1.).

Figure 3.1.1.

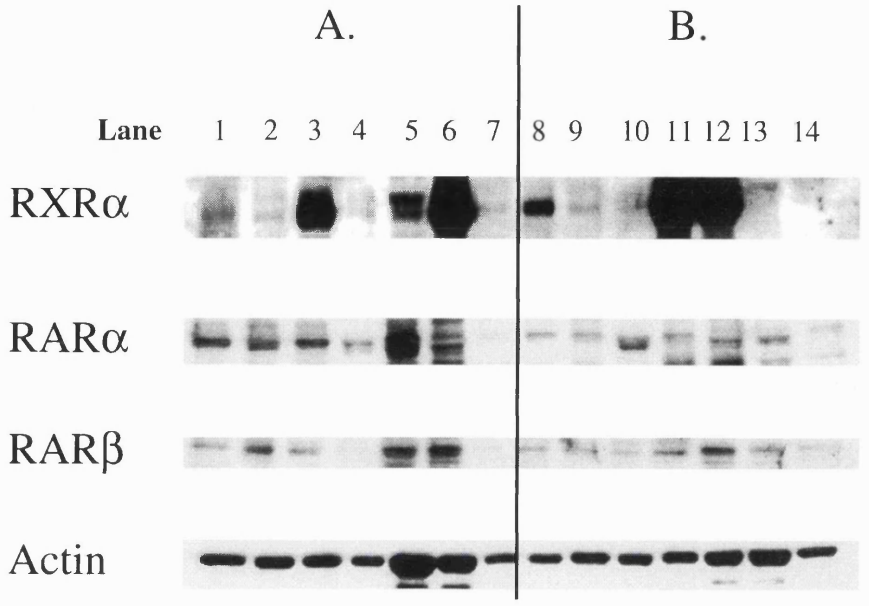

Figure 3.1.1. Expression of RXRα, RARα, and RARβ in peripheral blood monocytes during differentiation.

Monocytes were isolated from peripheral blood (see section 2.1.) taken from the same volunteer on two separate occasions (experiment A = lanes 1-7; experiment B = lanes 8-14). Untreated day 0 monocytes are located in lanes 1 and 8. Monocytes were cultured in the presence of either DHCC for 1 day (lanes 2 and 9), or for 7 days (lanes 7 and 14); with 2% human AB serum for 1 day (lanes 3 and 11), or for 7 days (lanes 7 and12); with IL4, GM-CSF, and TNFα for 1 day (lanes 4 and 10), or for 7 days (lanes 5 and 13). Lysates were run on SDS-polyacrylamide gels, and expression levels determined by immunoblotting (see section 2.4.) The filter used for the RXRα blot was stripped and incubated for expression of actin, to act as a control for protein levels in each lane (lower panel). A seperate filter, but with the same amount of protein loaded, was used for assessing RARα and RARβ expression.

Table 3.1.1.

Experiment A							
Lane	1	2	3	4	5	6	7
Day	0	1	1	1	7	7	7
Treatment	-	DHCC	AB sera	cytokine	cytokine	AB sera	DHCC
RXRα	1.71	0.63	2.78	0.57	1.32	2.46	1.71
RARα	1.25	1.15	1.12	0.96	1.46	1.19	0.42
RARβ	0.45	0.66	0.35	0.46	0.73	0.69	0.34
Actin	1	1	1	1	1	1	1

Experiment B							
Lane	8	9	10	11	12	13	14
Day	0	1	1	1	7	7	7
Treatment	-	DHCC	cytokine	AB sera	AB sera	cytokine	DHCC
RXRα	2.69	1.37	2.76	4.44	2.97	0.71	0.67
RARα	0.62	0.66	1.01	1.01	1.13	0.64	0.55
RARβ	0.71	0.61	0.53	0.7	0.68	0.46	0.45
Actin	1	1	1	1	1	1	1

Table 3.1.1. Normalised expression of RXRα, RARα, and RARβ in peripheral blood monocytes during differentiation.
Densitometry (NIH Image) was performed on the immunoblots shown in Figure 3.1.1., RXRα, RARα, and RARβ protein expression was normalised to the amount of actin shown in the lower panel of Figure 3.1.1.

3.1.2. Expression of RXRα, RARα, and RARβ in U937 transfectants.

U937 transfectants were cultured and cells treated with 9-*cis* RA, or with cadmium ions for 24 hours. Cells were then counted and lysed, and expression of proteins determined by immunoblotting.

3.1.2.1. Expression of RXRα in the U937 transfectants.

Figure 3.1.2.1A. shows that the level of expression of RXRα is higher in the αG2S cell line, and lower in the αB5A cell line, when compared to that in the control MEP cell line. These differences in RXRα expression are increased upon the addition of cadmium ions to the cells. Thus, αG2S cells hyper-express RXRα, and this expression is inducible with activation of the metallothionein promoter; αB5A cells hypo-express RXRα, and this inhibition of expression is again inducible with activation of the metallothionein IIa promoter. Figure 3.1.2.1B. shows the relative amounts of protein expressed in each lane, normalised for the amount of protein loaded, as measured by the level of actin in each lane.

Although the presence of cadmium ions was shown here to augment the differences in RXRα expression, addition of cadmium ions did not augment differences in cell function (data not shown), suggesting that the level of expression seen without cadmium ions is sufficient to saturate the response elements and heterodimeric partners in the αG2S cell line. Therefore, for the functional studies outlined below cadmium ions were not added. The level of transfected gene expression seen without the addition of cadmium ions is presumably due to activation of the metallothionein promoter by divalent ions contained in the media in which the cells are grown, or to "leaky" cadmium ion independent expression of the promoter.

Figure 3.1.2.1.

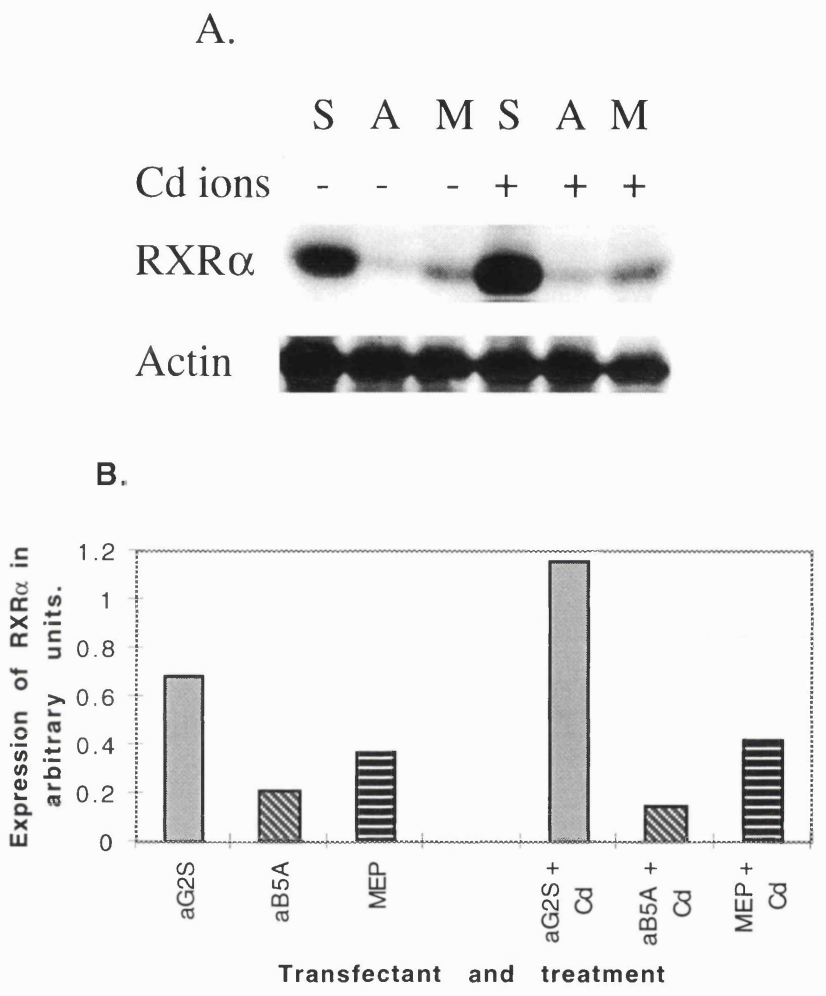

Figure 3.1.2.1. Expression of RXRα in the U937 transfectants.

10^7 αG2S cells (S), or αB5A cells (A), or MEP cells (M), untreated or treated with 20μM $CdCl_2$,were lysed in a 2% SDS lysis buffer. Lysates were run on 10% SDS-polyacrylamide gels and protein levels determined by immunoblotting (see section 2.4.) with a polyclonal RXRα antibody (C20) (upper panel). The blot was then stripped and incubated with an anti-actin mAb, to act as a control for protein levels in each lane (lower panel) (A.). Densitometry (NIH Image) was performed on the immunoblots shown in (A.), RXRα protein expression was normalised to levels of actin (B.).

3.1.2.2. Expression of RARα and RARβ in the U937 transfectants.

Figure 3.1.2.2A. shows that both RARα and RARβ were expressed in the three U937 transfectant cell lines. RARα was expressed at equal levels in all three cell lines, and this level did not change on addition of cadmium ions. However, expression was reduced in all three cell lines on addition of 9-*cis* RA. This could be due to 9-*cis* RA binding and inducing a conformational change of RARα, which masks the binding epitope of the RARα antibody used in the immunoblot, or that 9-*cis* RA down-regulates RARα expression. RARβ was expressed in equal amounts in all three cell lines and its levels were not effected by cadmium ions or 9-*cis* RA. Figure 3.1.2.2B. shows the relative amounts of protein expressed in each lane, normalised for the amount of protein loaded, as measured by the level of actin in each lane.

3.1.3. Expression of cell surface proteins on the U937 transfectants.

Previously it had been shown that there were differences in cell surface protein expression between the three U937 transfectants (Brown et al., 1997; Brown T.R.P., 1995). Only limited experiments had been done previously and these had shown that FcγRs, CD16, CD32, and CD64, were all expressed equally on all three cell lines, with or without prior 9-*cis* RA treatment. The expression of integrin chains CD18 and CD11 was also previously investigated. These results showed that CD11a and CD18 were expressed on 100% of all three U937 transfectants, and that the density of expression was not effected by 9-*cis* RA treatment. Expression of CD11b and CD11c increased following 9-*cis* RA treatment in all three cell lines, with expression of CD11b on sense αG2S cells further augmented upon 9-*cis* RA treatment.

Figure 3.1.2.2.

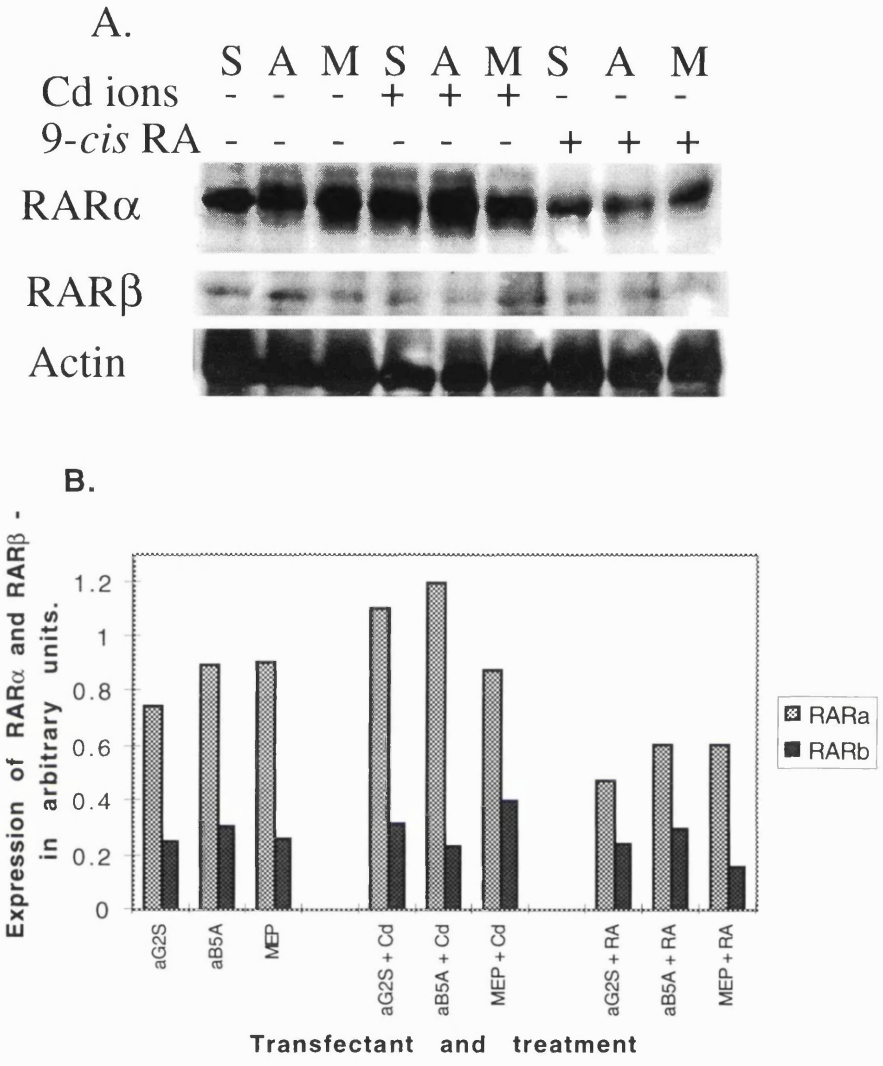

Figure 3.1.2.2. Expression of RARα and RARβ in the U937 transfectants.
αG2S (S), αB5A (A), or MEP cells (M), untreated or treated for 24 hours with 1μM 9-*cis* RA or 20μM $CdCl_2$,were lysed in a 2% SDS lysis buffer. Lysates were run on 10% polyacrylamide gels and expression determined by immunoblotting (see section 2.4.) with either a polyclonal RARα antibody (C19) (upper panel), or a polyclonal RARβ antibody (C18) (middle panel). The blot was then stripped and incubated with an anti-actin mAb, to act as a control for protein levels in each lane (lower panel) (A.). Densitometry (NIH Image) was performed on the immunoblots shown in (A.), RARα and RARβ protein expression was normalised to levels of actin (B.).

3.1.3.1. Expression of ICAM molecules on the U937 transfectants.

Table 3.1.3.1. shows the levels of expression of ICAM-1 (CD54), ICAM-2 (CD102), and ICAM-3 (CD50) on 9-*cis* RA-treated and untreated U937 transfectants, as determined by FACS analysis (see Appendix I, for details of mAbs). ICAM-1 was the predominantly expressed member of this family in all three cell lines. On treatment with 9-*cis* RA, expression of ICAM-1 was increased on αG2S cells, the levels on αB5A and MEP cells remaining unchanged. Expression of ICAM-2 was very low on 9-*cis* RA-treated and untreated αG2S and MEP cells. In contrast, both 9-*cis* RA-treated and untreated αB5A cells expressed ICAM-2 on a high percentage of cells, ableit at low density. No expression of ICAM-3 was detected on any cell line, under either condition.

Table 3.1.3.1.

	αG2S - RA		αG2S + RA		αB5A - RA		αB5A + RA		MEP - RA		MEP + RA	
Specificity	%+ve	MFI	%+ve	MFI	%+ve	MFI	%+ve	MFI	%+ve	MFI	%+ve	MFI
CD54	90	416	99	677*	99	437	99	410	94	456	96	443
CD102	6	11	5	14	98*	88*	97*	72*	6	18	9	18
CD50	7	12	7	15	3	11	5	12	4	15	6	18

Table 3.1.3.1. Expression of ICAM molecules on 9-*cis* RA-treated and untreated U937 transfectants.

3.1.3.2. Expression of antigens targeted by mAbs from the myeloid panel of the 6th HLDA.

The expression of common myeloid antigens on 9-*cis* RA-treated U937 transfectants was assessed by FACS analysis. Appendix I shows the mAbs used in this study, these mAbs were from the blind (prefixed M), and the reference (prefixed MR) panels of the 6th HLDA. The expression of the proteins targeted by these mAbs is shown in Appendix IV. These results are shown in CD number order, followed by expression of antigens targeted by unclassified and then unknown mAbs.

In summary, two further CD11b mAbs bound to an increased percentage of 9-*cis* RA-treated αG2S cells and with increased density (MFI) to 9-*cis* RA-treated αG2S cells. Only one further CD11c mAb was tested, and this did not bind strongly to any of the U937 transfectants. However, a slight increase in expression was seen on αG2S cells. The β2 chain integrin (CD18) was shown to be expressed on more than 90% of all three U937 transfectants at equal density, as shown with both of the CD18 mAbs tested.

Three CD13 mAbs (aminopeptidase N), two CD33 mAbs, one CD36 mAb, two CD64 mAbs, one CDw65 mAb, one CD89 mAb, two CDw92 mAbs, two CDw93 mAbs, and one CD157 mAb bound to over 90% of all three 9-*cis* RA-treated U937 transfectants with equal density.

Three CD15 mAbs were used. One (BU60) bound to 99% of all three cell lines, another (HIM95) bound to 90% of αG2S and MEP cells, and to only 68% of αB5A cells, and a third (8D7) did not bind to any U937 transfectant. With three mAbs, CD34 was shown to be expressed at higher density on a larger percentage of αG2S cells, than on either αB5A or MEP cells (HIM80), whilst another CD34 mAb (9F2) bound to a low percentage of all three cell lines, a final mAb (NU-4A1) did not bind to any transfectant. Two CD63 mAbs were used. One (710F) bound to 45% of cells in all three cell lines, while the other mAb (VIM17) bound to a lower percentage of αB5A cells than of αG2S or MEP cells. A mAb against CD66b did not bind to any transfectant, whilst a mAb against CD66acde bound to 20% of cells in all three U937 transfectants. Three CD87 mAbs were tested. One (3B10) bound to 95% of all transfectants, another (VIM5) bound to a higher percentage of MEP cells than αG2S and αB5A cells, and the third (10G7) did not bind to any transfectant. Two CD98 mAbs were tested. One (J3-E1B) bound to 95% of all three transfectants, whilst the other (J1-G3B) bound more to MEP cells than to

αG2S or αB5A cells. Of two CD101 mAbs tested, one (BB27) bound to a lower percentage of αB5A cells than αG2S or MEP cells, whilst the other (V7.1) did not bind to any transfectant. Two CD148 were tested. One (143-41) bound to 90%, whilst the other (A3) bound to 50% of all three U937 transfectants. Two CD156 mAbs bound to a higher percentage of αG2S cells. Two CD163 mAbs bound to an increased percentage with higher density to αG2S cells.

One CDw12 mAb, four CD14 mAbs, one CDw17 mAb, one CD35 mAb, one CD39 mAb, three CD68 mAbs, one CD114 mAb, and an mAb against a carbohydrate structure (cho) did not bind to any of the three 9-*cis* RA-treated U937 transfectants.

A significant number of the mAbs in the myeloid panel still have unknown specificities, of these mAbs 1.83 (M7), BIRMA 65 (M26), X11 (M32), 5H1 (M43), ZCH-7-2D3 (M49), HIM15 (M60), HIM63 (M65), and HI247 (M67) bound to over 90% of all three 9-*cis* RA-treated U937 transfectants with equal density.

Unknown mAbs 4B5.F5, 4B4.E11, PMO-1, X7, X15, PM-1K, AM-3K, and HIM95 bound to an increased percentage of αG2S cells than to αB5A or MEP cells.

Unknown mAbs Ay19 and J2-E1F bound to a decreased percentage of αB5A cells than to αG2S or MEP cells.

Finally, unknown mAbs TAX64, BG6, M103, MEM-166, 1B12.1, Anti TF V-28, X3, X12, ZCH-7-4C3a, and AAA4 did not bind to any of the U937 transfectants.

The relevance of the expression of antigens recognised by these unclassified mAbs will only become clear after the mAbs have been designated, perhaps at the next HLDA.

3.1.4. 9-cis RA-treated U937 transfectants display differing efficiencies of immunophagocytosis.

In order to assess the extent of differentiation and activation in the U937 transfectants, the process of immunophagocytosis, a primary function of the monocyte/macrophage lineage, was investigated in these cells.

3.1.4.1. Morphological features of differing efficiencies for uptake of opsonised SRBC (op-SRBC).

The morphological features of 9-*cis* RA-treated U937 transfectants, exposed to op-SRBC, indicated different efficiencies of op-SRBC uptake, as illustrated in Figure 3.1.4.1. After two hours of co-culture with the op-SRBC, a different pattern of rosetting was clearly identifiable. The αG2S transfectant was more efficient than either the MEP control transfectant cell line or αB5A transfectants. The αG2S cells bound the op-SRBC, and also formed large aggregates, suggesting more activation and more efficient phagocytosis (A). The αB5A cells bound to the op-SRBC, but did not form any large aggregates either with other transfectants or with op-SRBC (B). The control MEP cells bound to the op-SRBC and formed small clusters of cells (C).

Figure 3.1.4.1.

A. αG2S

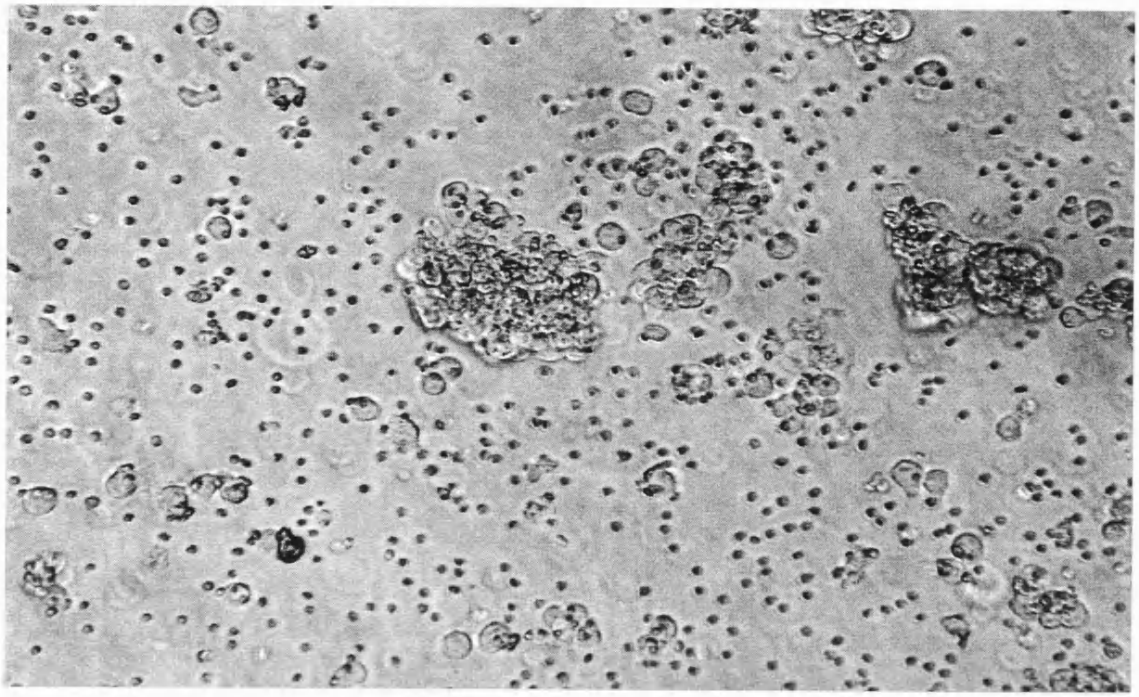

B. αB5A

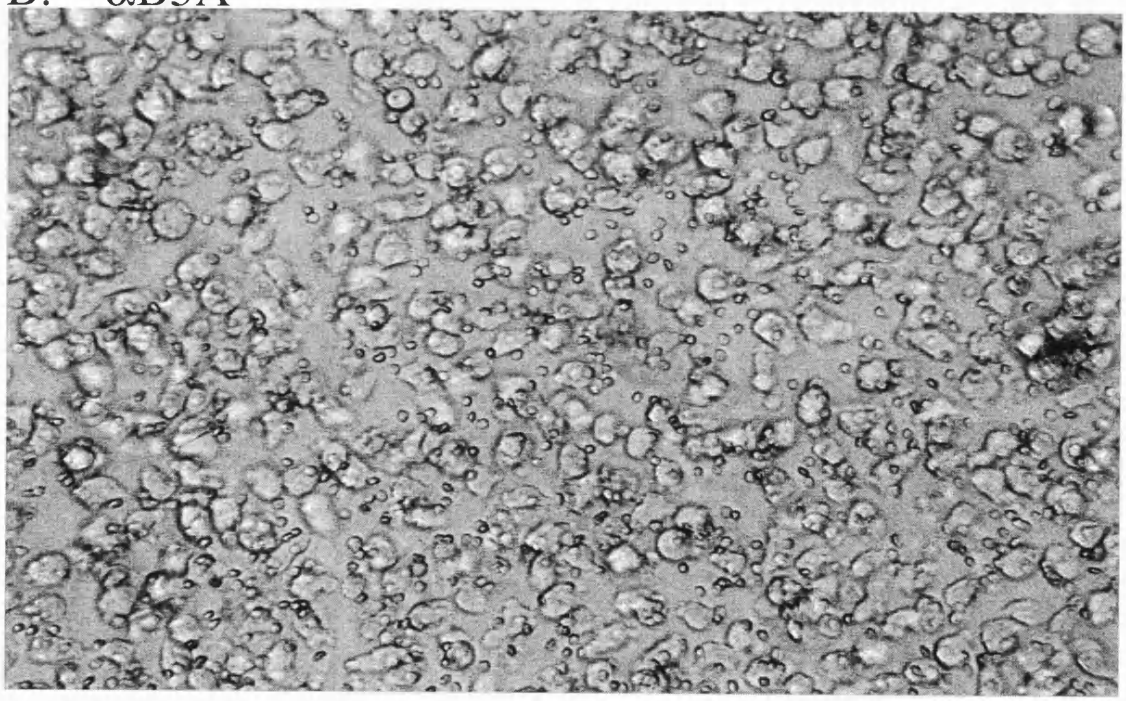

C. MEP

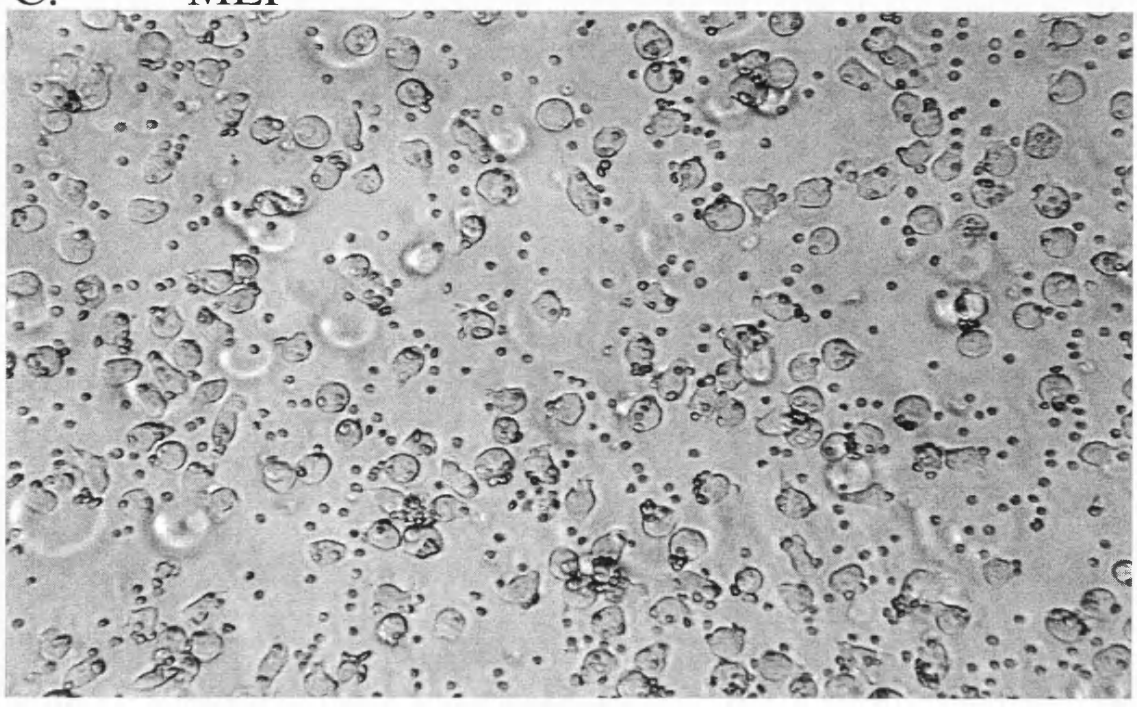

Figure 3.1.4.1. Assessment of immunophagocytic efficiency by the U937 transfectants by microscopy.

$2x10^7$ opsonised SRBC (op-SRBC) were added to 10^6 αG2S (A), αB5A (B), or MEP cells (C), which had been treated with 1μM 9-*cis* RA. Cells were cultured for two hours and then photographs taken at X40 magnification.

3.1.4.2. Quantitation of the increase in immunophagocytosis by αG2S cells.

The observation that αG2S cells are more efficient at immunophagocytosis was confirmed by measuring uptake of ^{51}Cr-op-SRBC (Figure 3.1.4.2.). The αG2S cells took up significantly more label than MEP cells, which in turn took up more label than αB5A cells.

Figure 3.1.4.2.

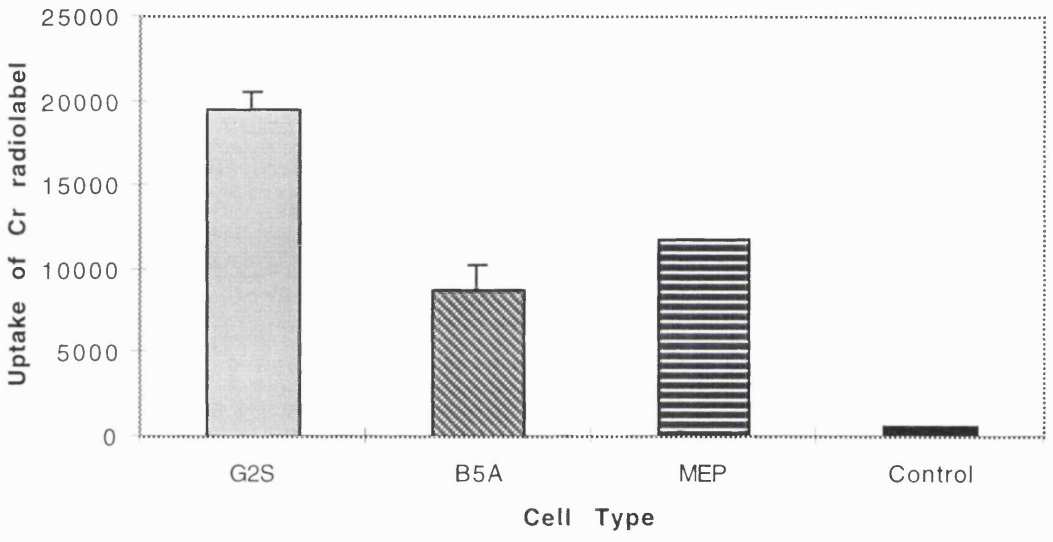

Figure 3.1.4.2. Assessment of immunophagocytic efficiency by the U937 transfectants by uptake of radiolabelled opsonised SRBC (^{51}Cr-op-SRBC). 2x10^6 9-*cis* RA-treated αG2S (A), or αB5A (B), or MEP cells (C), were cultured for 2 hours with 4x10^7 ^{51}Cr-op-SRBC. Uptake of radioisotope in the cell pellets was measured by gamma counter. The column labelled control is a measure of non-specific uptake of ^{51}Cr when αG2S cells were cultured with un-opsonised ^{51}Cr- SRBC. The values shown are the mean cpm of triplicates from each cell line +/- the standard deviation from the mean from one representative experiment.

3.1.4.3. Actin staining of U937 transfectants after two hours of exposure to op-SRBC.

Rearrangement of cytoskeletal actin is essential for the process of engulfment of opsonised particles. Therefore, effects of immunophagocytosis on cellular actin distribution was assessed and similar results were observed with all three U937 transfectants (data not shown). This suggests that differences in immunophagocytic efficiency were quantitative rather than qualitative. Figure 3.1.4.3. shows MEP control cells as an example of these experiments. MEP cells exposed for two hours to the op-SRBC, or un-exposed, were stained for actin using phalliodin, and examined by confocal microscopy. Figure 3.1.4.3A. shows a cell which has completely internalised op-SRBC, shows clearly that during immunophagocytosis that actin becomes much more organised, and has more surface processes. This can be seen by comparing the actin distribution in Figure 3.1.4.3A. with that seen in Figure 3.1.4.3B., where no pre-exposure to op-SRBC has occurred, the actin staining is much more granular, and less concentrated to the cell membrane.

3.1.5. Immunophagocytosis by the U937 transfectants was inhibited by Fcγ receptor III mAbs (CD16).

Immunophagocytosis by monocytes and macrophages is known to be mediated by Fcγ receptors. Therefore, to confirm that Fcγ receptor mediated phagocytosis is occurring in this experimental system, and to confirm which Fcγ receptors are important in immunophagocytosis by the U937 transfectants, a panel of Fcγ receptor mAbs were used to attempt to inhibit uptake of ^{51}Cr-op-SRBC (see Appendix II).

Figure 3.1.4.3.

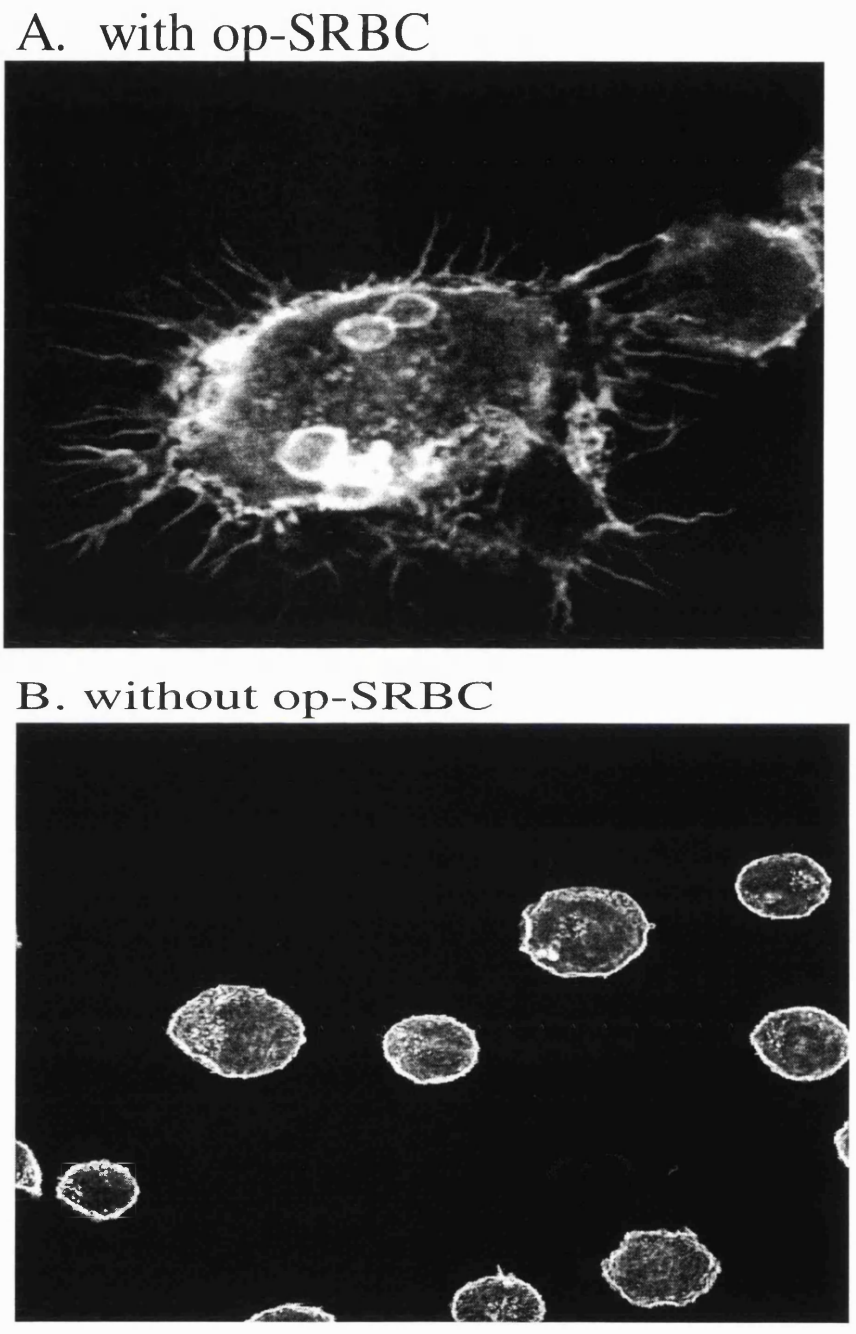

Figure 3.1.4.3. Visualisation of actin after two hours exposure to op-SRBC.

$2x10^6$ 9-*cis* RA-treated MEP cells were cultured for 2 hours with $4x10^7$ op-SRBC (A), or were not exposed to any op-SRBC (B). The cells were then stained for actin, fixed, bound to poly-l-lysine coated cover slips, and visualised with confocal microscopy.

3.1.5.1. Immunophagocytosis was inhibited by Fc receptor γIII mAbs (CD16), but not FcR γII (CD32), or FcR γI (CD64).

Figure 3.1.5.1. shows that incubation of two CD16 (FcγRIII) (3G8 and leu-11-b) mAbs, inhibited uptake of ^{51}Cr-op-SRBC into all three U937 transfectant cell lines, whilst incubation with CD32 (FcγRII) (IV3) or CD64 (FcγRI) (32) mAbs did not.

Figure 3.1.5.1.

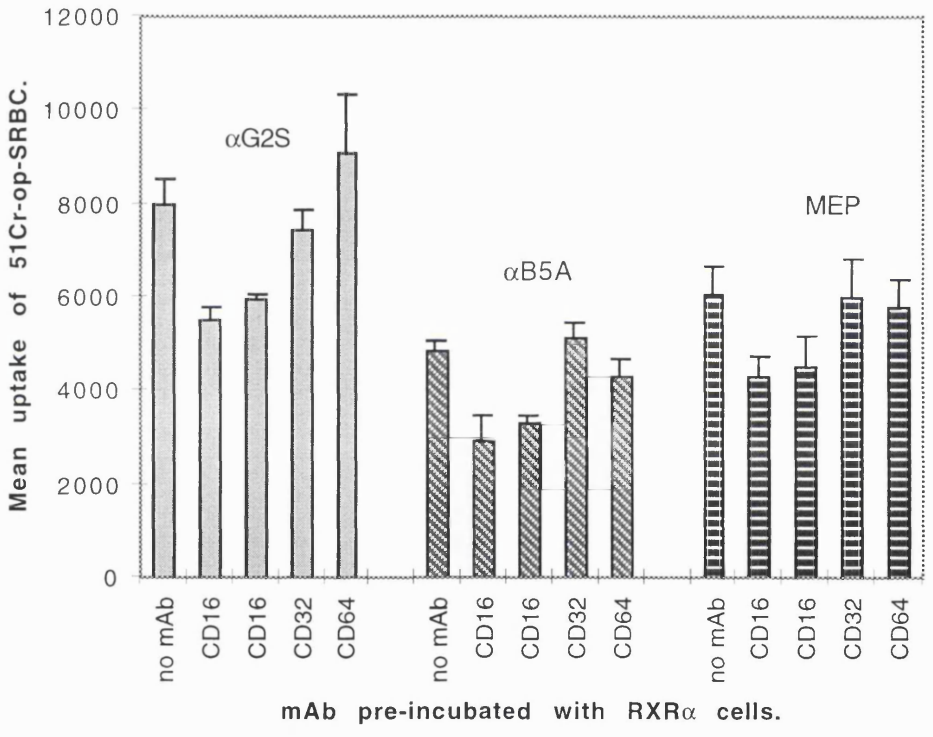

Figure 3.1.5.1. Blockade of immunophagocytosis by Fcγ receptor mAbs. 10^7 9-*cis* RA-treated αG2S, αB5A, or MEP cells were incubated with 1:50 dilutions of Fcγ receptors mAbs for 1 hour at 4°C. The ability of these cells to immunophagocytose was assessed by uptake of ^{51}Cr-op-SRBC (see sections 2.7. and 2.8.). The values shown are the mean cpm of triplicates from each cell line +/- the standard deviation from the mean from one representative experiment.

3.1.5.2. Further investigation of Fcγ receptor mAb inhibition of immunophagocytosis.

As shown in Figure 3.1.5.1., the two CD16 mAbs inhibited immunophagocytosis by around 20%. To examine whether this was an effect of mAb concentration, a titration of the same Fcγ receptor mAbs were pre-incubated with the MEP cell line. Figure 3.1.5.2. shows that increased CD16 mAb concentration increased the inhibition of uptake of ^{51}Cr-op-SRBC by MEP cells. This suggests that the low inhibition seen in all three U937 transfectants previously, was due mAb concentration, as inhibition was dose-dependent. Increased concentrations of CD32 and CD64 mAbs had no effect on uptake of ^{51}Cr-op-SRBC.

3.1.6. Immunonophagocytosis by the U937 transfectants is inhibited mAbs which recognise CD13, and CD18.

To investigate the nature of other molecules on the cell surface involved in immunophagocytosis by these cells, mAbs from the myeloid panel of the 6th Human Leukocyte Differentiation Antigen workshop (6th HLDA) (see appendix II) were incorporated into the quantitation assays.

3.1.6.1. Initial screen of effects of mAbs from the myeloid panel on immunophagocytosis.

Appendix V shows an example of the initial screening protocol where αG2S cells were pre-incubated with mAbs and then exposed to chromium labelled op-SRBC (^{51}Cr-op-SRBC) for two hours. All the mAbs used in this assay had been previously shown to bind to the U937 transfectants (see section 3.1.3.2.), except for M3, which served as a non-binding mAb control. Identical experiments were performed using the αB5A, and MEP cell lines (data not shown).

Figure 3.1.5.2.

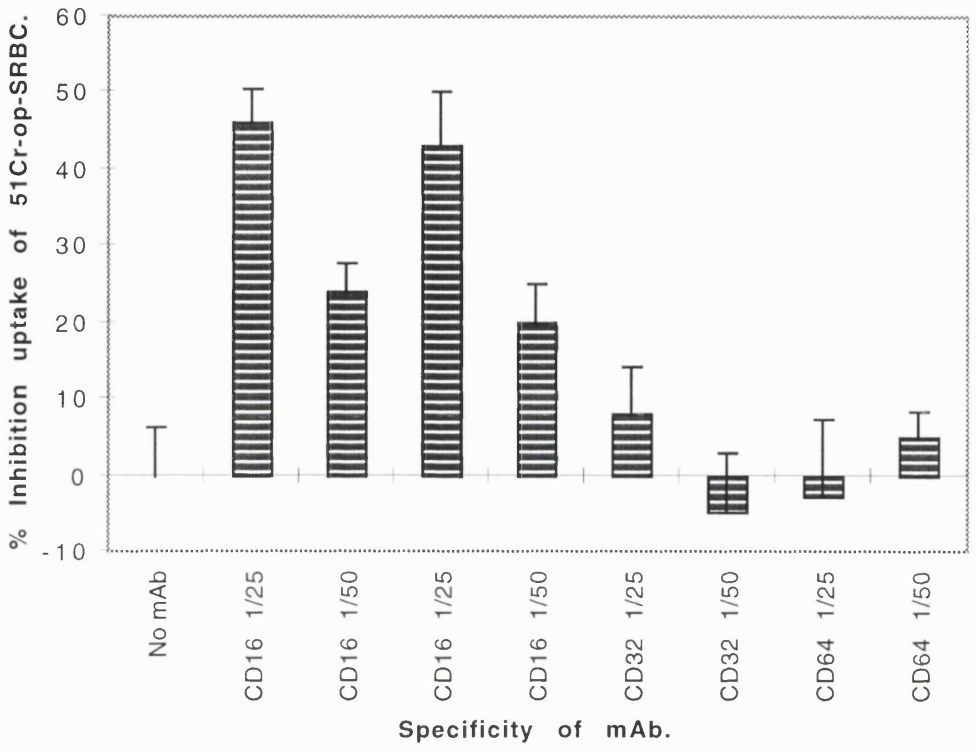

Figure 3.1.5.2. Blockade of immunophagocytosis by a titration of Fcγ receptor mAbs.

10^7 9-*cis* RA-treated MEP cells were incubated with 1:50 or 1:25 dilutions of Fcγ receptors mAbs for 1 hour at 4°C. The ability of these cells to immunophagocytose was assessed by uptake of ^{51}Cr-op-SRBC (see sections 2.7. and 2.8.). The values shown are the mean % inhibition of ^{51}Cr-op-SRBC uptake, compared to the no mAb control sample (value 11007 cpm), +/- the % error from triplicate wells.

3.1.6.2. Two mAbs from the myeloid panel, CD13 (7H5), and CD18 (BU87-M2), inhibited uptake of ^{51}Cr-op-SRBC into the U937 transfectants.

From the initial screening experiments, any mAb that caused any inhibition of uptake of ^{51}Cr-op-SRBC (Appendix V), was chosen for further study, and these experiments repeated in triplicate. Figure 3.1.6.2. show examples of this further screening done on the myeloid panel of mAb. This shows that of all the mAbs tested only two mAbs directed against particular surface molecules, CD13 (7H5 - code number M50), and CD18 (BU87-M2 - code number M16) inhibited uptake of ^{51}Cr-op-SRBC into all three U937 transfectants. This is consistent with the preliminary screen (Appendix V), where these two mAbs were also the most inhibitory. All mAbs shown in Figures 3.1.6.2. were shown to bind to all three transfectant cell lines by FACS analysis, including the two inhibitory mAbs each of these were expressed at equal levels on all three cell lines (section 3.1.3.2.).

3.1.7. Expression of p47-phox, but not of p67-phox is upregulated in αG2S cells, but not in αB5A cells.

To further investigate the increase in efficiency of immunophagocytosis of the sense αG2S cell line, expression of proteins that are indicative of a differentiated phenotype was assessed. p47-phox and p67-phox form part of the enzymatic complex NADPH oxidase, which are involved in superoxide production that is a feature of mature phagocytes. 9-*cis* RA-or cadmium ion-treated αG2S, αB5A or MEP cell lysates probed for p47-phox and p67-phox expression by immunoblotting. Figure 3.1.7. shows that there are low levels of p47-phox in the unstimulated cells. These increased significantly in 9-*cis* RA-treated αG2S cells, and to a lesser extent in MEP cells under the same conditions. No increase in expression was seen in αB5A cells after 9-*cis* RA treatment. Furthermore, there was no change in p47-phox expression in any cell line upon cadmium ion treatment, suggesting either that overexpression of RXRα was not itself

sufficient to increase expression of p47-phox. In contrast with p47 phox, no expression of p67 phox was seen in the U937 transfectants under these conditions (Figure 3.1.7.).

Figure 3.1.6.2.

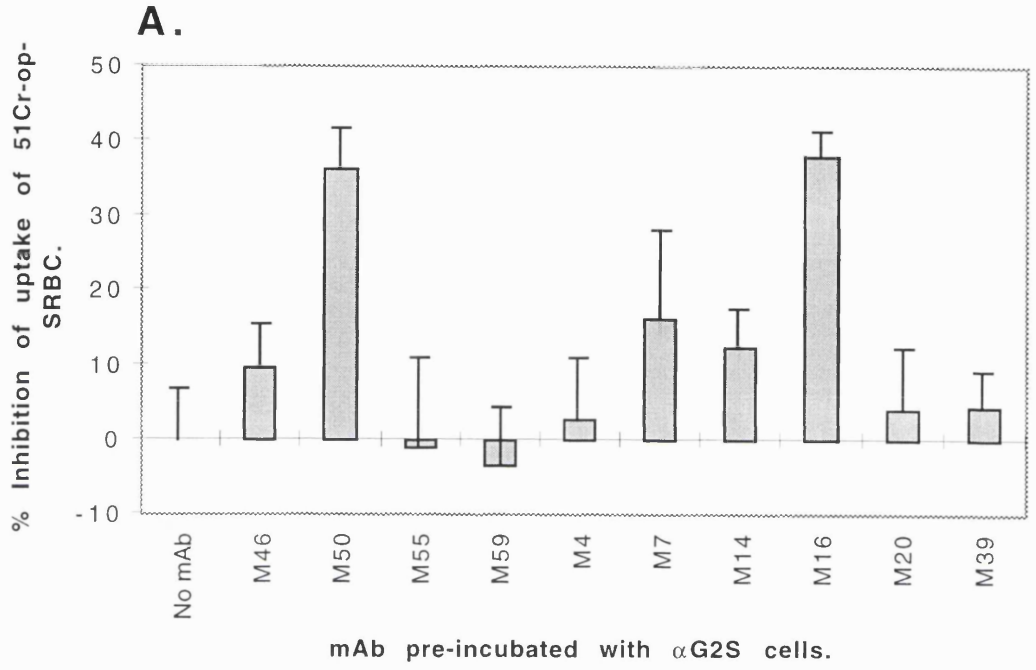

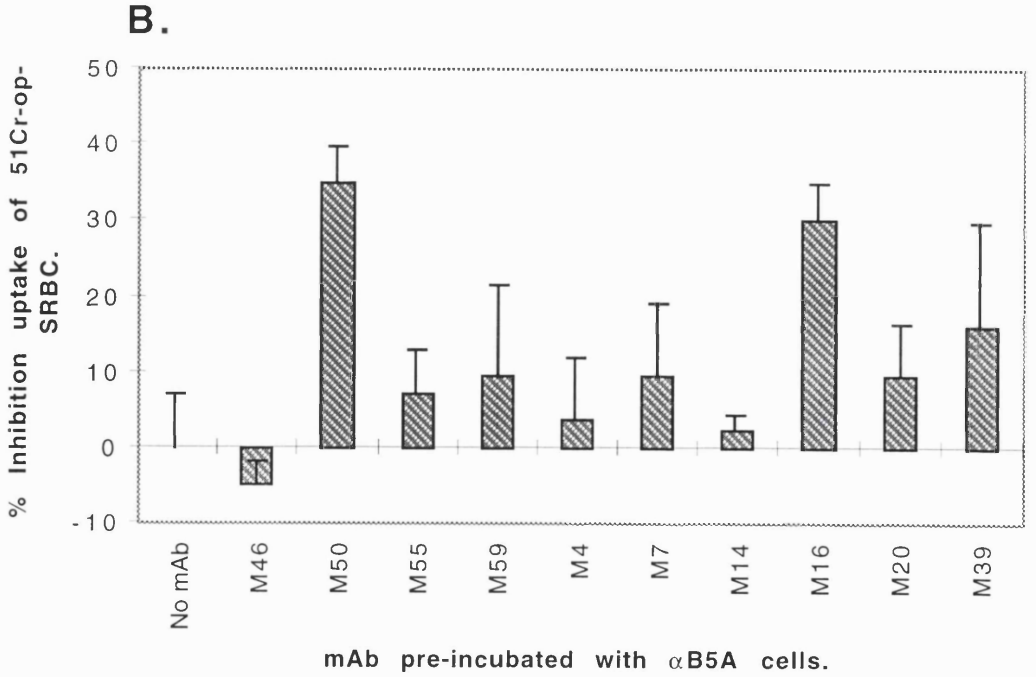

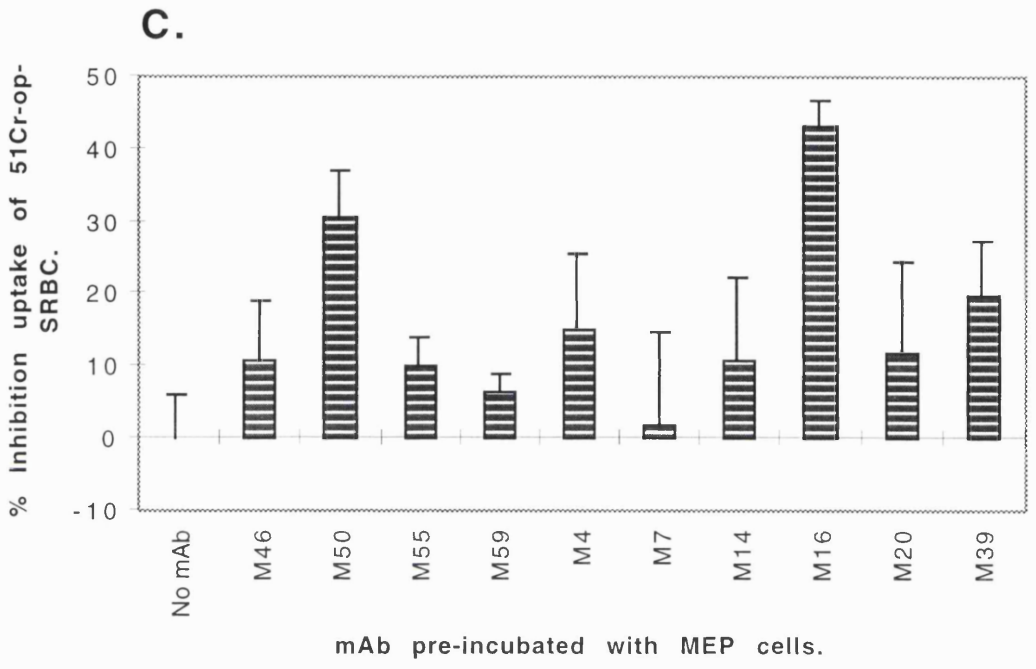

Figure 3.1.6.2. Immunophagocytosis by the U937 transfectants is inhibited by a CD13 mAb (M50 - 7H5), and a CD18 mAb (M16 - BU87-M2).

9-*cis* RA-treated αG2S (A), αB5A (B), or MEP cells (C), were incubated with 1:50 dilutions of mAbs from the myeloid panel which had been shown to have any inhibitory effect in the initial screen for 1 hour at 4°C. The ability of these cells to immunophagocytose was assessed by uptake of ^{51}Cr-op-SRBC (see sections 2.7. and 2.8.). The values shown are the mean inhibition of uptake of ^{51}Cr-op-SRBC of triplicates wells from each cell line +/- the % error, compared to the no mAb control, from one representative experiment. The mAbs used in the assay shown are directed against, CD11b (M46 or ZCH-7-4FB); CD13 (M16 or 7H5); CD36 (M55 or UN7); CD34 (M59 or HIM80); CD148 (M4 or A3); a unclassified mAb (M7 or 1.83); CD15 (M14 or BU60); CD18 (M16 or BU87-M2); CD63 (M20 or V1M17); and CD163 (M39 or D11).

Figure 3.1.7.

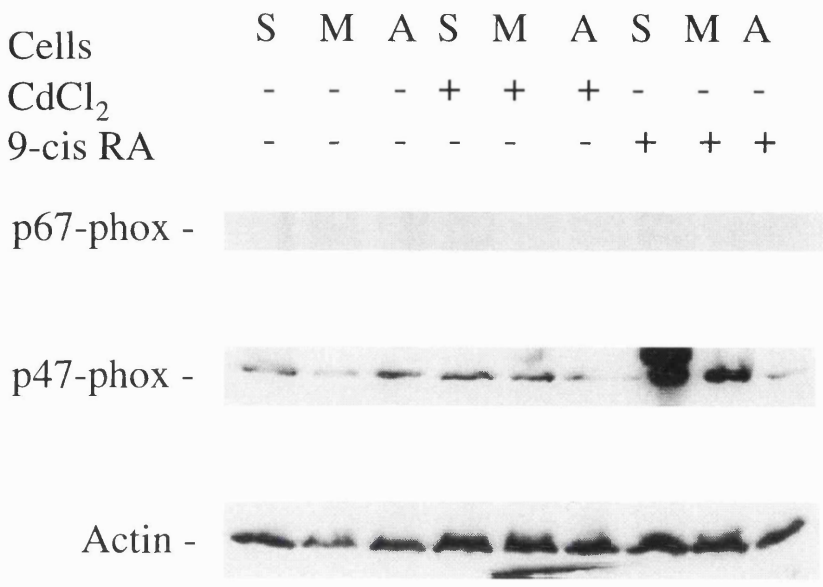

Figure 3.1.7. Expression of p47-phox, and p67 phox in the U937 transfectants. 9-*cis* RA- or $CdCl_2$ - treated or untreated αG2S (S), αB5A (A), or MEP cells (M), were lysed, and lysate from 10^6 cells electrophoresed in each lane of a SDS-polyacrylamide gel. Immunoblotting with a p47-phox antibody (middle panel), or a p67 phox antibody (upper panel) was performed (see section 2.4.). As a control for protein loading, the p47 phox blot shown was stripped and incubated with an anti-actin mAb (lower panel).

3.1.8. Immunophagocytosis by the U937 transfectants induces rapid tyrosine phosphorylation of numerous proteins.

The mechanism of Fcγ receptor mediated phagocytosis has previously been shown to be correlated to phosphorylation of many proteins inside the phagocytic cell (see section 1.2.). Based upon the findings regarding the differences in phagocytic efficiencies of the U937 transfectants, the effects on phosphotyrosine signalling in the transfectants following op-SRBC exposure were compared.

3.1.8.1. Pattern and intensity of tyrosine phosphorylation differs between 9-*cis* RA-treated U937 transfectants in response to op-SRBC.

Figure 3.1.8.1. shows that addition of op-SRBC to 9-*cis* RA-treated U937 transfectants induced extensive tyrosine phosphorylation. In αG2S cells, this response was apparent within 1 minute of op-SRBC addition, was maximal between 10 and 30 minutes, and began to decrease by 2 hours. In contrast the response of αB5A cells to op-SRBC was less intense and rapid, not being apparent until 5 minutes after addition of op-SRBC. The αB5A response was maximal between 10 and 30 minutes, and began to decrease by 2 hours. The response to op-SRBC of MEP cells was also rapid, though not as intense as in αG2S cells. The MEP response occurred within 1 minute, was maximal between 10 and 30 minutes, and began to decrease by 2 hours.

Figure 3.1.8.1.

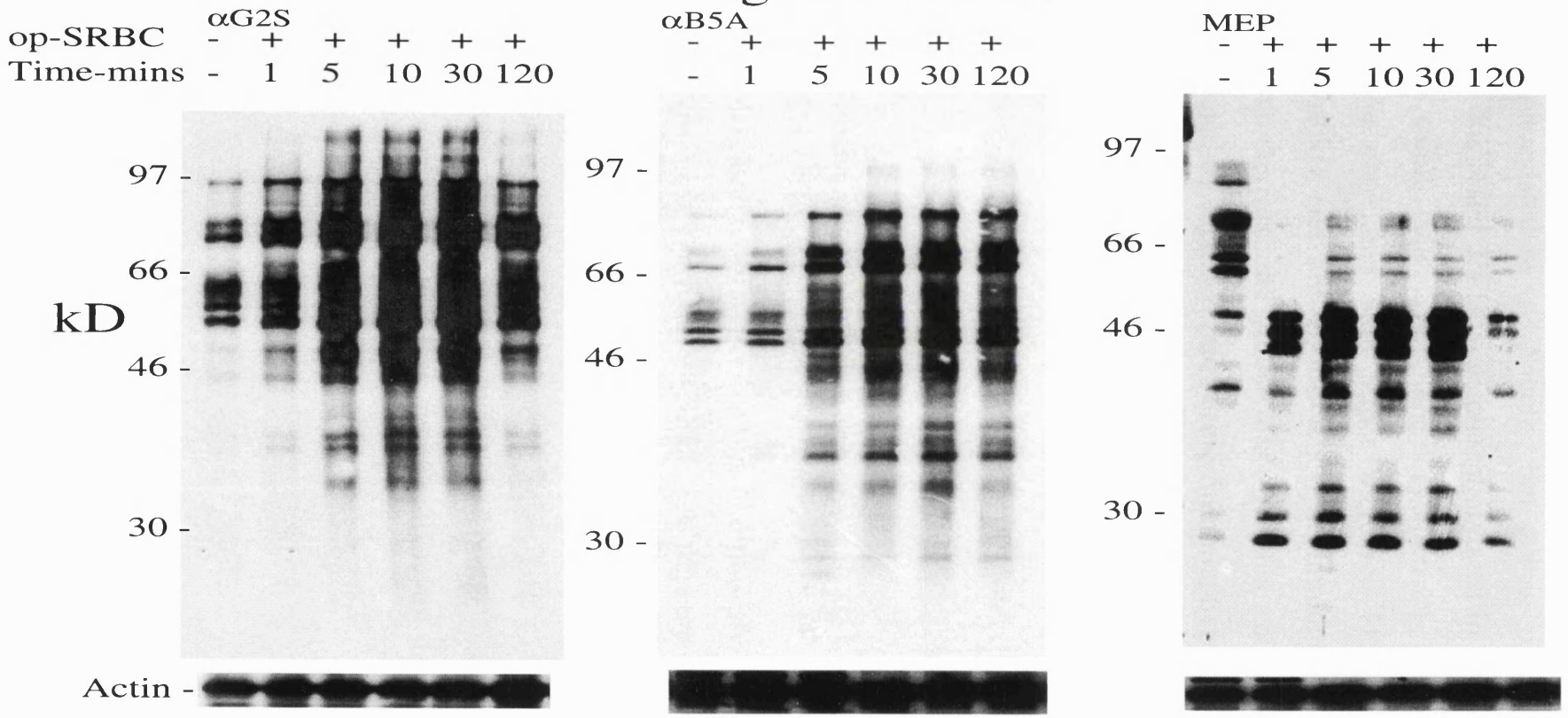

Figure 3.1.8.1. Immunophagocytosis induces differential patterns of tyrosine phosphorylation in the U937 transfectants. 9-*cis* RA-treated αG2S, αB5A or MEP cells were cultured with $4x10^7$ op-SRBC for the time points indicated. Cell lysates (equivalent of $4x10^5$ cells per lane) were run on 10% SDS-polyacrylamide gels, and anti-phosphotyrosine (with mAb 4G10) immunoblotting performed (see section 2.4.). As a control for protein levels, the blot shown was stripped and incubated with an anti-actin mAb (lower panel).

There were also several qualititative differences in tyrosine phosphorylation in the three cell lines. Proteins of MW 120kD, and 68kD, were phosphorylated in αG2S cells, but not in αB5A or MEP cells. Proteins of 46kD and 28kD were phosphorylated in αB5A or MEP cells, but not in αG2S cells. The phosphorylation of these proteins could therefore be correlated with either increased (120kD or 68kD), or decreased (46kD and 28kD) efficiency of immunophagocytosis. Table 3.1.8.1. summarises the molecular weights of proteins tyrosine phosphorylated by each cell line during immunophagocytosis.

The lower panels of blots shown in Figure 3.1.8.1. are the results of the same filters, stripped and incubated with an anti-actin mAb. These results confirm that approximately equal amounts of protein were present in each sample.

3.1.8.2. Tyrosine phosphorylation responses to op-SRBC are similar in DHCC-treated U937 transfectants.

To assess whether the differences in tyrosine phosphorylation between the three cell lines in response to op-SRBC are dependent upon RXRα/9-*cis* RA, the cells were treated with 500nM DHCC 24 hours prior to the assay. Figure 3.1.8.2 shows that the differences in tyrosine phosphorylation seen after 9-*cis* RA treatment do not occur upon DHCC treatment. All three DHCC-treated cell lines responding in a similar way. The response in αG2S cells was noticeably less intense than in the 9-*cis* RA-treated transfectants.

Table 3.1.8.1.

Protein size kD	Phosphorylated during phagocytosis αG2S	αB5A	MEP
115	**YES**	**NO**	**NO**
96	YES	YES	NO
85	YES	YES	NO
81	YES	YES	NO
68	**YES**	**YES**	**NO**
64	YES	YES	NO
60	YES	YES	YES
57	YES	YES	YES
48	YES	YES	YES
46	**NO**	**YES**	**YES**
44	YES	YES	YES
42	NO	YES	YES
39	YES	NO	YES
38	YES	YES	YES
37	YES	YES	YES
35	YES	YES	YES
28	**NO**	**YES**	**YES**
27	NO	NO	YES

Table 3.1.8.1. Proteins phosphorylated during immunophagocytosis in the U937 transfectants.

Proteins phosphorylated in Figure 3.1.8.1. are summarised above, proteins of particular interest are shown in bold (see text).

3.1.9. mAbs inhibitory of immunophagocytosis do not inhibit the phosphotyrosine response to op-SRBC.

The mAbs that had previously been shown to inhibit immunophagocytosis (see sections 3.1.5. and 3.1.6.) were also examined for their effects on the phosphotyrosine response to op-SRBC (see section 3.1.8.).

3.1.9.1. Fcγ receptor mAbs did not inhibit the phosphotyrosine response to op-SRBC.

Figure 3.1.9.1. shows the phosphotyrosine response to op-SRBC when Fcγ receptor mAbs were pre-incubated with 9-*cis* RA-treated U937 transfectants before addition of op-SRBC. Addition of these antibodies did not affect the phosphotyrosine response of the transfectants to op-SRBC. This suggests that whilst the CD16 mAbs inhibit the uptake of op-SRBC (see section 3.1.5.) they do not physically block the interaction of op-SRBC with Fc receptors on the cell surface.

3.1.9.2. The inhibitory mAbs CD13 (7H5) and CD18 (BU87-M2) do not inhibit the phosphotyrosine response to op-SRBC.

Figure 3.1.9.2. shows that when CD13 or CD18 mAbs were pre-incubated with 9-*cis* RA treated transfectants before addition of op-SRBC, the phosphotyrosine response to op-SRBC shown by αG2S, αB5A, and MEP cells did not alter. However, one band of 46kD was phosphorylated in response to addition of CD13 (7H5) to MEP cells.

Figure 3.1.8.2.

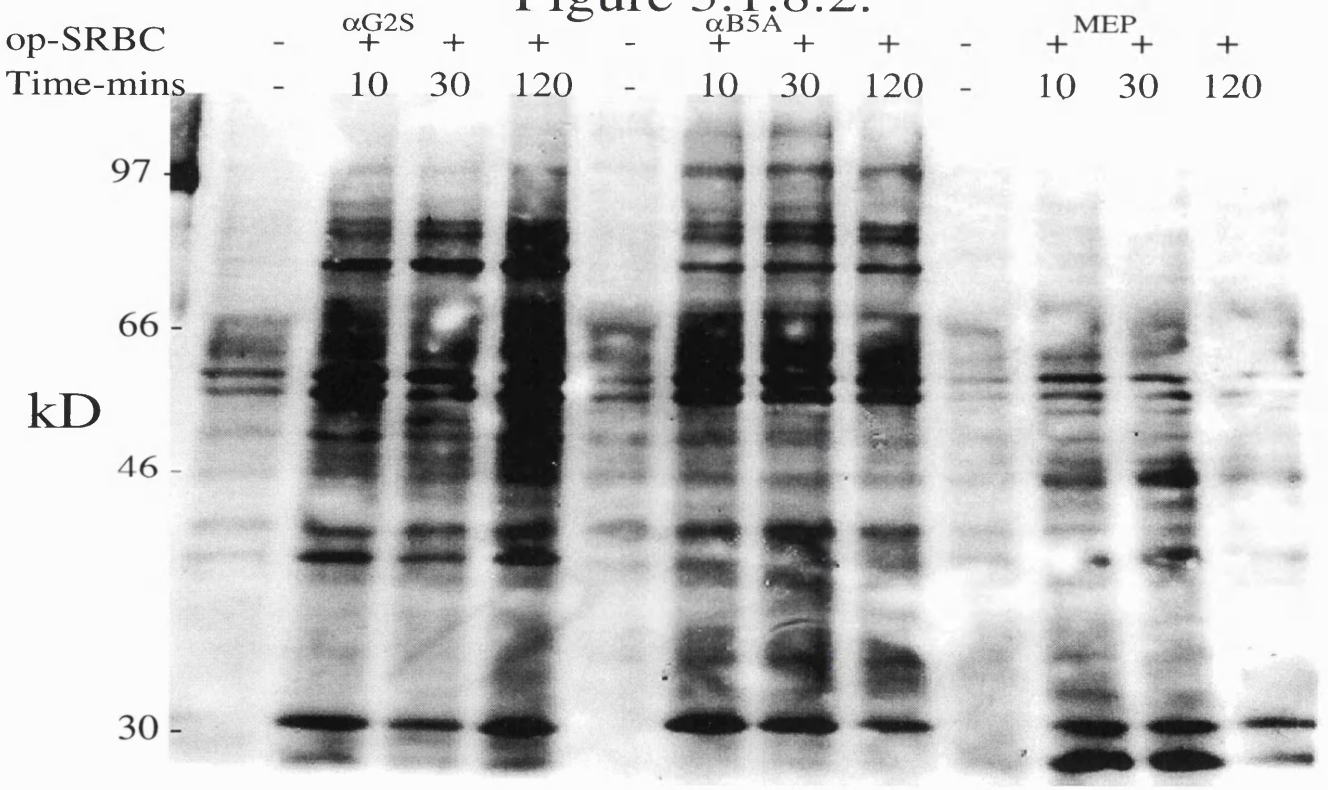

Figure 3.1.8.2. DHCC-treatment does not induce differential tyrosine phosphorylation responses to op-SRBC in the U937 transfectants. DHCC-treated αG2S, αB5A, or MEP cells were cultured with $4x10^7$ op-SRBC for the time points indicated. Cell lysates (equivalent of $4x10^5$ cells per lane) were run on 10% SDS-polyacrylamide gels, and anti-phosphotyrosine (with mAb 4G10) immunoblotting performed (see section 2.4.).

Figure 3.1.9.1A.

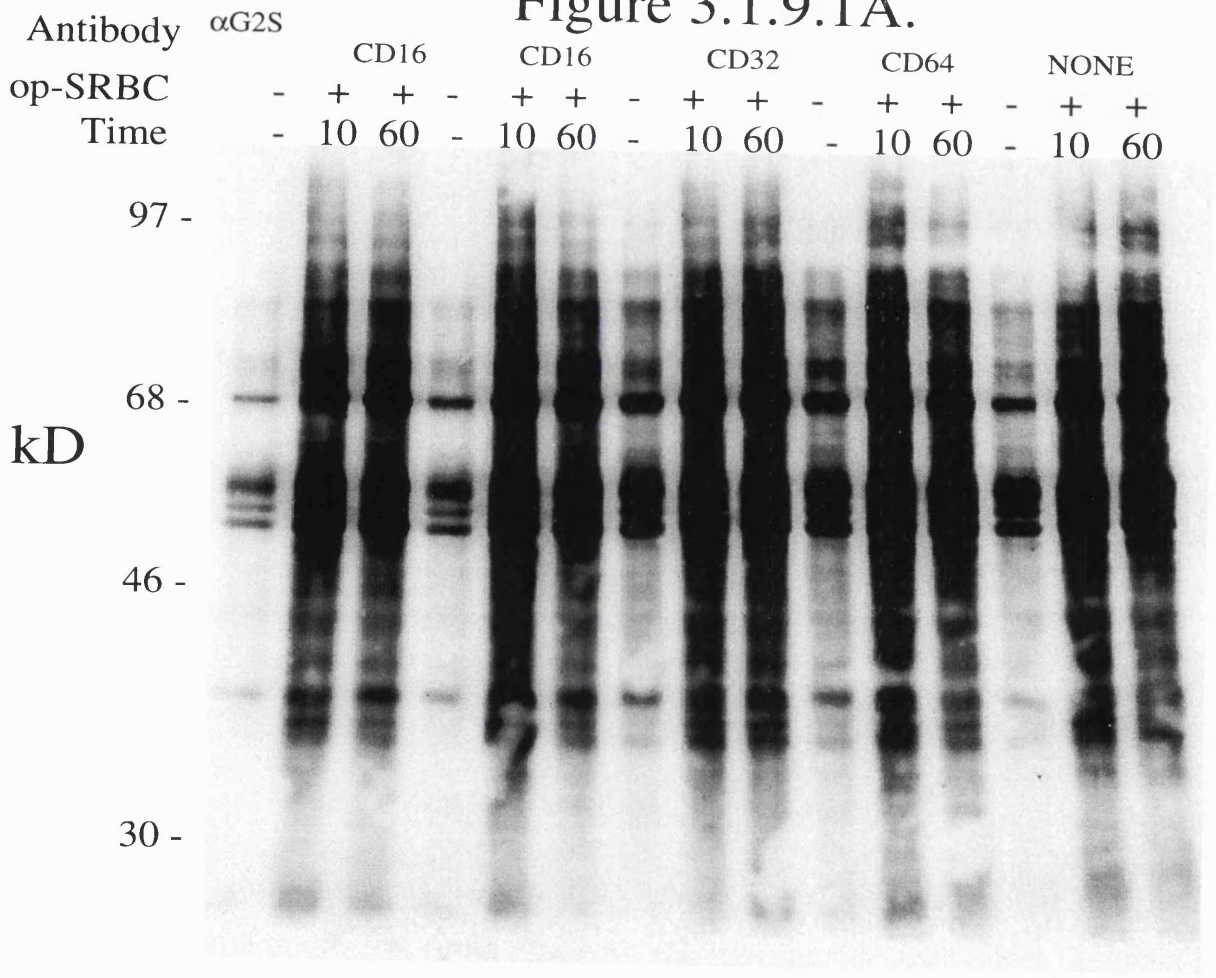

Figure 3.1.9.1B.

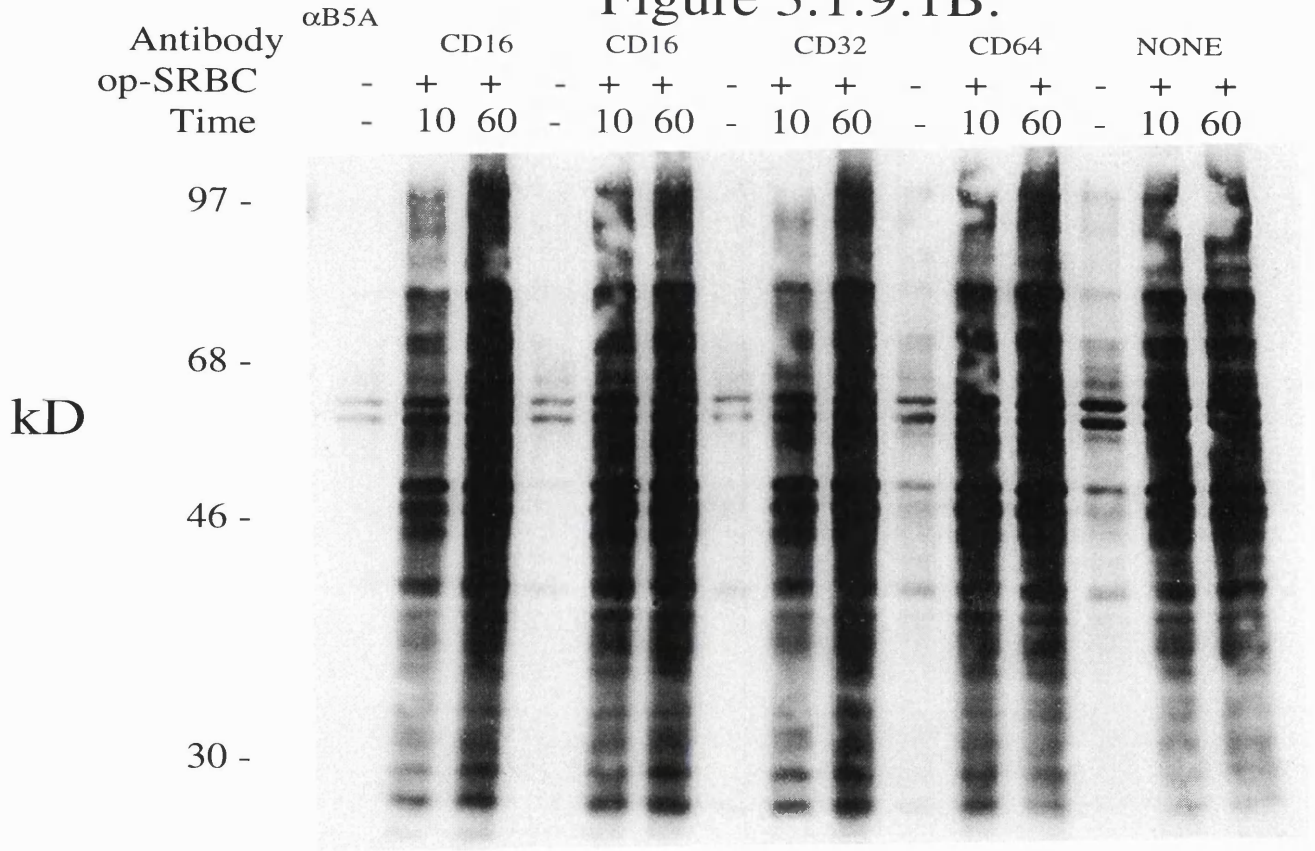

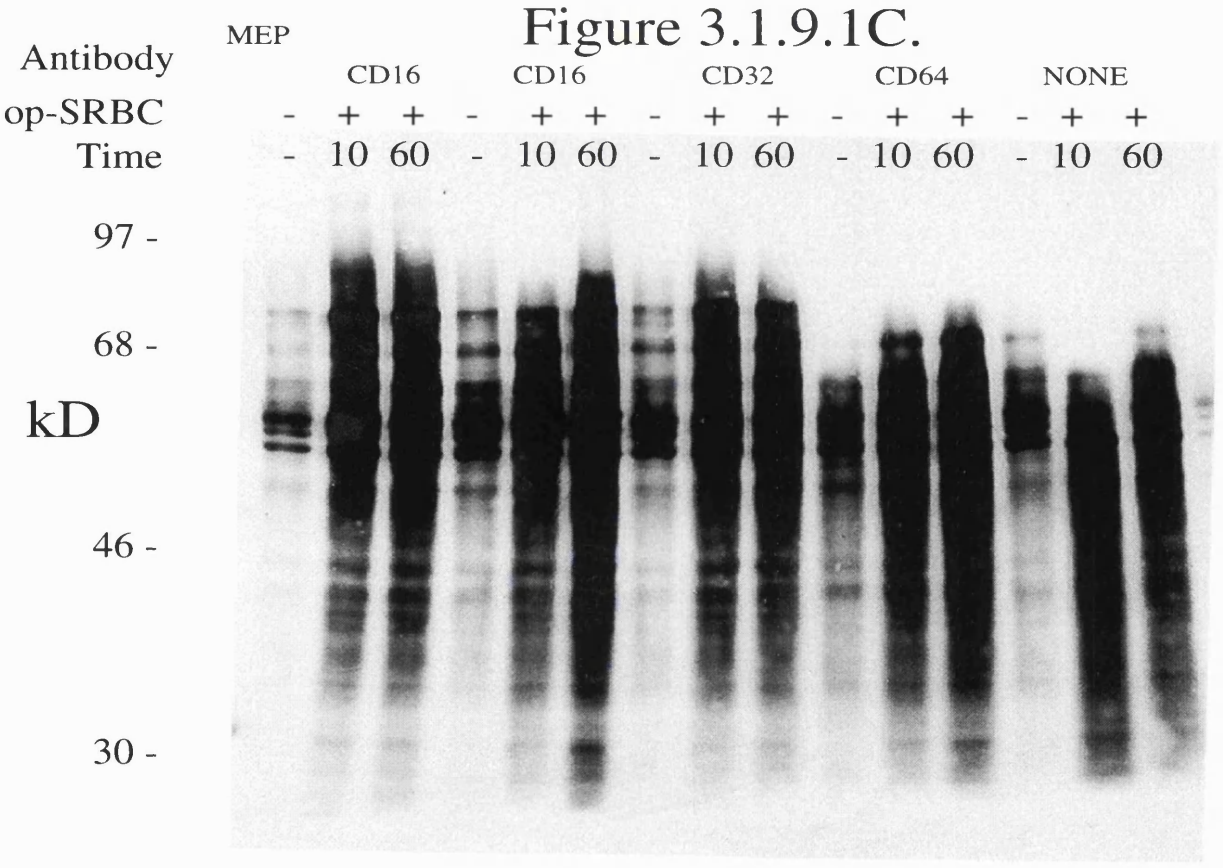

Figure 3.1.9.1. Effects of binding Fcγ receptor mAbs on the phosphotyrosine response to op-SRBC. 9-*cis* RA-treated αG2S (A), αB5A (B), or MEP cells (C), were incubated with anti-Fcγ receptor mAbs (3G8, Leu-11, IV3 and 32), then cultured for 10 minutes and 1 hour with op-SRBC. Cell lysates (equivalent of $4x10^5$ cells per lane) were electrophoresed on 10% SDS-polyacrylamide gels, and anti-phosphotyrosine (with mAb 4G10) immunoblotting performed (see section 2.4.).

Figure 3.1.9.2.

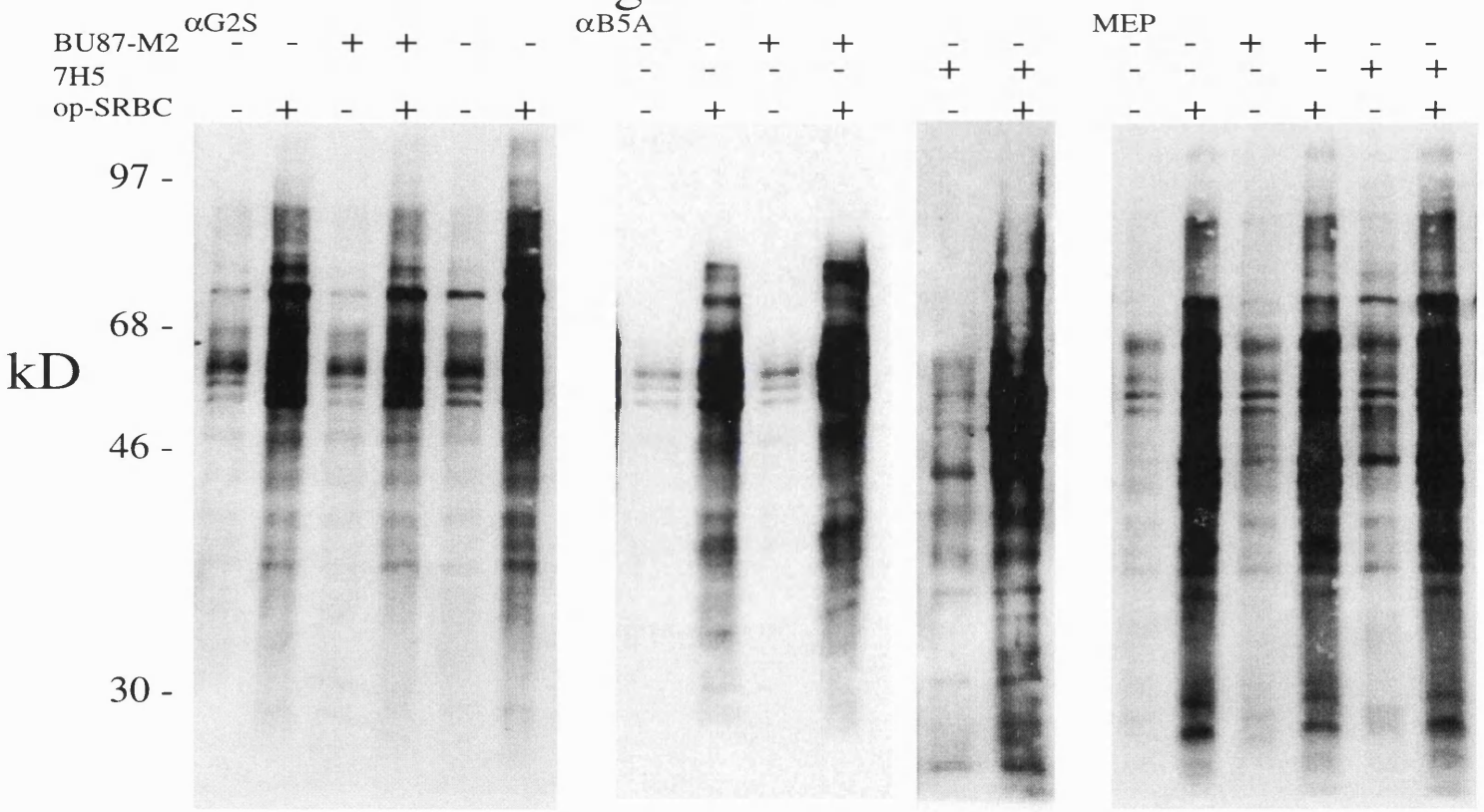

Figure 3.1.9.2. Effects of binding anti-CD13 (7H5), and anti-CD18 (BU87-M2) mAbs on the phosphotyrosine response to op-SRBC. 9-*cis* RA-treated αG2S, αB5A, or MEP cells were incubated with anti-CD13 (7H5) and anti-CD18 (BU87-M2) mAbs, then cultured with op-SRBC for 0 or 10 mins. Cell lysates (equivalent of $4x10^5$ cells per lane) were electrophoresed on 10% SDS-polyacrylamide gels, and anti-phosphotyrosine (with mAb 4G10) immunoblotting performed (section 2.4.).

Chapter 3.2. Discussion.

A role for retinoid receptors in monopoiesis has been suggested by the ability of RA and DHCC to mediate differentiation of monoblastic cell lines to mature monocytes. In a previous study from our laboratory (Brown et al., 1997; Brown T.R.P., 1995). we found that differentiation of the monoblastoid U937 cell line, induced by PMA, led to increased expression of RXRα and RXRβ mRNA, which suggested a role for RXRs in this differentiating step. Furthermore, studies of stably transfected U937-derived cell lines, indicated that growth arrest induced by RA and DHCC was mediated, at least in part, by dimers containing RXRα. Thus the role of RXRα in the differentiation and activation of monoblastic cells was examined, using these U937 transfectants as a model system.

Changes in phenotype of the U937 transfectants following 9-*cis* RA treatment are mediated by RAR-RXR dimers which promote transcription at DR2 and DR5 RARE and inhibit transcription at DR1 RARE; or by RXR-RXR dimers which promote transcription at DR1 RARE (reviewed by Mangelsdorf et al., 1995). The increase in intracellular RXRα concentration in αG2S cells could increase the formation of these heterodimers, and of RXR-RXR homodimers.

3.2.1. RXRα, RARα and RARβ are expressed in peripheral blood monocytes.

To examine the relevance of our previous findings regarding the importance of RXRs in monocyte development in leukeamic cell lines, expression of RXRα and other retinoic acid receptors was examined in human peripheral blood monocytes. Expression was also examined following addition of various differentiation-inducing stimuli (Figure 3.1.1.). In two separate experiments, RXRα was shown to be expressed in isolated monocytes, and this expression increased after 1 and 7 days treatment with human AB serum, but not upon DHCC or cytokine (IL-4, GM-CSF and TNFα) treatment.

Human AB serum and DHCC are agents that induce macrophage development (Andreesen et al., 1990; Kreutz and Andreesen, 1990; Kreutz et al., 1993), whilst IL-4-, GM-CSF- and TNFα-treated monocytes are often used to differentiate cells to dendritic cells (Pickl et al., 1996; Thomas et al., 1993; Xu et al., 1995). Human AB serum contains factors that induce differentiation, but the exact nature of these factors is not clear. This observation suggests that RXRα may be involved in AB serum-induced differentiation. It would be interesting to identify the factors/mechanism that increased RXRα expression so dramatically. DHCC is the ligand for VDR, and presumably induces differentiation via VDR-RXR, or in some cases VDR-VDR, dimers (Carlberg et al., 1993). The observation that DHCC treatment does not increase RXRα expression suggests that RXRα or RXRβ are present in sufficient concentration in day 0 monocytes, to act as dimerisation partners for liganded VDR, or that VDR-VDR dimers mediate DHCC-induced differentiation. In a previous study in our laboratory, growth arrest associated with DHCC-induced differentiation of the U937 transfectants to monocytes, was presumed to be mediated by VDR-RXRα dimers (Brown et al., 1997; Brown T.R.P., 1995). As the cells used in the present study are monocytes already, it is possible that VDR-RXRβ dimers are more important when differentiation to monocyte has already taken place.

The observation that AB serum treatment induced increased RXRα expression and that DHCC treatment did not suggests that monocyte-macrophage development can occur by more than one mechanism. This difference in mechanism of differentiation to a macrophage fate may be indicative of the fact that AB serum and DHCC induce different phenotypes of mature macrophage, respectively.

The observation that IL-4-, GM-CSF- and TNFα-treatment did not induce increased expression of RXRα, but that the level of expression was

maintained, suggests that RXRα may also be involved in directing monocytes to become dendritic cells, rather than macrophages.

The expression of RARα and RARβ was also assessed in these cells. Both these proteins were expressed in monocytes, and upon differentiation. Expression was at a lower level than when compared to RXRα, as much longer exposures of RAR immunoblots were required to achieve a similar band intensity to that of RXRα immunoblots. Although proteins were expressed upon treatment with the differentiation-inducing stimuli, no increase in expression of either protein was observed. This suggests that RARα and RARβ may play only a small role in monocytic differentiation. Evidence from HL-60 cells suggests that RARα is important in the differentiation of cells to become granulocytes (Collins et al., 1990), and that expression of RARs are decreased upon differentiation to become monocytes (McTernan et al., 1998). This suggests that RARs, and in particular RARα, do not have an important role in monocyte and macrophage development.

3.2.2. RXRα, RARα and RARβ are expressed in the U937 transfectants.

The levels of RXRα in the U937 transfectants had not previously been directly examined by immunoblotting. These data confirmed previous data which suggested that different amounts of RXRα protein were expressed in the three U937 transfectants (Figure 3.1.2.1.). Sense (αG2S) cells expressed higher levels of RXRα than the MEP control cell line, which in turn expressed more RXRα than antisense (αB5A) cells. These differences in expression were potentiated by the addition of Cd^{++} ions, which induced the hMTIIa promoter which controlled expression RXRα. It was noticeable that even in the absence of Cd^{++} ions there were substantial differences in the expression of RXRα, this was due to either the leakiness of the promoter, or due to the promoter interacting with heavy metals, such as Zn^{++} ions, contained within the media.

The expression of RARα and RARβ was also examined in the U937 transfectants (Figure 3.1.2.1.). Both RARα and RARβ were expressed in all three U937 transfectants. These levels were largely unaffected by addition of Cd^{++} ions to further induce RXRα expression. These data show that over-expression of RXRα does not effect the levels of these other retinoid receptors. However, the level of RARα was decreased in all three transfectants following 9-*cis* RA treatment. This could be due to a conformational change in RARα upon 9-*cis* RA binding, or could indicate that 9-*cis* RA binding to RARα leads to a decrease in expression. Although this decrease was seen in all three U937 transfectants, it could also be mediated by RXR, by either the low level of RXRα in αB5A cells, or by RXRβ, which is expressed in the parent U937 cell line (Brown et al., 1997; Brown T.R.P., 1995). This decrease could be particularly important in monocyte differentiation as in HL-60 cells induced to differentiate with DHCC to become monocytes, RAR expression is also decreased (McTernan et al., 1998). Consistent with this it has also been demonstrated that RARα is involved in neutrophilic differentiation of HL-60 cells (Collins et al., 1990), thus suggesting that "suppression" of RARα expression is an important step in monocytic differentiation. Expression of RARβ was not affected by 9-*cis* RA treatment.

3.2.3. Cell surface protein expression on the U937 transfectants.

Figure 3.2.3. shows U937 cell differentiation induced by 9-*cis* RA. This shows the cell surface molecules that were tested in this section, expression of which may be indicative of a either a immature or mature monocyte phenotype.

Figure 3.2.3.

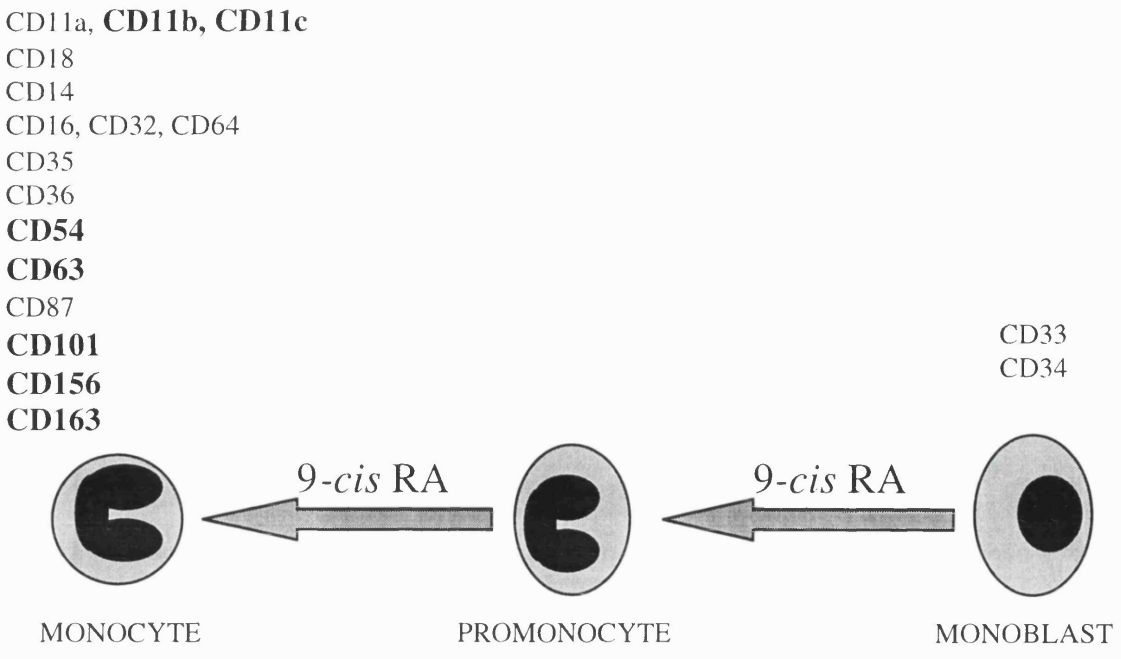

Figure 3.2.3. Schematic representation of cell surface protein expression during monoblast (U937) differentiation. The proteins written above monoblasts and monocytes are those that the expression of is indicative of either a mature or immature monocyte phenotype. The proteins shown in bold are those that have increased expression on 9-*cis* RA-treated αG2S cells, and or decreased expression on 9-*cis* RA-treated αB5A cells, thus indicating that αG2S cells are more mature and αB5A cells are less mature, than the control MEP cell line.

3.2.3.1. Expression of ICAM molecules.

Expression of ICAM molecules was assessed on the U937 transfectants (Table 3.1.3.1.). ICAM-1 (CD54) was the predominantly expressed ICAM on all three cell lines, and expression of ICAM-1 increased upon 9-*cis* RA treatment only in αG2S cells. ICAM-2 (CD102) was only expressed on untreated and 9-*cis*-RA-treated αB5A cells, whilst ICAM-3 (CD50) was not expressed on any transfectant.

Monocytes express moderate levels of ICAM-1, and increases in expression are normally associated with treatment of inflammatory

cytokines, such as IFN-γ and TNF-α (Springer, 1990). This suggests that retinoid receptors could play a role in activating these cells to more activated phenotype. In previous studies both U937 cells, and U937 cells stably transfected with RARα cDNA, exhibited increased expression of CD54 upon all-*trans* RA treatment (Aldinucci et al., 1997). This further suggests that the increase in ICAM-1 expression seen in 9-*cis*-RA-treated αG2S cells was due to RARα-RXRα dimers, and that liganded RARα may be functionally important in this process. ICAM-1 is the receptor for the integrins LFA-1 (CD11a/18), and Mac-1 (CD11b/18) (Springer, 1990). Through these interactions ICAM-1 has roles in adhesion and in co-stimulation of T-cell responses. The increased expression in 9-*cis*-RA-treated αG2S cells of ICAM-1 and CD11b (Brown et al., 1997) and section 3.2.3.2.), may be the reason why these cells become slightly adherent to plastic and each other after 48 hours 9-*cis*-RA-treatment (data not shown).

ICAM-2 is a further receptor for LFA-1, but not Mac-1 (Springer, 1990). ICAM-2 is predominantly expressed on vascular endothelial cells, which suggests a role in leukocyte trafficking. It is also expressed on some populations of monocytes and lymphocytes, but not on neutrophils, and this expression is not induced by inflammatory cytokines, as is ICAM-1 (de Fougerolles et al., 1991). The observation that αB5A cells express less ICAM-2, suggests that RXRα may be involved in the inhibition of ICAM-2 expression in monocytes. This possible RXRα-mediated inhibition may be important in why some populations of monocytes express ICAM-2 and others do not.

ICAM-3 (CD50) is expressed only on cells of leukocyte origin, and acts as the third receptor for LFA-1 (de Fougerolles and Springer, 1992). ICAM-3 expression is not induced by inflammatory cytokines. RXRα expression or ligation appeared to play no role in regulation of CD50 expression.

3.2.3.2. Expression of integrins.

To confirm the differences in expression previously observed (Brown et al., 1997; Brown T.R.P., 1995), expression of integrins in the U937 transfectants was examined. As before, CD18 (β2 chain) was found to be highly expressed on all U937 transfectants. Two further CD11b mAbs confirmed that expression of this molecule was increased on 9-*cis*-RA-treated αG2S cells. One further CD11c mAb suggested that expression of this molecule was also increased on 9-*cis*-RA-treated αG2S cells. Increased expression of these integrin molecules is associated with a more mature monocyte phenotype (see Chapter 1, section 1.1.). Integrins are involved in important monocyte/macrophage processes such as adherence to other cells and extracellular matrix (CD11a/18 (LFA-1), CD11b/18 (Mac-1) and CD11c/18), as well as in immunophagocytosis (CD11b/18 (Mac-1) and CD11c/18) (Springer, 1990). This suggests that 9-*cis*-RA-treated αG2S cells are more differentiated than MEP or αB5A cells, and that RXRα plays a role in inducing the expression of these important functional molecules.

3.2.3.3. Expression of other cell surface molecules.

mAbs against CD13, CD33, CD36, CD64, CDw65, CD89, CDw92, CDw93 and CD157 bound to over 90% of all three U937 transfectants with equal density.

- CD13 (aminopeptidase N), is a protein expressed as a homodimer on the surface of developing and mature monocytes/macrophages and neutrophils. CD13 is a zinc-binding metalloprotease that catalyses the removal of single amino residues from the N-terminal end of small peptides (Goyert, 1997a). As expression of CD13 is stable throughout monocyte development it is not surprising expression was similar in the U937 transfectants.
- CD33 is a sialic acid-dependent cytoadhesion molecule, that acts as a dimer to bind carbohydrates. Expression of CD33 is limited to

monocyte/macrophage and neutrophil precursors, and expression decreases upon maturation. For this reason this molecule has been used as a useful marker for myeloid leukaemias. The function of CD33 remains unknown (Peiper and Guo, 1997). The observation that CD33 expression was similar in all three transfectant cell lines suggests that αG2S cells cannot be considered to be mature monocytes by this measure.

- CD36 is a major scavenger receptor for oxidised low density lipoproteins, and has been implicated in the production of macrophage foam cells during atherosclerosis. It has also been implicated in macrophage recognition and phagocytosis of apoptotic cells. In leukocytes CD36 is expressed on mature monocytes, macrophages, some dendritic cells and platelets (De Haas and Von Dem Borne, 1997). The fact that this molecule is expressed on all three cell lines suggests that U937 cells have passed the stage of monopoiesis at which CD36 expression is induced. This also suggests that RXRα plays no role in increasing expression of CD36.
- CD64 (FcγRI) is a high affinity receptor for IgG, and is involved in amongst other things, IgG mediated phagocytosis and ADCC (see Chapter 1 section 1.2.). CD64 is expressed on all monocytes, macrophages and dendritic cells. Expression can be increased on monocytes and macrophages by activation with inflammatory cytokines (Sun et al., 1997). The fact that this molecule is expressed on all three cell lines suggests that U937 cells have passed the stage of monopoiesis at which CD64 expression is induced. This also suggests that RXRα plays no role in increasing expression of CD64.
- The CDw65 mAb used in this study recognises the non-sialylated form of this protein. CDw65 is expressed on monocytes, neutrophils, on most myeloid progenitors and myeloid leukaemic cell lines. The functions of this protein are unknown (Kniep et al., 1997).
- CD89 (FcαR) is the high affinity receptor for IgA, and is involved in IgA mediated phagocytosis and degranulation (of neutrophils). CD89 is

expressed on immature and mature monocytes and neutrophils, and on some populations of macrophages (Kubagawa et al., 1997).

- CDw92 is a protein of unknown function that is expressed on monocytes, neutrophils and myeloid cell lines (Goyert, 1997b).
- CDw93 is a sialylglycoprotein of unknown function that is also expressed on monocytes, neutrophils and myelomonocytic cell lines (Goyert, 1997c).
- CD157 (BST-1) is expressed on both mature and precursor neutrophils and monocytes, some macrophages and most myelomonocytic cell lines. CD157 is a GPI linked molecule that has ADP-ribosyl cyclase and cyclic ADP-ribose hydrolase activities. The product of these enzymatic activities have been shown to release Ca^{++} ions from the endoplasmic reticulum inside cells, but the role of these products extracellularly is unknown (Ishihara et al., 1997).

Of three CD15 mAbs tested, each bound differently to the U937 transfectants. This result could be due to extensive post-translational modification, such as addition of sialyl groups, that this protein undergoes. The forms of this protein act as adhesion molecules, interacting with CD62 (E-, P- and L-selectin), and some reports have suggested homotypic CD15-CD15 interactions. CD15 is expressed on monocytes, neutrophils and also on many cancer cell lines (Kannagi, 1997). The decrease in expression seen with one mAb in αB5A cells could be an RXRα mediated event, but this is unclear. As CD15 is present on most cancer cells, expression seen in all three cell lines could be due to the fact that these cells are leukaemic cell derived.

With two CD34 mAbs, CD34 was expressed with increased density and on an increased percentage of 9-*cis*-RA-treated αG2S cells. CD34 is an important marker of haemopoietic progenitor cells. It is thought to be involved in cell-cell adhesion and with inhibition of cell proliferation and differentiation. Although its exact functions remain unknown. CD34 mAb

recognise four different classes of epitope, which are dependent on the type of CD34 glycosylation. The reason that one CD34 mAb did not bind is that it recognises a Class II CD34 epitope, whilst the other two mAbs both recognise Class III CD34 epitopes (Nishio et al., 1997). The reason why 9-*cis*-RA-treated αG2S cells express more of this progenitor marker, when they appear to be more differentiated in most other ways, is not clear.

One CD63 mAb, bound to a lower percentage of 9-*cis*-RA-treated αB5A cells. CD63 is a member of the tetraspan protein family. CD63 is expressed on the lysosome of most leukocytes, and is expressed on the cell surface following cell activation/degranulation. Its function is again unknown (De Haas et al., 1997). This lower expression on αB5A cells may be indicative of a less activated cell phenotype.

One CD66b mAb did not bind to any U937 transfectant, whilst one CD66acde mAb bound equally to a small percentage of each transfectant. CD66 are neutrophil and neutrophil precursor markers, that bind selectins as well as other CD66 isoforms. They are involved in neutrophil activation, are thought to mediate integrin dependent adhesion, and mediate signal transduction by interacting with Src family kinases (Skubitz et al., 1997).

CD87 (urokinase plasminogen activator receptor-uPAR), is a GPI linked receptor for uPA. CD87 is expressed on activated leukocytes, predominantly at the leading edge of leukocytes migrating through the extracellular matrix (ECM). This protein can initiate a process that leads to hydrolysis of ECM, that is impeding migration of the leukocyte, by plasmin. In this way CD87 is thought to contribute to neoplastic and inflammatory cell invasion of tissues (Todd et al., 1997). Expression of CD87 in the U937 transfectants could be indicative of an activated phenotype, or could be due to the leukaemic nature of the cell lines. In

our laboratory, CD87 has been implicated as a possible co-stimulatory molecule that is highly expressed on peripheral blood dendritic cells (Woodhead et al., 1998).

CD98 is a disulphide-linked heterodimer of a 80kD protein and a undefined 45kD protein. CD98 is widely expressed, and expression is induced upon cell activation. CD98 has been shown to have slight homology to amino acid transporters (Diaz et al., 1997a). More recently, CD98 has been associated with regulation of β1 integrin signalling (Fenczik et al., 1997). One mAb (J3-E1B) binds to the U937 transfectants and the other (J1-G3B) mAb does not bind as well. This is due to J3-E1B being targeted against the heavy chain of CD98 (80kD), whilst J1-G3B co-precipitates a 45kD protein closely associated with the heavy chain which may be the disulphide linked chain (Diaz et al., 1997a). A more extensive discussion of CD98 can be found in Chapter 5.2.

CD101 is widely expressed on mature monocytes, neutrophils, dendritic cells and T-cells. There is evidence that CD101 is important in T-cell activation, CD101 positive T cells being highly responsive to CD28 signalling. With the same mAbs U937 cells have previously shown to be negative for CD101. This suggests that CD101 may be a marker of a mature U937 phenotype. Thus 9-*cis* RA-treated αG2S and MEP cells may be more mature than αB5A cells. The two mAbs tested recognise separate epitopes of CD101, which have different patterns of expression (Boumsell et al., 1997). This may be the reason that one mAb and not the other bound to the U937 transfectants.

CD148 (p260 phosphatase) is a receptor protein tyrosine phosphatase that does not have any defined functions. CD148 is expressed widely on neutrophils, monocytes and dendritic cells. Both mAbs used recognise the same epitope, so the differences in percentage cells bound was probably due to mAb affinity or concentration (Schraven et al., 1997).

CD156 (ADAM 8) is a metalloprotease, that is expressed on monocytes, neutrophils and myelomonocytic cell lines. CD156 has been previously shown to be upregulated by RA and DHCC treatment. CD156 is thought to play a role in the digestion of the basement membrane, and remodelling of the ECM, during leukocyte migration (Higuchi et al., 1997). The observation that αG2S express more CD156 again suggests that these cells are of a more mature phenotype.

CD163 is a member of the scavenger receptor family, expression of which is restricted to monocytes and macrophages. The ligand and functions of CD163 are unknown. Previously U937 cells have been shown to express CD163 following PMA treatment (Pulford et al., 1997). Therefore, the increase in expression of this antigen in 9-*cis*-RA-treated αG2S cells can be considered as a measure of cell maturation.

Of the antigens that were not present on any of the U937 transfectants the most relevant were CD14 and CD35. CD14 is a monocyte specific marker. This protein is a GPI linked LPS receptor, and is important in monocyte responses to bacterial products (Goyert et al., 1997d). It has been shown previously that RA treatment will not induce CD14 expression of U937 cells (Sellmayer et al., 1994). This data confirms this, and suggests RA will not differentiate U937 cells to fully mature monocytes, but to an intermediate stage. Furthermore, it demonstrates that increasing RXRα expression does not overcome this differentiative block. It suggests that other mechanisms are involved in induction of CD14, and full monocyte phenotype.

CD35 (CR1) is a complement receptor that is expressed on mature phagocytes. CD35 binds C3b and C4b, and plays a role in FcγR mediated phagocytosis (Nickells et al., 1997). The lack of this antigen also suggests

that none of the U937 transfectants had reached a fully mature monocyte phenotype.

3.2.4. Immunophagocytosis by the U937 transfectants.

3.2.4.1. Differences in efficiency of immunophagocytosis.

U937 cells acquire when induced to differentiate with factors such as PMA, RA and DHCC, monocyte/macrophage phenotypic functions. One of these functions is immunophagocytosis (Harris and Ralph, 1985). Therefore, as a further measure of U937 differentiation the process of immunophagocytosis was investigated. Two independent measures showed that 9-*cis*-RA-treated αG2S cells had increased efficiency of immunophagocytosis when compared to MEP cells, which in turn were more efficient than αB5A cells (Figures 3.1.4.1. and 3.1.4.2.). The differences seen in levels of immunophagocytosis was not due to altered expression of Fcγ receptors on the U937 transfectants, as all three transfectants expressed equal amounts of Fcγ receptors (Brown et al., 1997; Brown T.R.P., 1995).

Overall, the increase in immunophagocytic capability of αG2S cells is consistent with the theory that over-expression of RXRα makes it possible for the cells to develop a more mature monocyte/macrophage phenotype in response to 9-*cis* RA than is possible without excess RXRα.

Furthermore, cytoskeletal actin staining showed that the immunophagocytosed op-SRBC were fully internalised by the transfectants, not just bound at the membrane, and that this was associated with striking changes in cell configuration, with development of numerous cytoplasmic processes when compared to cells that had not been exposed to the immunophagocytic stimulus (Figure 3.1.4.3.). Actin staining revealed that all three cell lines reacted in similar ways in response to op-SRBC, with no qualitative differences in the amount of

organisation of the cytoskeleton. This suggested that other mechanisms be involved in the quantitative differences in immunophagocytosis.

3.2.4.2. Proteins involved in immunophagocytosis.

To investigate cell surface molecules involved in immunophagocytosis, mAbs were pre-incubated with the transfectants prior to addition of ^{51}Cr-op-SRBC. Two mAbs against CD16 (FcγRIII) (3G8 and leu-11-b) inhibited the quantitative assay, whilst CD32 (FcγRII) (IV3) and CD64 (FcγRI) (32) mAbs did not (Figure 3.1.5.1.). Furthermore, the CD16 mAbs inhibited uptake in a dose-dependent manner (Figure 3.1.5.2.). Theoretically, any FcγR could have been involved in immunophagocytosis.

Although some studies have found that CD16 (FcγRIII) is not expressed on U937 cells (Ninomiya et al., 1994). Other studies have found expression of CD16 on U937, or that expression can be induced upon differentiating stimuli, such as TNFα (Faulkner et al., 1993; Gessl et al., 1994; Ikewaki et al., 1993). In previous studies in our laboratory it has been shown that CD16 was expressed on all three U937 transfectants, regardless of any differentiating stimuli (Brown et al., 1997; Brown T.R.P., 1995). This could be due to differences in U937 clones from one laboratory to another, or that the media that the U937 transfectants are maintained in contains factors that induce expression of this protein.

Another possibility for increased immunophagocytic ability of αG2S cells, is increased expression of other molecules involved in FcγR mediated phagocytosis. The complement receptors CR3 (Mac-1 or CD11b/18) and CR4 (CD11c/18) are such molecules (see Chapter 1, section 1.2). It has been shown that CR3 is required for efficient FcγR mediated phagocytosis (Gresham et al., 1991), and that CD16 (FcγRIII) and CR3 are physically associated by a lectin link (Zhou et al., 1993). As shown previously (Brown et al., 1997; Brown T.R.P., 1995), and in this

thesis (see section 3.1.3.2.), 9-*cis* RA treatment increased the expression of CD11b and CD11c on the U937 transfectants. This increase in expression was augmented further in 9-*cis* RA-treated αG2S cells. In contrast, CD18 was highly expressed equally on all U937 transfectants, and levels were not affected by 9-*cis* RA treatment. Previously, it has been shown that that a CD18 deficiency also leads to a lack of cell surface expression of CD11b and CD11c. Therefore, it is a possibility that the increase in efficiency of immunophagocytosis was due to increased expression of the components of CR3 (CD11b) and CR4 (CD11c) in αG2S cells. CR1 (CD35), another complement receptor was shown not to be expressed on any U937 transfectant (see Appendix IV).

Confirming a possible role for CR3 and or CR4, a mAb directed against CD18 (BU87-M2), inhibited immunophagocytosis in a dose-dependent manner (Figures 3.1.6.1. and 3.1.6.2.). This demonstrated that CR3 and or CR4 play a role in immunophagocytosis by all three U937 transfectants, and that increased phagocytic abilities may be due to the increased levels of CR3 and or CR4 on αG2S cells. However, in the same set of experiments, a further CD18 mAb (BU86) did not inhibit immunophagocytosis (Figure 3.1.6.1). This suggests that the epitope targeted by CD18 mAbs may be important in its inhibitory activity. Also in the same experiments, CD11b and CD11c mAbs did not inhibit immunophagocytosis (Figure 3.1.6.1). This suggests that CD18 is the important component of CR3 and CR4 in mediating phagocytosis. However, another alternative, is that the epitopes recognised by the particular CD11b and CD11c mAbs, do not recognise functionally relevant parts of the protein could not be excluded. These data do not discount that LFA-1 (CD11a/18), is involved in phagocytosis, although there is no previous evidence for this.

In these studies, one other mAb inhibited immunophagocytosis in a dose-dependent manner. This mAb was targeted against CD13 (7H5) (Figures

3.1.6.1. and 3.1.6.2.). CD13 (aminopeptidase N), is a molecule that cleaves N terminal peptide residues. This protein was shown to be expressed equally on all U937 transfectants (see Appendix IV and section 3.2.3.3. for a brief description of CD13). CD13 has been shown to have a role in regulating the immune system. It has been shown to participate in the trimming of peptides bound to MHCII molecules (Larsen et al., 1996). CD13 also cleaves the chemokine MIP-1, and changes the target cell specificity of MIP-1 from basophils to eosinophils (Weber et al., 1996). No role for this molecule in immunophagocytosis has been previously reported.

3.2.4.3. Immunophagocytic induced tyrosine phosphorylation.

The increase in immunophagocytic efficiency in 9-*cis* RA-treated αG2S cells correlates with a more intense phosphotyrosine response to op-SRBC (figure 3.1.8.1.). This increase in signalling could be indicative of either more receptor-op-SRBC interactions at the cell surface, or of more efficient signalling, by the recruitment of different signalling cascades. In addition, the pattern of phosphotyrosine responses between the U937 transfectants was different, which suggests that more signalling cascades are recruited in αG2S cells. However, this difference could also be due to an increase in receptor-op-SRBC interactions, as more interactions may trigger signalling in αG2S cell specific cascades by moving the stimulus over a threshold level.

A detailed discussion of the changes seen in phosphotyrosine signalling, and the mechanisms involved in immunophagocytic signalling, in the 9-*cis* RA-treated U937 transfectants can be found in Chapter 4.2.

In contrast to the results with 9-*cis* RA-treated U937 transfectants, DHCC-treated U937 transfectants responded similarly to each other following exposure to op-SRBC (Figure 3.1.8.2.). This demonstrates that the differences in phosphotyrosine responses seen previously are 9-*cis*

RA/RXR dependent. If intensity of phosphotyrosine responses is correlated to increase in immunophagocytic efficiency, this suggests that DHCC treatment does not increase the phagocytic capability of αG2S cells above that of αB5A or MEP cells. This is not surprising as previous evidence from these cell lines has suggested that levels of VDR are limiting in some DHCC responses (Brown et al., 1997; Brown T.R.P., 1995).

3.2.4.4. Effects of inhibitory mAbs on immunophagocytic induced tyrosine phosphorylation.

The mAbs, against CD13, CD16 and CD18, previously shown to be inhibitory of immunophagocytosis did not inhibit the phosphotyrosine response (Figure 3.1.9.1. and 3.1.9.2.). This suggests that the mAbs inhibited immunophagocytosis not by blocking interaction of op-SRBC with the phagocytic receptor complex, but by blocking engulfment of op-SRBC. In order for this theory to be correct the CD16 mAbs must not bind to an epitope that blocks the IgG binding site. The primary signal transduced during phagocytosis, is by crosslinking FcγR (Metzger and Kinet, 1988). This crosslinking leads to phosphorylation of ITAM of FcγR or of associated γ chains (Santana C. et al., 1996), this then leads to downstream signal transduction. Another explanation for the phosphotyrosine response observed in the presence of CD16 mAbs, could be due to unsaturated CD16, as CD16 mAbs did not completely inhibit the uptake of ^{51}Cr-op-SRBC.

The inhibition of engulfment by both CD13 and CD18 mAbs suggests that these molecules co-localise with CD16, which presumably mediates the initial signal transduction. CD18 has been shown to be physically linked to CD16 (Zhou et al., 1993), but no evidence for any interaction between CD13 and CD16 exists. Additionally, CD13 mAb in isolation, induces phosphorylation of a 46 kD protein in MEP cells, CD13 is a

transmembrane protein with an intracellular region, but there is no previous evidence that this peptidase has signalling potential.

3.2.5. Expression of NADPH oxidase components.

NADPH oxidase is activated during phagocytosis to produce superoxide, a precursor of microbicidal oxidants (Roos et al., 1996). During phagocytosis four sub-units of this enzyme assemble, and form an activated complex. gp91-phox and p22-phox are tightly associated membrane bound sub-units that comprise a *b*-type cytochrome. On phagocytosis this cytochrome migrates to the base of nascent phagosomes. For activation to occur two cytosolic proteins, p47-phox and p67-phox, must migrate to the membrane and associate with the cytochrome. This complex accepts electrons from NADPH on the cytosolic side of the membrane, and donates these to molecular oxygen on the inside of the phagosome, in this way superoxide is produced. The activity/migration of p67-phox and p47-phox is regulated by phosphorylation (Bolscher et al., 1989; Dusi and Rossi, 1993). Mutations of any component of the NADPH oxidase leads to chronic granulomatous disease, a genetic disease characterised by the inability of phagocytes to produce ROS, which are needed for intracellular killing of pathogens.

The expression of p67-phox and p47-phox was investigated in 9-*cis* RA-treated U937 transfectants, and results used as a measure of monocytic maturation, and as a possible functional reason that αG2S cells may be more efficient phagocytes. These data showed that 9-*cis* RA-treated αG2S cells expressed more p47-phox, than MEP cells. 9-*cis* RA-treated αB5A cells showed no expression of p47-phox. In contrast, no expression of p67-phox was detected in any U937 transfectant. This suggests that 9-*cis* RA-treated αG2S cells are of a more mature phenotype than MEP cells, which themselves are more mature than αB5A cells. It is also possible that the increased p47-phox expression is RXR dependent, and that p67-phox expression is regulated by different mechanisms. As NADPH oxidase

requires all of its sub-units to produce superoxide, it is unlikely that the increased levels of p47-phox has any functional effect on phagocytic efficiency, as no p67-phox was expressed by any cell.

Chapter 4

4.1. Results

Signalling processes involved in immunophagocytosis by the U937 transfectants.

Once immunophagocytosis, and associated cell activation has occurred, then the consequences are likely to be reflected in the activation status of common intracellular signalling cascades that have been identified. Therefore, 9-*cis* RA-treated U937 transfectants were exposed to op-SRBC for various time points, cell lysates prepared, and the activation state of several "signalling" proteins examined in order to determine which cascades are involved in immunophagocytosis by the U937 transfectants, and more specifically, which proteins are activated differentially in response to op-SRBC in the three cell lines. Next, a panel of glutathione-SH2 domain fusion proteins was used to screen op-SRBC exposed cell lysates, to determine which SH2 domains interact with tyrosine phosphorylated proteins. Lastly, the phosphorylation of candidate proteins that may be functionally related to the increase in immunophagocytic ability in αG2S cells was examined. Information on the signalling mechanisms considered here has been reviewed in Chapter 1, section 1.3.

4.1.1. Mitogen activated protein kinases (MAPK) are phosphorylated in response to addition of op-SRBC.

Members of the MAPK family of tyrosine kinases have been identified as being phosphorylated during phagocytosis mediated by FcεR (Hirasawa et al., 1995; Jabril Cuenod et al., 1996). Furthermore, Jnk and ERK-2 are proteins of 46 and 44 kD respectively, and therefore were candidate proteins for the 46kD protein that is phosphorylated in αB5A and MEP cells, but not αG2S cells. Therefore, the phosphorylation states of three

members of the MAPK family were assessed, either by immunoblotting with antibodies specific for the phosphorylated forms of Jnk or p38, or by the usage of a specific ERK-1 and ERK-2 mAb that recognises both unphosphorylated and phosphorylated forms. This was accomplished by observing a shift in mobility of ERK proteins that occurs upon phosphorylation, so that phosphorylated ERK-1 and ERK-2 proteins appear larger than unphosphorylated forms (Meighan Mantha et al., 1997; Santini and Beaven, 1993).

4.1.1.1. ERK-1 phosphorylation in response to op-SRBC.

Figure 4.1.1.1. shows phosphorylation of ERK-1 protein in response to ten of minutes exposure to op-SRBC in all three of the U937 transfectants. This is demonstrated by a shift in mobility of ERK-1 in response to addition of op-SRBC, from 42kD to 45kD. This change in mobility is a well recognised property of ERK phosphorylation (Meighan Mantha et al., 1997; Santini and Beaven, 1993). ERK-2 was not detected in any cell lysate.

4.1.1.2. p38 is phosphorylated in response to op-SRBC.

Figure 4.1.1.2. shows phosphorylation of p38 in response to ten minutes of exposure to op-SRBC in all three of the U937 transfectants. The top panel shows that addition of op-SRBC induced increased levels of phosphorylated p38 as defined by the increased signal in these lanes. This antibody recognises p38 phosphorylated on both tyrosine 182 and threonine 180. The lower panel shows the total expression of p38, demonstrating that p38 is found in all three cell lines and that similar amounts of protein are expressed in all lanes on the blot.

Figure 4.1.1.1.

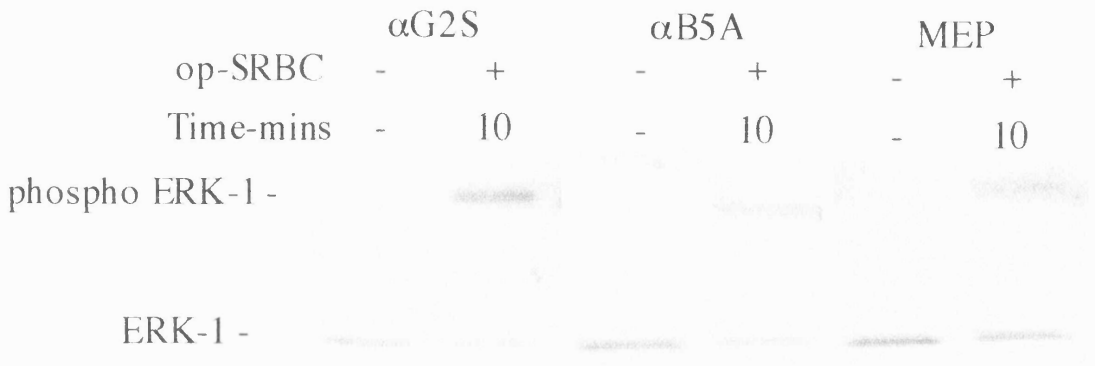

Figure 4.1.1.1. Phosphorylation of ERK-1 in the U937 transfectants upon exposure to op-SRBC.

$6x10^6$ 9-*cis* RA-treated αG2S, αB5A or MEP cells were cultured with 10^8 op-SRBC for the time points indicated. Cells were lysed in 1%NP40 lysis buffer. Cell lysates (equivalent of $5x10^5$ cells per lane) were run on 10% SDS-polyacrylamide gels. Separated proteins were transferred to nitrocellulose filters, filters were incubated with anti ERK-1 and ERK-2 immunoblots performed (see section 2.4.).

Figure 4.1.1.2.

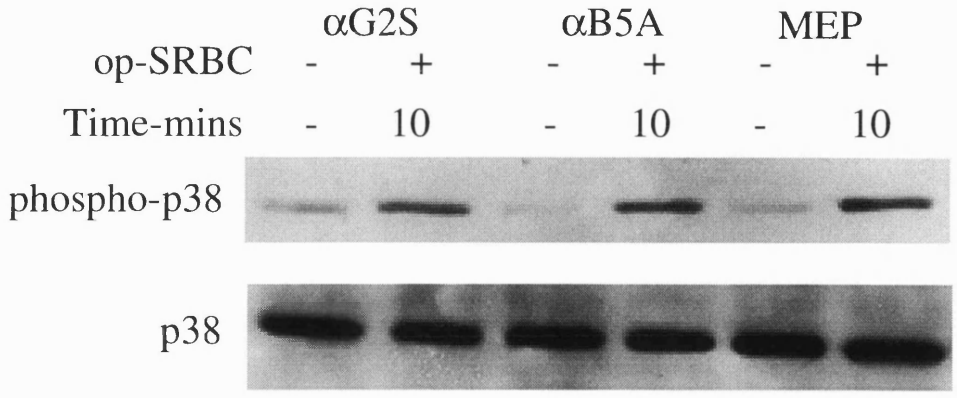

Figure 4.1.1.2. The p38 stress kinase is phosphorylated in the U937 transfectants upon exposure to op-SRBC.

$6x10^6$ 9-*cis* RA-treated αG2S, αB5A or MEP cells were cultured with 10^8 op-SRBC for the time points indicated. Cells were lysed in 1%NP40 lysis buffer. Cell lysates (equivalent of $4x10^5$ cells per lane) were run on 10% SDS-polyacrylamide gels. Separated proteins were transferred to nitrocellulose filters, filters were incubated with either anti p38 Ab (bottom panel), or anti phospho-p38 Ab (top panel) (see section 2.4).

4.1.1.3. Jnk is phosphorylated in response to op-SRBC.

Figure 4.1.1.3. shows phosphorylation of Jnk in response to ten and two hours exposure to op-SRBC in all three of the U937 transfectants. The top panel shows that addition of op-SRBC, induced increased levels of phosphorylated Jnk as defined by the increased signal in these lanes. This antibody recognises Jnk1 and Jnk2 which is phosphorylated on both tyrosine 185 and threonine 183. The lower panel shows the total expression of Jnk1 and Jnk2, demonstrating that Jnk is found in all three cell lines, but that ~~either~~ different amounts of protein were loaded on to this gel. Another possibility is that Jnk is differentially expressed in the U937 transfectant cell lines, as it appears from this gel that αG2S cells express more Jnk than either αB5A or MEP cells. This would be an interesting area of future research (also see Chapter 6.2.).

4.1.2. The activation state of the adaptor molecule Shc is not effected by exposure to op-SRBC.

Another protein that is involved in signal transduction in many systems is the adaptor molecule Shc. Its activation state is also controlled by phosphorylation. Shc has two forms, of 46 and 50kD respectively, and is involved in the Ras pathway. Figure 4.1.2. shows that the phosphorylation state of Shc was not affected by addition of op-SRBC, but that Shc was already phosphorylated prior to op-SRBC addition in both αG2S and MEP cells. This result also shows that Shc was not abundant enough to be detected by immunoblotting of lysates. Immunoprecipitation from these lysates with an anti-phosphotyrosine mAb shows that Shc is present and is phosphorylated, but that addition of op-SRBC does not effect this phosphorylation. The two lower bands seen on the blot correspond to the two forms of Shc (one of 46kD and one of 50kD). The third higher band is a Shc related protein with which the Shc antibody cross reacts, this protein was also phosphorylated in these cells.

Figure 4.1.1.3.

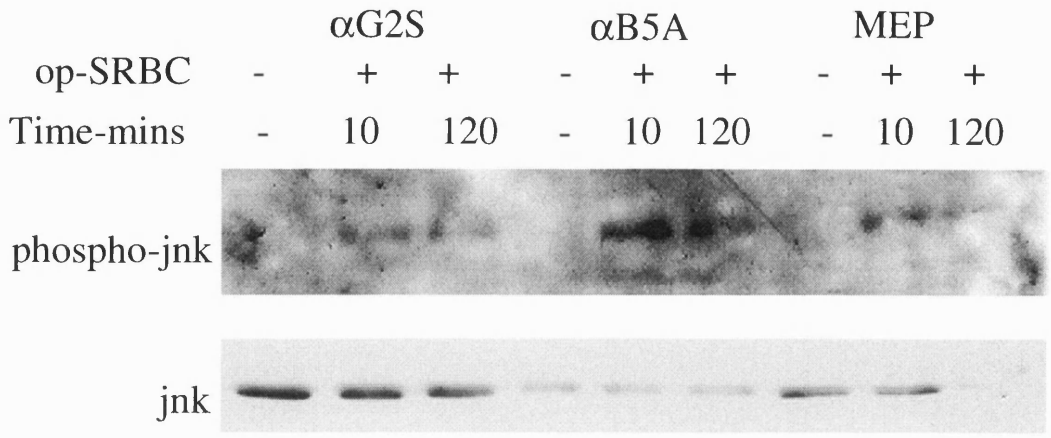

Figure 4.1.1.3. The Jnk stress kinase is phosphorylated in the U937 transfectants upon exposure to op-SRBC.

$6x10^6$ 9-*cis* RA-treated αG2S, αB5A or MEP cells were cultured with 10^8 op-SRBC for the time points indicated. Cells were lysed in 1%NP40 lysis buffer. Cell lysates (equivalent of $4x10^5$ cells per lane) were run on 10% SDS-polyacrylamide gels. Separated proteins were transferred to nitrocellulose filters, filters were incubated with either anti Jnk Ab (bottom panel), or anti phospho-Jnk Ab (top panel) (see section 2.4).

4.1.3. Expression of FRIP, a regulator of rasGAP, in the U937 transfectants.

FRIP is a novel protein of 54kD which has been recently described (Nelms et al., 1998). This protein has only been found in cells of T cell lineage and in some haematopoeitic cells. Activated FRIP binds and regulates RasGAP activity, which itself regulates the level of activation of Ras. Expression of this protein was investigated because of its possible role in down-regulation of the Ras activity. 9-*cis* RA-treated U937 transfectants were lysed and expression of FRIP assessed by immunoblotting. Figure 4.1.3. shows that both αG2S and MEP cells express FRIP whilst no expression was seen in αB5A cells. Primary human tonsillar CD4+ and CD8+ T cells were used as positive controls for expression of FRIP in these immunoblots.

4.1.4. Tyrosine phosphorylated proteins in the three U937 transfectants have differing associations with GST-SH2 fusion proteins of common signalling molecules.

A number of GST-SH2 fusion proteins derived from common signalling molecules were used to examine lysates of the three cell lines which had been exposed to op-SRBC. Fusion proteins containing Src SH2 (Figure 4.1.4A.), Grb-10 SH2 (Figure 4.1.4B.), Shc PTB (Figure 4.1.4C.), p85 (sub-unit of PI3-K) N and C terminal SH2 (Figure 4.1.4D. & E.), PLCγ C terminal SH2 (Figure 4.1.4F.) domains interacted with several proteins in each sample. The pattern of this interaction was different for lysates from each cell line, although there were also some similarities between the cell lines. PLCγ N terminal SH2 domain (Figure 4.1.4G.) did not interact with any

Figure 4.1.2.

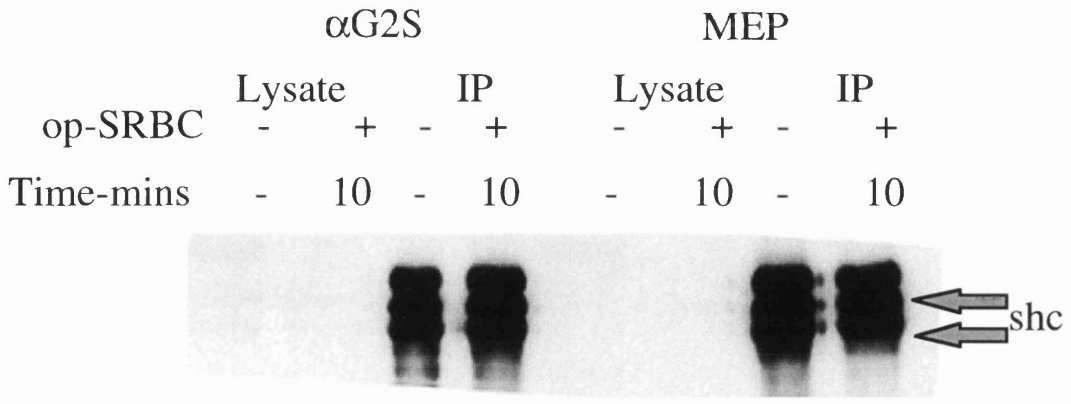

Figure 4.1.2. Activation of Shc is not affected in the U937 transfectants upon exposure to op-SRBC.

$6x10^6$ 9-*cis* RA-treated αG2S or MEP cells were cultured with 10^8 op-SRBC for the time points indicated. Cells were lysed in 1%NP40 lysis buffer. 150μl of each lysate was immunoprecipitated (IP) with 6μg of 4G10 anti-phosphotyrosine mAb (see section 2.13.). IP were run on 10% SDS-polyacrylamide gels along side non IP cell lysates (equivalent of $5x10^5$ cells per lane). Separated proteins were transferred to nitrocellulose filters and anti-Shc immunoblots performed (see section 2.4.)

Figure 4.1.3.

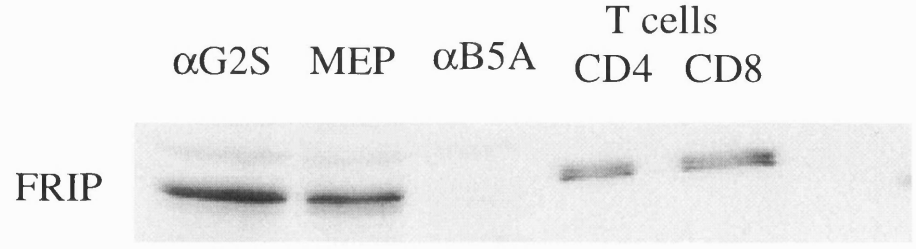

Figure 4.1.3. Expression of FRIP in the U937 transfectant cell lines.

$2x10^6$ 9-*cis* RA-treated αG2S, αB5A or MEP cells, and 10^7 purified human CD4+ or CD8+ tonsillar T cells were lysed in 1%NP40 lysis buffer. αG2S, αB5A and MEP cells (equivalent of $3x10^5$ per lane) and T cells (equivalent of 10^6 per lane), were run on 10% SDS-polyacrylamide gels. Separated proteins were transferred to nitrocellulose filters and anti-FRIP immunoblots performed (see section 2.4.).

phosphorylated proteins. Phosphorylated proteins from lysates of op-SRBC-exposed αG2S cells interacted with Shc SH2 (Figure 4.1.4H.) and Grb-2 SH2 (Figure 4.1.4I.) domains, whilst phosphorylated proteins from αB5A and MEP cell responses did not. The Shc-SH2 domain interacted with three phosphorylated proteins from αG2S cell lysates, of MW 72kD, 68kD, and 50kD. The Grb-2 SH2 domain also interacted with three phosphorylated proteins from αG2S cell lysates, of MW 68kD, 55kD, and 50kD. Figure 4.1.4J. shows the result of experiments on the same lysates using a control GST empty vector fusion protein, showing that no non-specific binding to GST alone was seen.

4.1.5. Phosphorylation of p47-phox and p67-phox was not induced in response to op-SRBC in the U937 transfectants.

Expression of the NADPH oxidase component p47-phox, but not of another component, p67-phox, was up regulated in 9-*cis* RA-treated αG2S cells (see section 3.1.7.). Previously it has been shown that phosphorylation of both p47- and p67-phox occurs during immunophagocytosis (Bolscher et al., 1989; Dusi and Rossi, 1993; Sumimoto et al., 1996). Therefore the phosphorylation states of these proteins were investigated in op-SRBC-exposed U937 transfectants. Figure 4.1.5A. shows that as previously shown p47-phox is expressed in αG2S cells but not in MEP or αB5A cells. It also shows that after anti-phosphotyrosine immunoprecipitations, followed by p47-phox immunoblotting, that little additional phosphorylation of p47-phox was seen. Figure 4.1.5B. shows that as before no p67-phox is expressed in any of these cells and that following anti-phosphotyrosine IP no phosphorylated p67-phox was detected. The bands seen in Figure 4.1.5B. are of 47 kD and probably represent the p67 phox antibody cross-reacting with p47 phox (personal communication with Prof AW Segal).

Figure 4.1.4.

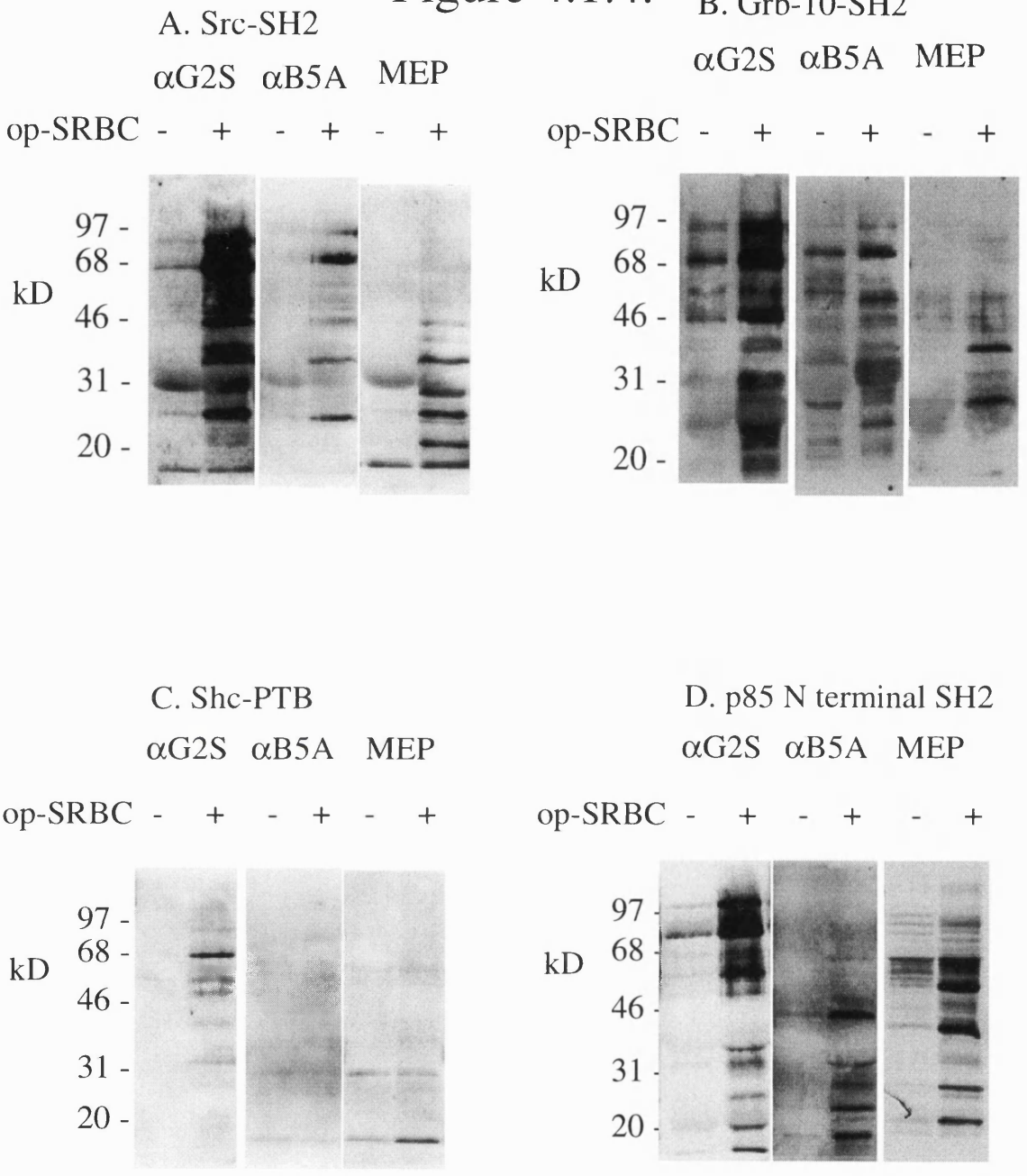
A. Src-SH2
αG2S αB5A MEP
op-SRBC - + - + - +
kD
97 -
68 -
46 -
31 -
20 -
B. Grb-10-SH2
αG2S αB5A MEP
op-SRBC - + - + - +
kD
97 -
68 -
46 -
31 -
20 -
C. Shc-PTB
αG2S αB5A MEP
op-SRBC - + - + - +
kD
97 -
68 -
46 -
31 -
20 -
D. p85 N terminal SH2
αG2S αB5A MEP
op-SRBC - + - + - +
kD
97 -
68 -
46 -
31 -
20 -

Figure 4.1.4.

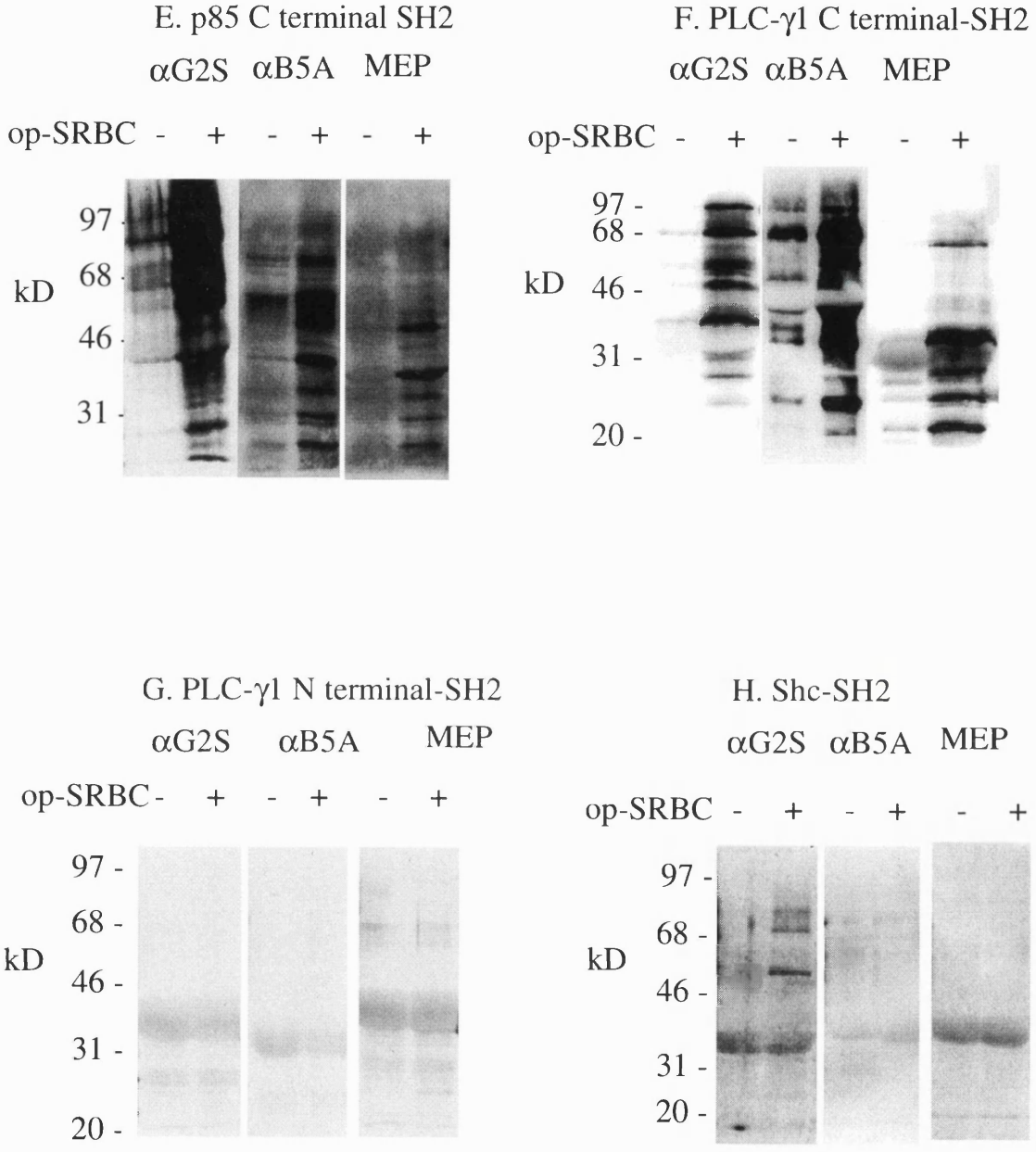
E. p85 C terminal SH2
αG2S αB5A MEP
op-SRBC - + - + - +
kD
97
68
46
31
F. PLC-γ1 C terminal-SH2
αG2S αB5A MEP
op-SRBC - + - + - +
kD
97
68
46
31
20
G. PLC-γ1 N terminal-SH2
αG2S αB5A MEP
op-SRBC - + - + - +
kD
97
68
46
31
20
H. Shc-SH2
αG2S αB5A MEP
op-SRBC - + - + - +
kD
97
68
46
31
20

Figure 4.1.4.

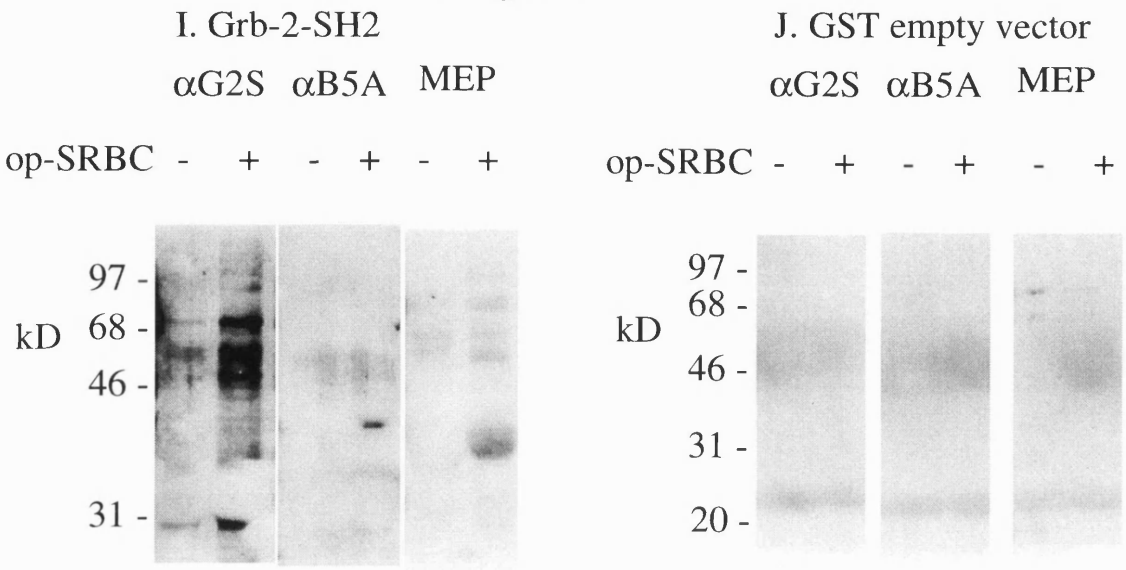

Figure 4.1.4. Tyrosine phosphorylated proteins from the U937 transfectants differentially interact with SH2 domains of signalling molecules.

$2x10^6$ 9-*cis* RA-treated αG2S, αB5A or MEP cells were cultured with $4x10^7$ op-SRBC for 0 or 10 minutes. Cells were lysed and lysates incubated with 10-20μg of glutathione bound agarose which had been preloaded with GST-SH2 fusion proteins. The resultant pellet boiled with 2x SDS denaturing loading buffer (see section 2.14 and 2.15.). 10μl of each sample was run on a 10% polyacrylamide gel, and anti-phosphotyrosine immunoblotting performed (see section 2.4.). The specific SH2 domain fusion proteins used are Src-SH2 (A), Grb-10 SH2 (B), Shc PTB (C), p85 N terminal SH2 (D), p85 C terminal SH2 (E), PLCγ C terminal SH2 (F), PLCγ N terminal SH2 (G), Shc SH2 (H), Grb-2 SH2 (I), and GST empty vector fusion protein (J).

4.1.6. Expression of paxillin in the U937 transfectants, and phosphorylation of paxillin in response to op-SRBC.

Paxillin is a protein of 68kD that is involved in the formation of focal adhesions and therefore in the organisation of the actin cytoskeleton. Phosphorylation of paxillin during immunophagocytosis has been demonstrated (Greenberg et al., 1994). Therefore, differential phosphorylation of this protein in the three cell lines could lead to a more organised cytoskeleton and more efficient immunophagocytosis. Figure 4.1.6A. shows that paxillin was expressed in all three U937 transfectants, and that the level of expression was unaffected by induction of RXRα expression with cadmium ions, or by induction of differentiation with 9-*cis* RA. Figure 4.1.6B. shows that in these cells no phosphorylation of paxillin occurred after exposure to op-SRBC. The bands seen in the IP's in these gels below 68kD were probably the secondary anti-mouse antibody used in immunoblotting, binding to the mouse anti-phosphotyrosine mAb used in the immunoprecipitation.

Figure 4.1.5.

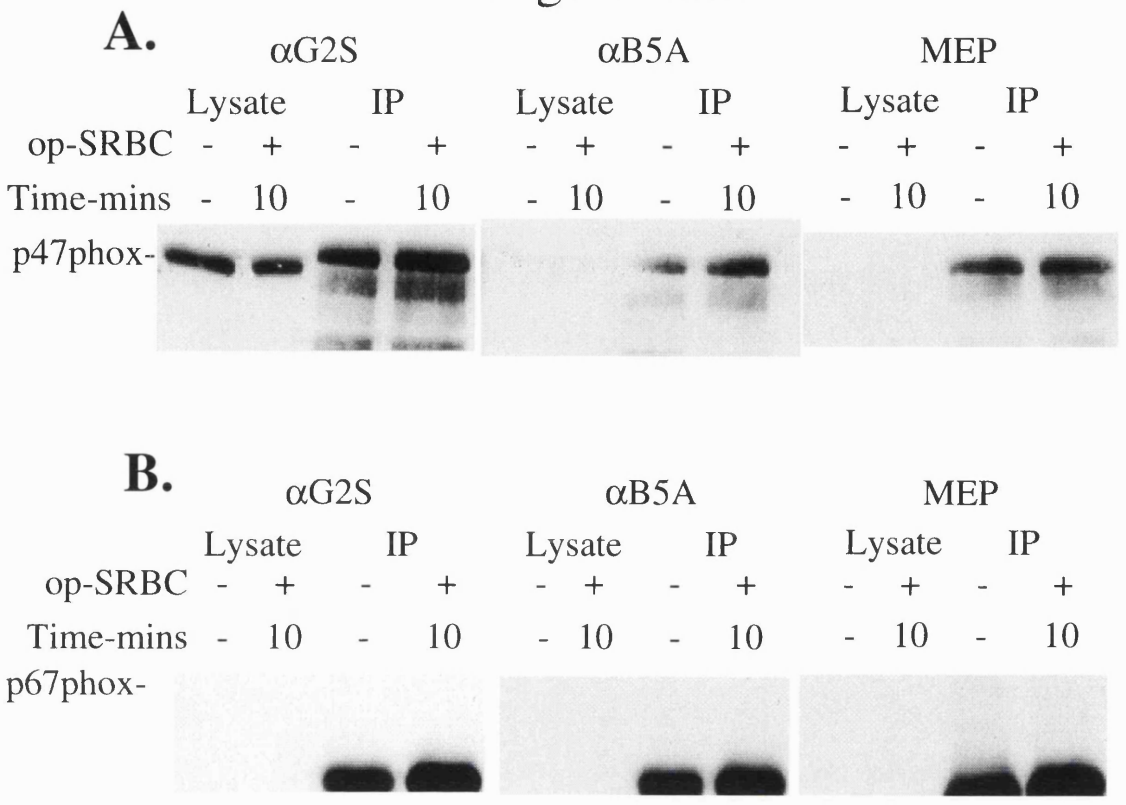

Figure 4.1.5. Phosphorylation of p47-phox and p67-phox is not induced in the U937 transfectants upon exposure to op-SRBC.

$6x10^6$ 9-*cis* RA-treated αG2S, αB5A or MEP cells were cultured with 10^8 op-SRBC for the time points indicated. Cells were lysed in 200μl of 1%NP40 lysis buffer. 150μl of each lysate was immunoprecipitated (IP) with 6μg of 4G10 anti-phosphotyrosine mAb (see section 2.13.). IP were run on 10% SDS-polyacrylamide gels along side non IP cell lysates (equivalent of $5x10^5$ cells per lane). Separated proteins were transferred to nitrocellulose filters and anti-p47-phox (A), or p67-phox (B) immunoblots performed (see section 2.4.)

Figure 4.1.6.

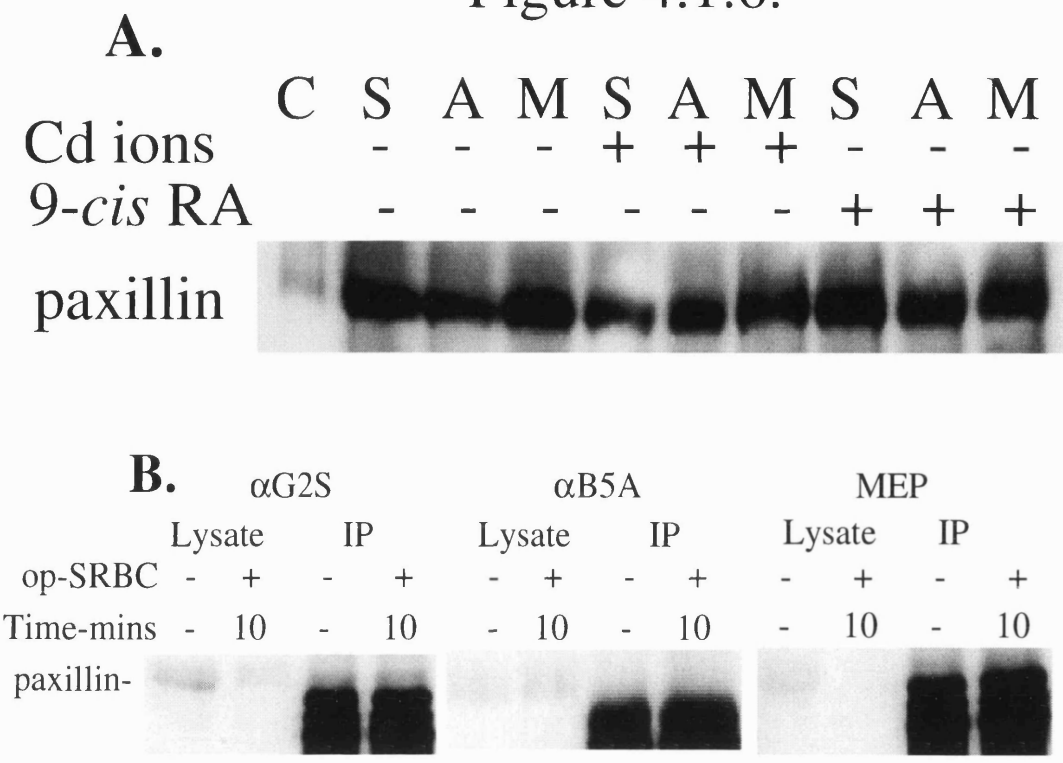

Figure 4.1.6. Expression of paxillin in the U937 transfectants; paxillin is not phosphorylated in response to op-SRBC.

(A.) 2x10^6 untreated αG2S (S), αB5A (A) or MEP (M) cells, or cells which had been treated with 9-*cis* RA or Cd^{++} ions, were lysed in 100μl of 1% NP40 lysis buffer. Lysates (equivalent of 3x10^5 cells per lane) were run on 10% SDS-polyacrylamide gels, and paxillin immunoblots performed (see section 2.4.). the lane labelled C, is 1mg of a paxillin positive cell lysate that was provided with the paxillin antibody. In (B). 6x10^6 9-*cis* RA-treated αG2S, αB5A or MEP cells were cultured with 10^8 op-SRBC. Cells were lysed in 200μl of 1%NP40 lysis buffer. 150μl of each lysate was immunoprecipitated (IP) with 6μg of 4G10 anti-phosphotyrosine mAb (see section 2.13.). IP were run on 10% SDS-polyacrylamide gels along side non IP cell lysates (equivalent of 5x10^5 cells per lane). Separated proteins were transferred to nitrocellulose filters and anti paxillin immunoblots performed (see section 2.4.)

4.2. Discussion.

The observation of the differential efficiencies of immunophagocytosis by 9-*cis* RA-treated U937 transfectants, prompted an examination of the intracellular tyrosine phosphorylation response to the immunophagocytic signal. Uptake of op-SRBC led to transient tyrosine phosphorylation in all U937 transfectants. The response of αG2S cells was more intense and more extensive than that of MEP or αB5A cells (Figure 3.1.8.1.). The response of αB5A cells was not as immediate, with no response observed until 5 minutes exposure, compared to that of αG2S or MEP cells (Figure 3.1.8.1.).

This difference can be explained in a number of ways. Although similar levels of FcγR were observed on the surface of these cells (Brown et al., 1997; Brown T.R.P., 1995), increased expression of CR3 and CR4 components was seen on αG2S cells (Appendix IV). These proteins are crucial co-factors for FcγR function (Graham et al., 1994; Gresham et al., 1991), and this increase could therefore lead to higher levels of signalling via FcγR or the CR proteins themselves. An alternative reason could be increased expression and phosphorylation of relevant intracellular signalling proteins or of functional proteins that are involved in the mechanics of phagocytosis.

4.2.1. Activation of ERK-1, Jnk and p38 during immunophagocytosis.

ERK-1 has previously been shown to be phosphorylated in response to FcεRI cross linking (Hirasawa et al., 1995; Jabril Cuenod et al., 1996). This activation occurred by Syk phosphorylation of Shc, which in turn led to Sos association and activation of Ras (to Ras-GTP). Ras-GTP then interacted with Raf, which induced phosphorylation of the ERK pathway (Hirasawa et al., 1995; Jabril Cuenod et al., 1996). In this study FcγR-mediated phagocytosis by U937 transfectants also induced phosphorylation

of ERK-1 (Figure 4.1.1.1.), suggesting that a similar pathway may operate in FcγR- as well as FcεR-mediated events.

Furthermore, in this study, the stress activated MAPKs, Jnk and p38 were shown to be phosphorylated following FcγR-mediated phagocytosis (Figures 4.1.1.2. and 4.1.1.3.). This is the first evidence for the participation of these proteins in a FcγR-mediated process. It is perhaps not surprising that Jnk and p38 are activated as the process of engulfment and the concomitant production of ROS, nitric oxide and other microbicidal factors must be a stressful process for the cell. One further observation was a possible increase in expression of Jnk in αG2S cells, although unfortunately no protein loading controls were done to confirm this (Figure 4.1.1.3.). A discussion of this effect is given in Chapter 6.2.2.

4.2.2. Phosphorylation of Shc is not affected by immunophagocytosis.

As outlined above Shc is phosphorylated following both FcγRIII (CD16), and FcεRI crosslinking (Galandrini et al., 1996; Jabril Cuenod et al., 1996). This is mediated by Syk (Jabril Cuenod et al., 1996). Phosphorylated Shc will complex with Grb-2 and Sos, and this complex is thought to interact with Ras-GDP. Thus, Sos will dissociate from Shc-Grb-2, bind Ras-GDP and induce the formation of active Ras-GTP (Galandrini et al., 1996; Jabril Cuenod et al., 1996). However, in this present study Shc was found to be phosphorylated at the same levels prior and during immunophagocytosis. The constitutive phosphorylation of Shc has been reported previously in cultured cells and can be minimised by the reduction of serum content in the medium (Jabril Cuenod et al., 1996; Turner et al., 1995). This observation is consistent with Shc having a role in induction of signals from growth factor receptors (Basu et al., 1994; Pronk et al., 1994). Therefore, in order to assess the role of Shc in immunophagocytosis in these cells, experiments need to be performed on cells maintained in low serum concentration. However, previous evidence,

and the fact that downstream ERK was phosphorylated in the U937 transfectants, does suggest that Shc is involved in immunophagocytosis.

4.2.3. FRIP is expressed in αG2S and MEP cells, but not αB5A cells.

FRIP is a protein that regulates the activity of RasGAP (Nelms et al., 1998). Activated RasGAP interacts with Ras-GTP, induces the GTPase activity of Ras, and hence promotes the formation of inactive Ras-GDP (Marshall, 1996). FRIP activates RasGAP by phosphorylation, and its own activity is itself regulated by phosphorylation by unknown proteins (Nelms et al., 1998). This protein was investigated because it has been found to be antagonistic of Shc-Grb-2-Sos in Ras activation, altering the balance of IL-4/IL-12 signalling in T-cells (Nelms et al., 1998). The protein is expressed in T-cells and some other haemopoietic cell lines, but had not been identified in monoblastoid cells and their derivations before.

FRIP was expressed in 9-*cis* RA-treated αG2S and MEP cells, but not in αB5A cells (Figure 4.1.3.). This suggests that expression of this protein increased upon differentiation of U937 cells, and that this process is mediated by RXRα. The expression of this protein could indicate that Ras activation has become more carefully regulated in 9-*cis* RA-treated αG2S and MEP cells, but not αB5A cells.

4.2.4. Interactions with GST-SH2 fusion proteins.

Although similarities exist in the phosphoproteins found in op-SRBC-treated U937 transfectants that interact with each specific SH2 domain, fundamental differences were apparent. The SH2 domains selected for investigation were chosen as the proteins that these domains are derived from have all been shown to be involved in immunophagocytosis (see Chapter 1.2.). This study was undertaken to try to identify phosphoproteins on the basis of which SH2 domains they interacted with

in vitro. However, identifying *in-vitro* interactions does not prove *in vivo* binding.

4.2.4.1. Src SH2 interactions.

Src and other members of this family of tyrosine kinases are associated with inactive FcγR (Bolen, 1991; Santana C. et al., 1996). Dephosphorylation and activation of Src family kinases by PTPases (possibly CD45), allows Src family kinases to bind to p-Tyr residues on ITAMs of FcγR or associated proteins (Adamczewski et al., 1995; Ghazizadeh et al., 1994).

This study has shown that Src SH2 domains interacted with many more phosphoproteins from αG2S cell lysates, than αB5A cell lysates, and that MEP cell lysates showed a completely different pattern of interaction (Figure 4.1.4A.). Surprisingly as Src interacts with p-Tyr residues in the ITAM of γ chain, no band of 18kD was observed. A band of 40kD was also observed in all three cell lysates, which could indicate interactions with FcγRII (CD32). The many bands recognised by Src SH2 implicates Src as having an possible role in immunophagocytosis by the U937 transfectants. However, it must be noted that *in vitro* binding does not necessarily indicate that any *in vivo* binding occurs.

4.2.4.2. Grb-2 and Grb-10 SH2 interactions.

Grb-2 and Grb-10 are adaptor molecules involved in many signal transduction systems. These proteins bind to phosphorylated tyrosines of receptor tyrosine kinases (RTK) and associated molecules, including Shc, via SH2 domains. Grb-2 and Grb-10 also contain two SH3 domains which bind other proteins such as Sos and SLP-76 (Buday and Downward, 1993). Therefore, these SH2 domains bind to upstream signalling molecules, with downstream signalling mediated by proteins attached to SH3 domains. The Grb-2-Sos complex has been implicated in activating

the Ras/MAPK pathway during phagocytosis (Galandrini et al., 1996; Jabril Cuenod et al., 1996).

The differences in bands that interacted with the two SH2 domains demonstrate the differences in specificity of these closely related proteins. Grb-10 SH2 interacted with many proteins from αG2S cell lysates, and with fewer proteins from αB5A and MEP cell lysates (Figure 4.1.4B.). In contrast, Grb-2 SH2 domains interacted only with three proteins from αG2S cell lysates (Figure 4.1.4I.). Both SH2 domains interact with a 46kD protein from op-SRBC exposed αG2S cell lysates, and this could be due to interaction with Shc. Although Shc has shown to be constitutively phosphorylated in these cells (Figure 4.1.2.), the Shc-Grb-2/Grb-10 interactions may only occur during immunophagocytosis. A 72kD phosphoprotein from op-SRBC exposed αG2S cell lysates also interacted with both Grb-2 and Grb-10 SH2 domains. One possibility is that this protein is Syk, the phosphorylation of which is essential for phagocytosis (Agarwal et al., 1993; Cox et al., 1996). Syk has also been shown to be responsible for the activation of the Shc-Grb-2-Sos complex (Jabril Cuenod et al., 1996). Grb-10 SH2 also interacted with a 18kD phosphoprotein from op-SRBC exposed αG2S cell lysates, which could be the FcγR associated γ chain.

4.2.4.3. Shc SH2 and PTB interactions.

Shc is another adaptor protein, the functions of which have previously been discussed in section 4.2.2. Shc SH2 and PTB domains bind phosphorylated RTKs and associated molecules (Pawson and Scott, 1997). This allows the phosphorylation of tyrosine residues in Shc, which act as docking sites for other proteins such as Grb-2. Therefore, these SH2 and PTB domains bind to upstream signalling molecules, with downstream signalling mediated by proteins attached to Shc p-Tyr residues.

Shc SH2 domain interacted with three proteins of 72kD, 68kD and 50kD from op-SRBC exposed αG2S cell lysates, but with no proteins from either MEP or αB5A cell lysates (Figure 4.1.4H.). The 72kD protein is consistent with Syk, which has previously been shown to phosphorylate Shc during phagocytosis (Jabril Cuenod et al., 1996). The Shc PTB domain also bound three proteins of 68kD, 55kD and 50kD from op-SRBC exposed αG2S cell lysates, with only proteins of 68kD and 18kD from MEP cell lysates, but with no proteins from αB5A cell lysates (Figure 4.1.4C.). The 18kD protein may be the γ chain.

Thus, one possible reason for the increased efficiency of phagocytosis by αG2S cells may be phosphorylation and recruitment of Syk, which could not be detected in the p-Tyr immunoblots because it is present at low levels in total cell lysates (Figure 3.1.8.1.).

4.2.4.4. p85 SH2 interactions.

p85 is the regulatory sub-unit of PI3-K and contains both N- and C-terminal SH2 domains (reviewed by Carpenter and Cantley, 1996). PI3-K has been implicated in phagocytosis, as a specific PI3-K inhibitor, wortmannin, inhibits phagocytosis (Ninomiya et al., 1994).

The p85 N-terminal SH2 domains interacted with phosphoproteins from αG2S and MEP cell lysates, and fewer from αB5A cell lysates (Figure 4.1.4D.). The C-terminal SH2 domain interacted with very many phosphoproteins from αG2S cell lysates, and fewer but still a substantial number of αB5A and MEP cell lysates (Figure 4.1.4E.). The C-terminal SH2 domain was also the only construct that interacted with a 115kD phosphoprotein, that was only present in αG2S cells (Figure 3.1.8.1.). A protein of this size has previously been found to interact with p85 SH2 domains during phagocytosis (Ninomiya et al., 1994). It has been hypothesised that this protein could be focal adhesion kinase (FAK), a kinase important in F-actin and focal adhesion formation. However,

another study found no induction of FAK phosphorylation during phagocytosis (Greenberg et al., 1994)

4.2.4.5. PLC-γ1 SH2 interactions.

PLC-γ1 and PLC-γ2 have been shown to be activated by FcγR crosslinking in a PTK dependent manner (Azzoni et al., 1992; Ting et al., 1992; Windebank et al., 1988). Activation of these proteins leads to production of IP3 and DAG, which mobilises intracellular calcium and activates PKC respectively (Toker, 1998). The protein kinases that activate PLCγ are presently unknown.

The PLC-γ1 C-terminal SH2 domain interacted with many proteins from all three of the cell lysates, whilst the N-terminal SH2 domain did not interact with proteins from any cell lysates. This observation indicates that only the C-terminal SH2 domain is involved in mediating the phagocytic signal, and that the different SH2 domains may be used in different cellular processes in which PLC-γ is involved.

4.2.5. Phosphorylation of p47-phox and p67-phox is not induced by immunophagocytosis.

As shown in Chapter 3, increased levels of p47-phox was expressed in 9-*cis* RA-treated αG2S cells, whilst lower levels were expressed in αB5A cells, when compared to MEP cells (Figure 3.1.7.). The phosphorylation of this and another component of the NADPH oxidase, p67-phox, was assessed. These molecules are phosphorylated and migrate to phagosomes upon phagocytosis and complex with a cytochrome that forms the other half of functional NADPH oxidase (Bolscher et al., 1989; Dusi and Rossi, 1993; Roos et al., 1996). This activated complex produces superoxide inside phagosomes, which increases the microbicidal activity of these phagosomes.

Therefore, differences in phosphorylation of p47-phox and p67-phox could be important in explaining the differential efficiencies of phagocytosis and also the differential phosphotyrosine pattern. However, no phosphorylation of either of these proteins was detected in any cell line (Figure 4.1.5.). This supports previous data shown that p47-phox was expressed at higher levels in 9-*cis* RA-treated αG2S cells than in MEP or αB5A cells.

This suggests that the U937 transfectants whilst being able to phagocytose did not possess the ability to produce superoxide, and thus kill engulfed pathogens. This demonstrates that 9-*cis* RA-treated αG2S cells are not fully differentiated monocytes, but have an intermediate phenotype.

4.2.6. Expression but not phosphorylation of paxillin in the U937 transfectants.

Paxillin has been previously shown to be tyrosine phosphorylated in macrophages following FcγR mediated phagocytosis (Greenberg et al., 1994). Paxillin has been shown to localise to focal adhesions with F-actin and talin (Turner C.E. et al., 1990). Furthermore, F-actin and phosphorylated paxillin localise to the sub-membranous area beneath nascent phagosomes during phagocytosis (Greenberg et al., 1994). In a further study, F-actin assembly has been shown to require intact ITAMs and Syk activation (Cox et al., 1996).

The process of actin polymerisation and formation of focal adhesions is thought to be essential for engulfment of IgG coated pathogens. In this study we have shown that immunophagocytosis induces a more defined pattern of actin staining, as well as inducing surface processes that are indicative of F-actin formation (Figure 3.1.4.3.).

Paxillin was shown to be expressed equally in all three U937 transfectants, and expression was not effected by 9-*cis* RA treatment (Figure 4.1.6A.).

No phosphorylation of paxillin was detected following immunophagocytosis in any cell line (Figure 4.1.6B.). In contrast to the U937 transfectants, macrophages, in which phosphorylation of paxillin was detected, the phosphotyrosine response and engulfment of IgG coated particles was maximal after three minutes, and F-actin was detected at the phagosome after thirty seconds (Greenberg et al., 1991). Therefore, the lack of paxillin phosphorylation could explain differences in efficiency of phagocytosis between these monoblasts and mature macrophages.

4.2.7. Summary.

The increase in efficiency of immunophagocytosis by the αG2S cells, correlates with an increased and differential pattern of tyrosine phosphorylation. This increase in efficiency and tyrosine phosphorylation may be due to increased expression of CR3 and CR4 on αG2S cells, which have been shown to be vital co-factors in FcγR mediated phagocytosis.

Figure 4.2.7. shows a schematic representation of possible signalling pathways utilised following immunophagocytosis by the U937 transfectants. In these cells FcγRIII cross-linking leads to phosphorylation of ITAMs on the FcγR associated γ chains. Although the initial processes of ITAM phosphorylation are unclear, Src kinase family members have been previously implicated (Ghazizadeh et al., 1994). This study has shown that Src-SH2 domain constructs bind many phosphoproteins, but no protein of 18kD that may be the γ chain. As Src family kinases are localised to the cell membrane, it seems likely that these proteins are involved in early signal transduction events.

In this study, SH2 and PTB domains of the adaptor proteins Shc, Grb-2 and Grb-10 interacted with more phosphoproteins from the αG2S cell line, than from αB5A or MEP cells. Of particular interest was a 72kD protein that was only found in αG2S cell lysates. This protein could be Syk, a protein that has been shown previously to phosphorylate Shc

during immunophagocytosis. It could be differential activation of Syk in αG2S cells that causes the increased efficiency of immunophagocytosis by these cells. Shc-Grb-2 complexes with Sos, which is a stimulator of Ras activation.

Downstream of Ras, ERK-1 was phosphorylated following immunophagocytosis by all three of the U937 transfectants. Furthermore the stress MAPKs, p38 and Jnk, were also phosphorylated in all three cell lines.

Also in this study, PLCγ, and PI3-K SH2 domains were shown to interact with phosphoproteins in lysates of all three cell lines. This suggests that these proteins may also play a role in immunophagocytic signal transduction in these cells.

Figure 4.2.7.

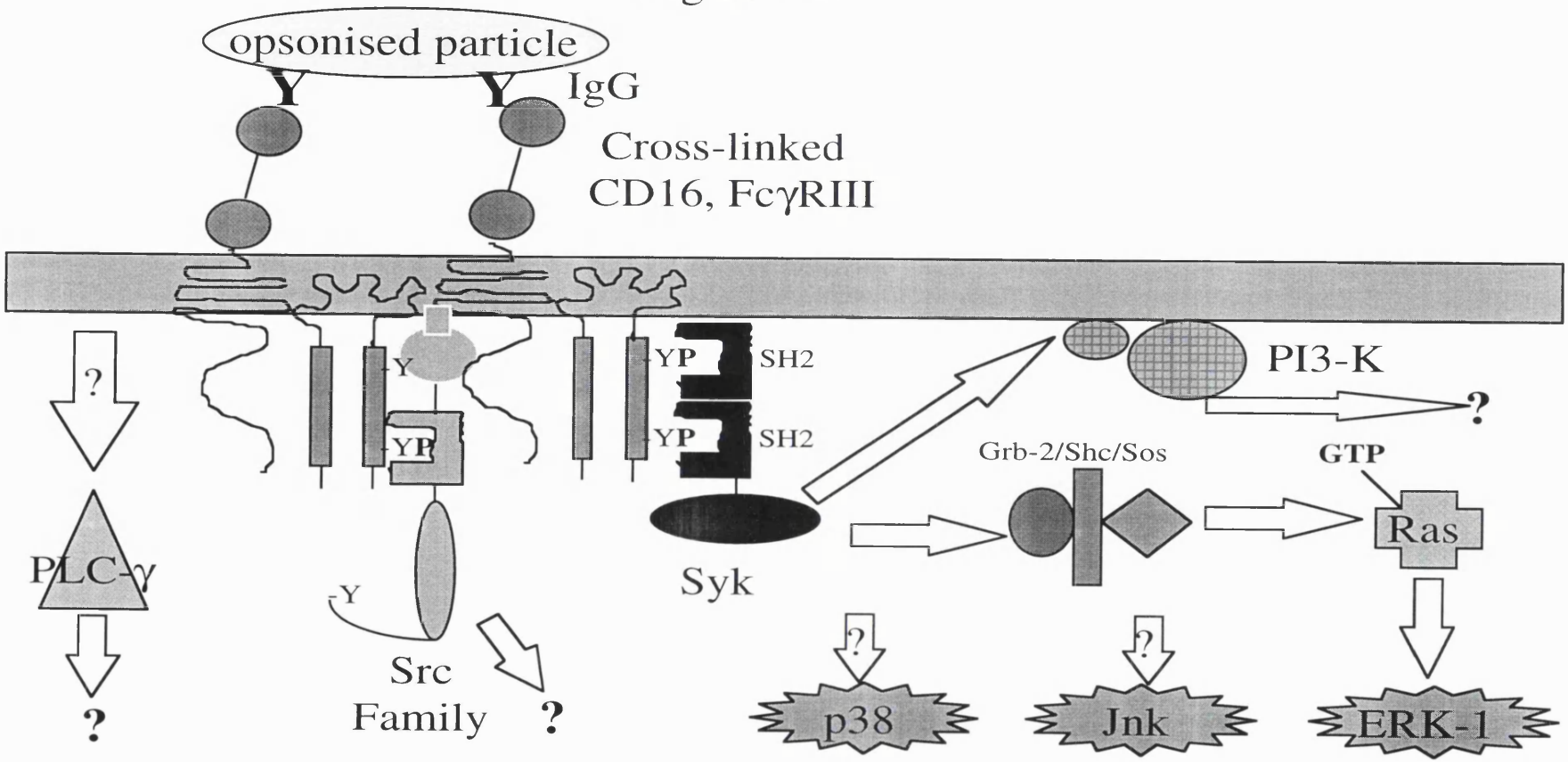

Figure 4.2.7. Schematic representation of possible signalling pathways utilised following immunophagocytosis by the U937 transfectants. See text for details.

Chapter 5

5.1. Results

Molecular characterisation of U937 dependent T-cell co-stimulation.

The activation of T-cells in response to antigen (Ag) requires at least two types of signals to be provided by an antigen presenting cell (APC) (Schwartz, 1992). The first of these is mediated via the interaction of the antigen specific T-cell receptor (TCR) with peptide that is associated with MHC molecules on the surface of the APC (Schwartz, 1985). As a result of this interaction, the TCR associated CD3 complex mediates intracellular signals that are necessary but not sufficient for T-cell clonal proliferation (Barber et al., 1989; Weiss and Littman, 1994). The second critical signal is mediated either by proteins on the T-cells that interact with co-stimulatory molecules on the surface of the APC (Jenkins et al., 1991b; Linsley et al., 1991a) or by soluble cytokines produced by APC acting on the T-cell. Unlike TCR mediated signals, these co-stimulatory signals are not Ag specific. The type of co-stimulatory signal that is delivered is dependent on several factors, including not only the type and activation status of the APC (Thomas et al., 1993), but also the type of T-cell (CD4+ or CD8+), and whether the T-cells are of naive or memory phenotype (Byrne et al., 1988).

Previously Johnson & Jenkins (1994) have demonstrated that the monoblastoid U937 cell line is itself capable of providing a co-stimulatory signal to T-cells in a CD3 mAb dependent assay. This co-stimulation was found to be independent of CD80/86 - CD28 interaction, and it was suggested that it was also independent of CD11a/18 - CD54 interaction. The aims of this study were:

- to confirm the co-stimulatory capability of U937 cells;
- to identify molecules on U937 cells involved in co-stimulation of T-cells;
- to characterise which subsets of T-cells are co-stimulated by U937 cells;
- to investigate how mAbs inhibitory of T-cell proliferation have their effects. .

These studies would form a basis for analysis of the role of the U937 transfectants in co-stimulation (see Chapter 6).

5.1.1. U937 cells provide a co-stimulatory signal to T-cells.

Initial experiments confirmed that the human monoblastoid U937 cell line has a co-stimulatory capacity in a CD3 dependent T-cell proliferation assay. Irradiated U937 cells ($5x10^3$ to $5x10^4$ cells per well), T-cells ($5x10^4$ to $8x10^5$ cells per well) and CD3 mAb (UCHT1) (0.1μg/ml or 0.2μg/ml) in soluble form, rather than bound to the culture well, were titrated into the assay. Figures 5.1.1A+B. show that the extent of T-cell proliferation was dependent on U937 cell number. When the number of U937 cells is increased with a constant T-cell number, the proliferation of T-cells increased in proportion to U937 cell number, at both concentrations of CD3 mAb tested. Since the T-cell proliferation observed in the presence of both 0.1μg/ml and 0.2μg/ml CD3 mAb was similar (compare 5.1.1A with 5.1.1B), these results suggest that CD3 is saturated at 0.1μg/ml. This concentration was therefore used in all subsequent experiments. Figures 5.1.1C+D. show that T-cell proliferation was also dependent on the number of T-cells added to the assay, but that proliferation reached a plateau once 10^5 T-cells were added to each well, and that the addition of $8x10^5$ cells to each well led to a reduction in proliferation that was probably due to overcrowding. T-cell proliferation using both 0.1μg/ml and 0.2μg/ml of CD3 mAb was again similar (compare 5.1.1C. with

5.1.1D.). Neither irradiated U937 cells alone, nor T-cells with CD3 alone, nor T-cells with U937 cells but without CD3 proliferated in this assay.

Figure 5.1.1.

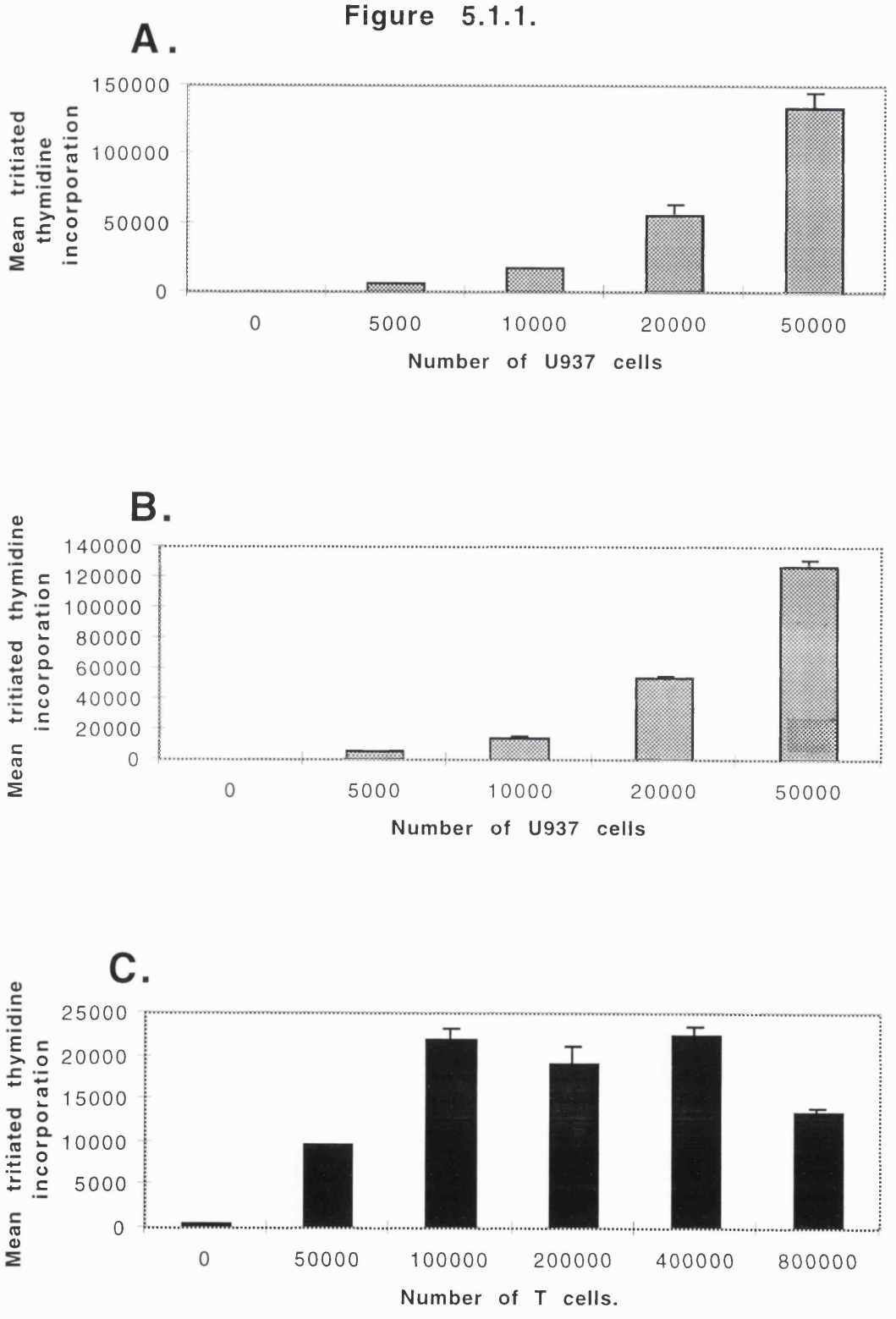

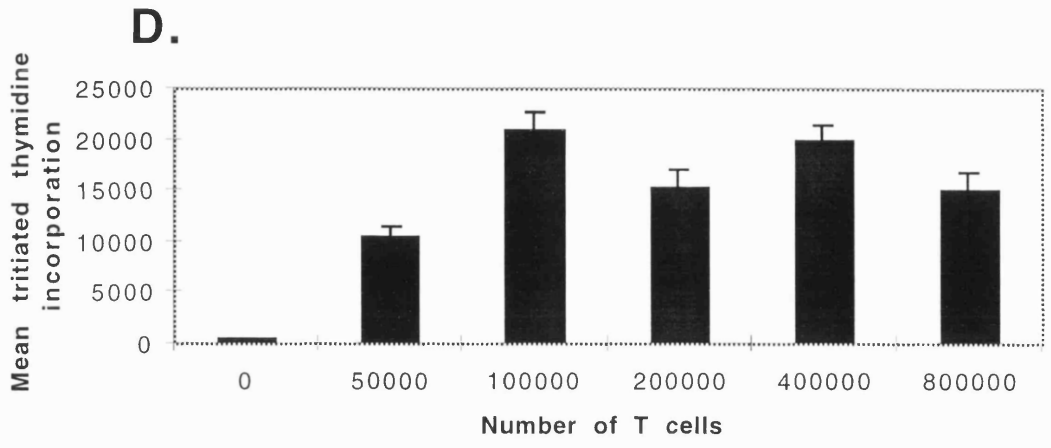

Figure 5.1.1. U937 cells co-stimulate T-cells in a CD3 dependent proliferation assay.
(A+B). Increasing numbers of irradiated U937 cells were co-cultured with $2x10^5$ purified tonsillar T-cells, in the presence of (A) 0.1μg/ml or (B) 0.2μg/ml CD3 mAb (UCHT1). (C+D). Increasing numbers of T-cells were co-cultured with 10^4 irradiated U937 cells, in the presence of (C) 0.1μg/ml or (D) 0.2μg/ml CD3 mAb (UCHT1) (see section 2.17.). T-cell proliferation was assessed by ^3H thymidine incorporation between 48 and 64 hours of culture. T-cells and U937 together without CD3 mAb, and T-cells with CD3 mAb but no U937 cells did not elicit a T-cell response. $5x10^4$ irradiated U937 cells alone gave thymidine incorporation values of 2000 cpm. The values shown are the mean ^3H thymidine incorporation of triplicate wells +/- SD from one experiment. Similar results have been found in at least two other experiments.

All further proliferation assays in this study used 10^4 irradiated U937 cells, $2x10^5$ T-cells and 0.1μg/ml of CD3 mAb. This was selected deliberately so that a sub optimal T-cell response would be detected, which would enable stimulatory as well as inhibitory effects on T-cell proliferation to be identified.

5.1.2. U937 cells and T-cells form large cell clusters during T-cell proliferation.

Under the conditions used in this study with soluble CD3 mAb (rather than bound to the culture well), T-cell activation could be observed visually. There was gradual formation of large clusters of cells, containing many U937 and T-cells (Figure 5.1.2A). In the absence of CD3 mAb, clusters were also sometimes observed, but they were much smaller and included a much smaller percentage of the cells (Figure 5.1.2B).

5.1.3. Role of CD11a /18 and CD54 in U937 induced T-cell activation.

5.1.3.1. CD11a /18 and CD54 mAbs inhibit T-cell activation.

The next stage in confirming the results of the previous study (Johnson and Jenkins, 1994) was to examine the effects of CD11a/18 and CD54, which were not inhibitory in previous work. A panel of mAbs against different epitopes on CD11a, CD18 and CD54 (See Appendix III), blocked U937 dependent T-cell activation significantly (Table 5.1.3.1.). All mAbs to CD11a/CD18, except one (AZN L21), blocked proliferation by 80% or more. Some antibodies to CD54 also blocked proliferation by greater than 90%, indicating that in this model, alternative CD11a/CD18 ligands (e.g. ICAM-2 or 3) are not effective substitutes for CD54. In agreement with this finding, mAbs to CD50 (ICAM-3) had only a very small effect on T-cell activation; with one CD50 mAb (MEM-171) giving 21% inhibition, and another (BL-A5) only 4% inhibition. Figure 5.1.3.1. shows that the inhibition of T-cell proliferation induced by CD11a/CD18 and CD54 mAbs also blocked the formation of U937-T-cell clusters (compare with Figure 5.1.2A.).

Figure 5.1.2.

A.

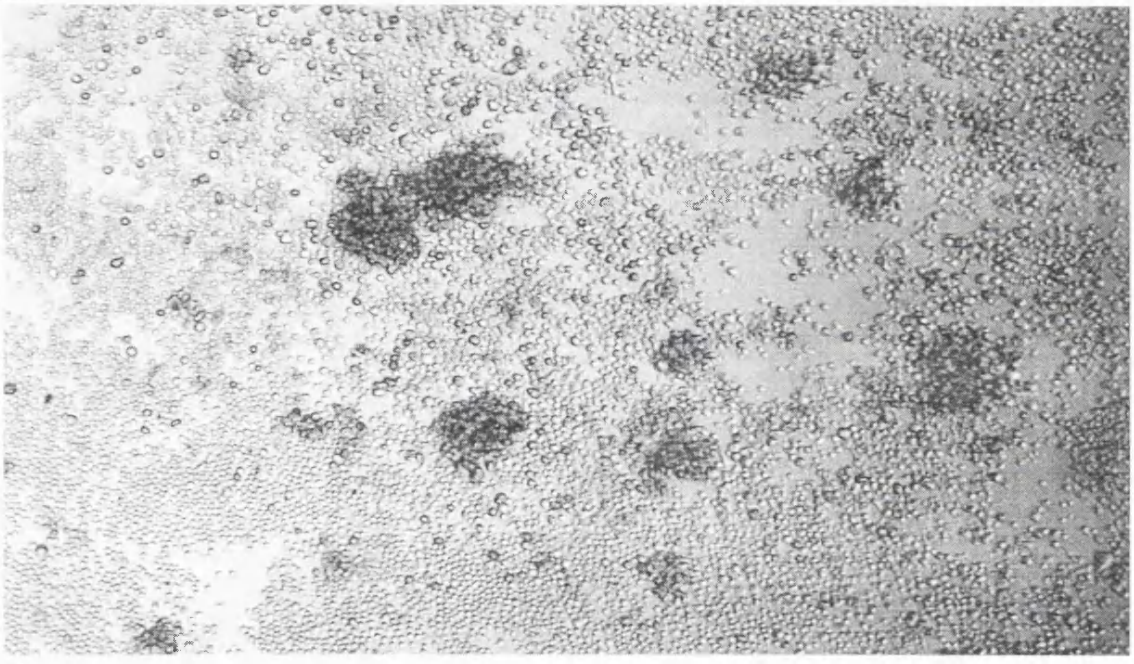

B.

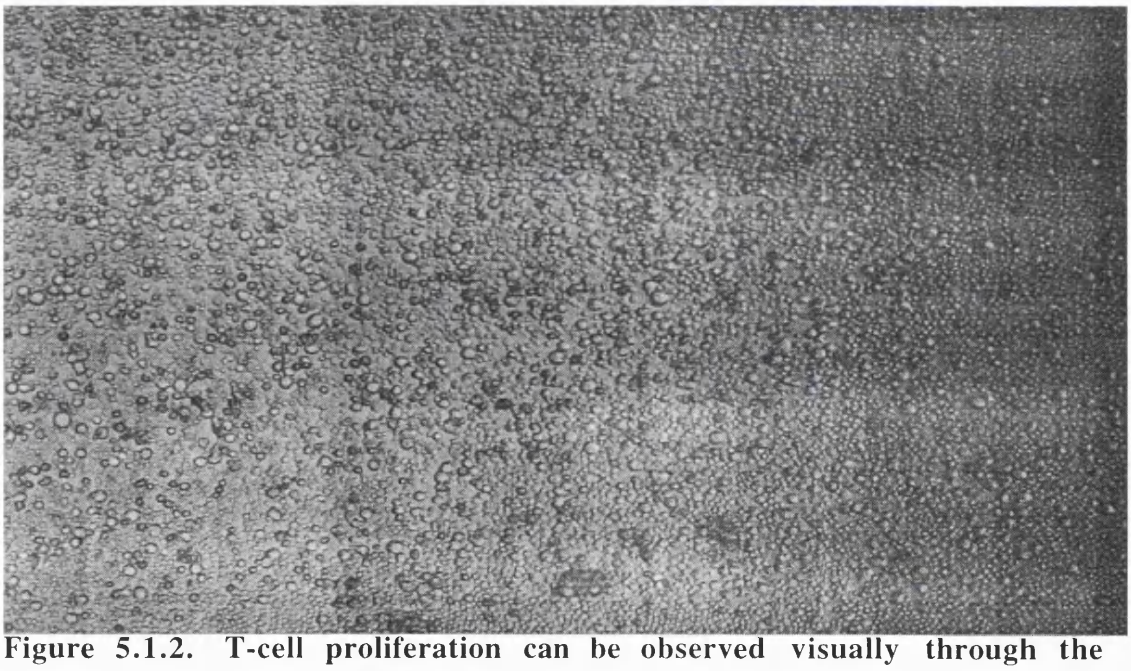

Figure 5.1.2. T-cell proliferation can be observed visually through the formation of large U937 / T-cell clusters.

Typical U937 / T-cell clusters seen at x40 magnification, approximately 48 hours after the start of the assay (see section 2.17.). (A). $2x10^5$ purified tonsillar T-cells, 10^4 irradiated U937 cells, and CD3 mAb (0.1μg/ml). (B). As for A, but without the addition of CD3 mAb.

Table 5.1.3.1.

Antibody/Specificity	3H Thymidine Incorporation	SD	% Inhibition	% Error
U937	661	132	-	-
T CELLS	285	13	-	-
T CELLS+U937	937	73	-	-
T CELLS+CD3	585	99	-	-
T CELLS+U937+CD3	40582	3264	0	8
CD11a				
CD11a 5E6	105	12	99	0.1
CD11a 6B7	530	58	98	0.2
AZN L27	1401	462	96	1.1
AZN L21	32514	1625	19	4
CD18				
7E4	1318	171	96	0.4
MEM 148	4893	255	87	0.6
AZN L18	7786	1245	80	3.1
CD54				
6.5B5	8059	306	80	0.8
D8H10	2217	296	94	0.7
MEM 111	1648	560	95	1.4
MEM 112	683	341	98	0.8

Table 5.1.3.1. CD11a, CD18 and CD54 mAbs inhibit the T-cell response. 10^4 irradiated U937 cells, $2x10^5$ purified T-cells and 0.1μg/ml CD3 mAb (UCHT1) (see section 2.18.) were cultured in either the presence of a 1/400 dilution of CD11a/18 and CD54 mAbs, as shown in column 1. T-cell proliferation was assessed between 48 and 64 hours of culture by measurement of ^3H thymidine incorporation. The results are expressed as the mean thymidine incorporation of triplicate wells +/- SD from one representative experiment, and the percentage inhibition +/- % error when test antibody is added to the assay compared to the no test antibody control. Similar results have been obtained in at least two other experiments.

Figure 5.1.3.1.

A. CD11a

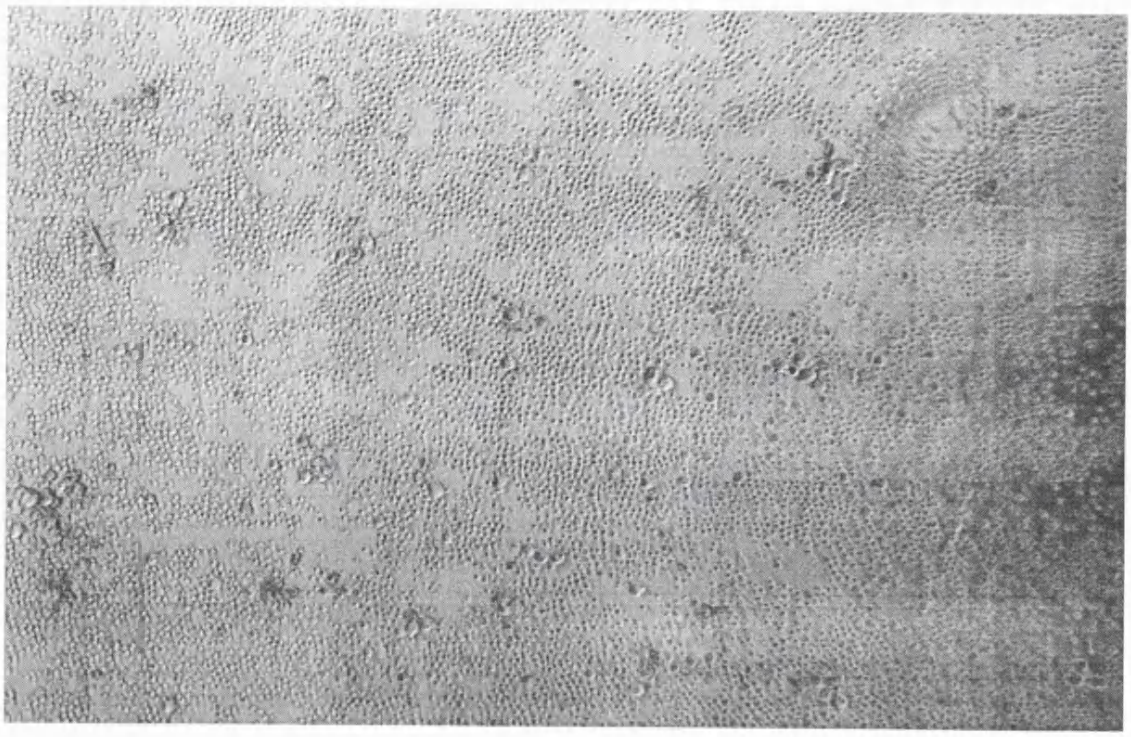

B. CD18

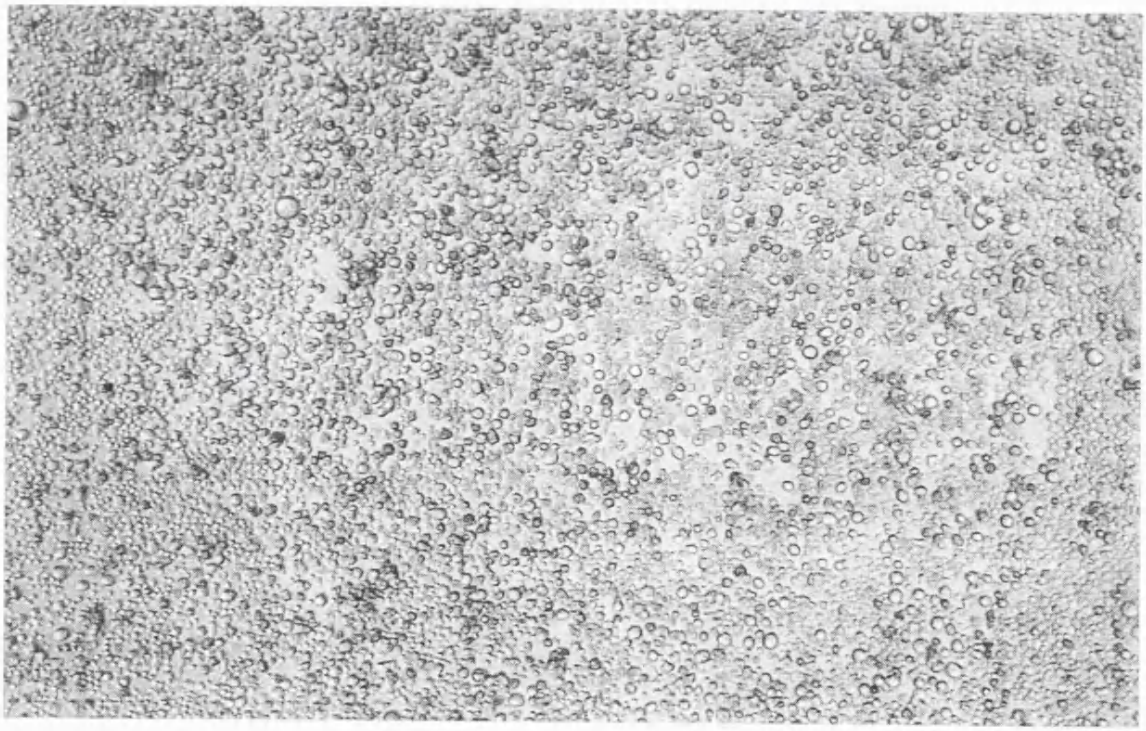

C. CD54

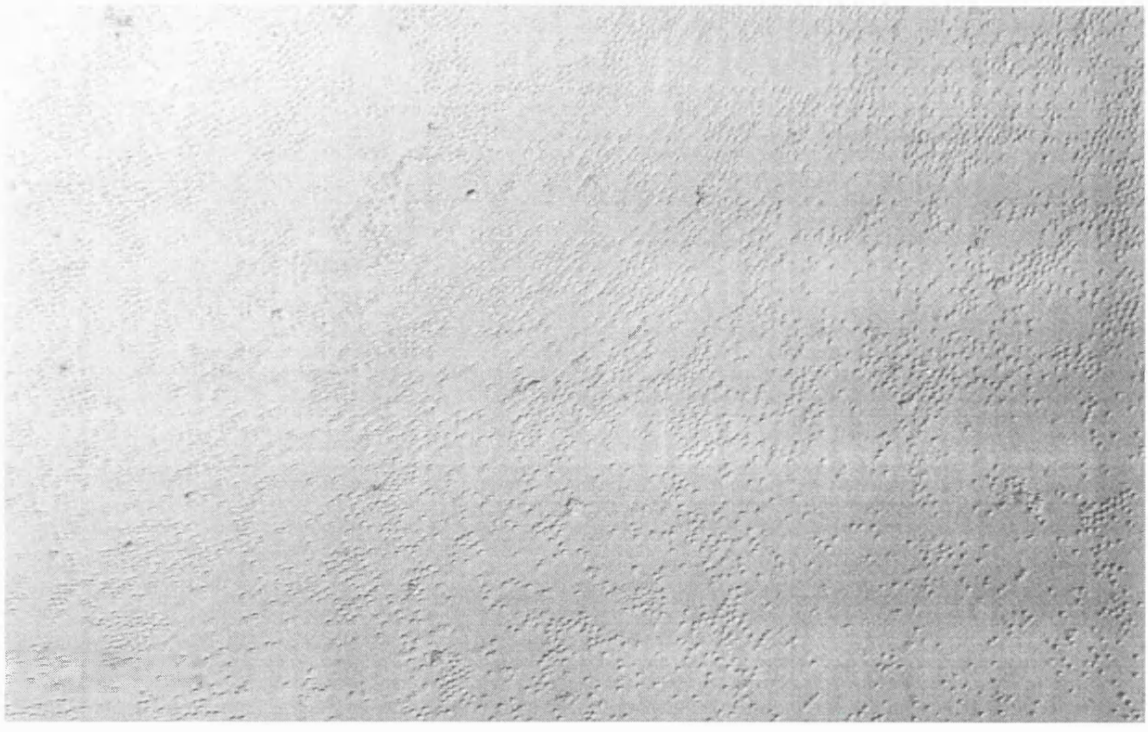

Figure 5.1.3.1. CD11a/CD18 and CD54 mAbs inhibit the formation of U937 - T-cell clusters.
(A). CD11a mAb CD11a-6B7, (B). CD18 mAb 7E4 and (C). CD54 mAb MEM-112 (all at 1/400 dilution) were added to 10^4 irradiated U937 cells, $2x10^5$ purified tonsillar T-cells, and 0.1μg/ml of CD3 mAb (UCHT1) and cluster formation assessed visually at x40 magnification (see section 2.18.). Cluster formation was inhibited compared to Figure 5.1.2A. Similar results were obtained with other CD11a/CD18 and CD54 mAbs.

5.1.3.2. Investigation of CD11a/18 and CD54 mAb induced inhibition.

The inhibition caused by the CD11a/18 and CD54 mAbs tested was dose-dependent and was not due to cytotoxicity, as measured by trypan blue exclusion (Figure 5.1.3.2.).

5.1.3.3. Levels of expression of CD11a/18 and CD54 on U937 and T-cells.

Flow cytometry with the same set of mAbs showed high levels of CD11a on U937, and much lower levels on purified T-cells. CD18 was present on both U937 and T-cells, albeit at much lower levels. In contrast, CD54 was expressed only on U937 cells, and not on the surface of T-cells (Table 5.1.3.3.). Only the mean fluorescence intensity (MFI) is given in this Table as a more relevant measure of the density of the protein on the surface of the cell than percentage of cells positive.

5.1.4. Screening panels of mAbs for effects on T-cell proliferation.

Two panels of mAbs from the 6th Human Leukocyte Differentiation Workshop (6th HLDA) were examined for their effects on T-cell proliferation. These were 152 mAbs from the non-lineage panel (i.e. not specific for myeloid, B- and T-cell); and 33 mAbs from the adhesion panel which included mAbs against molecules with putative adhesion roles. Appendix III shows all the mAbs used in the initial screen.

5.1.4.1. Results of primary screening.

Assays were performed as previously described, but with the addition of mAbs (Appendix III). These experiments were performed in triplicate wells, and each mAb was screened at least twice. Appendix VI shows the results of two of the initial screens. After the initial screens were completed, mAbs that consistently inhibited T-cell proliferation by ~70% or more in two or more experiments were selected for further study.

Figure 5.1.3.2.

Figure 5.1.3.2. CD11a/CD18 and CD54 mAbs inhibit T-cell proliferation in a dose-dependent manner and are not cytotoxic.
CD11a/CD18 and CD54 mAbs at 1/200 and 1/2000 dilutions were added to $2x10^5$ T-cells, 10^4 irradiated U937 cells, and CD3 mAb (0.1μg/ml). T-cell proliferation was assessed by ^3H thymidine incorporation (section 2.18.). The results are expressed as the mean % inhibition of T-cell proliferation in triplicate wells +/- % error, when test mAb was added compared to proliferation in the absence of test mAb (control = 42691 cpm). Similar results were obtained in at least one other experiment. The % figures given above bars measure cell viability. 1/200 dilutions of mAbs were added to the standard assay, and cell viability assessed by trypan blue exclusion (section 2.19.). The values shown are viable cells counted as % of the viable cells in the control, which contained $1.9x10^5$ viable cells/well, compared to $2.1x10^5$ cells/well that were originally added.

Table 5.1.3.3.

Antibody/Specificity	Mean fluorescence intensity	
	U937	T cell
anti mouse 2nd layer only	18	8
CD11a		
CD11a 5E6	356	112
CD11a 6B7	446	83
AZN L27	287	64
AZN L21	151	47
CD18		
7E4	132	89
MEM 148	105	51
AZN L18	189	56
CD54		
6.5B5	87	10
D8H10	118	11
MEM 111	71	7
MEM 112	89	21

Table 5.1.3.3. Levels of expression of CD11a, CD18 and CD54 on U937 and T-cells.
Mean fluorescence intensity (MFI) of U937 or T-cells stained with mAbs to CD11a, CD18 and CD54, analysed by flow cytometry (see section 2.5.).

Appendix VII lists the inhibitory mAbs that fitted these criteria and the amount of inhibition obtained with these mAbs in the primary screening experiments. Eleven CD45, six CD98, four unknown, two CD53, two CD147 and one each of CD18, CD55 and CDw108 mAbs were found to be highly inhibitory of T-cell proliferation. Therefore, these mAbs, along with other mAbs with the same specificities, were selected for further study.

The original plan was to investigate further mAbs that stimulated T-cell proliferation by >50% in this assay as well as those which inhibited, but none of the mAbs tested consistently caused an increase over two or more experiments (data not shown), so this plan was abandoned.

5.1.4.2. mAbs chosen for further studies.

Appendix VIII shows mAbs chosen for further study. The CD18 mAb - BL5 was not included, as the role of CD18 in this assay had already been investigated previously (see section 5.1.3.).

5.1.5. Role of CD45 in U937 induced T-cell proliferation.

5.1.5.1. CD45 mAbs inhibit T-cell proliferation.

Of eighteen CD45 mAbs tested, fourteen inhibited T-cell proliferation: eight of nine "pan-CD45" mAbs, two of five CD45RA mAbs, all three CD45RB mAbs and one CD45RO mAb. Generally, pan CD45 mAbs were potent inhibitors of T-cell proliferation, whereas mAbs directed against CD45 isoforms were less inhibitory of T-cell proliferation. This inhibition was dose-dependent (Figure 5.1.5.1.). All the inhibitory mAbs except ICO46 (pan CD45) had no cytotoxic effects on the assay; this mAb gave a % cell viability of 20% of the control value (Figure 5.1.5.1.), suggesting that inhibition was due to killing.

5.1.5.2. Expression of CD45 on U937 and T-cells.

U937 cells express high levels of CD45, but the function of this protein phosphatase in U937 cells (or indeed in other APCs) is not clear. In expression analysis with the CD45 mAbs, there was no correlation between quantitative expression (as judged by MFI) and the inhibitory capability of a particular mAb (Table 5.1.5.2.).

Figure 5.1.5.1.

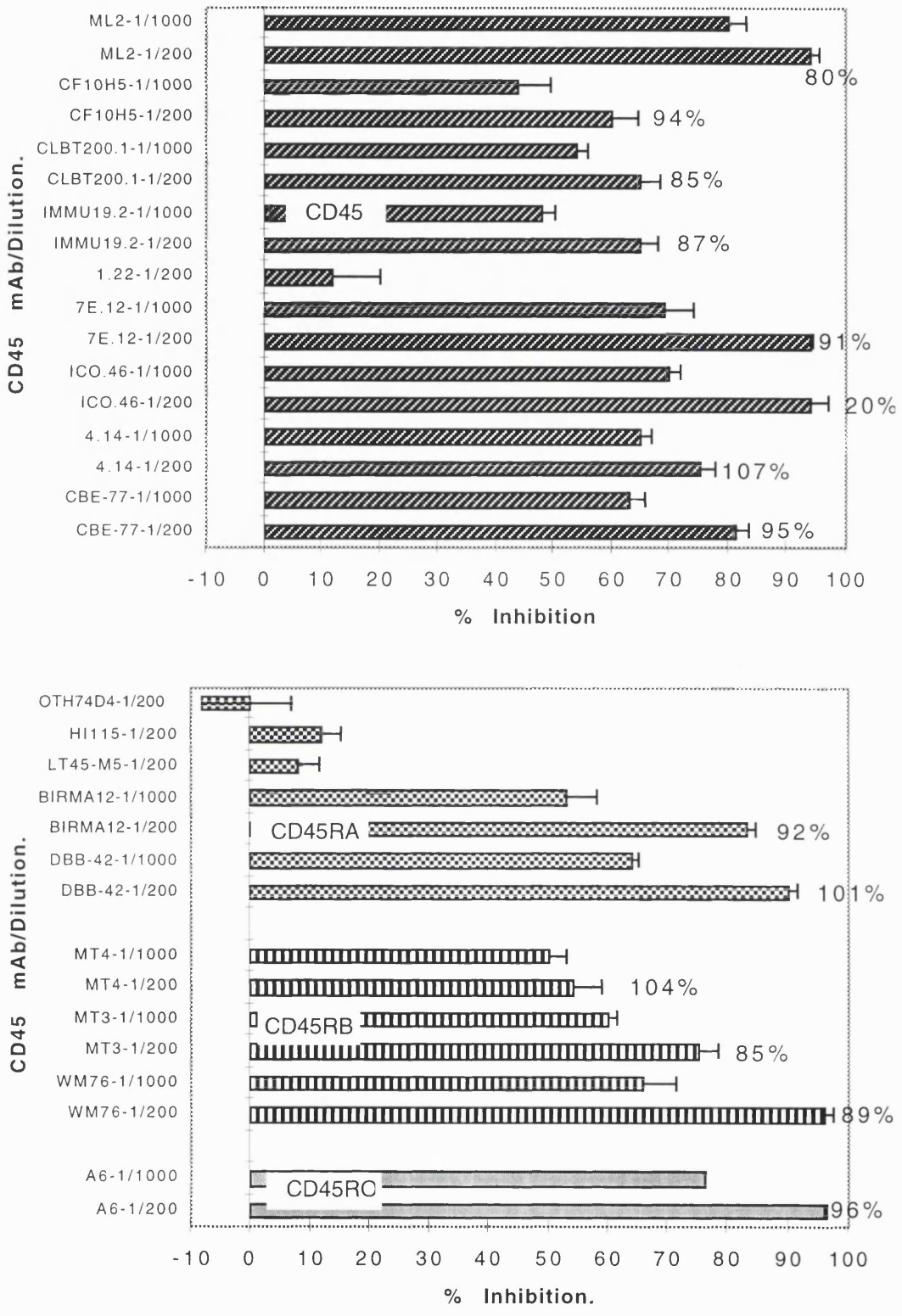
ML2-1/1000
ML2-1/200
CF10H5-1/1000
CF10H5-1/200
CLBT200.1-1/1000
CLBT200.1-1/200
IMMU19.2-1/1000
IMMU19.2-1/200
1.22-1/200
7E.12-1/1000
7E.12-1/200
ICO.46-1/1000
ICO.46-1/200
4.14-1/1000
4.14-1/200
CBE-77-1/1000
CBE-77-1/200
CD45 mAb/Dilution.
80%
94%
85%
CD45
87%
91%
20%
107%
95%
-10 0 10 20 30 40 50 60 70 80 90 100
% Inhibition
OTH74D4-1/200
HI115-1/200
LT45-M5-1/200
BIRMA12-1/1000
BIRMA12-1/200
DBB-42-1/1000
DBB-42-1/200
MT4-1/1000
MT4-1/200
MT3-1/1000
MT3-1/200
WM76-1/1000
WM76-1/200
A6-1/1000
A6-1/200
CD45 mAb/Dilution.
CD45RA
92%
101%
104%
CD45RB
85%
89%
CD45RO
96%
-10 0 10 20 30 40 50 60 70 80 90 100
% Inhibition.

Figure 5.1.5.1. Inhibition of T-cell proliferation induced by CD45 mAbs is dose-dependent and not due to cytotoxicity. (See previous page)
CD45 mAbs (at 1/200 or 1/1000) were added to $2x10^5$ purified T-cells, 10^4 irradiated U937 cells, and CD3 mAb (0.1μg/ml) (section 2.18.). Proliferation was assessed by ^3H thymidine incorporation between 48 and 64 hours of culture. The results are expressed as the mean % inhibition of T-cell proliferation in triplicate wells +/- % error, when test mAb was added to the assay compared to the proliferation in the absence of test mAb (control = 42691 cpm). Similar results have been obtained in at least one other experiment. The % values given above the bars measure cell viability. 1/200 dilutions of mAbs were added to the assay the number of viable cells was assessed by trypan blue exclusion (section 2.19.). The values shown are the number of viable cells as a % of the number of viable cells in the no test mAb control. This control contained $1.9x10^5$ viable cells/well, compared to $2.1x10^5$ cells/well that were originally added to the assay.

Table 5.1.5.2.

Specificity	mAb	Mean fluorescence intensity	
		U937	T cell
anti mouse 2nd layer only		18	8
CD45	CBE-77	145	258
CD45	4.14	306	521
CD45	ICO.46	314	402
CD45	7E.12	259	381
CD45	1.22	400	224
CD45	IMMU19.2	325	412
CD45	CLBT200.1	217	437
CD45	CF10H5	455	1037
CD45	ML2	360	624
CD45 RA	DBB-42	170	140
CD45 RA	BIRMA 12	44	80
CD45 RA	LT45-M5	32	109
CD45 RA	HI115	95	45
CD45 RA	OTH74D4	46	62
CD45 RB	WM76	348	618
CD45 RB	MT3	154	258
CD45 RB	MT4	113	281
CD45 RO	A6	192	145

Table 5.1.5.2. Levels of expression of CD45 on both U937 and T-cells. U937 and T-cells were stained with mAb as shown in columns 1 and 2 and MFI determined by flow cytometry (see section 2.5.).

5.1.5.3. CD45 mAbs induce the formation of larger U937 - T-cell clusters.

Paradoxically, CD45 mAbs, whilst inhibiting T-cell proliferation caused the formation of larger U937 - T-cell clusters, which were not seen on addition of any other mAbs. These clusters were identified readily by morphology (Figure 5.1.5.3A. compare with Figure 5.1.2A). Furthermore, inhibitory CD45 mAbs cause an increase in U937 - T-cell clustering without the addition of the CD3 antibody (Figure 5.1.5.3B. compare with Figure 5.1.2B). Although large U937 - T-cell clusters were observed in wells with CD45 mAb but without CD3, no T-cell proliferation was detected in these wells (data not shown).

5.1.6. Role of CD53 in U937 induced T-cell proliferation.

5.1.6.1. CD53 mAbs inhibit T-cell proliferation.

Of four CD53 antibodies tested, two mAbs were potent inhibitors (>75%) of T-cell proliferation. One mAb inhibited less well (~50%), and one antibody (WM65) had no effect. This inhibition was dose-dependent and was not due to cytotoxicity (Figure 5.1.6.1.).

5.1.6.2. Expression of CD53 on U937 and T-cells.

Table 5.1.6.2. shows the MFI of the four CD53 mAb tested (Figure 5.1.6.1.). Flow cytometry with the potent inhibitory mAb 202-24B showed that CD53 was expressed on U937 cells, and more strongly on T-cells. The non inhibitory CD53 mAb (WM 65) did not bind to either U937 cells or T-cells, which explains the lack of effect this mAb had in the functional assay.

Figure 5.1.5.3.

A.

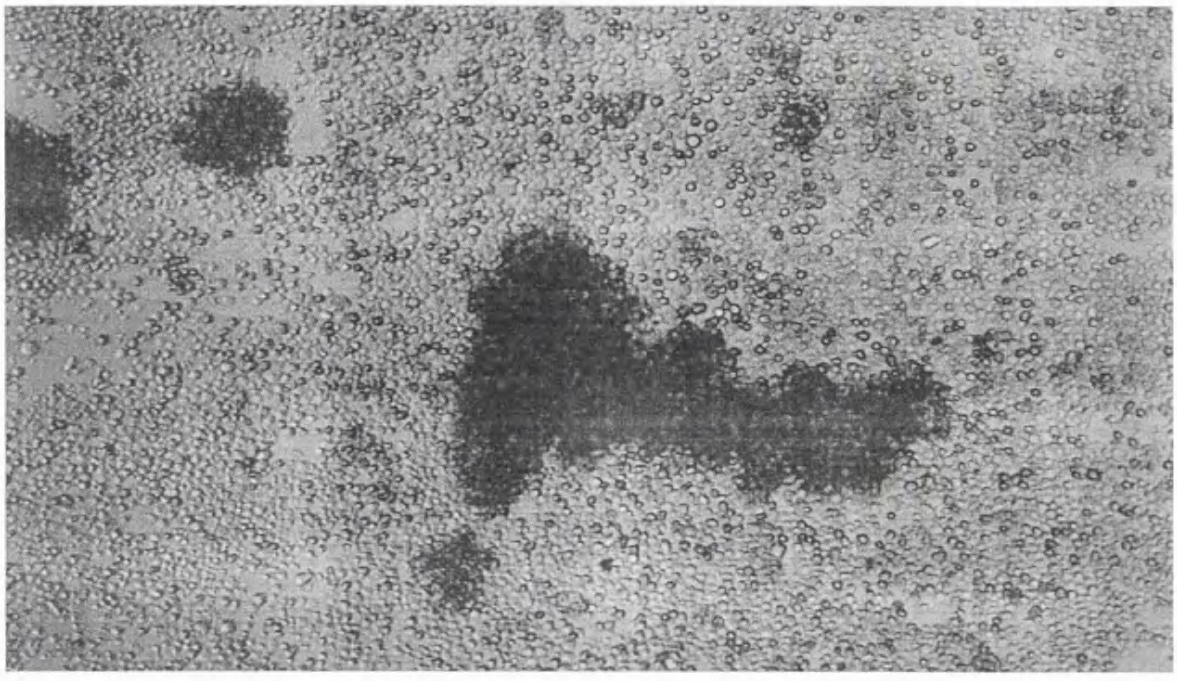

B.

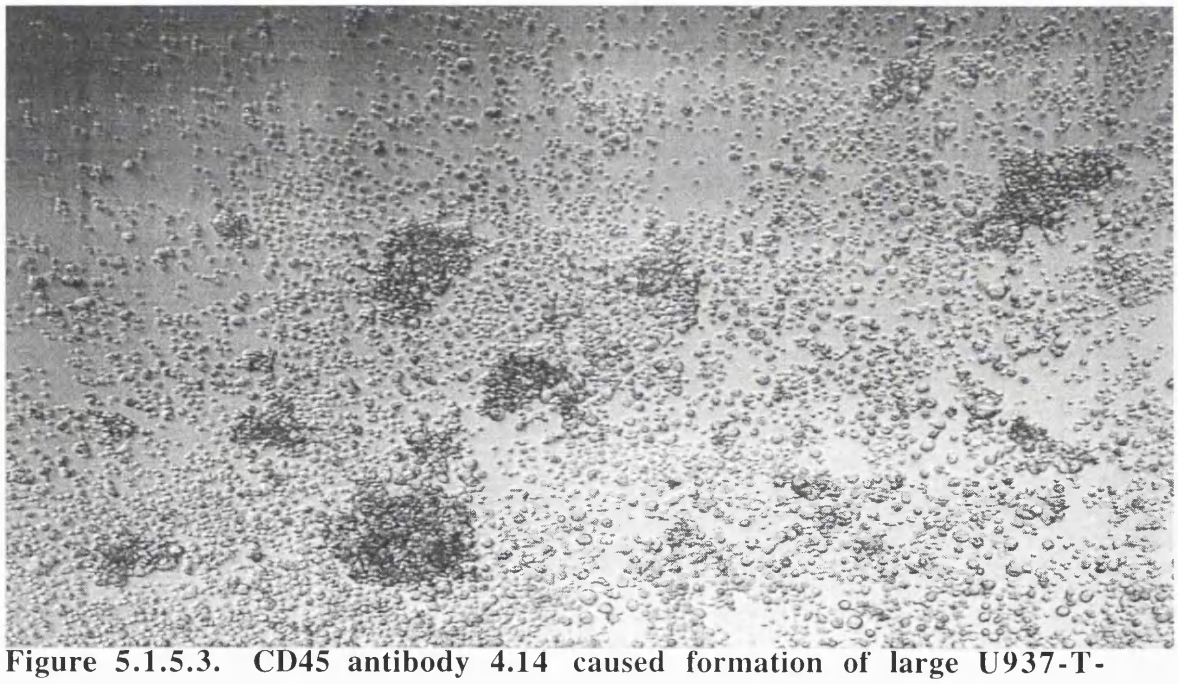

Figure 5.1.5.3. CD45 antibody 4.14 caused formation of large U937-T-cell clusters.

(A). CD45 mAb 4.14 (at 1/400) was added to 10^4 irradiated U937 cells, $2x10^5$ purified T-cells and 0.1μg/ml CD3 mAb (UCHT1) (section 2.18.). The cells were cultured for 48 hours and then photographed. In (B) culture conditions were the same but no CD3 mAb was added. Other inhibitory CD45 mAbs had the same effect of increasing U937 - T-cell clustering. The increased clustering was independent of CD45 isotype.

Figure 5.1.6.1.

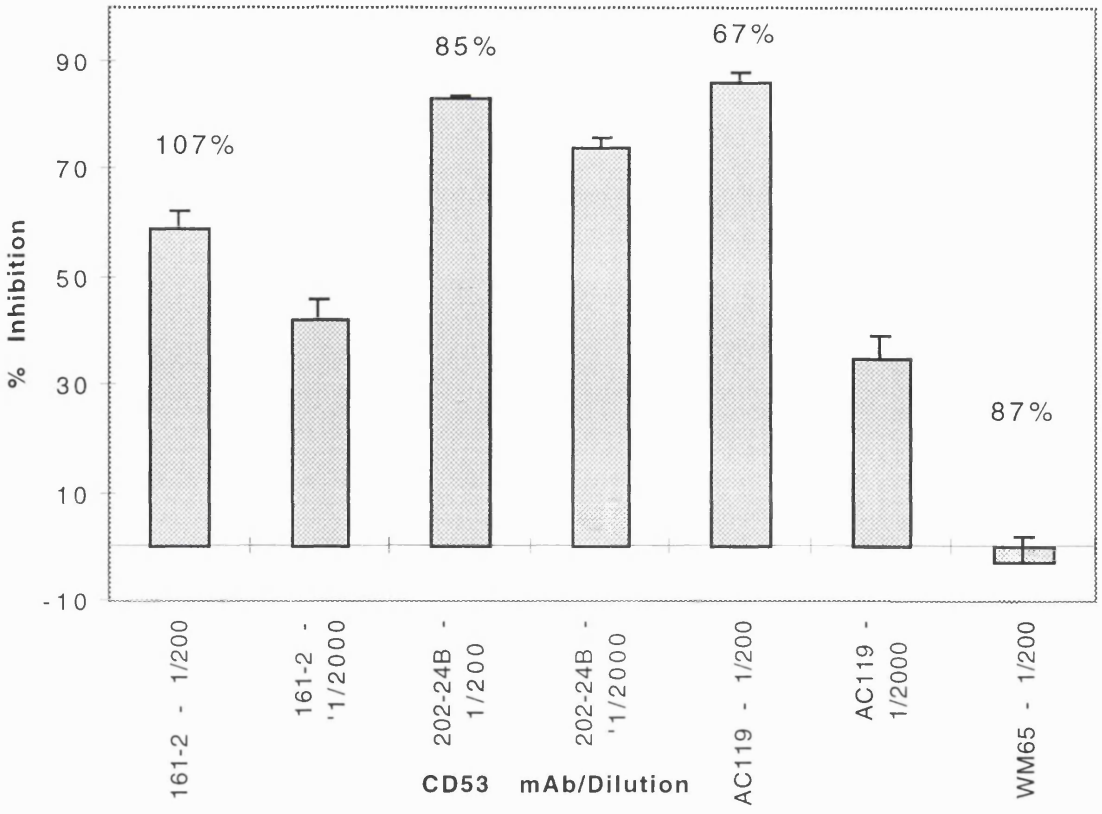

Figure 5.1.6.1. Inhibition of T-cell proliferation induced by CD53 mAbs is dose-dependent and not due to cytotoxicity.

Test mAbs (at 1/200 or 1/2000) were added to cultures of 10^4 irradiated U937 cells, $2x10^5$ T-cells and 0.1μg/ml CD3 mAb (UCHT1) (section 2.18.). Proliferation was assessed by measurement of ^3H thymidine incorporation. The response is shown as the mean % inhibition of T-cell proliferation in triplicate wells +/- % error, when test mAb is added to the assay compared to proliferation in the absence of test mAb. (control = 33200 cpm). Similar results were obtained in at least two other experiments. The % Figures given above the bars measure cell viability. 1/200 dilutions of mAbs were added to the assay, the number of viable cells was assessed by trypan blue exclusion (see section 2.19.). The values shown are the number of viable cells as a % of the viable cells in the no test mAb control. This control contained $1.9x10^5$ viable cells/well, compared to $2.1x10^5$ cells/well that were originally added.

Table 5.1.6.2.

CD53mAb	Mean fluorescence intensity	
	U937	T cell
anti mouse 2nd layer only	24	5
161-2	110	161
202-24B	165	236
AC119	105	203
WM65	15	33

Table 5.1.6.2. Levels of expression of CD53 on both U937 and T-cells. U937 and T-cells were stained with mAb as shown in column 1 and MFI determined by flow cytometry (see section 2.5.).

5.1.7. Role of CD55 in U937 induced T-cell proliferation.

One of two CD55 mAbs (JS 11) potently inhibited T-cell proliferation in a dose-dependent manner and this was not due to cytotoxicity (Figure 5.1.7.). Flow cytometry with these mAbs showed that CD55 was expressed mainly on T-cells but also at a lower level on U937 (Table 5.1.7.). Both mAbs bound equally, suggesting that simple quantitation could not account for differences in inhibitory ability.

5.1.8. Role of CD98 in U937 induced T-cell proliferation.

5.1.8.1. CD98 mAbs inhibit T-cell proliferation.

Out of nine CD98 antibodies tested, six mAbs (MEM 108, J1-G3B, J3-E1B, CAF7, IPO-T10, and BU89) were potent inhibitors (>75%) of T-cell proliferation, one mAb (BK 19.9) inhibited less well (~50%), and two mAbs (2E12 and BU53) had no effect on T-cell proliferation This inhibition was dose-dependent and was not due to cytotoxicity (Figure 5.1.8.1.).

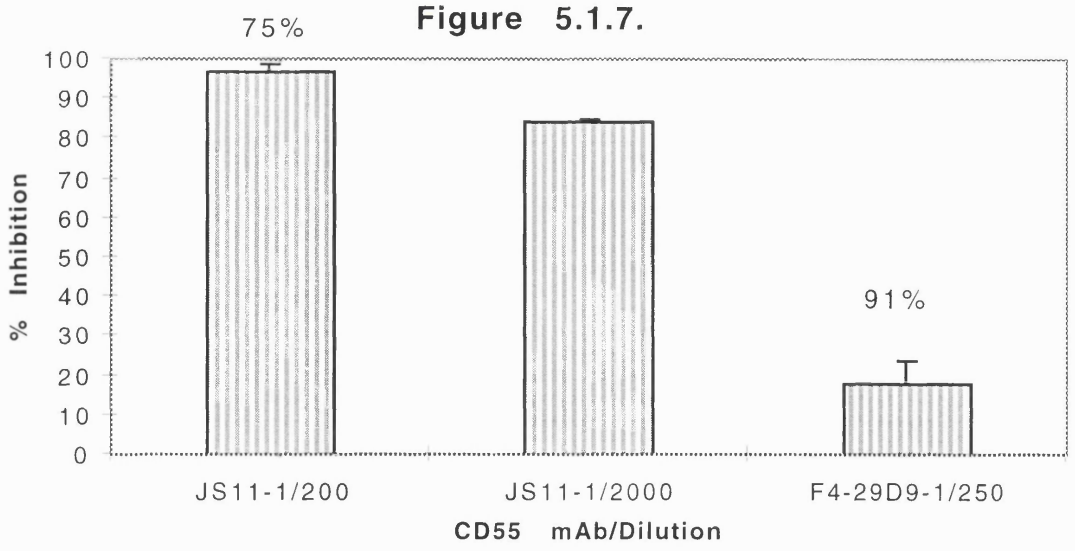

Figure 5.1.7. Inhibition of T-cell proliferation induced by CD55 mAbs is dose-dependent and not due to cytotoxicity.

Test mAbs (at 1/200 or 1/250 or 1/2000) were added to cultures of 10^4 irradiated U937 cells, $2x10^5$ T-cells and 0.1μg/ml CD3 mAb (UCHT1) (section 2.18.). Proliferation was assessed by measurement of ^3H thymidine incorporation. The response is shown as the mean % inhibition of T-cell proliferation in triplicate wells +/- % error, when test mAb is added to the assay compared proliferation in the absence of test mAb. (control = 42691 cpm). Similar results were obtained in two other experiments. The % Figures given above the bars measure cell viability. 1/200 dilutions of mAbs were added to the assay, the number of viable cells assessed by trypan blue exclusion (section 2.19.). The values shown are the number of viable cells as a % of the number of viable cells in the no test mAb control. This control contained $1.9x10^5$ viable cells/well, compared to $2.1x10^5$ cells/well that were originally added.

Table 5.1.7.

CD55 mAb	Mean fluorescence intensity	
	U937	T cell
anti mouse 2nd layer only	25	3
JS11	35	98
F4-29D9	41	112

Table 5.1.7. Levels of expression of CD55 on both U937 and T-cells. U937 and T-cells were stained with mAb as shown in column 1 and MFI determined by flow cytometry (see section 2.5.).

Figure 5.1.8.1.

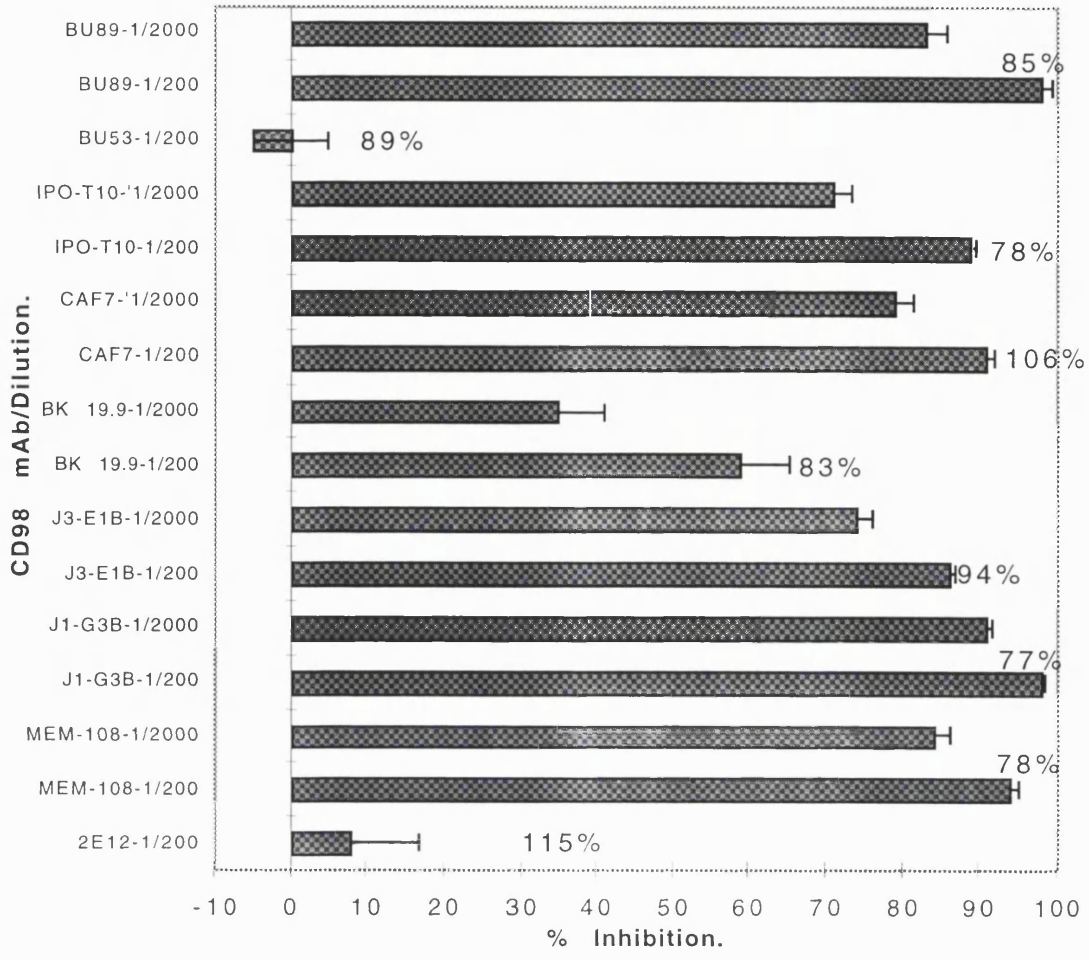

Figure 5.1.8.1. Inhibition of T-cell proliferation induced by CD98 mAbs is dose-dependent and not due to cytotoxicity.

Test mAbs (at 1/200 or 1/2000) were added to cultures of 10^4 irradiated U937 cells, $2x10^5$ T-cells and 0.1μg/ml CD3 mAb (UCHT1) (section 2.18.). Proliferation was assessed by measurement of ^3H thymidine incorporation. The response is shown as the mean % inhibition of T-cell proliferation in triplicate wells +/- % error, when test mAb is added to the assay compared to the proliferation in the absence of test mAb (control = 33200 cpm). Similar results were obtained in at least two other experiments. The % Figures given above the bars measure cell viability. 1/200 dilutions of mAbs were added to the assay, and numbers of viable cells assessed by trypan blue exclusion (section 2.19.). Values shown are numbers of viable cells as a % of the numbers of viable cells in the no test mAb control. This control contained $1.9x10^5$ viable cells/well, compared to $2.1x10^5$ cells/well that were originally added.

5.1.8.2. Expression of CD98 on U937 and T-cells.

Table 5.1.8.2. shows the MFI of the nine CD98 mAbs tested (Figure 5.1.8.1.), The potent inhibitory CD98 mAbs bound with similar patterns of high U937 cells, and low T-cell expression (U937 MFI range from 343 to 830; and T-cell MFI range from 19 to 41). The only exception was the CD98 mAb J1-G3B, which bound more strongly to T-cells (MFI 1266) than U937 cells (MFI 503). The less inhibitory CD98 mAb BK 19.9, bound less strongly to both U937 and to T-cells, and CD98 mAb 2E12 bound to neither U937 or T-cells, explaining the relative effects of these mAbs. The remaining non inhibitory CD98 mAb BU53 bound to both U937 cells (MFI 622), and to T-cells (MFI 30) thus again suggesting that simple quantitation could not account for this difference in inhibitory ability.

Table 5.1.8.2.

CD98 mAb	Mean fluorescence intensity	
	U937	T cell
anti mouse 2nd layer only	24	5
2E12	30	5
MEM-108	830	41
J1-G3B	503	1266
J3-E1B	1155	90
BK 19.9	151	13
CAF7	741	40
IPO-T10	27	4
BU53	622	30
BU89	343	19

Table 5.1.8.2. Levels of expression of CD98 on both U937 and T-cells. U937 and T-cells were stained with mAb as shown in column 1 and MFI determined by flow cytometry (see section 2.5.).

5.1.9. Role of CDw108 in U937 induced T-cell proliferation.

Only one CDw108 (MEM 150) was tested, and this was a potent inhibitor of T-cell activation. Inhibition was dose-dependent with a 1/400 dilution inhibiting T-cell proliferation by 82%, and a 1/4000 dilution inhibiting by 72%. This inhibitory effect was not due to cytotoxicity as the % cell viability compared to no test mAb control was 86%. CDw108 was shown to be expressed on T-cells (MFI 68). but not on U937 cells (MFI 16).

5.1.10. Role of CD147 in U937 induced T-cell proliferation.

5.1.10.1. CD147 mAbs inhibit T-cell proliferation.

Out of four CD147 mAbs tested, two mAbs (UM-8D6 and HI197) were potent inhibitors (>75%) of T-cell proliferation, one mAb (HIM6) inhibited less well (~50%), and one mAb (H84) had no effect on T-cell proliferation. This inhibition was dose-dependent and was not due to cytotoxicity (Figure 5.1.10.1.).

5.1.10.2. Expression of CD147 on U937 and T-cells.

Table 5.1.10.2. shows the MFI of the four CD147 mAbs tested (Figure 5.1.10.1.). The potent inhibitory CD147 mAbs, bound very strongly to U937, but less well to T-cells. The less inhibitory CD147 mAb (HIM6) also bound strongly to U937 cells and bound to T-cells. The non inhibitory CD147 mAb (H84), showed slightly lower but nonetheless significant binding to both U937 cells and T-cells, suggesting that simple quantitation could not account for this difference in inhibitory ability.

Figure 5.1.10.1.

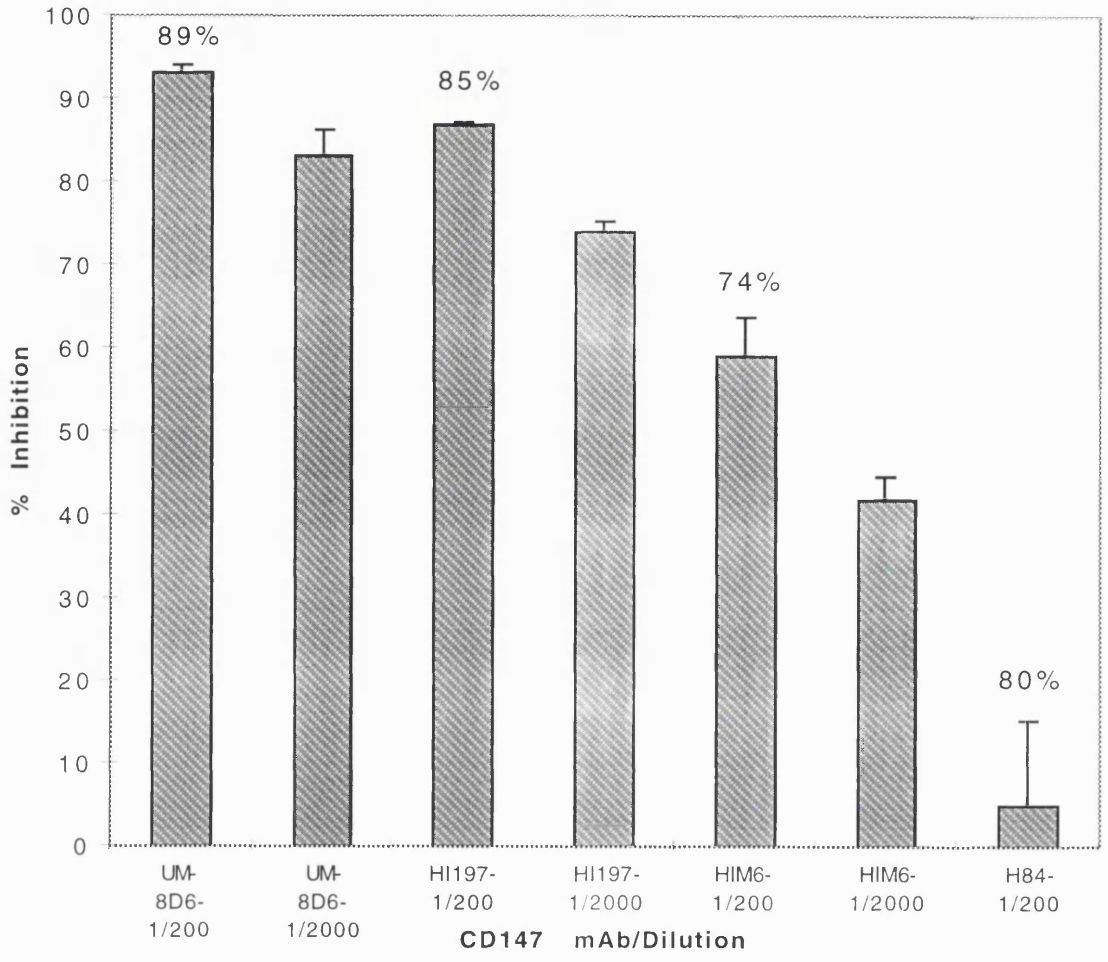

Figure 5.1.10.1. Inhibition of T-cell proliferation induced by CD147 mAbs is dose-dependent and not due to cytotoxicity.

Test mAbs (at 1/200 or 1/2000) were added to cultures of 10^4 irradiated U937 cells, $2x10^5$ T-cells and 0.1μg/ml CD3 mAb (UCHT1) (section 2.18.). Proliferation was assessed by measurement of ^3H thymidine incorporation. The response is shown as the mean % inhibition of T-cell proliferation in triplicate wells +/- % error, when test mAb is added to the assay compared to the proliferation in the absence of test mAb (control = 33200 cpm). Similar results were obtained in at least two other experiments. The % Figures given above the bars measure cell viability. 1/200 dilutions of mAbs were added to the assay, numbers of viable cells assessed by trypan blue exclusion (section 2.19.). Values shown are numbers of viable cells as a % of the numbers of viable cells in the no test mAb control. This control contained $1.9x10^5$ viable cells/well, compared to $2.1x10^5$ cells/well that were originally added.

Table 5.1.10.2.

CD147 mAb	Mean fluorescence intensity	
	U937	T cell
anti mouse 2nd layer only	24	5
UM-8D6	1085	76
HI197	1155	47
HIM6	1175	66
H84	864	67

Table 5.1.10.2. Levels of expression of CD147 on both U937 and T-cells. U937 and T-cells were stained with mAb as shown in column 1 and MFI determined by flow cytometry (see section 2.5.).

5.1.11. Role of unknown antigens in U937 induced T-cell proliferation.

5.1.11.1. mAbs of undefined specificity inhibit T-cell proliferation.

Four mAbs of undefined specificity inhibited T-cell proliferation by greater than 75%. (MEM 135, WM78, RmCB and K108). This inhibition was dose-dependent and was not due to cytotoxicity (Figure 5.1.11.1.).

5.1.11.2. Expression of these undefined antigens on U937 and T-cells.

Flow cytometry with these mAbs showed that two of the mAbs, MEM 135 and WM78, were strongly positive on U937 cells and less positive on T-cells. Expression of RmCB and K108 could not be detected on either cell type by FACS analysis (Table 5.1.11.2.).

Figure 5.1.11.1.

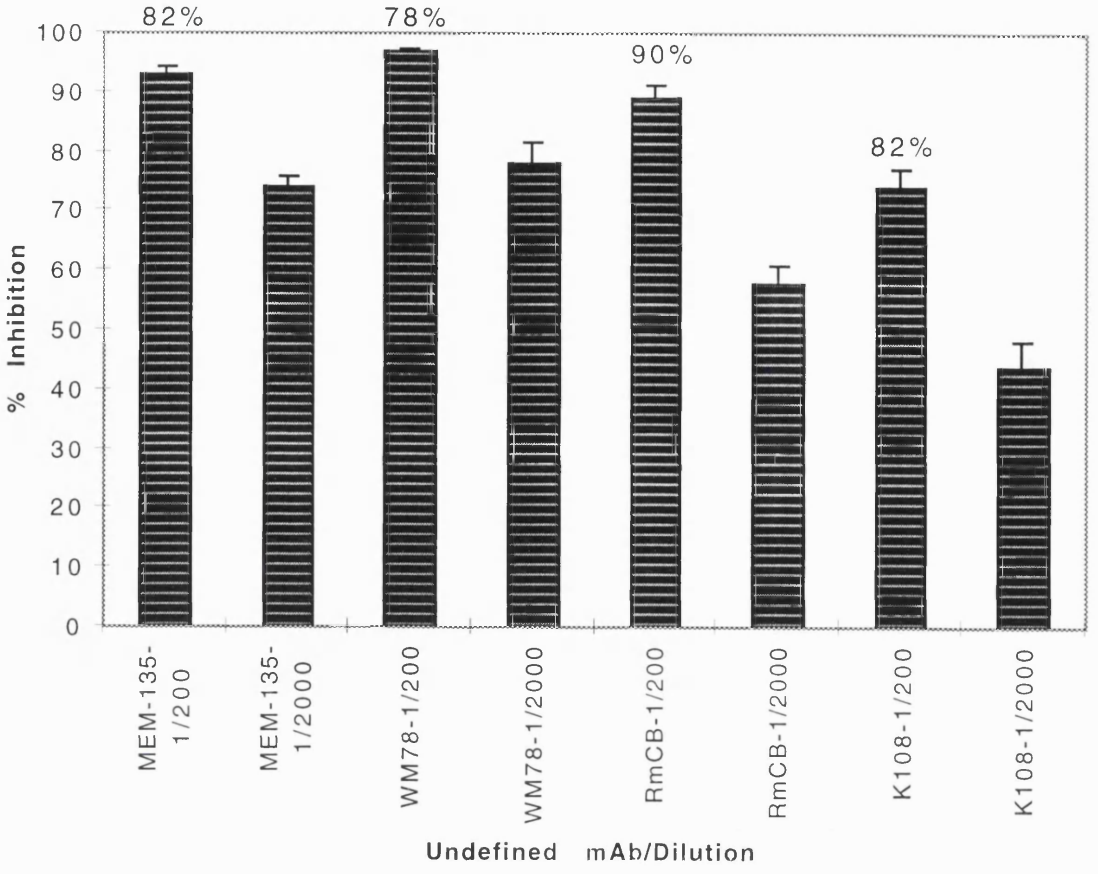

Figure 5.1.11.1. Inhibition of T-cell proliferation induced by mAbs of unknown specificity is dose-dependent and not due to cytotoxicity.
Test mAbs (at 1/200 or 1/2000) were added to cultures of 10^4 irradiated U937 cells, $2x10^5$ T-cells and 0.1μg/ml CD3 mAb (UCHT1) (section 2.18.). Proliferation was assessed by measurement of ^3H thymidine incorporation. The response is shown as the mean % inhibition of T-cell proliferation in triplicate wells +/- % error, when test mAb is added to the assay compared to the proliferation in the absence of test mAb (control = 33200 cpm). Similar results were obtained in at least two other experiments. The % Figures given above the bars measure cell viability. 1/200 dilutions of mAbs were added to the assay, numbers of viable cells assessed by trypan blue exclusion (section 2.19.). Values shown are numbers of viable cells as a % of the numbers of viable cells in the no test mAb control. This control contained $1.9x10^5$ viable cells/well, compared to $2.1x10^5$ cells/well that were originally added.

Table 5.1.11.2.

Unclassified mAb	Mean fluorescence intensity	
	U937	T cell
anti mouse 2nd layer only	24	5
MEM-135	466	93
WM78	483	89
RmCB	23	7
K108	25	8

Table 5.1.11.2. Levels of expression of undefined mAbs on both U937 and T-cells.
U937 and T-cells were stained with mAb as shown in column 1 and MFI determined by flow cytometry (see section 2.5.).

5.1.12. Non-inhibitory mAbs that bind to either U937 or T-cells.

To demonstrate that the inhibition seen previously was due to the specificity of the mAbs used rather than non specific functions of mAbs in general, flow cytometry was used to assess binding to U937 and T-cells of a selection of mAbs which have no inhibitory effects on T-cell proliferation. Table 5.1.12. shows the level of binding (MFI) of isotyped matched mAbs to U937 cells (range, MFI 76-1420), and T-cells (range, MFI 17-206). The last two columns show the negligible % inhibition (and % error) of T-cell proliferation caused by these mAbs (see section 5.1.4.).

5.1.13. CD53, CD55, CD98, CDw108, CD147 and the undefined mAbs do not inhibit U937/T-cell cluster formation.

Figure 5.1.13. shows that inhibitory mAbs against CD53, CD55, CD98, CDw108, CD147 and undefined mAbs did not inhibit formation of U937 / T-cell clusters. This contrasts with mAbs against CD11a /18 and CD54 mAbs which inhibited both T-cell proliferation and cluster formation

(Figure 5.1.3.1.), and with CD45 mAbs which caused an increase in cluster size (Figure 5.1.5.3), whilst inhibiting T-cell proliferation. This suggests that different mAbs cause inhibition via differing mechanisms; and that while clustering is necessary for T-cell proliferation, it is not sufficient.

Table 5.1.12.

Specificity	Antibody	Mean fluorescence intensity		%Inhibition	%Error
		U937	T cell		
anti mouse 2nd layer only		18	5		
CD30	11D1.H10	332	17	8	4
CD43	148-1C3	1420	59	-15	12
CD44	TA-9B1	356	206	7	5
CD48	156-4H9	85	98	10	9.5
CD48	BU91	76	121	-17	4
CD71	LT-4E3	854	24	-29	12.5
CD99	HI142	129	80	8	10

Table 5.1.12. Levels of expression of non inhibitory mAbs on U937 and T-cells, and inhibition of T-cell proliferation found with these mAbs. U937 and T-cells were stained with mAb as shown in column 1 and 2 and MFI determined by flow cytometry (see section 2.5.). In columns 5 and 6 the inhibition induced by these mAbs is shown (see section 2.19.). The results are expressed as the mean percentage inhibition of T-cell proliferation in triplicate wells +/- % error, when test mAb was added to the assay compared to the proliferation in the absence of test mAb (proliferation in control was 99172 cpm).

Figure 5.1.13.

A.

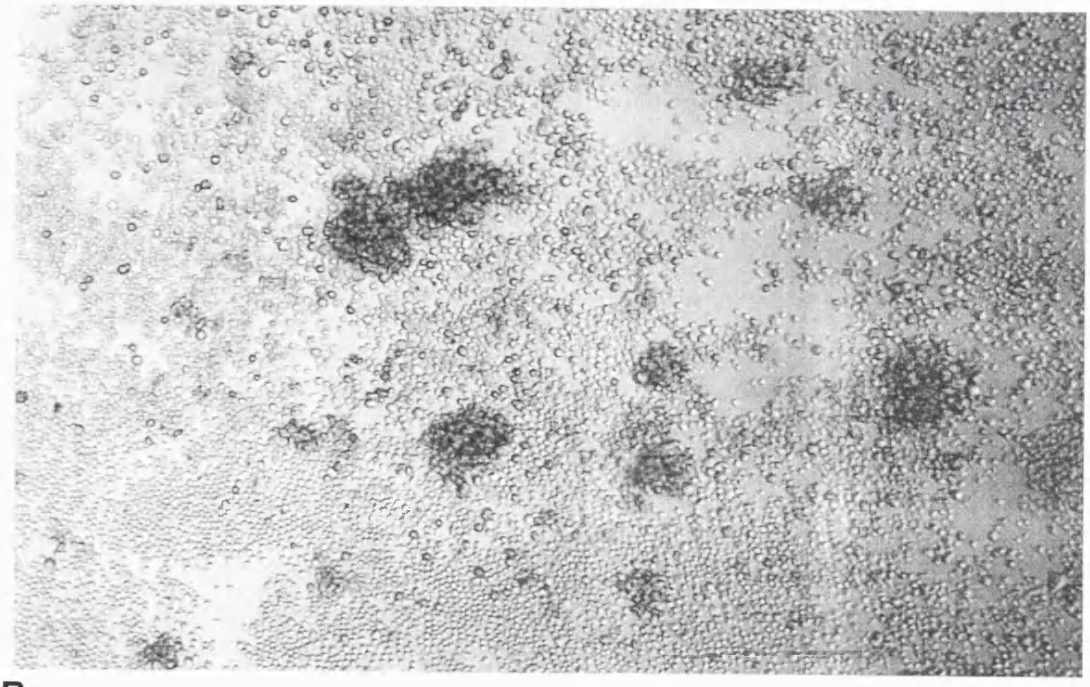

B.

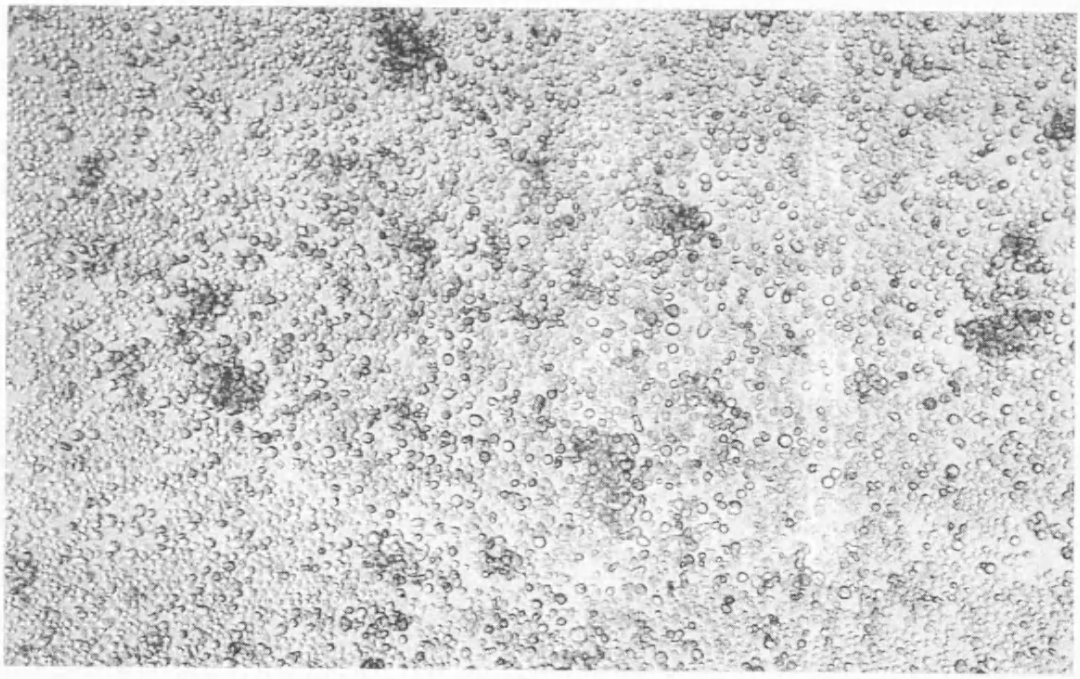

Figure 5.1.13.

C.

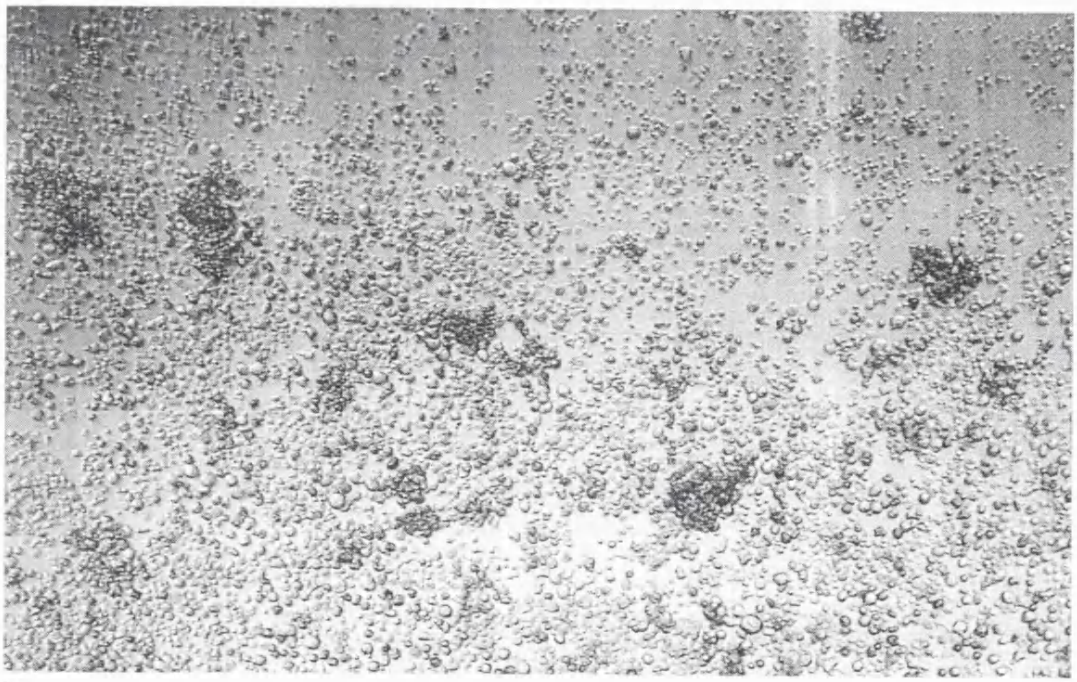

D.

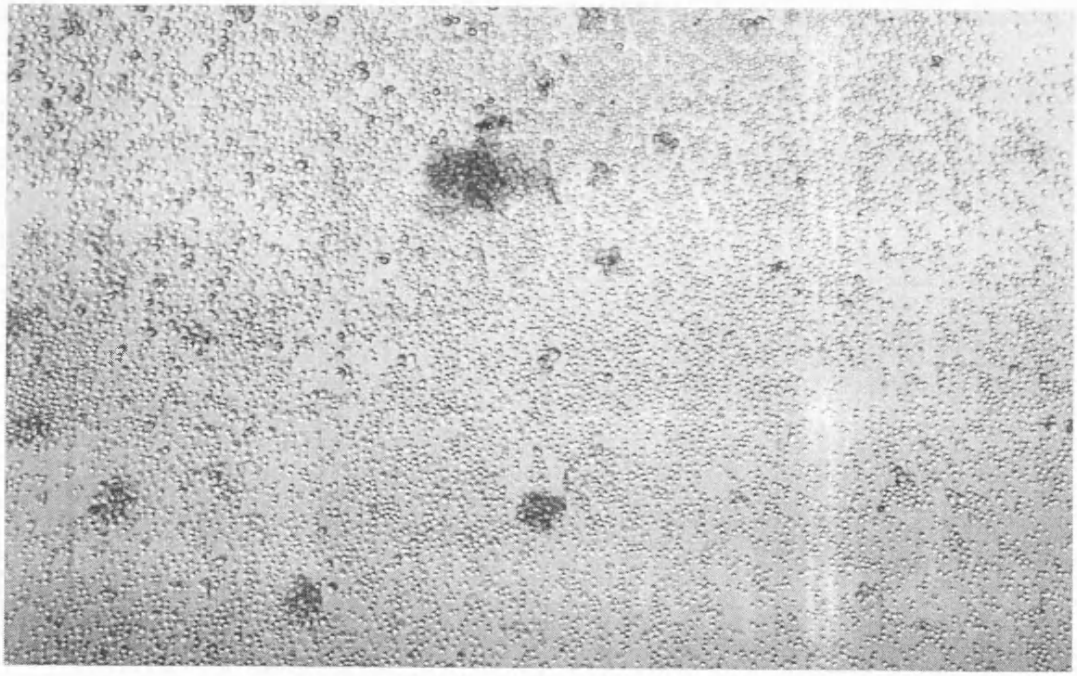

Figure 5.1.13.

E.

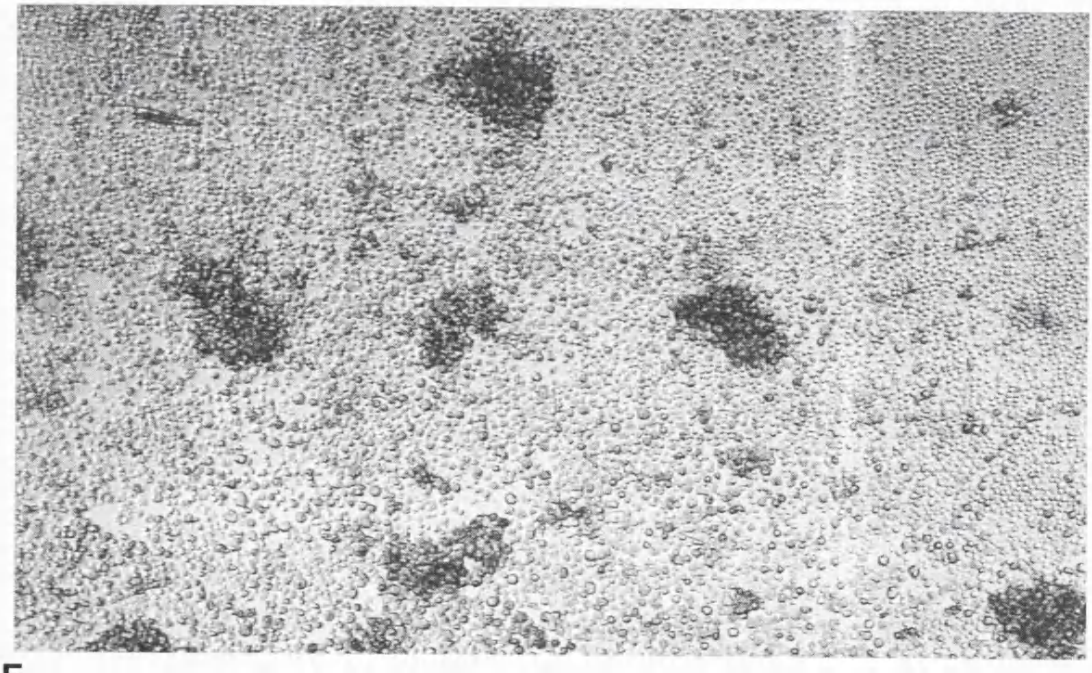

F.

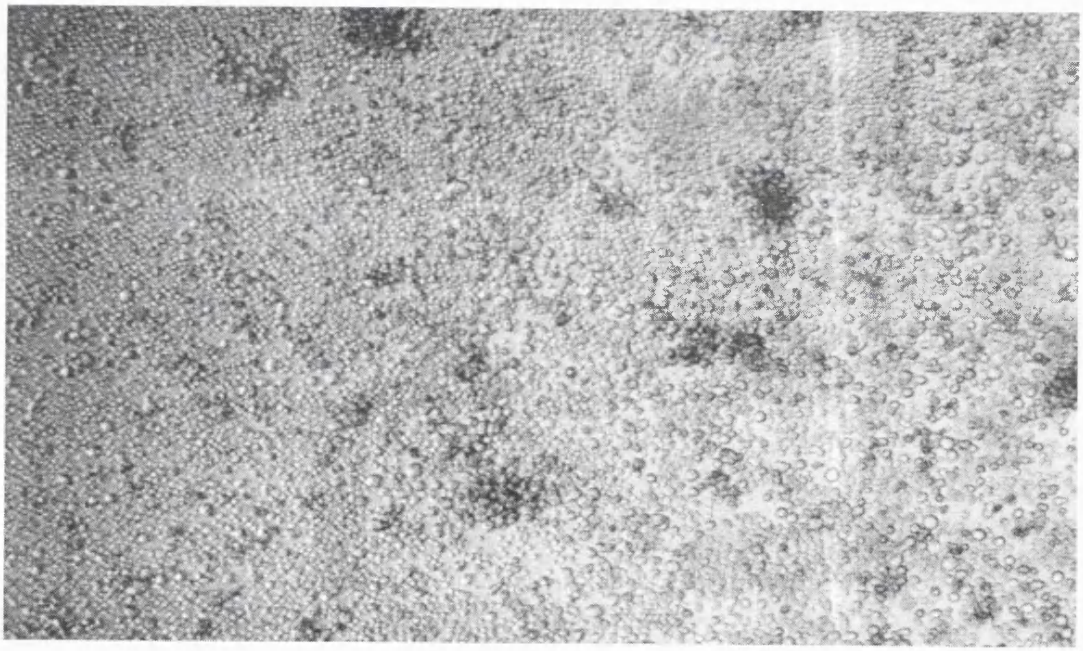

Figure 5.1.13.

G.

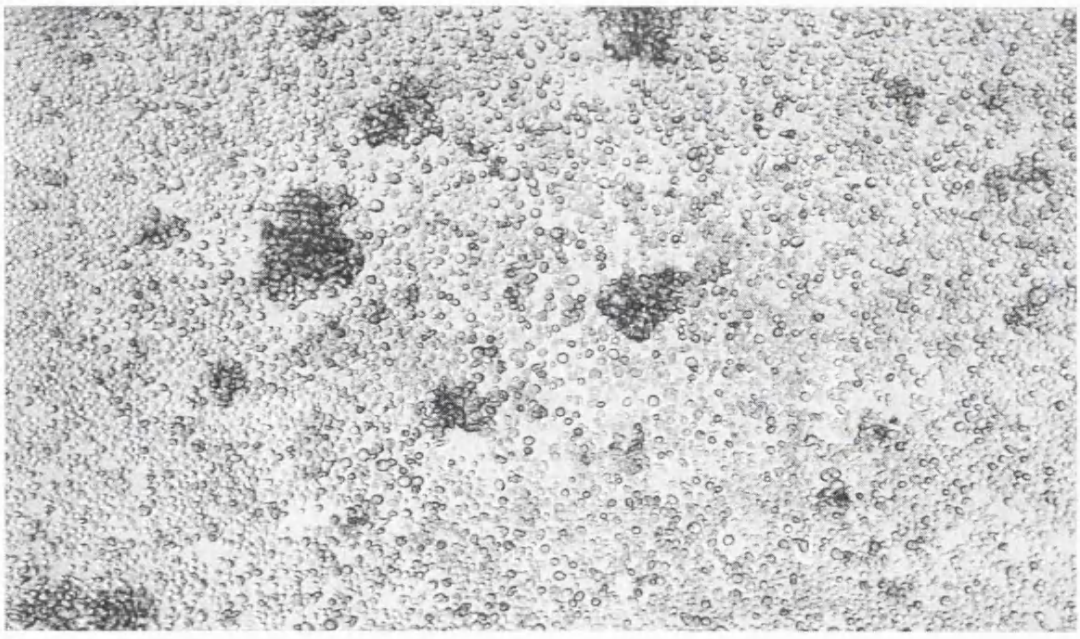

H.

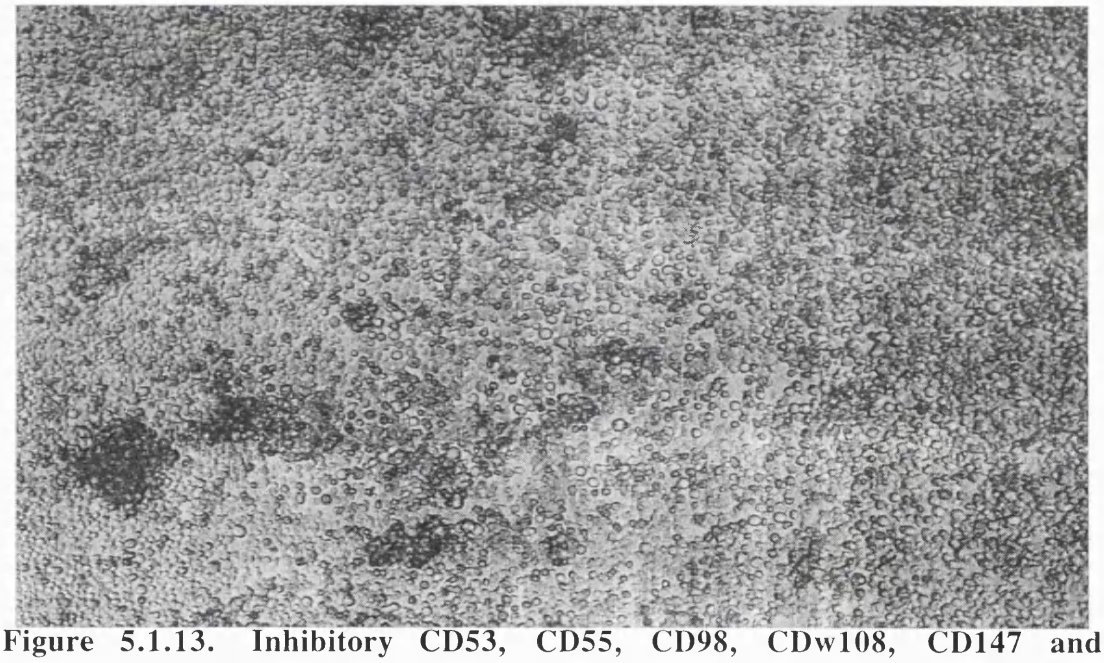

Figure 5.1.13. Inhibitory CD53, CD55, CD98, CDw108, CD147 and undefined mAbs do not effect U937 / T-cell cluster formation.

(A). 10^4 irradiated U937 cells, $2x10^5$ T-cells, and 0.1μg/ml CD3 mAb (UCHT1) were cultured for 48 hours (section 2.18.). Cluster formation assessed visually at x40 magnification. (B-H). As above, but with 1/400 dilution of: (B). CD53 mAb AC 119; (C). CD55 mAb JS 11; (D). CD98 mAb J3-E1B; (E). CDw108 mAb MEM 150; (F). CD147 mAb HI197; (G). undefined mAb WM78 and (H). undefined mAb MEM 135.

5.1.14. Pre-incubation of U937 cells with mAbs inhibits T-cell responses.

To investigate whether the mAbs that we had previously identified as inhibitors were having their effect on the co-stimulatory ability of U937 cells, or were acting via a direct effect on T-cells, U937 cells were pre-pulsed, excess antibody washed off, and then cells added into the T-cell proliferation assay as before. Figure 5.1.14. shows a representative experiment demonstrating that the majority of these mAbs were still inhibitors of T-cell responses, although generally mAbs did not give as high a percentage inhibition as in the standard assay, where the mAb was in solution. Thus, pre-incubation of U937 cells with mAbs to CD11a (CD11a-6B7), CD18 (7E4), CD54 (MEM112), CD98 (J3-E1B) and CD147 (HI 197) resulted in more than 60% inhibition of T-cell proliferation. This concurs with FACS analysis which showed that all these molecules were more abundant on U937 cells than on T-cells. The CD45 mAb (4.14) was ~40% inhibitory of T-cell proliferation, and the mAbs MEM 135 and WM78, which target unknown antigens, inhibited T-cell proliferation by 22% and 58% respectively. These results suggest that these mAbs inhibit T-cell proliferation by having an effect on accessory U937 cells, and not because of a direct effect on T-cells. In contrast, the CD53 mAb (AC119) showed no inhibitory ability in this assay, suggesting that this mAb has an inhibitory effect mediated via the T-cell. This is consistent with the observation that much more CD53 was present on T-cells than on U937 cells (Table 5.1.6.2.).

Figure 5.1.14.

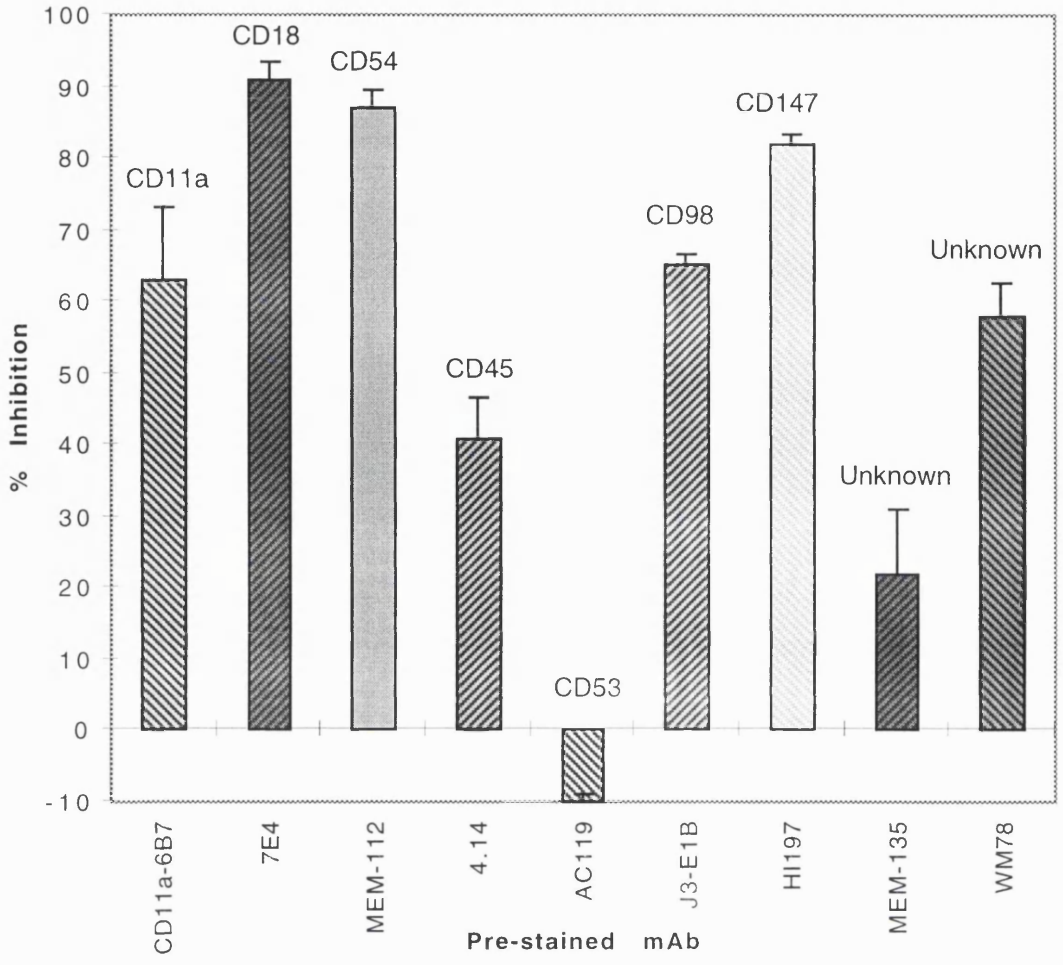

Figure 5.1.14. Inhibitory activity of antibodies when bound selectively to U937 cells.

MAbs (1/100) were incubated with U937 cells for 1 hour at 37°C and excess mAb removed by washing (section 2.20.). 10^4 of mAb/U937 cells were co-cultured with $2x10^5$ purified T-cells and 0.1μg/ml CD3 mAb (UCHT1) (section 2.17.). Proliferation was assessed by measurement of ^3H thymidine incorporation. The results are expressed as the mean % inhibition of T-cell proliferation in triplicate wells +/- % error, when test mAb was added compared to the proliferation in the absence of test mAb. The proliferation in the absence of test mAb was 92691cpm. Similar results were obtained in at least two other experiments.

5.1.15. Addition of inhibitory mAbs to a PMA/ionomycin dependent - U937 independent T-cell proliferation assay causes inhibition of T-cell activation.

In additional assays to assess the effect of the inhibitory mAbs directly on T-cells, tonsillar T-cells were activated in a U937/CD3 independent assay using the PKC activating compound PMA, and the calcium ionophore ionomycin. Figure 5.1.15. shows that mAbs to CD53, CD55, and CDw108, completely inhibited T-cell proliferation in this assay, thus agreeing with the FACS data that these mAbs bound to T-cells, not U937 cells. The unknown mAb MEM-135 also completely inhibited T-cell proliferation in this system, despite its target antigen being more highly expressed on U937 cells than on T-cells. These mAbs therefore appear to inhibit T-cell proliferation via T-cell, rather than by U937-T-cell interactions.

The mAbs against CD11a, CD18, CD54, and the two unknown antigens targeted by WM78 and RmCB, did not inhibit T-cell proliferation in this assay, and are thus likely to have inhibitory effects at the U937 -T-cell level. Of two mAbs directed against CD45 used in this assay, one (4.14) strongly inhibited T-cell proliferation, and another (CBE-77) inhibited by ~ 50%, suggesting that CD45 mAbs inhibit T-cell proliferation both via the T-cell, and the U937-T-cell interaction.

Of two mAbs directed against CD98 used in this assay, one J1-G3B completely inhibited T-cell proliferation and the other J3-E1B inhibited by ~ 60%. This agrees with the FACS data that J1-G3B binds strongly to T-cells and suggests that these CD98 mAbs inhibit T-cell proliferation both via the T-cell, and the U937-T-cell interaction.

Figure 5.1.15.

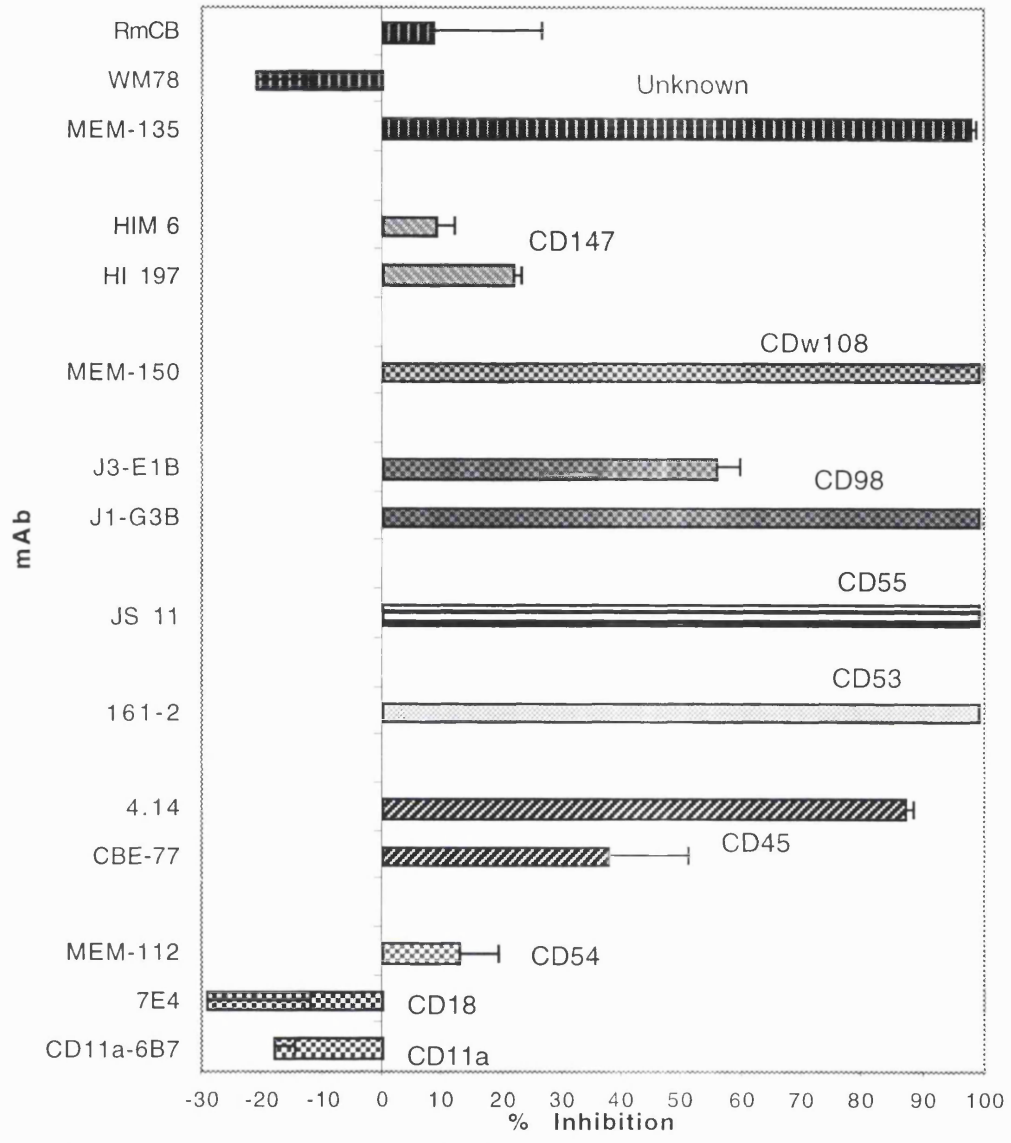

Figure 5.1.15. Some mAbs are inhibitory of T-cell proliferation in a U937 independent proliferation assay.

Dilutions (at 1/400) of inhibitory mAbs were added to $2x10^5$ purified T-cells to which 2μg/ml ionomycin and 25ng/ml PMA had already been added and cells cultured as before (section 2.21.). T-cell proliferation was assessed by measurement of ^3H thymidine incorporation. The results shown are the mean % inhibition of T-cell proliferation in triplicate wells +/- % error, when test mAb is added to the assay compared to proliferation in the absence of test mAb. (control = 11990 cpm). PMA or ionomycin in isolation induced no T-cell proliferation. Similar results were obtained in at least one other experiment.

Of two mAbs directed against CD147 used in this assay, one (HI 197) inhibited T-cell proliferation ~ 50%, and the other (HIM 6) inhibited T-cell proliferation only slightly. This again agrees with the FACS data that CD147 is expressed predominantly on U937 cells, and suggests that both these mAbs inhibit T-cell proliferation both via the T-cell, and the U937-T-cell interaction.

5.1.16. U937 cells are more efficient co-stimulators of CD8+ T-cells, than of CD4+ T-cells.

To define the nature of the U937/CD3 induced T-cell response further, tonsillar T-cells were sub-purified into CD4+ and CD8+ fractions by immunodepletion. The purity of these fractions was confirmed by FACS analysis to show that 99% of the CD8-depleted cells were CD4+, and conversely 98% of the CD4-depleted cells were CD8+.

5.1.16.1. CD8+ T-cells proliferate 3-10 fold more than CD4+ T-cells.

Figure 5.1.16.1. shows that U937 induced proliferation of CD8+ T-cells was significantly greater than that seen with both CD4+ cells and the mixed starting T-cells from the same tonsil. This difference in proliferation was consistent, although the relative increase was variable from tonsil to tonsil, with a range of 3-10 fold difference detectable between CD4+ and CD8+ T-cells from the same individual.

5.1.16.2. Previously described inhibitory mAbs inhibit CD4+ and CD8+ T-cells equally.

Assays with inhibitory mAbs were performed with the CD4+ or CD8+ T-cell fractions. Figure 5.1.16.2. shows that there was little qualitative difference in the inhibitory capability of the antibodies tested, as judged by percentage inhibition of T-cell proliferation with respect to each of the CD4+, CD8+ or the undepleted T-cells no test mAb controls.

5.1.17. CD28 mAb stimulates proliferation of CD4+ T-cells, but not of CD8+ T-cells.

Since the molecules we had identified as being involved in T-cell activation in this model were apparently required for both CD4 and CD8 T-cell activation, we tested whether the inability of U937 cells to stimulate CD4 cells as effectively as CD8 cells might be due to the absence of a CD28 ligand on these cells. Previous studies (Palmer and van Seventer, 1997) had reported that CD80 was absent on U937 cells, while CD86 was present at very low levels. We were unable to detect CD86 on U937 cells by flow cytometry (data not shown). In order to by-pass the requirement for CD80/86, an agonistic CD28 mAb, 15E9, was added to the U937/CD3 - T-cell proliferation assay (Figure 5.1.17.). The addition of CD28 mAb increased CD4+ T-cell proliferation 8 fold, and increased the proliferation of unseparated T-cells by 4.5 fold. However, the addition of CD28 antibody did not affect proliferation of CD8+ T-cells. In the presence of CD3 mAb, CD28 mAb, or U937 cells alone, no proliferation of any T-cell subset was found. The addition of both CD3 and CD28, in the absence of U937 cells, caused only a low level of T-cell proliferation, suggesting that CD28 signalling *per se* is insufficient to trigger the resting T-cells in this model. The difference in sensitivity to CD28 antibody between CD4+ and CD8+ T-cell proliferation in response to CD28 antibody was not due to differences in CD28 expression, as flow cytometry demonstrated that CD28 was expressed equally on both CD4+ T-cells (95% of cells positive, and an MFI of 62), and on CD8+ T-cells (96% of cells positive, and an MFI of 65).

Figure 5.1.16.1.

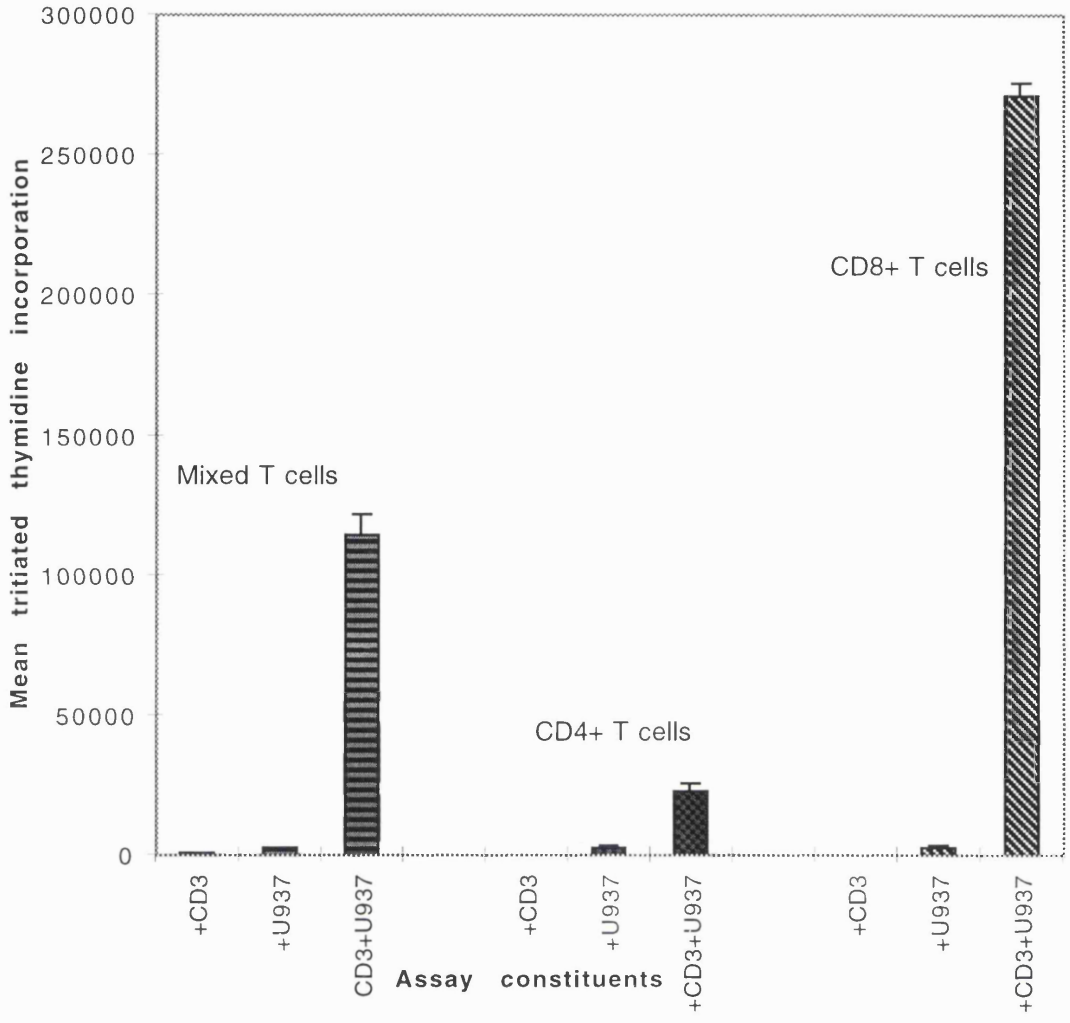

Figure 5.1.16.1. U937 cells preferentially stimulate CD8+ T-cells.
T-cells from one tonsil were purified into CD4+ and CD8+ fractions. $2x10^5$ T-cells of the appropriate population (CD4+, CD8+ or initial mixed population) were co-cultured with 10^4 irradiated U937 cells and 0.1μg/ml CD3 mAb (UCHT1) (section 2.17.). Proliferation was assessed between 48 and 64 hours of culture by measurement of ^3H thymidine incorporation. The data is expressed as mean T-cell proliferation of triplicate wells +/- SD, from one representative experiment. Similar results were obtained in at least two other experiments.

Figure 5.1.16.2.

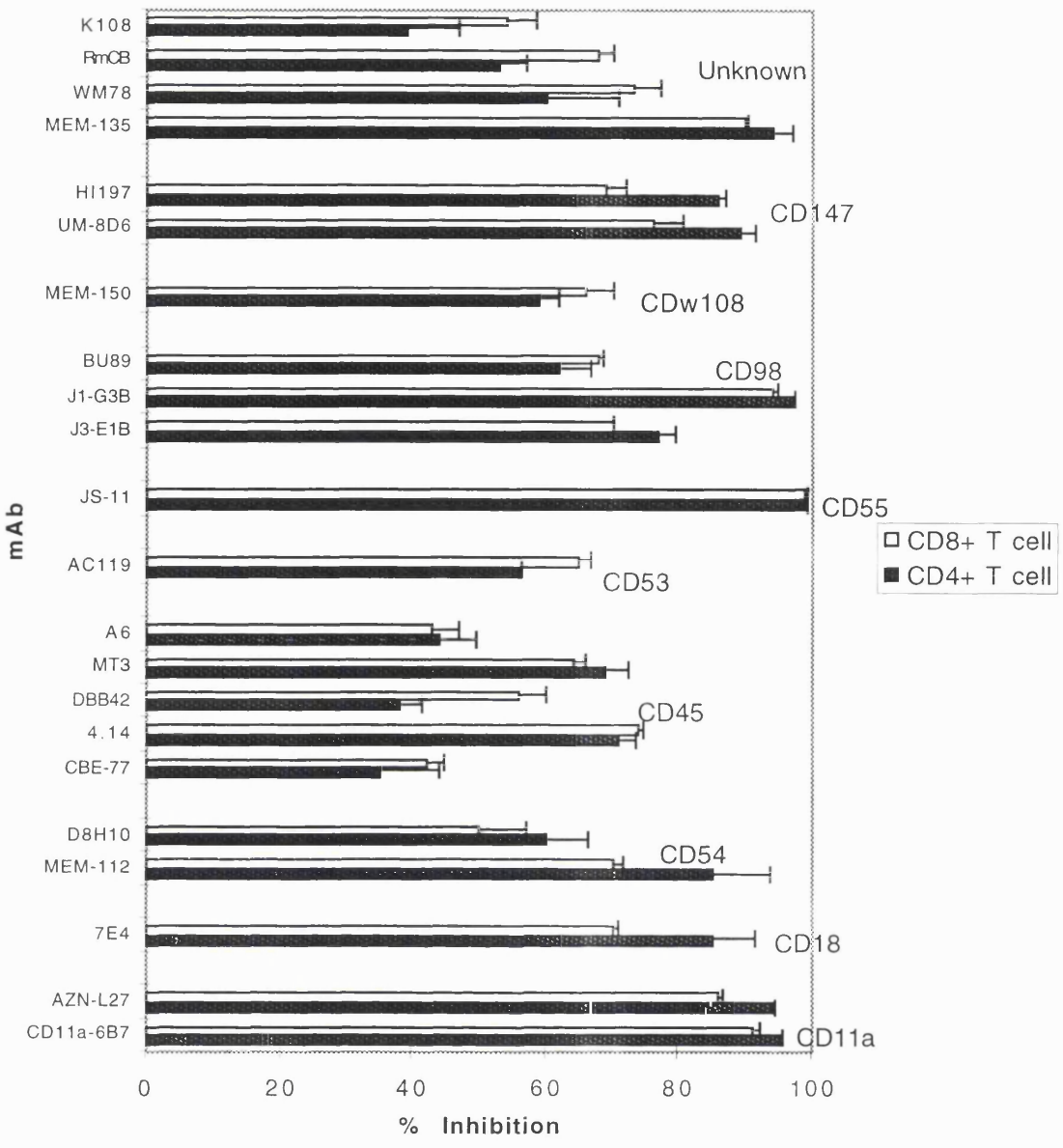

Figure 5.1.16.2. Inhibitory mAbs affect CD4+ and CD8+ T-cells equally. Test antibodies (at 1/400 dilution) were added to cultures containing 10^4 irradiated U937 cells, $2x10^5$ purified CD4+ or CD8+ T-cells and 0.1μg/ml CD3 mAb (UCHT1) (see section 2.18.). T-cell proliferation was assessed by the measurement of ^3H thymidine incorporation. The values shown are the mean % inhibition of T-cell proliferation in triplicate wells +/- % error, when test mAb is added to the assay compared to proliferation in the absence of test mAb. Mean proliferation in the absence of test mAb for CD4+ T-cells was 23203 cpm; and for CD8+ T-cells was 270838 cpm. Similar results were obtained in at least one other experiment.

Figure 5.1.17.

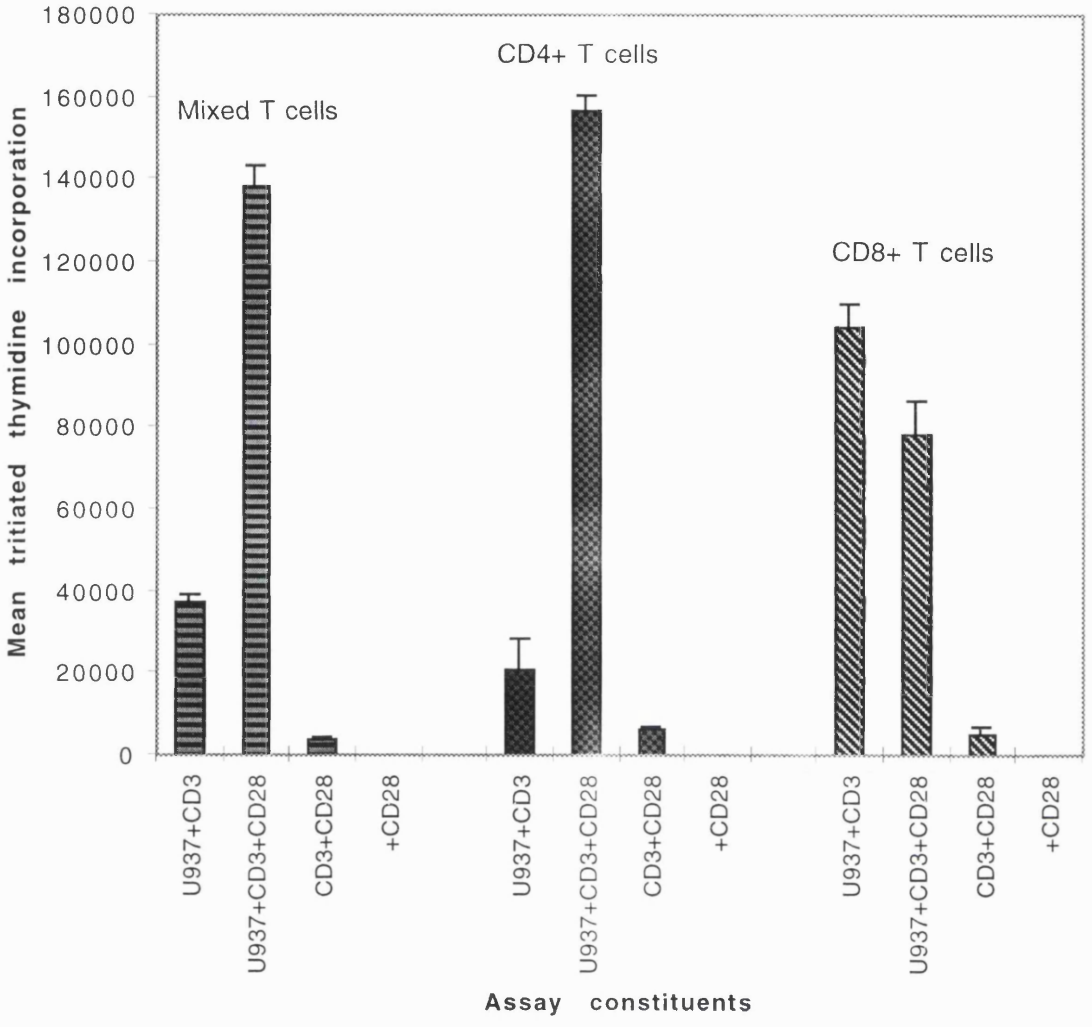

Figure 5.1.17. An agonistic CD28 antibody co-stimulates CD4+ T-cells, but has no effect on CD8+ T-cells.

The CD28 mAb 15E9 (1/20) was added to 10^4 irradiated U937 cells, either $2x10^5$ purified CD4+, CD8+ or mixed T-cells, and 0.1μg/ml CD3 mAb (UCHT1) (see section 2.18.). T-cell proliferation was assessed by measurement of ^3H thymidine incorporation. The values shown are the mean proliferation of triplicate wells +/- SD, from one representative experiment. Similar results were found in at least two other experiments.

5.1.18. The inhibitory mAbs previously described induce changes in tyrosine phosphorylation in both U937 and T-cells.

In order to further assess how the addition of the mAbs inhibits T-cell responses, purified T-cells and U937 cells were treated for various time points with the inhibitory mAbs, and anti-phosphotyrosine immunoblotting performed on cell lysates.

5.1.18.1. mAbs that induce tyrosine phosphorylation in U937 cells.

Examples of mAbs from some of the groups previously described as inhibitory were incubated with U937 cells for 10 or 60 minutes and the phosphotyrosine response to these mAbs was then assessed by immunoblotting. Figure 5.1.18.1 shows the phosphotyrosine response shown by U937 cells. The mAb CBE-77 (CD45) induced extensive tyrosine phosphorylation after 60 minutes, but not after 10 minutes. (Figure 5.1.18.1A. lanes 5 and 6). There was no difference in this response in the presence of CD3 mAb (lane 2). CD3 in isolation had no effect (lanes 3 and 4), CD28 also had no effect (lane 7).

Two CD98 mAbs were tested. J1-G3B, had an unusual expression pattern for CD98 in that it bound T-cells more than U937 cells, and J3-E1B had the normal CD98 expression of U937 cells high, T-cell low (Table 5.1.8.2). Both of these mAbs induced extensive tyrosine phosphorylation after 10 minutes, and this increased after 60 minutes. Although most phosphoproteins were common to cells incubated with either mAb, J3-E1B induced phosphorylation of a 26kD protein that was not induced by J1-G3B (Figure 5.1.18.1B.).

Figure 5.1.18.1.

A.

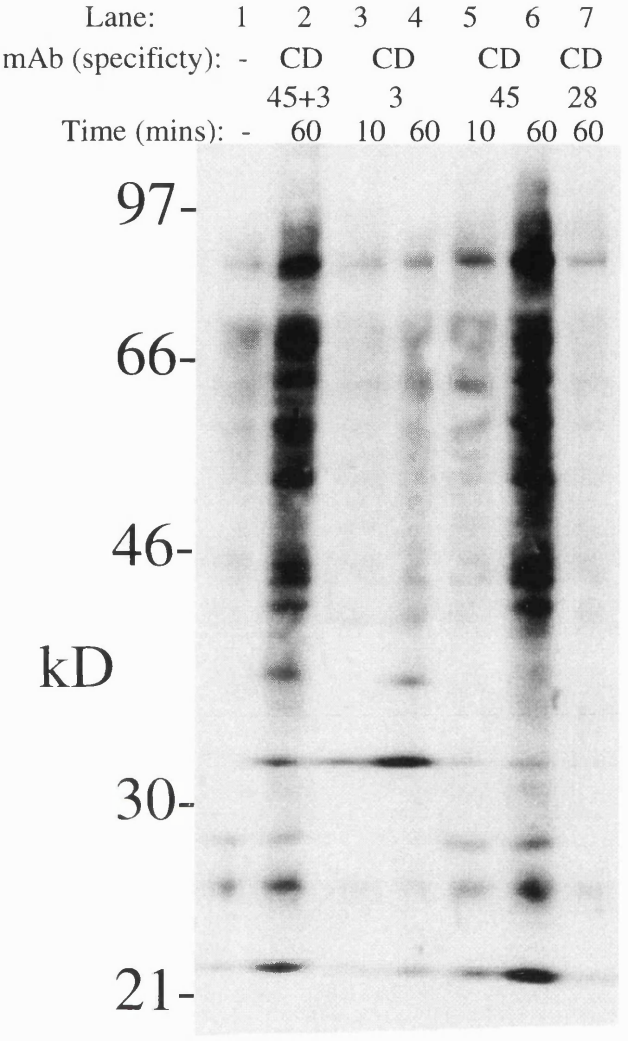

Figure 5.1.18.1.

B.

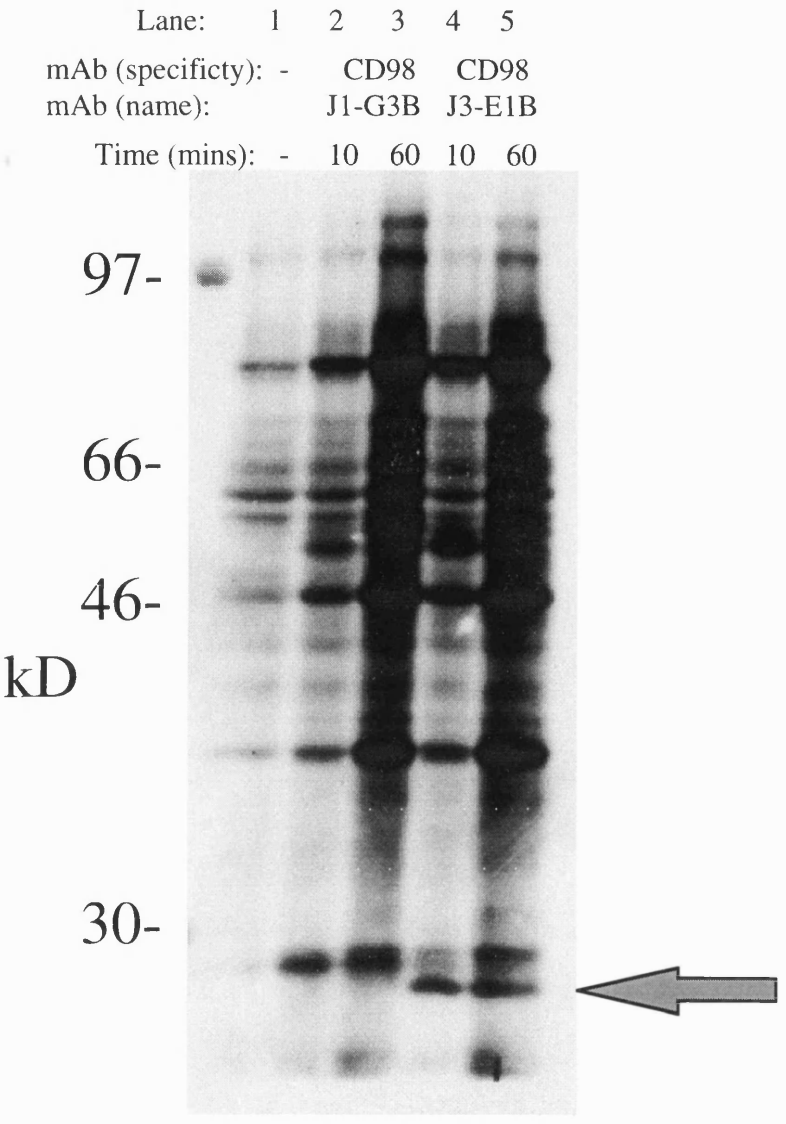

Figure 5.1.18.1.

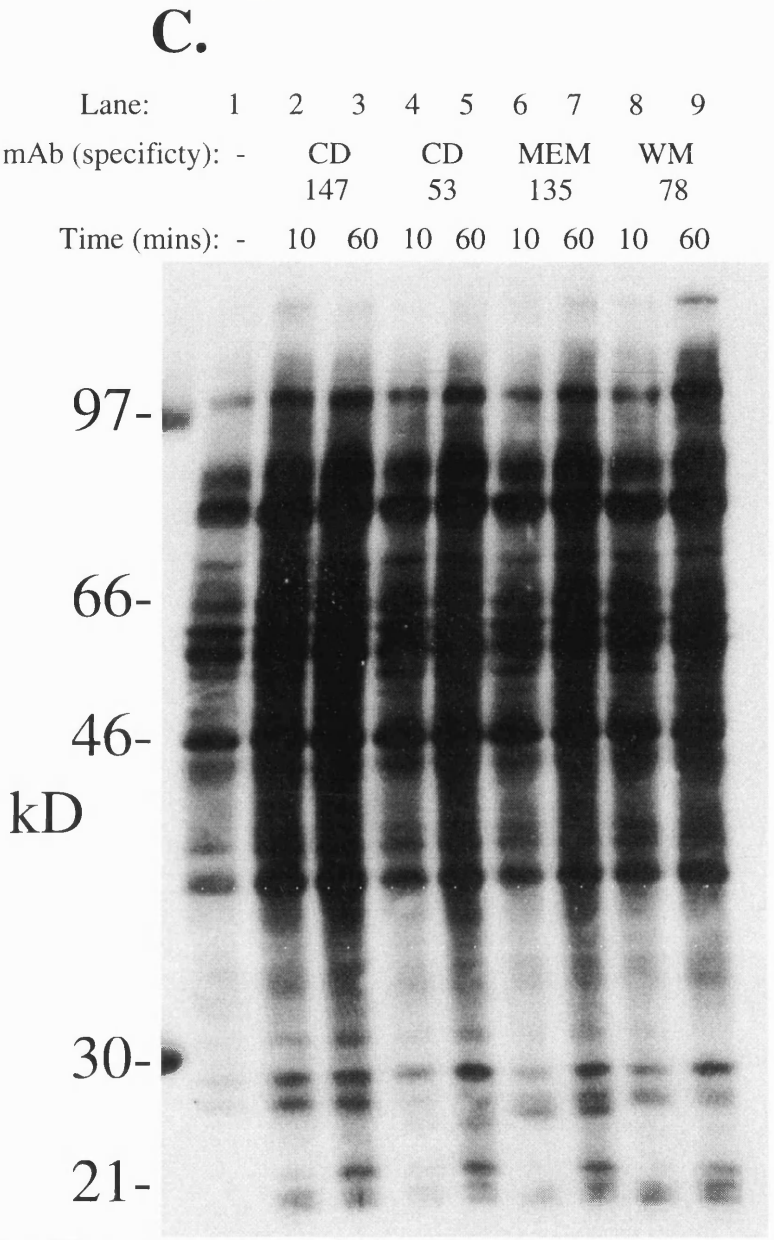

Figure 5.1.18.1. The effects of inihibitory mAbs on tyrosine phosphorylation of U937 cells.

1/100 dilutions of mAbs were added to $2x10^6$ U937 cells and cultured together for 10 or 60 minutes at 37° C. Cells were washed, spun and lysed in 100µl of a 1% NP40 buffer. Immunoblotting with an antiphosphotyrosine mAb (4G10) was performed on separated proteins (section 2.4.). The mAbs used in this study were CBE-77 (CD45), UCHT1 (CD3), and 15E9 (CD28) (A); J1-G3B and J3-E1B (both CD98) (B); 202-24B (CD53), HI197 (CD147), MEM-135 andWM78 (both unclassified) (C).

Figure 5.1.18.1C. shows the results of inhibitory mAbs HI197 (CD147) (lanes 2 and 3), 202-24B (CD53) (lanes 4 and 5), MEM-135 (lanes 6 and 7) and WM78 (lanes 8 and 9) (both unclassified), all induced small amounts of tyrosine phosphorylation especially of 15-40kD proteins. Overall, mAbs against CD45, CD98 and CD147 induced the most phosphorylation.

It is important to note that mAbs to CD28 (15E9) and CD3 (UCHT1) which are not expressed on U937 cells, did not induce tyrosine phosphorylation, suggesting that the signalling seen is genuine and not an artefact of mAbs cross linking Fc receptors thus triggering phosphorylation (Figure 5.1.18.1A.).

5.1.18.2. mAbs that induce tyrosine phosphorylation in purified T-cells.
The same mAbs used in the study on U937 cells (see 5.1.18.1.) were then used in an identical way on purified tonsillar T-cells. Figure 5.1.18.2. shows the phosphotyrosine response shown by T-cells. The mAb CBE-77 (CD45) induced extensive tyrosine phosphorylation (Figure 5.1.18.2A.) after 10 minutes addition. This level of phosphorylation was maintained after 60 minutes addition (lanes 2 and 3). The mAb UCHT1 (CD3) also induced tyrosine phosphorylation after 10 minutes. After 60 minutes this response was diminished slightly (lanes 4 and 5). The mAb 15E9 (CD28) induces tyrosine phosphorylation after 10 minutes addition, and after 60 minutes this level of phosphorylation increased (lanes 6 and 7). Surprisingly, the addition of a combination of CD3 and CD45 mAbs lead to only slight induction of phosphorylation, that was less than that induced by either mAb in isolation.

Of the two CD98 mAbs used (Figure 5.1.18.2B.), J1-G3B induced phosphorylation of two proteins, one of 54kD, and one of 28kD (lanes 2 and 3), whilst J3-E1B does not induce any phosphorylation (lanes 4 and 5). This is consistent with the expression data, as J1-G3B binds to T-cells,

whereas J3-E1B does not (Table 5.1.8.2). The CD53 mAb (202-24B) induces extensive tyrosine phosphorylation (lanes 6 and 7). The mAb of unclassified designation MEM-135 induced low levels of tyrosine phosphorylation of a protein of 26kD (lanes 10 and 11). The mAb HI197 (CD147) (lanes 8 and 9) and WM78 (lanes 12 and 13) (unclassified) did not induce tyrosine phosphorylation (Figure 5.1.18.2B.).

The no mAb control samples in this section (lane 1 on each Figure), have different levels of background phosphorylation because the exposures chosen were those that best demonstrated mAb induced phosphorylation, and not those that had standard background levels.

Figure 5.1.18.2.

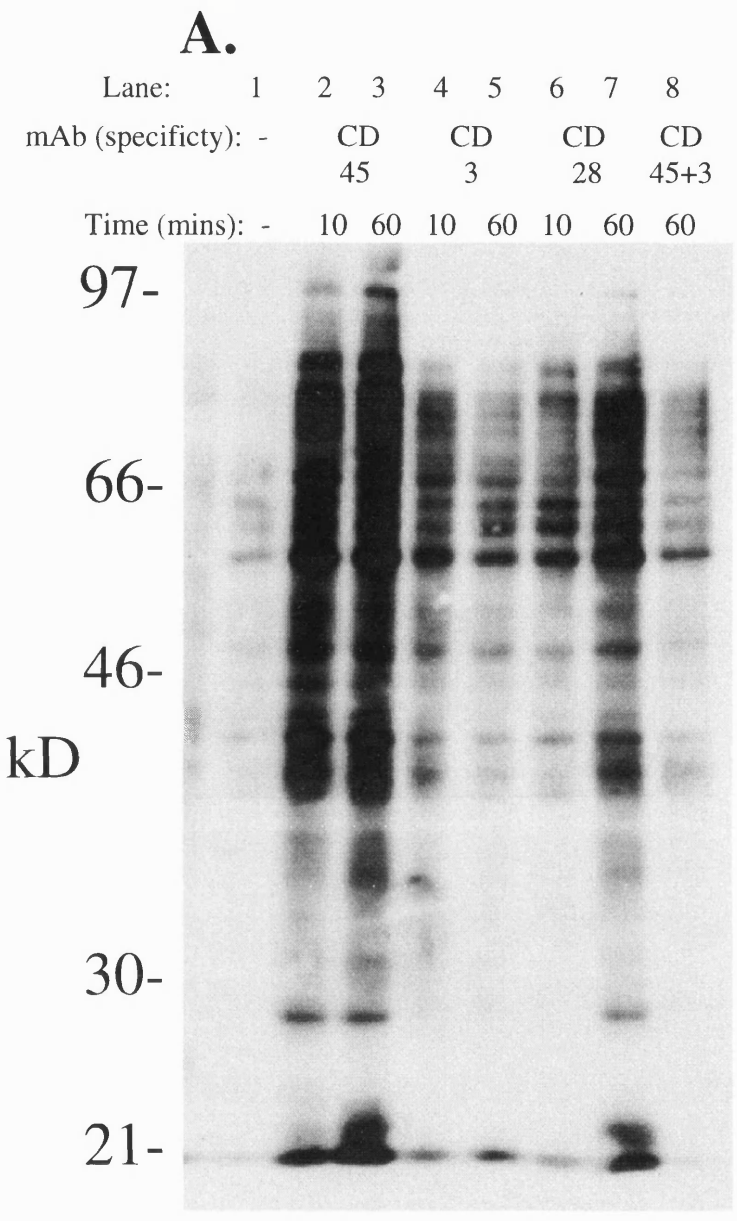

Figure 5.1.18.2.

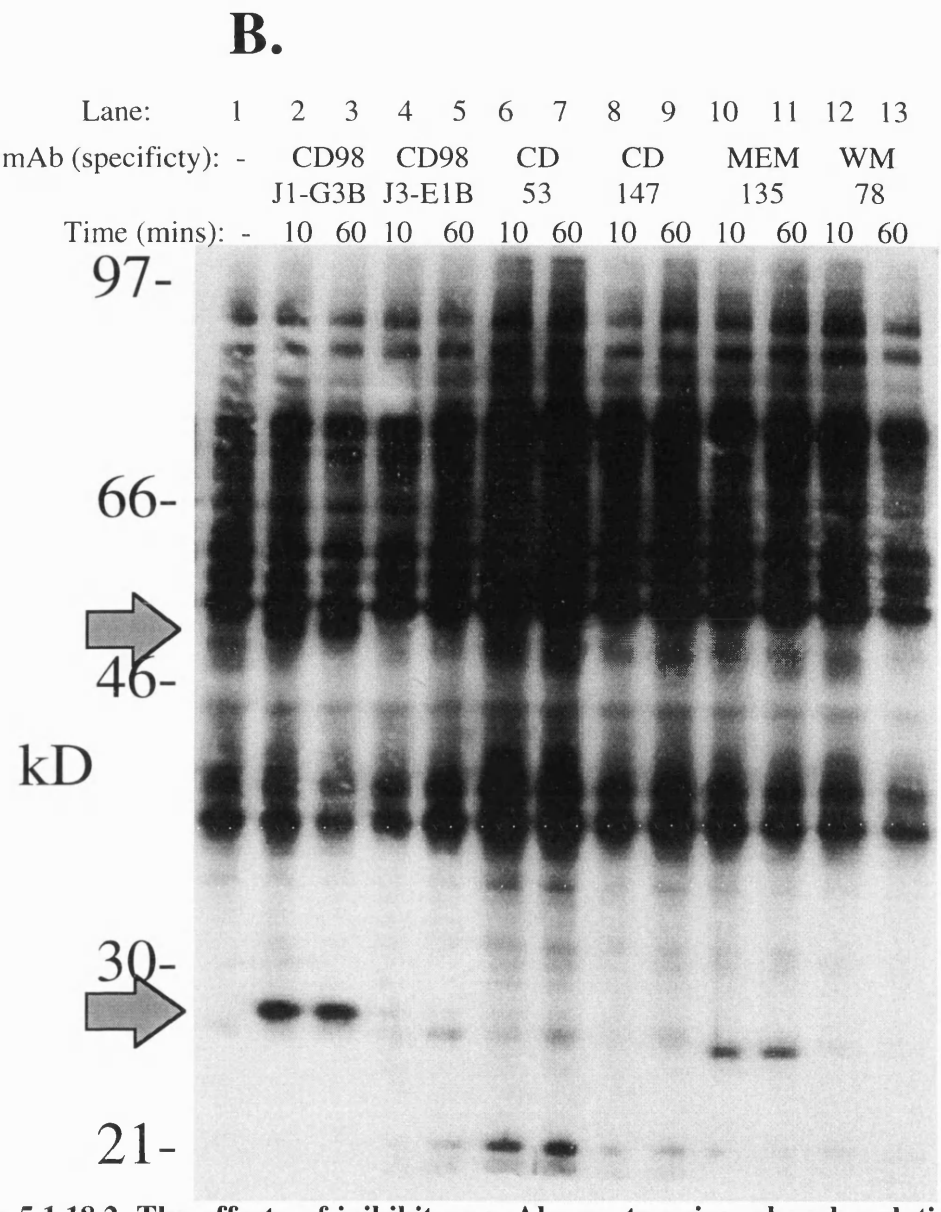

Figure 5.1.18.2. The effects of inihibitory mAbs on tyrosine phosphorylation of purified T-cells.

1/100 dilutions of mAbs were added to $4x10^6$ purified tonsillar T-cells and cultured together for 10 or 60 minutes at 37° C. Cells were washed, spun and lysed in 100µl of a 1% NP40 buffer. Immunoblotting with an antiphosphotyrosine mAb (4G10) was performed on separated proteins (section 2.4.). The mAbs used in this study were CBE-77 (CD45), UCHT1 (CD3), and 15E9 (CD28) (A); J1-G3B and J3-E1B (both CD98) (B); 202-24B (CD53), HI197 (CD147), MEM-135 andWM78 (both unclassified) (C).

5.2. Discussion.

The part played by accessory co-stimulatory molecules in the induction of immune responses has been explored extensively (Brown G.R. et al., 1995; Damle et al., 1992b; Jenkins and Johnson, 1993; Johnson and Jenkins, 1993; Mondino and Jenkins, 1994; van der Merwe et al., 1994; Van Seventer et al., 1990), and it is has been suggested that the nature and expression pattern of these molecules may help to determine outcome. For example, engagement of MHC molecules in the absence of co-stimulation can act as a tolerising rather than priming event (Boussiotis et al., 1995; Boussiotis et al., 1996). This observation is already being exploited in the clinic, both in attempts to render tumour cells immunogenic and thus activate and harness a host anti-tumour response (Chen, 1997), and in attempts to interfere with auto-immune T-cell activation (Boussiotis et al., 1994; Guinan et al., 1994).

The primary function of co-stimulatory molecules and their receptors on T-cells appears to give the appropriate cellular context to support antigen-specific T-cell activation, while at the same time preventing instigation of an immune response against a self-antigen expressed by non-immune cell.

Several different in vitro model systems have been used to define the role of these co-stimulatory molecules, ranging from primary cultures of APC and T-cells (Johnson and Jenkins, 1994) to single epitope transfectant analysis (Moudgil and Sercarz, 1993). A previous study in our laboratory looked at the early role of clustering as a co-stimulatory event using adherent cells produced by differentiation of the monoblastoid cell line, U937, as a model APC (King et al., 1990). This cell line, without differentiation, has also been used in T-cell activation studies, where a CD3 antibody simulates the role of antigen (Johnson and Jenkins, 1994).The conclusion of the latter study was that there are other co-stimulatory mechanisms for T-cell activation, which have not as yet been identified.

5.2.1. U937 cells provide a co-stimulatory signal to T-cells.

In this study, we have examined the U937/CD3 -T-cell model initially set up by Johnson and Jenkins in further detail. Our assay used high density (unactivated) tonsillar T-cells rather than peripheral blood T-cells, and soluble CD3 antibody rather than CD3 bound to the plastic surface, but is otherwise similar to the previous study (Johnson and Jenkins, 1994).

We confirmed that U937 cells are capable of acting as accessory cells in this CD3 dependent T-cell co-stimulation assay. U937 cells initiated T-cell proliferation in a dose-dependent manner in the presence of CD3 mAb (Figure 5.1.1.). U937 cells or CD3 mAb in isolation with T-cells did not induce proliferation (Figure 5.1.1. and data not shown). A titration of T-cells into the assay, revealed that proliferation measured peaked at 10^5 T-cells per well, and that addition of $8x10^5$ cells per well led to decreased proliferation (Figure 5.1.1.). This was presumably due to overcrowding of the assay. Two concentrations of CD3 mAb (0.1μg/ml and 0.2μg/ml) were tested initially. These concentrations induced similar levels of proliferation in this assay. This lack of dose-dependency suggests that CD3 was saturated at both concentrations of mAb. However, another report has observed that very much higher concentrations of CD3 mAb (50μg/ml) can, in isolation induce T-cell proliferation. This report also found that in the presence of a lower concentration of CD3 mAb, a larger co-stimulatory signal was needed to induce proliferation (Dubey et al., 1995). In this study, CD3 mAb at the concentrations used did not induce any proliferation, thus allowing the co-stimulatory signal provided by U937 cells to be examined.

In experiments in this study, CD3 mAb was given in a soluble form. Under these conditions, T-cell proliferation could be observed visually by the formation of large clusters that consisted of many U937 and T-cells (Figure 5.1.2A.). In the absence of CD3 mAb, much smaller clusters of

U937 and T-cells were observed (Figure 5.1.2B.). This suggests that U937 cell-T-cell interactions are necessary, but are not indicative of the extent of T-cell proliferation.

5.2.2. U937 cells preferentially co-stimulate CD8+ T cells.

The predominant response stimulated by U937 cells in this assay was of CD8+ rather than of CD4+ T-cells (Figure 5.1.16.1.), consistent with the expression of class I but not class II MHC on the U937 cell surface. This implies a selective role for MHC-TCR interactions even in the presence of the CD3 mAb. Interactions between the constant region of MHC I and CD8 or MHC II and CD4, have been shown to stabilise APC-T-cell interactions (Lustgarten et al., 1991). In this study this would not be possible for CD4+ T-cells, due to the lack of expression of MHC II on U937 cells. This stabilisation could be a factor which explains why CD8+ T-cells proliferate more efficiently than CD4+ T-cells.

Another co-stimulatory pathway that has been explored extensively in many model systems is the APC CD80/CD86 interaction with CD28 on T-cells. Since U937 cells do not express either CD80 (Palmer and van Seventer, 1997) and this study, data not shown) or CD86 (data not shown), then an agonistic CD28 mAb should synergise with a CD3 mAb to increase T-cell proliferation. Surprisingly, the CD28 mAb only induced increased proliferation of CD4+ T cells, with proliferation of CD8+ T-cells remaining unaffected. The presence of the CD28 mAb increased the proliferation of CD4+ T-cells 8 fold, and that of the mixed T-cell population 3-4 fold (Figure 5.1.17.). The difference in stimulation by the CD28 mAb was not due to differences in expression of CD28 itself, as this molecule was expressed on ~95% of both CD4+ and CD8+ T-cells. Therefore, the difference in response must be due to differences in the way that the CD28 signal is treated in the two T-cell subsets. CD28 ligation did have some effects on CD8+ T-cells, as addition of both CD28 and CD3 mAbs, without U937, induced low levels of proliferation of

CD8+ T-cells. This proliferation was similar to the response of CD4+ and mixed T-cell populations in the same conditions (Figure 5.1.17.). CD28 ligation has been shown to induce IL-2 production (Linsley et al., 1991a), and this cytokine stimulates CD4+ T-cells more effectively than CD8+ T-cells (Costello et al., 1993; Taga et al., 1991; Winkelstein et al., 1990). These data imply that there are differential co-stimulation as well as MHC requirements for the two forms of T-cell (Costello et al., 1993; Ghiotto-Rageneau et al., 1996).

A recent study investigating U937 cell, CD3 dependent co-stimulation of CD4+ naive peripheral blood T-cells, found that the proliferative T-cells were specifically of Th-1 phenotype. Furthermore, U937 cells transfected with B7.1 (CD80) supported the proliferation of both Th-1 and Th-2 T-cells. This suggests that B7/CD28 interactions not only preferentially co-stimulate CD4+ T-cells, but also direct the immune system to Th-1 or Th-2 responses (Palmer and van Seventer, 1997).

This cumulative data shows that studies of co-stimulation in the absence of the CD80-CD86/CD28 interaction, may be necessary to reveal some of the more subtle interactions that modulate and control T-cell responses. This may be especially true for the study of CD8+ T-cell activation.

5.2.3. CD11a/18 (LFA-1)-CD54 (ICAM-1) interactions co-stimulate T-cell responses.

In the previous study, CD11a and CD18 mAbs did not co-stimulate U937/CD3-dependent T-cell responses (Johnson and Jenkins, 1994). In this study, CD11a/CD18-CD54 (LFA-1-ICAM-1 complex) clearly did play a role, as evidenced by inhibitory effects of several mAbs (Table 5.1.3.1. and Figure 5.1.3.2.). The only CD11a mAb which was not inhibitory, AZNL21, also does not block other CD11a-mediated assays (Hogg, 1997), despite the fact that it does bind to CD11a transfectants.

Thus, this mAb may identify an epitope that is not implicated in the receptor-ligand association(s) of this molecule.

A possible explanation for the discrepancy between our study and the lack of inhibitory activity seen with CD18 mAbs in previous studies was that in the latter (Johnson and Jenkins, 1994) CD3 was immobilised on the bottom of the tissue culture well. When T-cells respond to CD3 mAb orientated in such a two dimensional fashion across the bottom of the well, adhesion molecules may not be as important as when three dimensional clusters are formed between T-cells and U937 cells with multiple contact sites. The inability of agonist mAbs to CD18 to substitute for U937 cells (Johnson and Jenkins, 1994) does, however, suggest that activation via this ligand is not by itself sufficient. If this is correct, then adhesion between U937 and T-cell may be a pre-requisite for additional secondary co-stimulatory interactions to work. In support of this CD11a, CD18 and CD54 mAbs inhibited the formation of U937-T-cell clusters (Figure 5.1.3.1.). This demonstrates the importance of APC-T-cell interactions in the induction of the immune response, and the importance of CD11a/18 and CD54 in this process.

Experiments to determine the site of action of these inhibitory mAbs revealed that CD11a, CD18 and CD54 mAbs inhibited T-cell proliferation when selectively pre-bound to U937, prior to the addition of T-cells (Figure 5.1.14). This suggested that CD11a/18 and CD54 regulate T-cell responses via U937-T-cell interactions. In an accessory cell independent assay, CD11a, CD18 and CD54 mAbs did not inhibit T-cell responses at all (Figure 5.1.15). This could suggest that the response is mediated only at the U937 level. However, this assay used PMA and ionomycin to activate T-cells, and so it is not surprising that with each T-cell being activated without binding accessory cells, there would be little effect in interfering with cell-cell adhesion.

The interaction between CD11a/18 and CD54 is not purely one of adhesion. This complex also mediates signal transduction that is thought to be important in T-cell activation (Van Seventer et al., 1992; Van Seventer et al., 1991; Vyth Dreese et al., 1993). ICAM-1-LFA-1 interaction leads to prolonged phospholipase C activation, and a sustained increase in intracellular levels of free Ca^{++} (Van Seventer et al., 1992), that contributes to increased T-cell activation. LFA-1 and other integrin molecule ligation is also associated with activation of the Rho family of GTPases. Rho is closely associated with the actin cytoskeleton, mobilisation of the cytoskeleton is crucial in forming close contacts between APC and T-cell reviewed by (Howe et al., 1998).

The cytotoxic effects of CD11a, CD18 and CD54 mAbs, and all subsequent inhibitory mAbs, were assessed by dye exclusion. These experiments showed that only one mAb (CD45-ICO46) was cytotoxic to cells in the assay. This was presumably due to antibody dependent cellular cytoxicity (ADCC), or high concentrations of azide being present in the mAb solution. There was not enough ICO-46 at the end of these studies to attempt to remove azide in the solution by dialysis, so the exact nature of cytotoxicity induced by this mAb was not discovered. The results of viable cells were given as a percentage compared to the no mAb control assay. The only mAb that was cytotoxic (ICO-46) gave 20% cell viability, all other mAbs had viabilities of over 70% and were therefore considered to have no cytotoxic effects.

5.2.4. CD45 mAbs inhibited T-cell proliferation.

By direct observation, one of the most striking effects seen was with a well-established leukocyte cell surface marker, CD45 and its isoforms. CD45 mAbs caused substantial inhibition of proliferation (Figure 5.1.5.1.) but enhanced U937-T-cell cluster formation (Figure 5.1.5.3.). The fact that CD45 mAbs increased cluster formation suggested that these

mAbs are agonistic. Indeed a mAb (CBE-77) that had both anti-proliferative and pro-clustering properties induced tyrosine phosphorylation in both U937 and T-cells (Figures 5.1.18.1. and 5.1.18.2.). This implies that ligation of CD45 leads to increased cell mobility and affinity for T-cells to bind U937 cells. The effect of CD45 on clustering, which (as in our previous study) (King et al., 1990) was independent of the presence of CD3, and was therefore not linked to TCR signal transduction, implies that CD45 is involved in the adhesion arm of co-stimulation, perhaps through amplification of the CD11a/18-CD54 pathway.

The cell clustering data from CD45, CD11a/18 and CD54 mAbs demonstrates that whilst interaction of U937 and T-cells is vital for the induction of T-cell activation (Figure 5.1.3.1.), it is not itself enough, as increased U937-T-cell clustering does not lead to increased T-cell proliferation (Figure 5.1.5.3.). In further clustering studies, with other mAbs directed against other cell surface proteins (see section 5.2.5.), U937-T-cell clustering was not effected by mAbs that inhibited T-cell proliferation in this assay (Figure 5.1.13.). This again suggests that cluster formation is not on its own sufficient to induce T-cell activation.

CD45 is a PTPase that has been shown to be vital in the early stages of TCR mediated signal transduction (reviewed by Altin and Sloan, 1997). As the clustering and signalling data suggest an agonistic role for the mAbs, the finding that these mAbs inhibit proliferation is puzzling. The most logical explanation is that the mAbs sequester CD45 away from the TCR-CD3 complex, thus impairing the initial processes of TCR mediated signalling (see section 1.4.1.). Evidence for this theory can be found in Figure 5.1.18.2A. (lane 9), where a combination of CD3 and CD45 mAb incubated with T-cells induced less tyrosine phosphorylation than either mAb in isolation. This suggests that CD3 and CD45 are closely associated

proteins, and if this association is hindered by the addition of both mAbs, this inhibits proper signalling activity.

Interfering with CD45 activity has previously been shown to block dephosphorylation of the regulatory C terminal domains of the CD4/CD8-associated Lck tyrosine kinase (Guttinger et al., 1992; Ledbetter et al., 1993) and/or of the TCR-associated Fyn tyrosine kinase (Ledbetter et al., 1993; Shiroo et al., 1992), and hence to inhibit intracellular signalling mediated by the TCR. In contrast, CD45-mediated inhibition of CD3-TCR complex activation has also been documented (Kiener and Mittler, 1989), and it has been suggested that CD45 ligation blocks the intracellular calcium flux normally associated with TCR signalling (Shivnan et al., 1996).

Experiments using an accessory cell free T-cell proliferation assay confirmed that CD45 mAbs acted directly on T-cells. Two mAbs inhibited T-cell proliferation, one by 40% and another by 90% (Figure 5.1.15.). However, in the U937/CD3-T-cell assay, a CD45 mAb also inhibited T-cell proliferation (40%) when selectively pre-bound to U937 cells before addition of T-cells (Figure 5.1.14). This demonstrates that CD45 also inhibits activation via U937-T-cell interactions.

5.2.5. Identification of novel molecules involved in T-cell activation.

A major aim of the present study was to identify which novel co-stimulatory molecules were implicated in U937-dependent T-cell activation using mAb - mediated inhibition as a starting point.

5.2.5.1. CD53 mAbs inhibited T-cell proliferation.

An inhibitory effect on T-cell proliferation was seen with three of the four CD53 mAbs (Figure 5.1.6.1.). All mAbs so far raised against this molecule recognise the same epitope (Conjeaud et al., 1997), thus

suggesting that the lack of effect of one mAb may have been due to its affinity for CD53. This molecule, a member of the tetraspan superfamily of surface molecules, is known to be induced on T-cells by TCR engagement during repertoire selection (Pieters et al., 1994), to trigger nitric oxide release via a protein kinase C dependent pathway (Bosca and Lazo, 1994), and to be associated with a tyrosine phosphatase activity, that is not CD45 (Carmo and Wright, 1995). In human tonsillar B cells, CD53 can form part of a multicomponent MHC II complex (Angelisova et al., 1994).

CD53 mAb-mediated inhibition was not seen in pre-incubating experiments (Figure 5.1.14.), implying that the CD53 role is likely to be mediated at the T-cell level rather than via U937 cells. In support of these data, CD53 was predominantly expressed on T-cells (Table 5.1.6.2.), a CD53 mAb completely inhibited T-cell proliferation in an accessory cell independent assay (Figure 5.1.15.), and the same CD53 mAb induced extensive tyrosine phosphorylation when incubated with T-cells (Figure 5.1.18.2.).

5.2.5.2. CD55 mAbs inhibited T-cell proliferation.

One of two CD55 mAbs inhibited T-cell responses (Figure 5.1.7.). Evidence suggests that this mAb inhibited directly via an effect on T-cells, as CD55 was predominantly expressed on T-cells (Table 5.1.7.) and the CD55 mAb completely inhibited T-cell proliferation in an accessory cell independent assay (Figure 5.1.15.). The two mAbs used in this assay may recognise different epitopes of CD55 (Loveland and Szokolai, 1997), and this may be the reason for the different effects of the two mAbs.

CD55, also known as decay accelerating factor, is a widely expressed GPI-linked molecule that is involved in the protection of cells from attack by complement. There is evidence that cross-linking of this protein will

lead to signal transduction, and a role in T-cell activation has been previously suggested (Liszewski et al., 1996).

5.2.5.3. CD98 mAbs inhibited T-cell proliferation.

Seven of nine CD98 mAbs inhibited T-cell responses (Figure 5.1.8.1.). CD98 is a dimer of CD98 heavy chain (CD98hc), which is an 80kD protein, and CD98 light chain (CD98lc), which is a 45kD protein (Diaz et al., 1997a). Previously, mAbs to two distinct CD98hc epitopes have been produced, and all the mAbs used in this study, except J1-G3B and BU89, recognise the same epitope (CD98-1). BU89 recognised neither of the epitopes previously identified, but did immunoprecipitate an 80kD protein (Diaz et al., 1997a). Therefore, this mAb probably recognises a novel epitope of CD98hc. In contrast, J1-G3B immunoprecipitated an undefined 42kD protein, which has been shown to be tightly associated with CD98hc, and may be CD98lc. The J1-G3B antigen bound to CD98hc transfectants, and not to the parent cell line, suggesting that this protein requires the presence of CD98hc for its own cell surface expression (Diaz et al., 1997a). However, in this study we have shown that the antigen recognised by J1-G3B was highly expressed on T-cells, whilst the expression of CD98hc was very low (Table 5.1.8.2.). This suggests that either the J1-G3B antigen is expressed in isolation from other CD98hc epitopes on resting T-cells, or that it is indeed a separate but closely associated surface molecule.

CD98, a type II transmembrane glycoprotein, has been implicated in many processes in a range cell types. CD98 is strongly expressed on all activated cells, whilst low levels are expressed on resting monocytes (Hemler and Strominger, 1982). CD98 has been shown to be important in cell survival during haemopoietic cell development (Warren et al., 1996), in the formation of HIV-induced multinucleate giant cells (Ohgimoto et al., 1995; Suga et al., 1997), and has been shown to mediate a calcium influx when bound by its ligand Galectin 3 (Dong and Hughes, 1997).

Very recently two reports have identified the CD98lc, and have reported a role for CD98hc-CD98lc dimers in the transport of large neutral amino acids (Kanai et al., 1998; Mastroberardino et al., 1998). CD98 also co-precipitates with CD3 in extracts derived from a human thymoma cell line (Cerny et al., 1996), which would suggest a role for CD98 at the T-cell level. Indeed a CD98hc mAb (J3-E1B) inhibited T-cell proliferation by 50% in an accessory cell independent assay, whilst the mAb against the CD98hc associated protein (J1-G3B) inhibited the same assay by 95% (Figure 5.1.15.). These data fit with the expression data which showed that J1-G3B bound to T-cells much more than J3-E1B (Table 5.1.8.2.). Incubation with J1-G3B also induced tyrosine phosphorylation in T-cells, whilst incubation with J3-E1B did not (figure 5.1.18.2.). This suggests that J1-G3B exerts its inhibitory effects predominantly via direct interactions with T-cells.

A CD98hc mAb (J3-E1B), also inhibited T-cell proliferation by 70%, in U937 cell pre-incubating experiments (Figure 5.1.14.). This suggests that CD98hc mAbs also have inhibitory effects predominantly via effects on U937 cells, as well as some direct effects on T-cells (Figure 5.1.15.). This is supported by expression data which showed that CD98hc was expressed at high levels on U937 cells, and at low levels on T-cells (Table 5.1.8.2.), and that incubation with a CD98hc mAb (J3-E1B), induced high levels of tyrosine phosphorylation in U937 cells (Figure 5.1.18.1.). Further evidence that CD98 has a co-stimulatory role is that it is expressed at much higher levels on dendritic cells than on resting T-cells (Woodhead et al., 1998).

Interestingly, incubation with the J1-G3B mAb, also induced high levels of tyrosine phosphorylation in U937 cells (Figure 5.1.18.1.). The pattern of phosphorylation induced was similar to that induced by J3-E1B, but an extra 26kD protein was phosphorylated in response to J3-E1B. This

supports the idea that the antigens recognised by these two mAbs are distinct, and that they may have differing functional roles.

Two recent studies have revealed more about the functions of this molecule, and support a co-stimulatory role. CD98 has been shown to have a controlling mechanism on integrin mediated cell-cell adhesion (Fenczik et al., 1997). These data suggest that CD98 could inhibit T-cell activation by interfering with integrin interactions and signalling. However, this seems unlikely as no inhibition of U937-T-cell clustering was observed with these mAbs (Figure 5.1.13.). This lack of effect on clustering suggests that CD98hc mAbs inhibits T-cell proliferation by other mechanisms. However, evidence for a role for CD98 in regulating adhesion was found during these studies, with the observation that CD98hc mAbs induce adherence to plastic of primary human dendritic cells after as little as 10 minutes incubation (data not shown). Confirming a role for CD98 on monocytes, Diaz et al (1997b) have reported that addition of CD98hc mAbs to peripheral blood mononuclear cells (PBMC), blocked superantigen and lectin induced cell proliferation. CD98hc mAbs inhibited IL-2 receptor expression and progression of T-cells from G1 to S phase. However, if the same experiments were repeated with monocyte depleted PBMC, no inhibition of T-cell responses was found upon addition of CD98hc mAb. In further experiments using murine splenocytes as accessory cells, instead of human monocytes, CD98hc mAbs again did not inhibit T-cell proliferation. Therefore, inhibition of T-cell responses by CD98hc mAbs was mediated through monocyte accessory cells in their assay system, all this supports our independent findings in these assays.

5.2.5.4. A CDw108 mAb inhibited T-cell proliferation.

One CDw108 mAb inhibited T-cell proliferation (see section 5.1.9.). CDw108 is a GPI linked protein that contains the JMH blood group

antigen (Mudad et al., 1995), CDw108 has also been shown to co-precipitate with CD3 in a human thymoma cell line (Cerny et al., 1996).

The inhibitory CDw108 mAb appeared to have its effects directly via T-cells, as CDw108 was expressed on T-cells, but not on U937 cells (see section 5.1.9.), and the CDw108 mAb inhibited T-cell proliferation completely in an accessory cell independent assay (Figure 5.1.15.).

5.2.5.5. CD147 mAbs inhibited T-cell proliferation.

Three of four CD147 mAbs inhibited T-cell proliferation (Figure 5.1.10.1.). CD147, also known as neurothelin or basigin, is a 54kD type I transmembrane glycoprotein, which consists of two extracellular Ig like domains (Seulberger et al., 1992). CD147 was first identified because of its role in the development and maintenance of the blood-brain barrier (Schlosshauer, 1991), and which is known to be involved in actin co-localisation and polarisation of endothelial cells (Schlosshauer et al., 1995). CD147, is however, widely distributed, including expression on mitogen activated T-cells (Kasinrerk et al., 1992). CD147 knockout mice have an increased mitogenic response in mixed leukocyte reactions, and repeatedly visited acetic acid soaked filter paper, indicating a changed behaviour to odour reception (Igakura et al., 1996).

A CD147 mAb inhibited T-cell proliferation by 80%, in U937 cell pre-incubating experiments (Figure 5.1.14.), and CD147 was expressed at high levels on U937 cells, and at low levels on T-cells (Table 5.1.10.2.). However, CD147 mAbs both inhibited T-cell proliferation by 10-30%, in an accessory cell independent assay (Figure 5.1.15.). This suggests that CD147 has inhibitory effects predominantly at the U937 cell level, but also a small effect directly via T-cells.

5.2.5.6. Unknown mAbs inhibited T-cell proliferation.

Four mAbs of yet unknown classification inhibited T-cell proliferation in the same assay. WM78 appeared to have inhibitory effects at the level of the U937 cell. Evidence for this was that this mAb inhibited T-cell proliferation by 65%, in U937 cell pre-incubating experiments (Figure 5.1.14.); was expressed at high levels on U937 cells, and at low levels on T-cells (Table 5.1.11.2.); and did not inhibit T-cell proliferation in an accessory cell independent assay (Figure 5.1.15.). MEM-135 although binding to U937 cells more than to T-cells (Table 5.1.11.2.), appeared to have inhibitory effects directly at the level of the T-cell. MEM-135 inhibited T-cell proliferation by 95%, in an accessory cell independent assay (Figure 5.1.15.); and did not significantly inhibit in the U937 cell pre-incubating experiments (Figure 5.1.14.).

The two remaining mAbs, RmCB and K108, did not bind to either U937 or T-cells (Table 5.1.11.2.), and RmCB did not inhibit an accessory cell independent assay (Figure 5.1.15.). This suggests that the antigens recognised by these two mAbs must be up-regulated on either U937 or T-cells during the assay.

5.2.5.8. Inhibitory mAbs inhibited CD4+ and CD8+ T-cells equally.

CD53, CD55, CD98, CDw108, CD147 and the inhibitory undefined mAbs, as well as mAbs against CD11a, CD18, CD54 and CD45, inhibited not only the dominant CD8+ T-cell response but also the CD4+ T-cell response to an equal extent (Figure 5.1.16.2.). This confirmed that the co-stimulatory effects are applicable to both T-cell subsets, and that the selective increase in CD8+ T-cell proliferation induced by U937 cells was not likely to be due to any of these molecules.

5.2.6. PBDC-CD3-dependent T-cell proliferation assay.

In support of the findings discussed above, a further CD3 dependent assay was developed that used human peripheral blood dendritic cells (PBDC),

as accessory cells, which co-stimulated autologous T-cells. In this assay T-cell proliferation was also inhibited by the same CD98 and CD147 mAbs. Furthermore, in non CD3-dependent assays, that involved prior activation of T-cells with periodate, or allogeneic reactions, CD98 and CD147 mAbs consistently inhibited T-cell proliferation (Woodhead et al., 1998). This demonstrates that CD98 and CD147 plays a role in T-cell activation mediated by diverse APCs. (Data not shown).

CD98 and CD147 are both molecules that would be present at sites of inflammation: CD98 as an activation antigen, and CD147 at sites of endothelial outgrowth. They may therefore play a role in induction of both innate and adaptive immunity. Delivery of either of these molecules to tumours may be a way to enhance their immunogenicity, and hence potentiate immunotherapeutic intervention in cancer. Conversely, the ability to block these alternative co-stimulatory pathways may provide another strategy to modulate the pathological immune reactions associated with auto-immunity.

5.2.7. Summary.

In conclusion, therefore, the U937/CD3-T-cell proliferation model has been used, and the classic accessory molecules (CD11a, CD18, CD54 and CD45) have been shown to be important for co-stimulation. Novel molecules, in particular CD98 and CD147, are also implicated in this process, most probably acting at the level of the APC rather than the T-cell. In addition CD53, CD55 and CDw108 were implicated in having effects directly at the T-cell level. There are three possible explanations as to how the inhibitory effects of the antibodies on U937 function are mediated: by blocking signalling into the APC, and hence production of a key mediator; by altering a critical pattern of surface expression of known co-stimulatory molecules; or by blocking direct receptor-ligand interaction with a molecule on the T-cell surface.

The inhibition observed with these mAbs was due to the specificity of these mAbs, and not their isotype. This was demonstrated by other mAbs tested in the same assay which did not inhibit T-cell proliferation (see Appendices III and VI). These mAbs did not inhibit simply because they do bind U937 or T-cells, as a series of non-inhibitory mAbs were shown to bind to either U937 or T-cells (Table 5.1.12.).

Chapter 6

6.1. Results

Investigation of X-irradiation induced cell death in the U937 transfectant cell lines; ability of U937 transfectants to co-stimulate T cells.

The next stage of the study was to have been an investigation of the co-stimulatory capabilities of the U937-derived RXRα transfectant cell lines (see chapters 3 and 4), in the CD3 dependent T cell proliferation assay (see chapter 5). This was planned in order to examine the effects of RXRα expression on the accessory cell capabilities of the U937 cell line. However, unexpectedly, the three RXRα transfectant cell lines responded differently to the X-ray treatment that was given prior to the assay. This Chapter contains preliminary data demonstrating that 9-*cis* RA treated αG2S cells are more resistant, and αB5A cells more susceptible, to X-ray induced apoptosis, than the MEP control cell line.

The co-stimulatory capabilities of the U937 transfectants in the CD3 dependent T cell proliferation assay were therefore assessed, using mitomycin C, rather than X-irradiation, to inhibit U937 transfectant proliferation.

6.1.1. Proliferation of 9-*cis* RA-treated αG2S, αB5A and MEP cells differs following X-irradiation.

Figure 6.1.1. shows that X-irradiation inhibits proliferation of 9-*cis* RA-treated αG2S, αB5A and MEP cells, to different degrees. At all doses of X-irradiation, αG2S proliferation was inhibited less than that of MEP cells. In turn inhibition of MEP cell proliferation was less than that of αB5A cells. This effect was most noticeable after exposure to 2000 rads.

In similar experiments to that shown in Figure 6.1.1., non-X-irradiated U937 transfectants all proliferated equally, incorporated between 350,000 and 400,000 cpm (data not shown).

6.1.2. Differences in proliferation on X-irradiated αG2S, αB5A and MEP cells is dependent upon 9-*cis* RA treatment.

To determine whether the differences in proliferation following X-irradiation were retinoid dependent, U937 transfectants were X-irradiated with or without 9-*cis* RA or DHCC treatment.

6.1.2.1. Proliferation by untreated αG2S, αB5A and MEP cells is inhibited equally following X-irradiation.

Figure 6.1.2.1. shows the proliferation of equal numbers of untreated and 9-*cis* RA-treated αG2S, αB5A and MEP cells, between 48 and 64 hours after exposure to 4000 rads. As shown before (see Figure 6.1.1.), 9-*cis* RA activated αG2S proliferate more than MEP cells which in turn proliferate more than αB5A cells. However, untreated U937 transfectants proliferate equally, demonstrating that over expression of RXRα is not itself sufficient to induce the differences seen cell proliferation following X-irradiation. It was noticeable that 9-*cis* RA treatment resulted in increased proliferation of all the U937 transfectants, including the αB5A cells, when compared to untreated cells.

6.1.2.2. Proliferation by DHCC-treated αG2S, αB5A and MEP cells is inhibited equally following X-irradiation.

Figure 6.1.2.2. shows the proliferation of equal numbers of DHCC- and 9-*cis* RA-treated αG2S, αB5A and MEP cells, between 48 and 64 hours after exposure to 4000 rads. Differences in proliferation between the cell lines were apparent after 9-*cis* RA treatment, but not after DHCC treatment.

Figure 6.1.1.

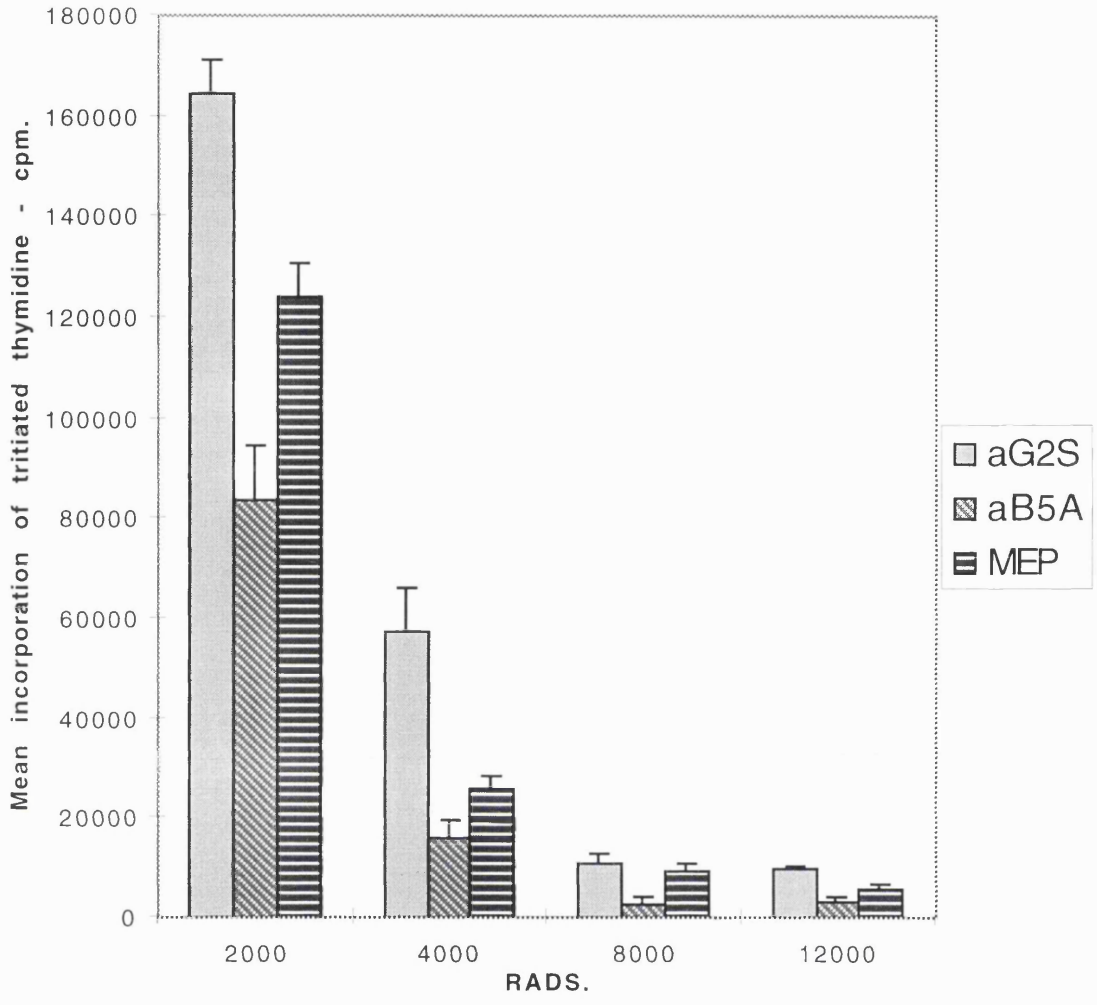

Figure 6.1.1. 9-*cis* RA-treated αG2S cells proliferate more, and αB5A cells less than MEP cells, following X-irradiation.

10^7 9-*cis* RA-treated αG2S, αB5A, or MEP cells, were exposed to 2000, 4000, 8000, or 12000 rads of X-irradiation. $2x10^4$ viable cells were plated in triplicate wells of 96 well plates, and proliferation assessed between 48 and 64 hours of culture by incorporation of ^3H thymidine (see section 2.25.). The data are expressed as mean incorporation of triplicate wells +/- the standard deviation, from one representative experiment.

Figure 6.1.2.1.

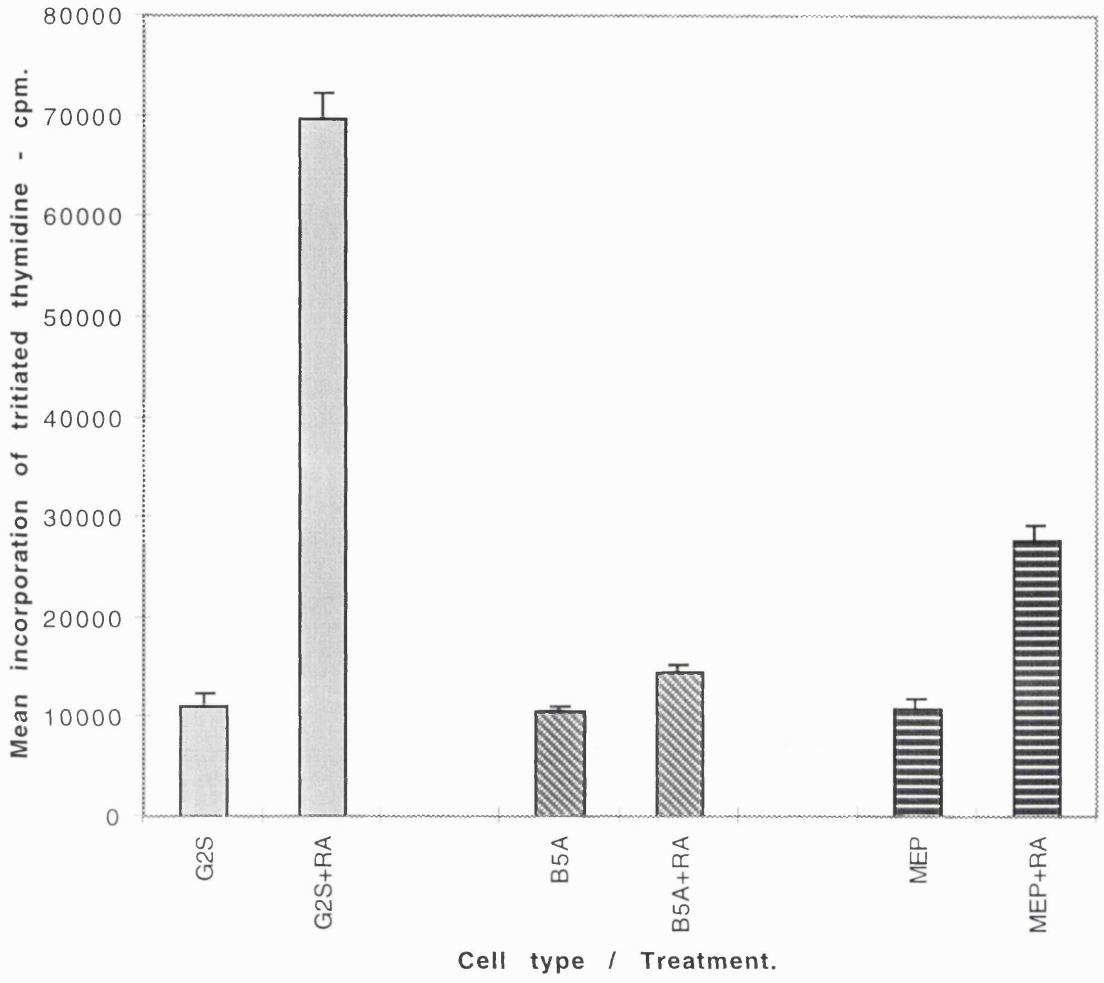

Figure 6.1.2.1. Proliferation by untreated αG2S, αB5A and MEP cells is inhibited equally following X-irradiation.

10^7 untreated or 9-*cis* RA-treated αG2S, αB5A, or MEP cells, were exposed to 4000 rads of X-irradiation. $2x10^4$ viable cells were plated in triplicate wells of 96 well plates, and proliferation assessed between 48 and 64 hours of culture by incorporation of ^3H thymidine (see section 2.25.). The data are expressed as mean incorporation of triplicate wells +/- the standard deviation, from one representative experiment.

Figure 6.1.2.2.

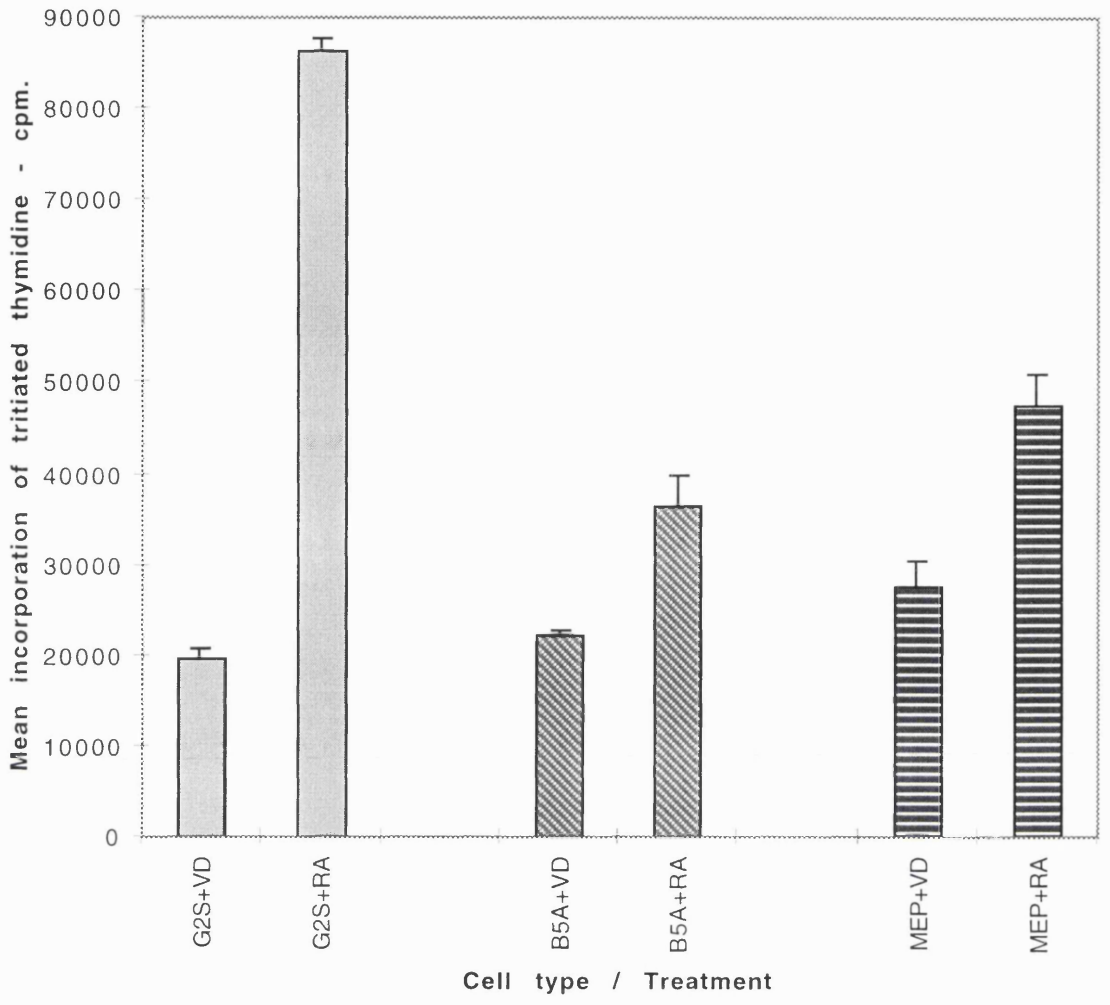

Figure 6.1.2.2. Proliferation by DHCC-treated αG2S, αB5A and MEP cells is inhibited equally following X-irradiation.

10^7 9-*cis* RA- (+RA), or 500nM DHCC- (+VD) treated αG2S, αB5A, or MEP cells, were exposed to 4000 rads of X-irradiation. $2x10^4$ viable cells were plated in triplicate wells of 96 well plates, and proliferation assessed between 48 and 64 hours of culture by incorporation of ^3H thymidine (see section 2.25.). The data are expressed as mean incorporation of triplicate wells +/- the standard deviation, from one representative experiment.

Taken together, Figures 6.1.2.1. and 6.1.2.2., demonstrate that the differences in proliferation following X-irradiation in the U937 transfectants are dependent upon 9-*cis* RA treatment.

6.1.3. Proliferation by 9-*cis* RA-treated αG2S, αB5A and MEP cells is inhibited equally following UV-irradiation.

The proliferation of 9-*cis* RA-treated αG2S, αB5A and MEP cells, between 48 and 64 hours after exposure to various doses of short wavelength UV light was assessed. Even a low dose of ten seconds, induced identical inhibition of proliferation in the three U937 transfectant cell lines. ^{3}H thymidine incorporation for all three cell lines was of the order of 100 cpm, per $2x10^{4}$ UV-exposed cells (data not shown).

6.1.4. Increased numbers of viable 9-*cis* RA-treated αG2S cells after X-irradiation.

Figure 6.1.4. shows double staining of 9-*cis* RA- treated αG2S (A), αB5A (B) and MEP cells (C), 24 hours after exposure to 4000 rads. Using TdT mediated dUTP nick end labelling (TUNEL) to identify apoptotic nuclei (green), and propidium iodide labelling (PI) to identify viable nuclei (red). Table 6.1.4. shows the percentages of apoptotic and viable cells counted in five different field of views for each cell line. Note that more αG2S cells, viable and apoptotic, were counted than MEP cells, and more MEP cells were counted than αB5A cells. This was because cells that die during the 24 hours following X-irradiation in the latter two cell lines, i.e. prior to the TUNEL assay, would not be available to bind to the poly-l-lysine coated cover slips, so that they could be included in the count.

Figure 6.1.4.

A.-αG2S

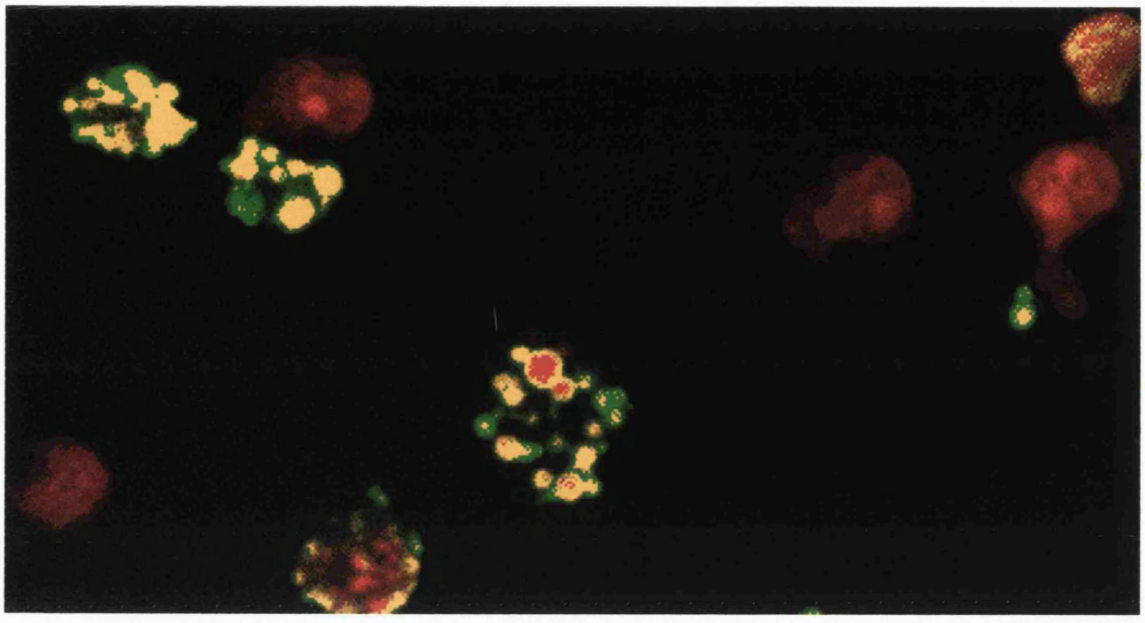

B.-αB5A

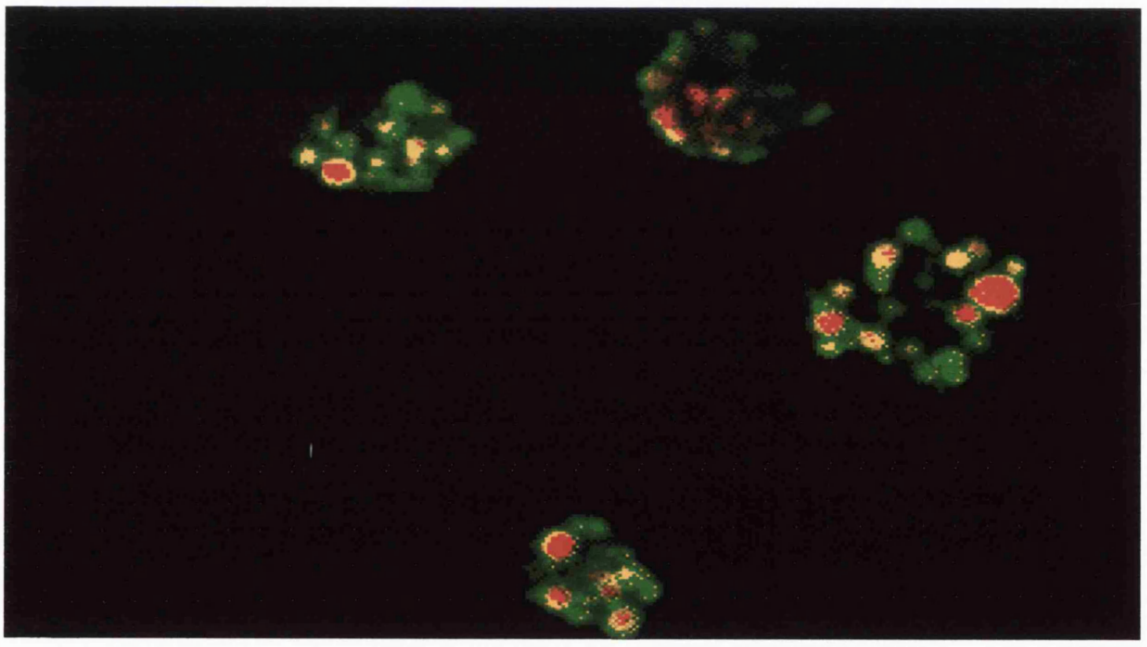

Figure 6.1.4.

C.-MEP

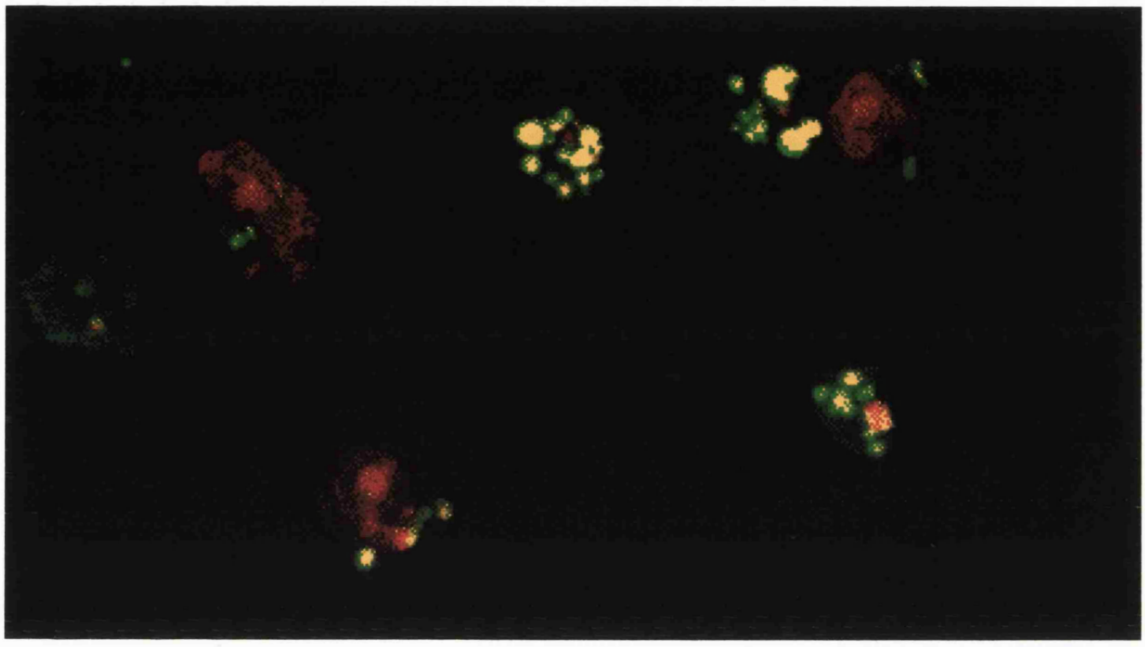

Figure 6.1.4. Increased numbers of viable 9-*cis* RA activated αG2S cells after X-irradiation.

10^7 9-*cis* RA-treated αG2S, αB5A, or MEP cells were exposed to 4000 rads of X-irradiation, and viable cells recultured in 10ml CM for 24 hours. $3x10^6$ cells from each sample were fixed in 4% paraformaldehyde, and permeabilised in 0.1% Triton X100 in a 0.1% sodium citrate solution on ice. The cells were then allowed to attach to poly-l-lysine-coated cover-slips and incubated with TUNEL reaction mixture and 50μg/ml of propidium iodide solution added and viewed with a confocal microscope (see section 2.26.).

Table 6.1.4.

Field of view	% Live cells αG2S	% Live cells αB5A	% Live cells MEP
1	48.1	8	36.8
2	47.8	5.9	39.6
3	51.1	6.9	33.7
4	47.1	10.9	39.2
5	50.8	3.2	29.1
Mean =	49% +/-1.8%	7% +/-2.8%	35.7% +/-4.4%

Table 6.1.4. Increased numbers of viable 9-*cis* RA-treated αG2S cells after X- irradiation.

10^7 9-*cis* RA-treated αG2S, αB5A, or MEP cells were exposed to 4000 rads of X-irradiation, and viable cells recultured in 10ml CM for 24 hours. $3x10^6$ cells from each sample were fixed in 4% paraformaldehyde, and permeabilised in 0.1% Triton X100 in a 0.1% sodium citrate solution on ice. The cells were then allowed to attach to poly-l-lysine-coated cover-slips and incubated with TUNEL reaction mixture and 50μg/ml of propidium iodide solution added and viewed with a confocal microscope (see section 2.26.). The number of viable cells (red), and apoptotic (green) cells were counted. Data are shown as the mean % of viable cells in five separate fields of view.

6.1.5. Increased numbers of 9-*cis* RA-treated αG2S cells complete the cell cycle after X-irradiation.

Table 6.1.5. shows increased numbers of viable αG2S cells in various stages of the cell cycle, after X-ray irradiation, as measured by propidium iodide labelling. In αG2S cells 28% of cells are viable and in some part of the cell cycle, compared to only 0.5% viable and cycling αB5A cells, and 16% viable and cycling MEP cells. This supports the previous data that 9-*cis* RA-treated αG2S cells are protected from X-irradiation induced cell death.

Table 6.1.5.

		% of irradiated cells		
Cell type	**Not viable**	**G1**	**S**	**G2m**
αG2S	72	13	10	5
αB5A	98.5	1	0.4	0.1
MEP	84	1	8	7

Table 6.1.5. Increased numbers of 9-*cis* RA-treated αG2S cells are viable and complete the cell cycle after X-irradiation.
10^7 9-*cis* RA-treated αG2S, αB5A, or MEP cells were exposed to 4000 rads of X-irradiation, and viable cells recultured in 10ml CM for 24 hours. $5x10^6$ cells from each sample were fixed in ice cold 100% ethanol, and washed twice in ice cold HBSS. Fixed cells were then treated with RNase 1, 50μg/ml of propidium iodide solution added a minute prior to FACS analysis, results analysed ungated using WinMDI software (see section 2.27.). Results are expressed as the percentage of the total number of events (cells) that are either not viable or in G1, S, or G2m phases of the cell cycle.

6.1.6. αG2S cells are more capable co-stimulators of T cell activation than MEP or αB5A cells.

The co-stimulatory capability of U937 transfectants was investigated by replacing the U937 cells with U937-derived RXRα transfectants in the CD3 dependent T cell proliferation assay (see chapter 5). The effect of immunophagocytosis 24 hours prior to the proliferation assay on co-stimulatory capability was also investigated. These experiments explored if immunophagocytic and accessory cell capabilities are mutually exclusive, and also by inference to see if immunophagocytosis influences expression of co-stimulatory molecules on the U937 transfectants. However, as the U937 transfectants were affected by X-irradiation in different ways, it was impossible to use X-irradiation to inhibit U937 transfectant growth. Therefore, an alternative method of inhibiting transfectant cell growth was used. For this purpose Mitomycin C was added to the cells for 16-18 hours prior to the assay. This had the desired

effect, inhibiting cell growth in each cell type, and to a similar extent. Thus, transfectant cells were treated with 9-*cis* RA for twenty four hours, and the cells split into two aliquots, one of which was exposed to op-SRBC, whilst the other was left unexposed. After excess op-SRBC had been removed and the cells washed, 10μg of mitomycin C were added per 10^6 cells and left overnight. The cells were washed five times the next morning, and then placed in the assay. The same basic assay was performed, with 10^4 U937 transfectant cells, $2x10^5$ purified T cells, and 0.1μg/ml CD3 mAb. Figure 6.1.6. shows that αG2S cells were significantly better co-stimulators of T cell activation in a CD3 dependent assay than MEP cells which were themselves better co-stimulators of T cells than αB5A cells. Cells set up in parallel and exposed to op-SRBC for two hours, twenty four hours before the start of the assay, showed no difference in their ability to co-stimulate T cells.

Figure 6.1.6.

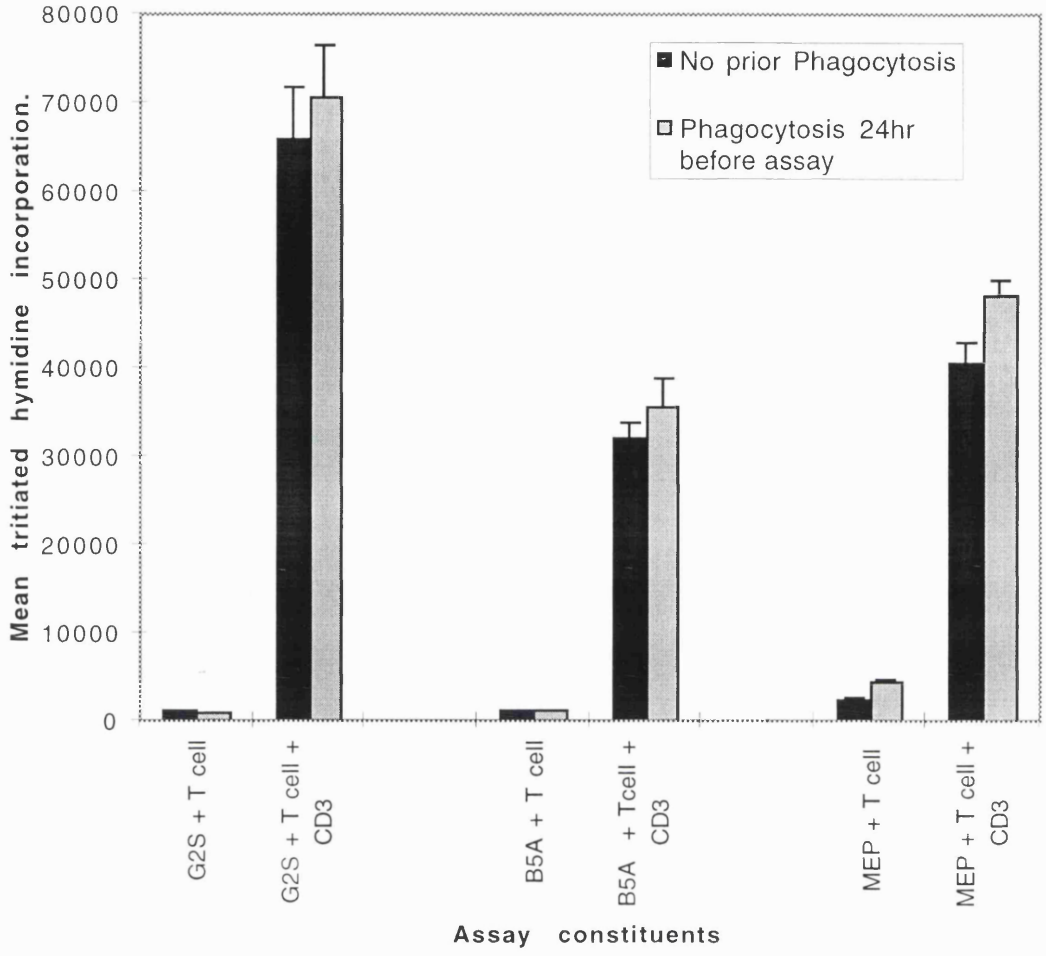

Figure 6.1.6. αG2S cells are more capable co-stimulators of T cell activation than MEP or αB5A cells.

10^7 9-*cis* RA-treated αG2S, αB5A, or MEP cells, were either exposed or not exposed to op-SRBC for two hours. 10μg of mitomycin C were added per 10^6 cells and the cells cultured overnight, the next morning cells were washed 5 times. To 10^4 of each cell line, $2x10^5$ tonsillar T cells and 0.1μg/ml of a CD3 mAb were added (see section 2.28.). T cell proliferation was assessed between 48 and 64 hours of culture by the incorporation of ^3H Thymidine. The data are expressed as mean T cell proliferation of triplicate wells +/- the standard deviation, from one representative experiment.

6.2. Discussion.

Results from this Chapter suggest that ligand binding to over-expressed RXRα, led to resistance to X-irradiation induced cell death in αG2S cells. This property of these cells made it impossible to assess the T-cell co-stimulatory capabilities of the U937 transfectants, using X-irradiation to inhibit accessory cell proliferation.

6.2.1. Differences in proliferation between X-irradiated U937 transfectants are 9-*cis* RA dependent.

X-irradiation inhibited proliferation of 9-*cis* RA-treated αG2S, αB5A and MEP cells, to different degrees in a dose-dependent manner. At all doses of X-irradiation, αG2S proliferation was inhibited less than that of MEP cells, which itself was inhibited less than that of αB5A cells (Figures 6.1.1., 6.1.2.1. and 6.1.2.2.). Proliferation was inhibited to the same extent in all three transfectants when untreated or DHCC-treated (Figures 6.1.2.1. and 6.1.2.2. respectively). This demonstrates that these differences in inhibition of proliferation are mediated by ligand bound RAR-RXR, or RXR-RXR dimers, and that ligand bound VDR-RXR dimers did not induce the same effect. It is noticeable that 9-*cis* RA treatment led to protection from X-irradiation induced death in all three transfectants, although the effect was very limited in αB5A cells (Figure 6.1.2.1.). This effect on αB5A cells suggests that the effect on proliferation could also be mediated by RXRβ, or by the residual levels of RXRα in these cells (Figure 3.1.2.1.).

In summary, the protection from X-irradiation induced cell death was dependent on RXR concentration. The observation that 9-*cis* RA-treated MEP cells were protected from cell death, in response to X-irradiation also demonstrated this to be a property of the parental U937 cell line.

In similar non X-irradiated samples, all 9-*cis* RA-treated cell lines proliferated equally (data not shown). This is in contrast to previous

results that showed that αG2S cells were more sensitive and αB5A cells resistant to growth arrest in the presence of 9-*cis* RA (Brown et al., 1997; Brown T.R.P., 1995). This was because in this study, cells were treated with 9-*cis* RA prior to X-irradiation, and after X-irradiation, cells cultured in 9-*cis* RA free media. This demonstrates that differences in growth arrest previously shown requires the presence of 9-*cis* RA at all times during the assay, whilst the differences in proliferation following X-irradiation requires only that the cells have been pre-treated with 9-*cis* RA. This suggests that two separate RXRα mechanisms are involved in these properties of the U937 transfectants.

6.2.2. Differences in inhibition of proliferation were caused by differential induction of apoptosis.

Further studies demonstrated that the differences in inhibition of proliferation were mediated by different efficiencies of apoptosis. Following X-irradiation, greater numbers of viable αG2S cells, and lower numbers of viable αB5A cells were present, when compared to viable MEP cells. (Figure 6.1.4. and Tables 6.1.4. and 6.1.5.). Viable cells were identified using PI, which binds to intact nuclei, thus indicating intact cells. Of the viable αG2S cells, equal numbers were in G1, S and G2m phase of the cell cycle. Viable MEP cells were predominantly in the S and G2m phase, very few being in G1, whilst very few αB5A cells were viable in any stage of the cell cycle (Table 6.1.5.). The process that caused cell death was shown to be apoptosis (Figure 6.1.4.), as judged by a TUNEL reaction which recognises 3'-OH termini of oligonucleotides that occur following nuclear disintegration and DNA cleavage. These DNA fragments are specific to apoptotic cells, as these fragments do not occur during necrosis, a further method of cell death.

Apoptosis is a process that controls cell populations during a wide range of biological events including embryogenesis, the immune response, and neoplasia. Apoptosis is also a method for removing cells that have been

damaged by toxic stimuli in a way that does not release toxic intracellular components into surrounding areas. To achieve this, the cell membrane of apoptotic cells is preserved until late in the process, enabling packaging of cellular contents into membrane bound vesicles. These cellular fragments are phagocytosed by surrounding cells or macrophages, in a way that does not induce an inflammatory reaction. Apoptosis can be induced by a number of physiologic and stress stimuli that trigger one of several distinct signalling pathways. The specific pathway activated is dependent on the stimulus and on the cell type affected (reviewed by Fraser and Evan, 1996).

Apoptosis can be induced by a number of stimuli. Two stimuli known to induce apoptosis in certain conditions, are Fas-ligand and TNF-α. These proteins interact with specific receptors on the cell surface, which induce apoptosis via death domains located in the cytoplasmic tail of each receptor. TNF receptor-associated death domain (TRADD), and Fas-associated death domain (FADD) proteins interact directly with specific caspases that induce apoptosis (as reviewed by Fraser and Evan, 1996). Caspases are proteins that exist in cells as pro-enzymes, that are proteolytically cleaved to form heterodimeric complexes. During apoptosis, it is the trans-cleavage and activation of caspases that is responsible for the apoptotic disassembly of cellular organelles.

Other important regulators of apoptosis are situated in the mitochondrial membrane. Two such factors in particular, apoptosis inducing factor (AIF), which is a caspase, and cytochrome c (Cyt c), are important pro-apoptotic co-factors. Thus, disruption of the mitochondrial transmembrane potential (MTP) causes the uncoupling of the respiratory chain, and the release of calcium, glutathione, as well as these two pro-apoptotic factors (reviewed by Fraser and Evan, 1996). Anti-apoptotic proteins are also situated in the mitochondrial membrane of mammalian cells, including Bcl-2 and BCL-$_{XL}$. Furthermore, there are also other

members of the same Bcl-2 family, e.g. Bax, Bad, and Bak, which may be pro-apoptotic. One possible suggestion is that heterodimerisation of an anti-apoptotic factor (Bcl-2), with a pro-apoptotic factor (Bad), will signal apoptosis, whilst the dissociation of these complexes results in protection from apoptosis. In contrast, Bcl-2 homodimers have anti-apoptotic effects by inhibiting the release of factors such as calcium, AIF and Cyt-c from the mitochondria (Kluck et al., 1997).

Apoptotic stimuli such as TNF and Fas-ligand also activate the stress-activated MAPK: Jnk, which increases the transcriptional activity of Jun by phosphorylation (Verheij et al., 1996). Jun forms heterodimers with proteins such as Fos, and activates transcription at AP-1 sites (see section 1.3). In fibroblasts the simple over-expression of Jun was sufficient to induce apoptosis, and that the transcriptional activity of Jun was required for this phenomenon (Bossy Wetzel et al., 1997). This Jun induced apoptosis was blocked by inhibition of caspase activity, confirming that c-Jun induces apoptosis indirectly through protease intermediates. In PC12 cells, withdrawal of NGF resulted in apoptosis, which was associated with activation of Jnk and p38, and a concomitant inactivation of ERK. Thus the balance of Jnk/p38 and ERK signalling may be important in deciding cell fate (Xia et al., 1995). Jnk activation is associated with many different processes, including cell proliferation and differentiation as well as apoptosis. A possible explanation for the heterogeneity of Jnk response, is that different stimuli may activate specific Jnk isoforms. A recent study supporting this hypothesis showed that a dominant negative form of Jnk1, but not of Jnk2, inhibited stress induced apoptosis in a lung cancer cell line (Butterfield et al., 1997).

Another pathway implicated in signalling to induce apoptosis is mediated via the lipid second messenger ceramide. Formation of ceramide is capable of inducing apoptosis in many different cell types in an efficient and uniform manner. However, ceramide also acts as a second messenger

for other processes such as proliferation of fibroblasts and differentiation of promyelocytes (as reviewed by Kolesnick and Kronke, 1998). Ceramide can be produced in cells in several ways. The most important process in rapid ceramide production is the catabolic hydrolysis of sphingomyelin (SM) to ceramide, by both acidic sphingomyelinases (A-SMase) and neutral sphingomyelinases (N-SMase). A-SMases activities are localised to acidic compartments such as the lysosome and endosome, whilst N-SMases are localised in the cell membrane. Both A-SMase and N-SMase have been shown to be rapidly and transiently activated by exogenous stimuli, and appear to be responsible for the rapid increase in ceramide levels within a time frame of seconds to minutes (as reviewed by Spiegel et al., 1996).

The distinct functions of ceramide may be regulated by the site of its production within the cell. For example, TNF is able to signal both proliferation and apoptosis, both of which depend on ceramide production. In apoptosis, the death domain of TNF-receptor induces ceramide production by A-SMases, which leads to apoptosis. Another domain on the TNF receptor is essential for N-SMase activation, which again produces ceramide, but in this case proliferation is the end result (as reviewed by Kolesnick and Kronke, 1998). Further evidence that A-SMase is critical in ceramide induced apoptosis is provided by cells from patients with a deficiency of A-SMase (Neimann-Pick disease), which did not respond to ionizing radiation either with production of ceramide or by apoptosis (Santana P. et al., 1996).

The fact that ionising radiation induces ceramide production in isolated membranes, where no death domains exist, suggests that ionising radiation may signal SMase activation by different mechanisms (as reviewed by Kolesnick and Kronke, 1998). This stimulus may directly activate SMases, in a similar way that UV radiation has been shown to activate Src family kinases directly (Devary et al., 1992). Ionising radiation appears to utilise

caspases downstream of ceramide production to induce apoptosis (Emoto et al., 1995). Ceramide also appears to signal disruption of the MPT that is associated with Cyt-c and AIF release (Pastorino et al., 1996), and Bcl-2 inhibits ceramide induced disruption of the MPT and AIF release (Susin et al., 1997). Furthermore, ceramide can also signal direct activation of caspases to execute apoptosis, and this activation is inhibited by over-expression of Bcl-2 (Zhang et al., 1996). These studies link ceramide to the classic effectors of apoptosis.

Exposure of U937 cells to various apoptosis-inducing stresses, including ionising radiation, induced rapid ceramide generation and activation of the Jnk signalling pathway (Verheij et al., 1996). Addition of excess ceramide to cells, like stress, induced activation of the Jnk signalling pathway, but not the ERK signalling pathway. Furthermore over-expression of dominant negative forms of Jun inhibited TNF, Stress, and ceramide induced apoptosis (Verheij et al., 1996). These data strongly indicate that ceramide production induces activation of Jnk, and that this process is vital in the apoptotic response to various stresses.

With the available data it is not possible to give a definitive explanation as to why the ability to apoptose in response to X-irradiation should be mediated by ligand bound RXR. However, one known property of RXRα, and other retinoic acid receptors, does provide a possible explanation. This is the ability of RARs and RXRs to antagonise AP-1 activity. Ligand bound RARα, RARβ, RARγ and RXRα have been shown to bind and sequester Jun, thus inhibiting the ability of Jun to bind DNA and activate transcription at AP-1 sites (Salbert et al., 1993; Schule et al., 1991). Treatment with all-*trans* RA, or with RXR specific retinoids, has also been shown to inhibit expression of *fos* mRNA and Fos protein, another component of the AP-1 transcription factor complex (Lee H.Y. et al., 1998). Furthermore, the same study showed that all-*trans* RA treatment inhibited Jnk activity. All-*trans* RA did not decrease expression of Jnk,

but reduced its ability to phosphorylate and activate Jun, as shown by a luciferase reporter gene assay (Lee H.Y. et al., 1998).

The ability of RXRα to inhibit AP-1 activation was shown to be dependent on 9-*cis* RA treatment and on the concentration of retinoid receptors (Salbert et al., 1993), both of which mirror the requirements in the anti-apoptotic effects on αG2S cells. The interaction between RXRα and Jun was found to be blocked by mutations of specific residues in the ligand binding domain (LBD). These blocking mutations are in H10 of the LBD, a region previously associated with protein dimerisation (see section 1.5.3.2.). Furthermore, monomeric ligand bound RARs bind Jun, and RAR-RXR heterodimers did not bind Jun (Salbert et al., 1993). Thus it is probable that the anti-AP-1 activity of RXRα is mediated by, the formation of RA-dependent non-productive RXRα-Jun dimers, RA-dependent inhibition of *fos* mRNA and protein expression, and RA-dependent inhibition of Jnk activity.

Therefore, the probable reason for the RXRα concentration-dependent protection from apoptosis in U937 transfectants was the regulatory effects that these receptors have on AP-1 activity. Under normal conditions, exposure of U937 cells to ionising radiation induced apoptosis by rapid ceramide generation and downstream activation of Jnk (Verheij et al., 1996), and this was confirmed when over-expression of dominant negative forms of Jun was found to inhibit apoptosis (Verheij et al., 1996).

If this is correct, then an interesting future experiment to elucidate the activity of Jnk and Jun would be the transfection of a Jun controlled reporter gene into the U937 transfectants. These cells could then be X-irradiated and the response of the reporter gene assessed. Another experiment would be the transfection of a dominant negative Jun construct to attempt to block X-irradiation induced apoptosis.

As shown previously in this study, Jnk was shown to expressed in all U937 transfectants, Jnk was phosphorylated in response to op-SRBC in a similar fashion in all three cell lines (Figure 4.1.1.3.). This demonstrated that 9-*cis* RA treatment does not block Jnk phosphorylation, and suggests that the RA-dependent inhibition of Jnk activity described previously (Lee H.Y. et al., 1998), is not due to inhibition of Jnk phosphorylation. Interestingly, Jnk expression was possibly increased in 9-*cis* RA-treated αG2S cells (Figure 4.1.1.3.), although unfortunately this observation was not checked with an actin protein loading control. An increase may be an attempt by these cells to overcome 9-*cis* RA/RXR mediated down-regulation of Jnk activity.

As UV light does not induce similar differential effects on death of the U937 transfectants, it can be assumed that UV light induces cell death by other mechanisms. However, UV light is known to induce Jnk activation. Therefore, UV light must also induce cell death by other alternative pathways. This was demonstrated by the sensitivity to exposure of the U937 transfectants to UV light, with no proliferation being measured after as little as ten seconds exposure (see section 6.1.3.).

Under other circumstances RXR molecules have been shown to induce apoptosis. For example, RXR-RXR homodimers have been shown to be responsible for activation induced apoptosis in RA-treated HL-60 cells (Nagy et al., 1995). This supports the possible antagonistic functions of RXR-RXR homodimers and RXR-Jun dimers in the induction of apoptosis which has been shown here.

6.2.3. Co-stimulation of T-cell activation.

In a further assay using mitomycin-C to inhibit the progression of the U937 cells through the cell cycle. 9-*cis* RA-treated αG2S cells were shown to be better co-stimulators of T-cell proliferation than MEP cells,

whilst αB5A cells were less efficient accessory cells than MEP cells (Figure 6.1.6.).

This increase in efficiency of accessory cell function could be mediated by the increase in expression of CD54 (ICAM-1), observed on αG2S cells following 9-*cis* RA treatment (Table 3.1.3.1.). The increase in CD102 (ICAM-2) observed in αB5A cells did not increase accessory cell functions of these cells.

This increase in efficiency of αG2S cells, and the decrease in efficiency of αB5A cells, suggests a more mature and a less mature monocyte phenotype respectively. Furthermore, pre- and non-exposed op-SRBC U937 transfectants had equal efficiencies as accessory cells (Figure 6.1.6.). This suggests that these cells did not up-regulate any co-stimulatory molecules after phagocytosis. An important observation from this experiment was that increased efficiencies of immunophagocytosis and accessory cell functions are not mutually exclusive, suggesting that activated monocytes and macrophages can both be efficient phagocytes and APCs.

The original intention of the experiments described in this Chapter were to investigate the molecules found in Chapter 5 that were implicated in T-cell activation. However, in view of the unexpected results observed upon X-irradiation of these cells, these experiments were not performed. One particularly interesting future experiment would be to see if the U937 transfectants were more capable in co-stimulation of CD4+ T-cell responses, and another would be to analyse whether or not expression of CD80 and CD86 is induced on the 9-*cis* RA-treated U937 transfectants.

Chapter 7

Conclusions and further objectives.

7.1. Expression of RXRα by peripheral blood monocytes.

This study has determined that RXRα is expressed in peripheral blood monocytes and that its expression is induced during differentiation to macrophages induced by human serum, but not by DHCC (Chapter 3). Levels of RXRα expression were also maintained when the same cells were induced to differentiate towards dendritic cells by cytokines (Chapter 3). In contrast, expression of RARα and RARβ was not affected during monocytic differentiation (Chapter 3). These data confirm the role of RXRα in some forms of monocyte differentiation, and suggests that the macrophages produced from human serum- or DHCC-treated monocytes may have distinct phenotypes and functional properties.

7.2. U937 derived RXRα transfectants.

This study has confirmed that αG2S cells hyper-express, and that αB5A hypo-express RXRα, when compared to MEP empty vector control cells. 9-*cis* RA-treated U937 transfectants differentiate partially, but not fully towards monocytes. These 9-*cis* RA mediated effects were most prominent in αG2S cells, and less prominent in αB5A cells, when compared to the MEP cell line (Chapter 3). Furthermore, following 9-*cis* RA treatment, the expression of RARα was decreased in all U937 transfectants, suggesting that down-regulation of this dimeric partner is important in U937 differentiation (Chapter 3). Differentiation of the U937 transfectants induced by 9-*cis* RA was most likely mediated by RXR-RXR homodimers. However, the formation of RAR-RXR heterodimers would also be induced by 9-*cis* RA. In order to assess which properties of the U937 transfectants are mediated by RAR or RXR, the

transfectants could be treated with retinoids specific for either RAR or RXR.

7.2.1. Assessment of differentiation.

Differentiation of the U937 transfectants was demonstrated by the increased expression of CD11b, CD11c, CD54, CD63, CD101, CD156, CD163 and of components of the NADPH oxidase, on 9-*cis*-RA-treated αG2S cells (Chapter 3). These data suggest that 9-*cis* RA-treated αG2S cells are more differentiated than MEP or αB5A cells, and that RXRα plays a role in inducing the expression of these important monocytic functional molecules. However 9-*cis*-RA treatment only induced partial differentiation of the U937 transfectants, as expression of CD14 was not induced in these cells (Chapter3).

A further measure of differentiation was the increased efficiency of immunophagocytic uptake of op-SRBC by 9-*cis*-RA-treated αG2S cells, and the decreased efficiency of 9-*cis*-RA-treated αB5A cells, when compared to MEP cells (Chapter 3). This suggests that RXRα plays a role in inducing differentiation of U937 cells. The increase in efficiency of phagocytosis may be due to increased expression of CR3 and CR4 (CD11b/18 and CD11c/18) (Chapter 3).

Immunophagocytosis was inhibited by prior addition of CD16 (FcγRIII), demonstrating that this FcγR mediates uptake of op-SRBC in these cells. Furthermore, a CD18 mAb inhibited op-SRBC uptake, demonstrating the importance of CR3 and CR4 in immunophagocytosis. One other mAb, directed against CD13 also inhibited phagocytic uptake, suggesting a role for this aminopeptidase in phagocytosis.

7.2.2. Immunophagocytic signal transduction.

The increased efficiency of immunophagocytosis by 9-*cis*-RA-treated αG2S cells correlated with more extensive and more intense tyrosine

phosphorylation in response to op-SRBC (Chapter 3). Tyrosine phosphorylation in response to op-SRBC was not inhibited by CD13, CD16 or CD18 mAbs, which demonstrated that these mAbs, whilst inhibiting engulfment, did not inhibit FcγR cross-linking, which is the initial step in inducing signal transduction (Chapter 3).

Members of the MAPK family of protein kinases (ERK-1, Jnk and p38) were shown to be activated following immunophagocytosis in all three U937 transfectants (Chapter 4). No phosphorylation of p47-phox or paxillin, proteins involved in superoxide production and focal adhesion formation respectively, was demonstrated following op-SRBC exposure (Chapter 4). The adaptor protein Shc was phosphorylated both before and after op-SRBC exposure in all three cell lines (Chapter 4). Shc has previously been shown to be constitutively phosphorylated in response to high levels of serum, so to examine the role of Shc in immunophagocytosis further experiments should be carried out in reduced serum conditions.

Proteins phosphorylated in response to op-SRBC in all three cell lines interacted with fusion proteins containing specific SH2 domains from common signalling molecules (Chapter 4). There were differences and also similarities in binding of phosphorylated proteins by specific SH2 domains between the U937 transfectants. Amongst the constructs tested, Grb-2-SH2 and Shc-SH2 bound phosphorylated proteins from only αG2S cell lysates (Chapter 4). Of note, was a 72kD protein found only in αG2S cell lysates that bound to Shc-, Grb-10 and Grb-2 SH2 domains (Chapter 4). Previous evidence suggests that this protein may be Syk. Therefore, the differences in immunophagocytic properties may be may be mediated via activation of Syk in αG2S cells compared to the other cell lines. An interesting area for future research would be the further investigation of immunophagocytic signalling, in particular the role of Syk.

7.2.3. Co-stimulatory capabilities.

A further measure of differentiation of the U937 transfectants is their ability to act as accessory cells for T-cell activation in a CD3 dependent assay. This data demonstrated that αG2S cells were more efficient at co-stimulating T-cell proliferation, than MEP cells, which themselves were more efficient than αB5A cells (Chapter 6). This may be due to an increase in the co-stimulatory molecule CD54 (ICAM-1) in αG2S cells (Chapter 3). The U937 transfectants induced similar levels of T-cell proliferation respectively, whether or not they had previously been exposed to op-SRBC (Chapter 6). This demonstrates that increased efficiencies of phagocytosis and accessory cell functions are not mutually exclusive properties.

Further experiments which these observations suggest, include an assessment of the levels of expression of B7 (CD80 and CD86) on these cells, whether or not the same molecules that inhibited U937 dependent T-cell proliferation (see section 7.3.), also inhibited U937 transfectant dependent T-cell proliferation, and whether or not 9-*cis* RA-treated αG2S cells are capable of providing better co-stimulation of CD4+ T-cells specifically, compared to undifferentiated U937 cells (see section 7.3.).

7.2.4. X-irradiation induced cell death.

During the course of determining the co-stimulatory capabilities of the U937 transfectants it became apparent that X-irradiation inhibited proliferation of αG2S cells less than that of MEP cells, which in turn proliferated more than αB5A cells (Chapter 6). These post-irradiation differences in proliferation were detectable only after 9-*cis* RA treatment (Chapter 6). This was shown to be due to differences in the level of apoptosis in the three cell lines (Chapter 6). In U937 cells, X-irradiation induces the formation of ceramide which induces apoptosis, probably via Jnk and Jun. It is known that expression of dominant negative Jnk inhibits

X-irradiation induced apoptosis. 9-*cis* RA bound RXRα has been shown to sequester Jun, and RA treatment to inhibit expression of Fos, a dimeric partner of Jun. Therefore the X-irradiation resistant effects seen are probably due to anti-Jun and anti-Fos effects which result from the available high levels of RXRα in αG2S cells. This hypothesis could be investigated further by the transfection of a Jun dependent reporter gene into each U937 transfectant to determine comparative activity of the Jnk/Jun pathway. This finding could have significant implications for different therapeutic regimes. For example, treatment of leukaemia patients with 9-*cis* RA, may reduce the effectiveness of radiotherapy; and inversely selective modulation of RXRα may increase the resistance of normal cells to X-irradiation induced damage.

7.3. U937 cell dependent T-cell co-stimulation.

7.3.1. U937 cells act as accessory cells.

The ability of U937 cells to act as accessory cells for T-cell proliferation in a CD3 dependent assay was confirmed. This accessory cell function was more efficient for CD8+ T-cells than for CD4+ T-cells. As U937 cells express Class I, but no Class II MHC, this highlights the importance of Class I-CD8 and Class II-CD4 interactions during T-cell activation, even in the presence of a CD3 mAb which acts on both. This data also suggests the possibility that CD4+ and CD8+ T-cells may utilise separate co-stimulatory pathways. Neither B7.1 (CD80) or B7.2. (CD86) were expressed on U937 cells, the addition of an agonistic CD28 mAb which mimics the presence of B7 molecules induced a large increase in CD4+ T-cell proliferation, but not of CD8+ T-cells. Thus B7-CD28 interactions may be more important for activation of CD4+, than for activation of CD8+ T-cells (Chapter 5).

7.3.2. Molecules that inhibit T-cell proliferation.

The role of integrin (CD11a/18 or LFA-1)-ICAM-1 (CD54) interactions in T-cell proliferation was confirmed. Panels of mAbs against CD11a,

CD18 and CD54 inhibited U937/CD3 dependent T-cell proliferation. These mAbs also inhibited the formation of U937-T-cell clusters. CD11a, CD18, CD54 and mAbs, all act via the accessory cell (U937), rather than via T-cells. CD45 mAbs also inhibited proliferation, but induced the formation of large clusters of cells, even in the absence of CD3 mAb. This suggests that CD45 ligation encourages cell-cell adhesion. CD45 mAbs acts via both the accessory (U937), and T-cell (Chapter 5).

CD45, CD53, CD55, CD98, CDw108, CD147 and four undefined mAbs also inhibited T-cell proliferation in the same assay. CD53, CD55 and CDw108 and one undefined mAb (MEM-135), inhibited T-cell proliferation by direct effects on the T-cells. CD98, CD147 and one undefined mAb (WM78), inhibited T-cell proliferation via effects on the U937 cells, as well as directly on T-cells.

These data suggest that CD98 and CD147 may be novel co-stimulatory molecules. As evidence for this, CD98 and CD147 mAbs also inhibited T-cell proliferation in a peripheral blood dendritic cell (PBDC)/CD3 dependent assay (Woodhead et al., 1998).

To confirm the putative co-stimulatory capabilities of CD98 and CD147, alternative T-cell activating stimuli, such as periodate, could be used instead of CD3 mAb. This has been done previously in our laboratory and CD98 and CD147 mAbs inhibited T-cell proliferation in a PBDC dependent assay (Woodhead et al., 1998).

APPENDIX I
mAbs used in phenotyping of U937 transfectants.

Code	Specificity	mAb Name	Isotype	Species	Originator
-	CD50	KS128	G1	Mouse	
-	CD54	MEM-112	G1	Mouse	Horejsi
-	CD102	CBR-IC2/2	G1	Mouse	
M1	Unknown	4B5.F5	G1	Mouse	Ashman
M2	Unknown	4B4.E11	G1	Mouse	Ashman
M3	CD68	4C5.D12	G1	Mouse	Ashman
M4	CD148	A3		Mouse	Aversa
M5	Unknown	TAX64	G1	Mouse	Bensussan A.
M6	Unknown	Ay19	G1	Mouse	Bensussan A.
M7	Unknown	1.83	G1	Mouse	Boumsell
M8	Unknown	BG6		Mouse	Boumsell
M10	Unknown	M103	M	Mouse	Clark
M12	CD101	V7.1	G1	Mouse	Engleman
M13	CD14	61D3	G1	Mouse	Gregory
M14	CD15	BU60	M	Mouse	Hardie
M15	CD18	BU86	G1	Mouse	Hardie
M16	CD18	BU87-M2	G2a	Mouse	Hardie
M17	Unknown	MEM-166	G1	Mouse	Horejsi
M18	CD11b	MEM-174	G2a	Mouse	Horejsi
M19	cho	IGR-2 1A6	M	Mouse	Ingerpuu
M20	CD63	VIM17	G1	Mouse	Knapp
M21	CD15	8D7		Mouse	Koch
M22	CD87	10G7	G3	Mouse	Koch
M23	CD39	8H2	G1	Mouse	Koch
M24	CD63	710F	M	Mouse	Koyama
M25	Unknown	1B12.1	G1	Mouse	Masuhara
M26	Unknown	BIRMA65	G1	Mouse	McDonald
M27	Unknown	AntiTF VD8	G1	Mouse	Muller
M28	Unknown	PMO-1	G1	Mouse	Oravecz
M29	CDw93	X1	G1	Mouse	Peters
M30	Unknown	X3	G1	Mouse	Peters
M31	Unknown	X7	G1k	Mouse	Peters
M32	Unknown	X11		Mouse	Peters
M33	Unknown	X12		Mouse	Peters
M34	Unknown	X15	G1	Mouse	Peters
M36	CD11c	U4	G1	Mouse	Peters
M38	CD163	GH1/61	G	Mouse	Pulford

Code	Specificity	mAb Name	Isotype	Species	Originator
M39	CD163	D11	G	Mouse	Rudinskaya
M40	CD98	J1-G3B	G1	Mouse	Skubitz
M41	Unknown	J2-E1F	G1	Mouse	Skubitz
M42	CD98	J3-E1B	G1	Mouse	Skubitz
M43	Unknown	5H1	G	Mouse	Stckbauer
M44	Unknown	PM-1K	G2a	Mouse	Takeya
M45	Unknown	AM-3K	G1	Mouse	Takeya
M46	CD11b	ZCH-7-4F8	G1	Mouse	Tang
M47	CD14	ZCH-7-2F9	G1	Mouse	Tang
M48	Unknown	ZCH-7-4C3a	M	Mouse	Tang
M49	Unknown	ZCH-7-2D3	G3	Mouse	Tang
M50	CD13	7H5	G2a	Mouse	Taskov
M51	CD157	Mo5	G2a	Mouse	Todd
M55	CD36	UN7	G1k	Mouse	Venuta
M56	CD148	143-41	G1	Mouse	Vilella
M57	CD156	3-2-C		Mouse	Yamamoto
M58	CD156	1-11-G		Mouse	Yamamoto
M59	CD34	HIM80	G1	Mouse	Shen
M60	Unknown	HIM15	M	Mouse	Shen
M62	CD15	HIM95	M	Mouse	Shen
M63	Unknown	HI249	G1	Mouse	Shen
M65	Unknown	HIM63		Mouse	Shen
M66	Unknown	HIM94		Mouse	Shen
M67	Unknown	HI247		Mouse	Shen
M68	Unknown	AAA4	G1	Mouse	Hazenberg
MR1	CD14	RPA-M1	G2b	Mouse	Aversa
MR3	CD14	MoS39	G2a	Mouse	Goyert
MR4	CD64	22.2	G1	Mouse	Guyre
MR5	CD64	197	G2a	Mouse	Guyre
MR6	CDw92	VIM15	G1	Mouse	Knapp
MR7	CDw92	VIM15b	G2b	Mouse	Knapp
MR8	CDw93	VIMD2	G1	Mouse	Knapp
MR9	CDw93	VIMD2b	G1	Mouse	Knapp
MR10	CD33	4D3	G2b	Mouse	Knapp
MR11	CD34	9F2	G	Mouse	Knapp
MR12	CDw65	VIM8	M	Mouse	Knapp
MR13	CD87	VIM5	G1	Mouse	Knapp
MR14	CD66acde	F34-187	G1	Mouse	Kuroki
MR15	CD34	NU-4A1	G1	Mouse	Nakamura
MR16	CDw12	M-67	G1	Mouse	Reiber

Code	Specificity	mAb Name	Isotype	Species	Originator
MR17	CD13	MCS-2	G1	Mouse	Sagawa
MR18	CD66b	G10F5	M	Mouse	Thompson
MR19	CDw17	G035	M	Mouse	Thompson
MR20	CD87	3B10	G2a	Mouse	Todd
MR21	CD13	72a	G1	Mouse	Todd
MR22	CD114	129	G1	Mouse	Welte
MR23	CD68	Y-1/82a	G3	Mouse	Cordell
MR24	CD68	Y-2/131	G1	Mouse	Cordell
MR25	CDw65	88H7	G1	Mouse	van Agthoven
MR28	CD101	BB27	G1	Mouse	Boumsell
MR29	CD33	UN-248		Mouse	Peiper
MR30	CD89	A59	G1	Mouse	Kubugawa
MR31	CD35	Ber-Mac-drc	M	Mouse	Stein

Appendix II

mAbs used in immunophagocytosis experiments.

mAb Name	Specificity	Isotype	mAb Name	Specificity	Isotype
lue-11-b	CD16		GH1/61	CD163	G
3G8	CD16		D11	CD163	G
IV3	CD32		J1-G3B	CD98	G1
32	CD64		J2-E1F	Unknown	G1
			J3-E1B	CD98	G1
4B5.F5	Unknown	G1	5H1	Unknown	G
4B4.E11	Unknown	G1	AM-3K	Unknown	G1
A3	CD148	G1	ZCH-7-4F8	CD11b	G1
Ay19	Unknown	G1	ZCH-7-2D3	Unknown	G3
B-C12	PRR2	G2b	7H5	CD13	G2a
BU60	CD15	M	Mo5	CD157	G2a
BU86	CD18	G1	UN7	CD36	G1k
BU87-M2	CD18	G2a	143-41	CD148	G1
MEM-174	CD11b	G2a	3-2-C	CD156	
710F	CD63	M	1-11-G	CD156	
BIRMA65	Unknown	G1	HIM80	CD34	G1
PMO-1	Unknown	G1	HIM15	Unknown	M
X1	CDw93	G1	HIM220	ScavengerR	M
X7	Unknown	G1k	HI249	Unknown	G1
X11	Unknown	G1k	HIM63	Unknown	M
X15	Unknown	G1	HI247	Unknown	M

Appendix III
mAbs used in U937/CD3 T-cell proliferation assay.

Code	Specificity	mAb Name	Isotype	Species	Originator
N/A	CD11a	CD11a 5E6	G1	Mouse	Knapp W.
N/A	CD11a	CD11a 6B7	G1	Mouse	Knapp W.
N/A	CD11a	AZN L27	G1	Mouse	van Kooyk Y.
N/A	CD11a	AZN L21	G2b	Mouse	van Kooyk Y.
N/A					
N/A	CD18	AZN L18	G1	Mouse	van Kooyk Y.
N/A	CD18	MEM 148	G1	Mouse	Horejsi V.
N/A	CD18	7E4	G1k	Mouse	van Agthoven A.J.
N/A					
N/A	CD50	MEM 171	G1	Mouse	Horejsi V.
N/A	CD50	BL-A5		Mouse	Eichler W.
N/A					
N/A	CD54	MEM 111	G2a	Mouse	Horejsi V.
N/A	CD54	MEM 112	G1	Mouse	Horejsi V.
N/A	CD54	6.5B5	G1k	Mouse	Askaa J.
N/A	CD54	D8H10	M	Mouse	Fainboim L.
N-L001	CD43	CBF-78	G1	Mouse	Delsol G.
N-L002	CD45	CBE-77	G3	Mouse	Delsol G.
N-L003	Blood Grp H	BNH-9	M	Mouse	Delsol G.
N-L004	CD74	DND-53	M	Mouse	Delsol G.
N-L005	CD45RA	DBB-42	G1	Mouse	Delsol G.
N-L006	CD98	2E12	G	Mouse	Stockbauer P.
N-L007	CD45RA	LT45-M5	G1	Mouse	Filatov A.V.
N-L008	Unknown	LT-TD5	M	Mouse	Filatov A.V.
N-L009	CD71	LT-4E3	G2a	Mouse	Filatov A.V.
N-L010	Unknown	LT-TB5	G1	Mouse	Filatov A.V.
N-L011	CD45RO	A6	G1	Mouse	Aversa G.
N-L012	CD45	4.14	G1	Mouse	Aversa G.
N-L013	CD45	1.22	G1	Mouse	Aversa G.
N-L014	Unknown	A8	G1	Mouse	Aversa G.
N-L015	CD36	UN7	G1	Mouse	Venuta S.
N-L017	CD98	MEM-108	G1	Mouse	Horejsi V.
N-L018	CDw149	MEM-120	M	Mouse	Horejsi V.
N-L019	CDw149	MEM-133	M	Mouse	Horejsi V.
N-L020	Unknown	MEM-135	G1	Mouse	Horejsi V.
N-L021	Unknown	MEM-156	M	Mouse	Horejsi V.
N-L022	CD50	MEM-171	G1	Mouse	Horejsi V.
N-L023	CD97	MEM-180	G1	Mouse	Horejsi V.

Code	Specificity	mAb Name	Isotype	Species	Originator
N-L024	CD25	MEM-181	G1	Mouse	Horejsi V.
N-L025	CD71	MEM-189	G1	Mouse	Horejsi V.
N-L026	CD100	133-1C6	M	Mouse	Vilella R.
N-L027	CD148	143-41	G1	Mouse	Vilella R.
N-L028	CD43	148-1B6	G	Mouse	Vilella R.
N-L029	CD43	148-1C3	G2a	Mouse	Vilella R.
N-L030	CD43	148-3D4	G1	Mouse	Vilella R.
N-L031	CD48	156-4H9	G1	Mouse	Vilella R.
N-L032	CD46	158-2A5	G1	Mouse	Vilella R.
N-L033	CD53	161-2	G2a	Mouse	Vilella R.
N-L034	CD6	161-8	G1	Mouse	Vilella R.
N-L035	CD43	161-46	G1	Mouse	Vilella R.
N-L036	CD59	193-27	M	Mouse	Vilella R.
N-L037	CD100	196-48	M	Mouse	Vilella R.
N-L038	CD46	197-2B1	G2a	Mouse	Vilella R.
N-L039	CD26	202-36	G2b	Mouse	Vilella R.
N-L040	CD53	202-24B	G1	Mouse	Vilella R.
N-L041	CD43	8B4/20	M	Mouse	Fabbi M.
N-L042	CD98	JI-G3B	G1	Mouse	Skubitz K.M.
N-L043	Unknown	J2-E1F	G1	Mouse	Skubitz K.M.
N-L044	CD98	J3-E1B	G1	Mouse	Skubitz K.M.
N-L045	Unknown	BL-TZ	G2b	Mouse	Eichler W.
N-L046	CD50	BL-A5		Mouse	Eichler W.
N-L047	CD44	TA-9B1	G2b	Mouse	Kikuchi K.
N-L048	CD40L	M90	G1	Mouse	Armitage R.J.
N-L049	CD30L	M81	G2b	Mouse	Armitage R.J.
N-L050	Unknown	5D4	G2a+G1	Mouse	Seto M.
N-L051	CD32	K22-268	G1	Mouse	Boyd A.W.
N-L052	Unknown	3D7	G1	Mouse	Boyd A.W.
N-L053	Unknown	III.A4	G1	Mouse	Boyd A.W.
N-L054	Unknown	CJ1250	M	Mouse	Thorley-Lawson D.
N-L055	CD48	BJ40	G	Mouse	Boumsell L.
N-L056	CD100	BB18	G1	Mouse	Boumsell L.
N-L057	CD100	BD16	G1	Mouse	Boumsell L.
N-L058	CD43	RDP/AD9	G1k	Mouse	Petterson R.D.
N-L059	Unknown	RDP/IAM19	Mk	Mouse	Petterson R.D.
N-L060	CD55	JS11	G	Mouse	Bensussan A.
N-L063	CD55	67	G1	Mouse	Hogg N.
N-L065	CD26	EF51A3	G1	Mouse	Kahne T.
N-L067	CD26	EF61 1B10	G1k	Mouse	Kahne T.
N-L068	CD45RA	BIRMA 12	G1	Mouse	McDonald D.

Code	Specificity	mAb Name	Isotype	Species	Originator
N-L069	CD26	L272	G2a	Mouse	Warner N.L.
N-L070	Unknown	11G7	G1	Mouse	Buehring H.J.
N-L071	CD30	11D1.H10	G2a	Mouse	Ashman L.K.
N-L072	CD32	II1A5	G1	Mouse	Frey J.
N-L073	CD32	II8D2	G1	Mouse	Frey J.
N-L074	Unknown	B-L12	G1	Mouse	Vermot-Desroches C.
N-L076	Unknown	MAL7B	M	Mouse	Turner G.T.H
N-L078	CD26	BA5	G2ak	Mouse	van Agthoven A.
N-L079	CD98	BK19.9	G1	Mouse	van Agthoven A.
N-L080	CD48	BU70	G1	Mouse	Hardie D.L.
N-L081	CD48	BU91	G2a	Mouse	Hardie D.L.
N-L082	CD147	UM-8D6	G3	Mouse	Fox D.A.
N-L083	CDw150	1PO-3	G1	Mouse	Sidorenko S.
N-L084	Unknown	1E8	G1	Mouse	Nagasaki M.
N-L085	Unknown	1A9	M	Mouse	Nagasaki M.
N-L087	Unknown	WM78	G1	Mouse	Henniker A.J.
N-L088	CD45RB	WM76	G1	Mouse	Henniker A.J.
N-L089	Unknown	WM66	M	Mouse	Henniker A.J.
N-L091	CD101	V7.1	G1	Mouse	Englemen E.G.
N-L092	Unknown	RmCB	G1	Mouse	Finberg R.W.
N-L093	CD43	OH-01	G1	Mouse	Higashihara M.
N-L094	Unknown	J-51	G2a	Mouse	Pesando J.M.
N-L095	CD38	JS-30	G1	Mouse	Pesando J.M.
N-L096	CD29	J-1	G2a	Mouse	Pesando J.M.
N-L097	Unknown	J-183	G1	Mouse	Pesando J.M.
N-L098	Unknown	J-67	G1	Mouse	Pesando J.M.
N-L099	Unknown	SN2	G1k	Mouse	Seon B.K.
N-L100	Unknown	SN1	G1k	Mouse	Seon B.K.
N-L101	Unknown	ICO-166	G1	Mouse	Baryshisnikov A.J.
N-L102	CD45	ICO-46	G2b	Mouse	Baryshisnikov A.J.
N-L103	CD45	IMMU19.2	G1k	Mouse	van Agthoven A.J.
N-L104	Unknown	KI12	M	Mouse	Kunlong B.
N-L105	Unknown	K108	M	Mouse	Kunlong B.
N-L106	Unknown	K101	M	Mouse	Kunlong B.
N-L107	Unknown	K104	M	Mouse	Kunlong B.
N-L108	CD147	HI197	G1	Mouse	Shen D.C.
N-L109	CD147	HIM6	G1	Mouse	Shen D.C.
N-L110	CD43	HI165	G1	Mouse	Shen D.C.
N-L111	CD45RA	HI115	G1	Mouse	Shen D.C.
N-L112	CD99	HI142	M	Mouse	Shen D.C.
N-L113	CD43	HI161	G1	Mouse	Shen D.C.

Code	Specificity	mAb Name	Isotype	Species	Originator
N-L114	Unknown	CNA-42	M	Mouse	Delsol G.
N-L116	CD70	IPO-38	M	Mouse	Gluzman D.F.
N-L117	BST1	BEC7	G1	Mouse	Hirano T.
N-L118	BST1	RF3	G2a	Mouse	Hirano T.
N-L119	CD47	1/1A4	G2b	Mouse	Knapp W.
N-L120	CD55	F4-29D9	G1	Mouse	George F.
N-L121	CD45RC	OTH75E4	G1	Mouse	Hadam M.
N-L122	CD45	CBLT200.1	G1	Mouse	Connelly M.
N-L123	CD45	7E.12	G1	Mouse	Taskov H.
N-L124	CD98	CAF7	G1	Mouse	Taskov H.
N-L125	Unknown	5G7	G2a	Mouse	Taskov H.
N-L126	Unknown	OTH77A3	G2a	Mouse	Hadam M.
N-L127	CD45RA	OTH74D4	G1	Mouse	Hadam M.
N-L128	CD52	CF1D12	G3	Mouse	Hadam M.
N-L129	CD45	CF10H5	G1	Mouse	Hadam M.
N-L131	CD48	IIID3	M	Mouse	Hadam M.
N-L132	CD53	AC119	G1k	Mouse	Buck D.W.
N-L133	CD31	AC114	G1k	Mouse	Buck D.W.
N-L134	CD71	AC108	G2ak	Mouse	Buck D.W.
N-L135	CD71	AC102	G2ak	Mouse	Buck D.W.
N-L136	Unknown	6G7	G1	Mouse	Ball E.D.
N-L137	Unknown	B-Zg	G1	Mouse	Vermot-Desroches C.
N-L140	CD98	IPO-T10	M	Mouse	Gluzman D.F.
N-L141	Unknown	P105	G1	Mouse	Roth P.
N-L142	Unknown	P53	G1	Mouse	Roth P.
N-L143	Unknown	PCNA	G1	Mouse	Roth P.
N-L144	Unknown	P120	G1	Mouse	Roth P.
N-L145	Unknown	2.7	G1	Mouse	Roth P.
N-L146	CD70	BU69	G1	Mouse	Hardie D.L.
N-L147	CD98	BU53	G2a	Mouse	Hardie D.L.
N-L148	CD98	BU89	G1	Mouse	Hardie D.L.
N-L149	CD48	WM63	M	Mouse	Henniker A.J.
N-L150	CD48	WM68	G3	Mouse	Henniker A.J.
N-L151	CD53	WM65	G1	Mouse	Henniker A.J.
N-L152	CD85	H47	G1	Mouse	Sagawa K.
N-L153	Unknown	H105	M	Mouse	Sagawa K.
N-L154	Unknown	KS-2	G2a	Mouse	Sagawa K.
N-L155	CD147	H84	G2b	Mouse	Sagawa K.
N-L156	CDw108	MEM-150	M	Mouse	Horejsi V.
N-L157	Unknown	HI151	G1	Mouse	Shen D.C.
N-L158	Unknown	HI156	G2a	Mouse	Shen D.C.

Code	Specificity	mAb Name	Isotype	Species	Originator
N-L159	Unknown	HI172	G1	Mouse	Shen D.C.
N-L160	Unknown	HI175	M	Mouse	Shen D.C.
N-L161	Unknown	HI185	G1	Mouse	Shen D.C.
N-L162	CD45RB	MT3	G1	Mouse	Poppema S.
N-L163	CD45RB	MT4	G1	Mouse	Poppema S.
N-L165	CD45	ML2	G1	Mouse	Poppema S.
N-L166	CD43	1G10	G1k	Mouse	Huang E.C.
N-L167	CD26	2A6	G1k	Mouse	Poppema S.
A101	Unknown	4A11	M	Mouse	Koch A.E.
A102	Unknown	ASC-11	G1	Mouse	Skubitz A.P.N.
A103	Unknown	67A4	G1k	Mouse	van Agthoven A.J.
A104	CD14	61D3	G1	Mouse	Gregory C.D.
A105	Unknown	CJ1250	MK	Mouse	Thorley-Lawson D.A.
A106	Unknown	HIM62	M	Mouse	Shen D.C.
A107	Unknown	CNA42	M	Mouse	Delsol G.
A108	Unknown	AD2	G1	Mouse	Patel D.
A109	ALCAM	3A6	G1	Mouse	Patel D.
A110	RHAMM	3T3.5	G1	Mouse	Turley E.A.
A111	S-Endo 1	F435H-7	G1	Mouse	George-Dignat F.
A112	S-Endo 1	F432G-3	G1	Mouse	George-Dignat F.
A113	S-Endo 1	F439E	G1	Mouse	George-Dignat F.
A114	Unknown	9C4	G2b	Mouse	Buehring H.J.
A115	MGC-24	105A5	G3	Mouse	Buehring H.J.
A116	CD18	BL5	G1	Mouse	Brochier J.
A117	CD98	JI-G3B	G1	Mouse	Skubitz K.M.
A118	Unknown	J2-E1F	G1	Mouse	Skubitz K.M.
A119	CD98	J3-E1B	G1	Mouse	Skubitz K.M.
A120	Unknown	H8E3	G3	Mouse	Fainboim L.
A122	Sialyl-Lewis x	SY32	M	Mouse	Bovin N.V.
A123	Sialyl-Lewis a	SY51	M	Mouse	Bovin N.V.
A124	MGC-24	9E10	G3	Mouse	Simmons P.J.
A125	Unknown	M72	M	Mouse	Clark R.A.
A126	Unknown	RmCB	G2b	Mouse	Finberg R.W.
A127	Unknown	UN1	G1k	Mouse	Venuta S.
A128	Unknown	R1-20	G1k	Mouse	Nakamura S.
A129	Unknown	IGR-2 1A6	M	Mouse	Ingerpuu S.
A130	CD63	710F	M	Mouse	Koyama Y.
A025	CD105	F430C-5	G2a	Mouse	George-Dignat F.
A029	CD6 L	J3-119	G2a	Mouse	Pesando J.M.
A030	CD6 L	J4-81	G1	Mouse	Pesando J.M.

Appendix IV

Expression of myeloid mAbs on 9 *cis-RA* treated U937 transfectants, by FACS analysis.

				αG2S		αB5A		MEP
Specificity	Code	mAb Name	% positive	MFI	% positive	MFI	% positive	MFI
CD11b	M18	MEM-174	63	392	29.6	293	24	286
CD11b	M46	ZCH-7-4F8	40	276	16	214	21	228
CD11c	**M36**	**U4**	**18**	**227**	**6.4**	**181**	**8.8**	**192**
CDw12	MR16	M-67	1.8	237	1	213	1.5	231
CD13	**M50**	**7H5**	**96**	**546**	**94**	**532**	**97**	**585**
CD13	**MR17**	**MCS-2**	**99**	**666**	**99**	**657**	**99**	**704**
CD13	**MR21**	**72a**	**99**	**536**	**99**	**523**	**99**	**548**
CD14	M13	61D3	8.5	225	6.2	183	3.9	191
CD14	M47	ZCH-7-2F9	11.4	198	5.5	164	5.3	173
CD14	MR1	RPA-M1	5	235	2.5	225	2	218
CD14	MR3	MoS39	5	245	1.9	225	1.6	220
CD15	**M14**	**BU60**	**97**	**727**	**96**	**711**	**96**	**707**
CD15	**M21**	**8D7**	**4.6**	**221**	**3**	**210**	**2.5**	**220**
CD15	**M62**	**HIM95**	**81**	**733**	**68**	**643**	**91**	**775**
CDw17	MR19	G035	4.6	251	2.7	230	5.6	254
CD18	**M15**	**BU86**	**98**	**575**	**98**	**539**	**98**	**547**
CD18	**M16**	**BU87-M2**	**98.5**	**563**	**97**	**514**	**98**	**515**
CD33	MR10	4D3	98	526	98	521	99	520
CD33	MR29	UN-248	95	508	98	512	99	522
CD34	**M59**	**HIM80**	**84**	**337**	**68**	**302**	**52**	**282**
CD34	**MR11**	**9F2**	**36**	**332**	**17**	**277**	**40**	**335**

Specificity	Code	mAb Name	% positive	αG2S MFI	% positive	αB5A MFI	% positive	MEP MFI
CD34	**MR15**	**NU-4A1**	**1**	**230**	**1.6**	**214**	**1**	**223**
CD35	MR31	Ber-Mac-drc	5.4	240	3.6	213	5.1	245
CD36	**M55**	**UN7**	**97**	**601**	**89**	**503**	**94**	**584**
CD39	M23	8H2	4.4	220	6.8	198	5.2	216
CD63	**M20**	**VIM17**	**50**	**350**	**36**	**328**	**43**	**351**
CD63	**M24**	**710F**	**55**	**357**	**59**	**367**	**39**	**338**
CD64	MR4	22.2	98	479	94	441	95	440
CD64	MR5	197	95	452	83	419	86	407
CDw65	**MR12**	**VIM8**	**98**	**868**	**98**	**859**	**99**	**859**
CDw65	**MR25**	**88H7**	**95**	**770**	**98**	**769**	**93**	**749**
CD66acde	MR14	F34-187	15	287	16	285	22	305
CD66b	MR18	G10F5	2	235	1.6	215	2.2	241
CD68	**M3**	**4C5.D12**	**2.5**	**202**	**3.2**	**180**	**2.1**	**174**
CD68	**MR23**	**Y-1/82a**	**1**	**223**	**1.7**	**198**	**1.1**	**216**
CD68	**MR24**	**Y-2/131**	**1.6**	**225**	**1.6**	**203**	**1.5**	**223**
CD87	M22	10G7	4.1	184	5	169	2.2	170
CD87	MR13	VIM5	59	372	42	349	99	513
CD87	MR20	3B10	97	514	93	450	99	594
CD89	**MR30**	**A59**	**98**	**548**	**98**	**535**	**98**	**584**
CDw92	MR6	VIM15	98	526	99	525	96	530
CDw92	MR7	VIM15b	98	512	99	499	95	504
CDw93	**M29**	**X1**	**99**	**613**	**98**	**619**	**96**	**586**
CDw93	**MR8**	**VIMD2**	**98**	**669**	**98**	**682**	**94**	**667**

Specificity	Code	mAb Name	% positive	αG2S MFI	% positive	αB5A MFI	% positive	MEP MFI
CDw93	**MR9**	**VIMD2b**	**97**	**666**	**98**	**689**	**95**	**674**
CD98	M40	J1-G3B	7.5	**196**	5.1	166	28	255
CD98	M42	J3-E1B	94	**642**	97	657	96	673
CD101	**M12**	**V7.1**	**9.8**	**236**	**5**	**210**	**7.8**	**232**
CD101	**MR28**	**BB27**	**29**	**322**	**19**	**290**	**37**	**336**
CD114	MR22	129	3.8	267	3.7	244	2.9	248
CD148	**M4**	**A3**	**55**	**337**	**50**	**333**	**45**	**339**
CD148	**M56**	**143-41**	**93**	**372**	**84**	**336**	**88**	**338**
CD156	M57	3-2-C	39	236	20	250	15	200
CD156	M58	1-11-G	27	247	12	210	11	216
CD157	**M51**	**Mo5**	**97**	**600**	**97**	**598**	**97**	**506**
CD163	M38	GH1/61	90	**356**	55	289	51	285
CD163	M39	D11	99	727	72	722	75	754
cho	**M19**	**IGR-2 1A6**	**3.2**	**207**	**4.4**	**186**	**5.9**	**210**
Unknown	**M1**	**4B5.F5**	**32**	**304**	**5.1**	**234**	**9**	**234**
Unknown	**M2**	**4B4.E11**	**22**	**284**	**6.5**	**253**	**3**	**241**
Unknown	**M5**	**TAX64**	**3.3**	**195**	**2.7**	**179**	**2.4**	**183**
Unknown	**M6**	**Ay19**	**55**	**334**	**37.5**	**328**	**62**	**343**
Unknown	**M7**	**1.83**	**65**	**346**	**65**	**352**	**76**	**364**
Unknown	**M8**	**BG6**	**4.4**	**229**	**2.2**	**216**	**6.4**	**236**
Unknown	**M10**	**M103**	**3.2**	**177**	**3.7**	**165**	**2.4**	**178**
Unknown	**M17**	**MEM-166**	**3.8**	**208**	**5.3**	**176**	**3**	**177**

Specificity	Code	mAb Name	% positive	αG2S MFI	% positive	αB5A MFI	% positive	MEP MFI
Unknown	M25	1B12.1	3.4	173	6.4	165	4.7	188
Unknown	M26	BIRMA65	98	557	99	540	96	543
Unknown	M27	AntiTF VD8	8.3	205	4	174	10	199
Unknown	M28	PMO-1	98	368	75	319	60	280
Unknown	M30	X3	4.8	171	4.2	164	7.5	187
Unknown	M31	X7	96	385	78	319	67	304
Unknown	M32	X11	97	404	93	380	89	349
Unknown	M33	X12	6.6	196	6.5	183	6.1	183
Unknown	M34	X15	87	351	57	282	53	278
Unknown	M41	J2-E1F	52	270	21	182	76	339
Unknown	M43	5H1	97	410	93	380	94	399
Unknown	M44	PM-1K	27	260	7	198	12	222
Unknown	M45	AM-3K	85	353	71	321	68	303
Unknown	M48	ZCH-7-4C3	9.8	180	3.6	156	4.6	169
Unknown	M49	ZCH-7-2D3	96.9	508	95	462	98	522
Unknown	M60	HIM15	89	739	83	715	95	753
Unknown	M63	HI249	77	323	58	284	63	326
Unknown	M65	HIM63	96	645	94	650	97	654
Unknown	M67	HI247	91	684	89	690	94	685
Unknown	M68	AAA4	8	165	7.8	160	6.3	164

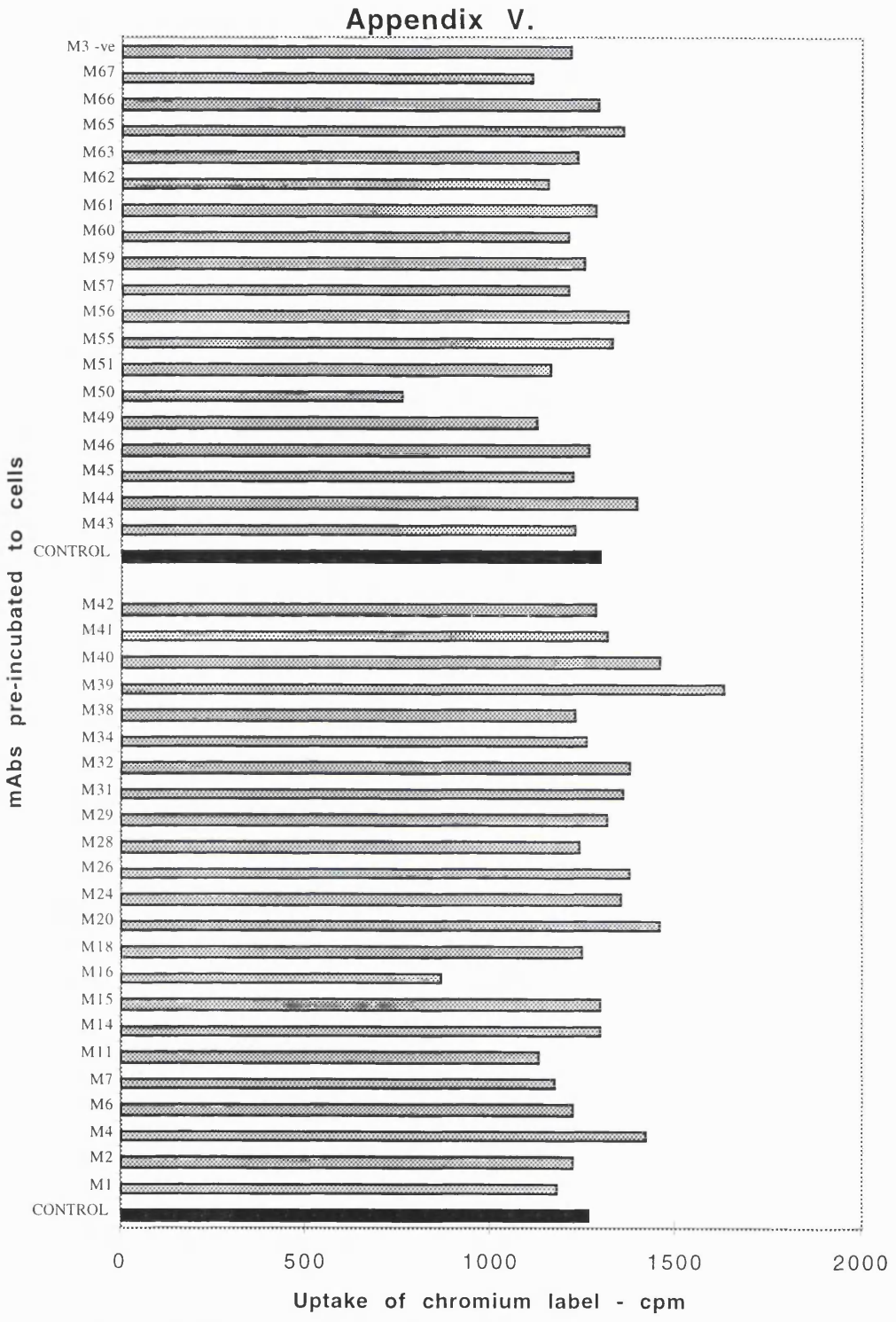

Appendix V. Screening of mAbs from the myeloid panel for effects on immunophagocytosis.
10^7 9-*cis* RA-treated αG2S cells were incubated with a 1:50 dilutions of mAbs from the myeloid panel of the 6th HLDA for 1 hour at 4°C. The ability of these cells to immunophagocytose was assessed by uptake of ^{51}Cr-op-SRBC (see sections 2.7. and 2.8.). The values shown are the cpm uptake of ^{51}Cr-op-SRBC from one experiment. The black bars shown are the control values, when no mAb was added to the assay.

Appendix VI. Part 1.

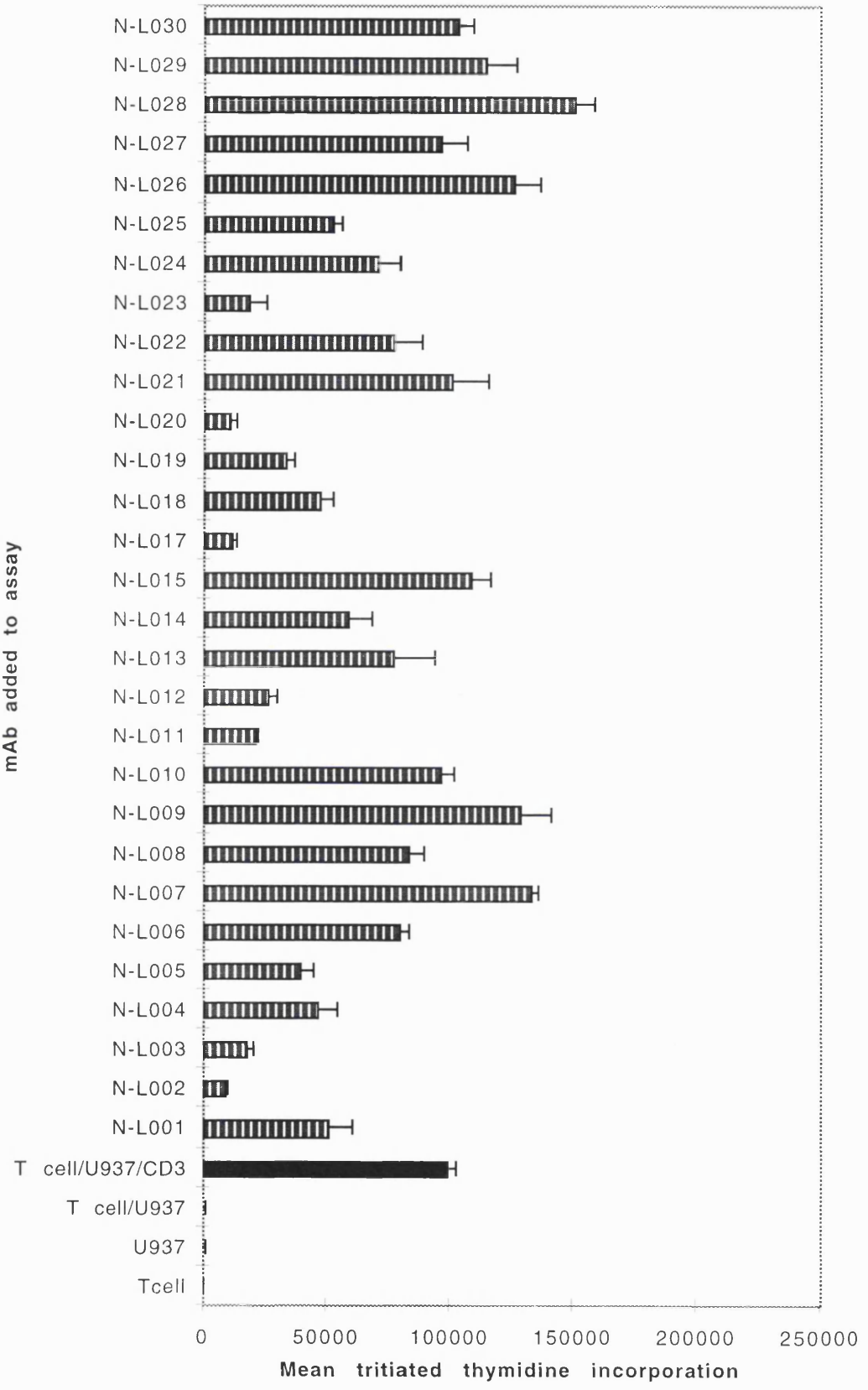

Appendix VI. Part 2.

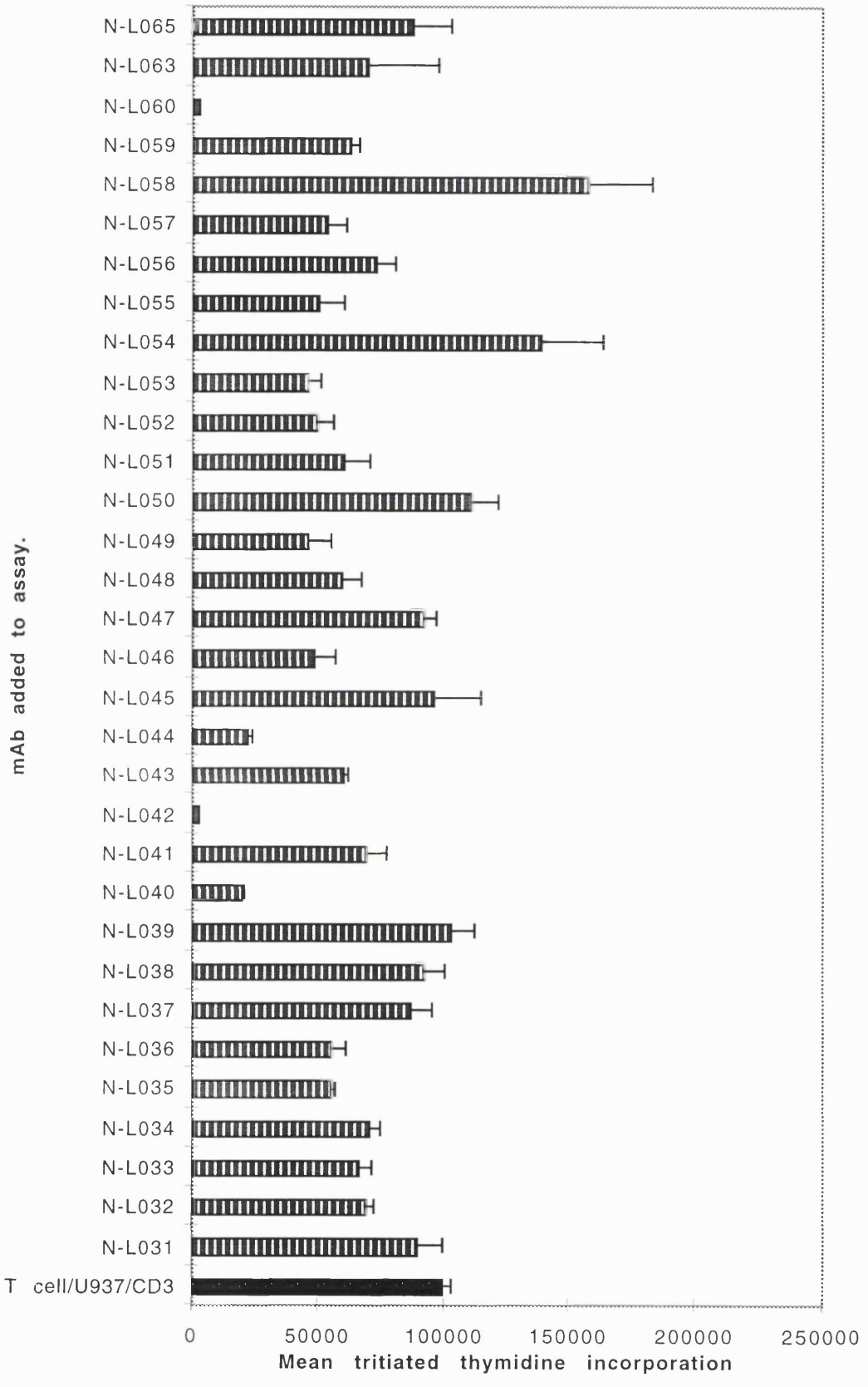

Appendix VI. Part 3.

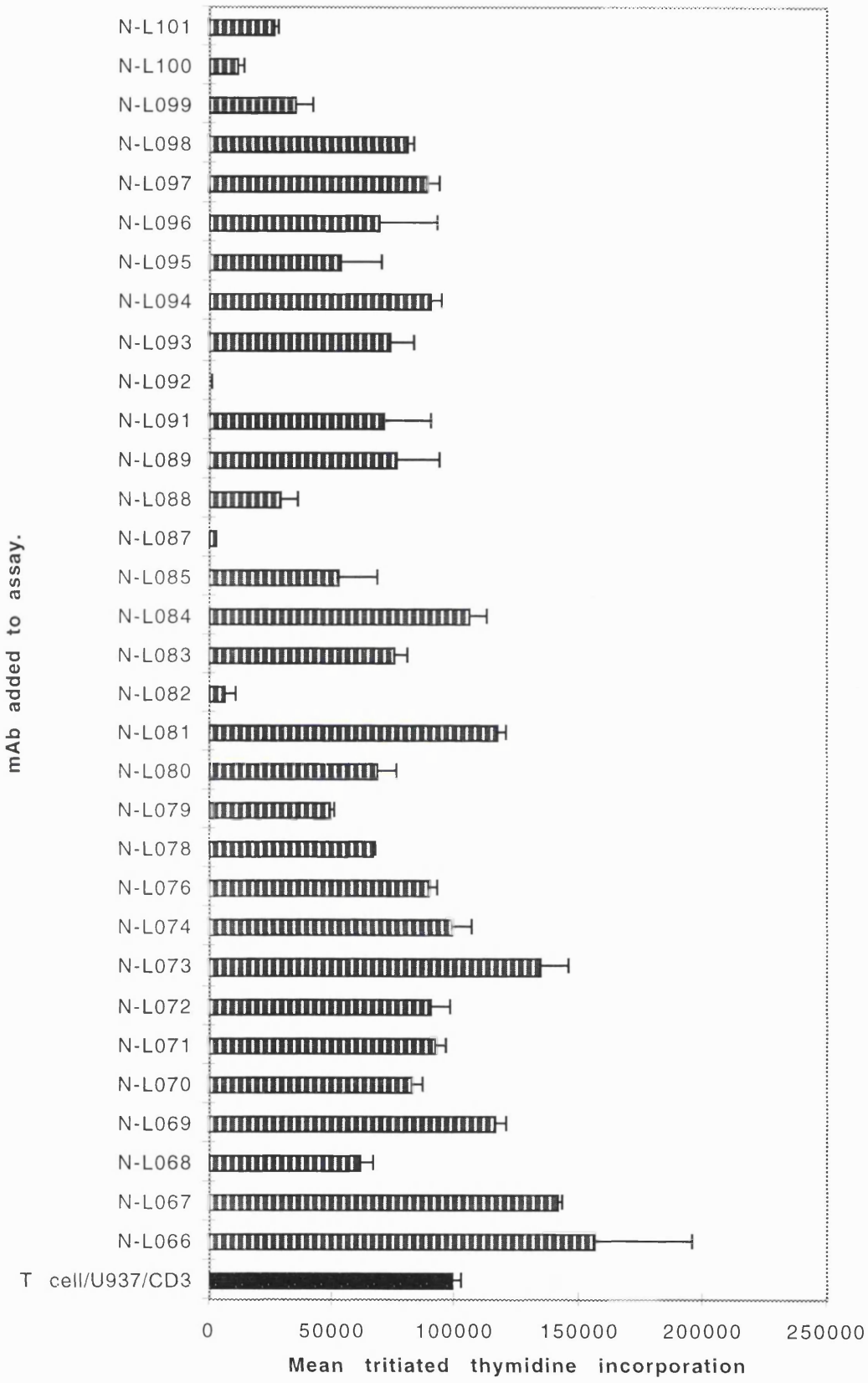

Appendix VI. Part 4.

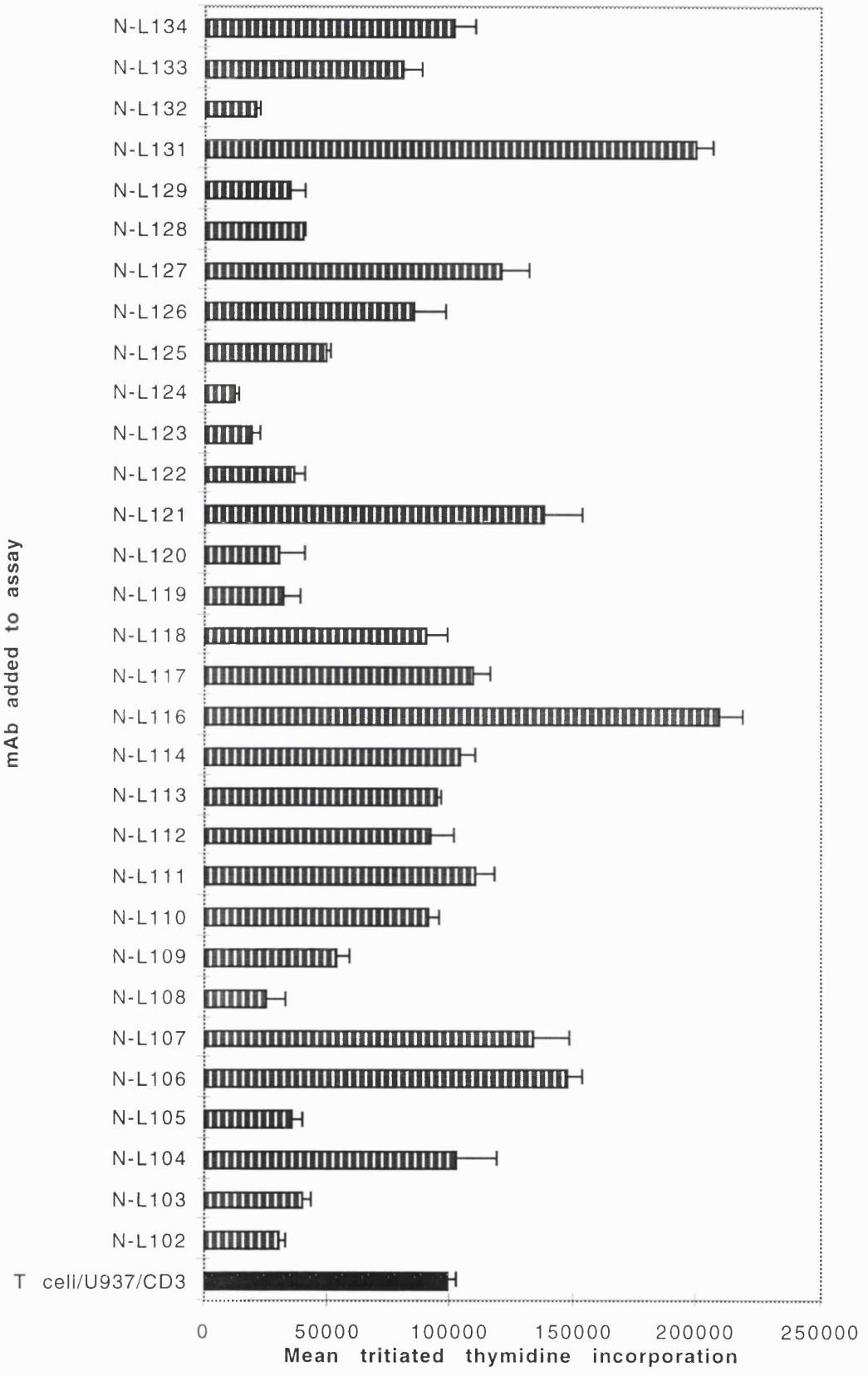

Appendix VI. Part 5.

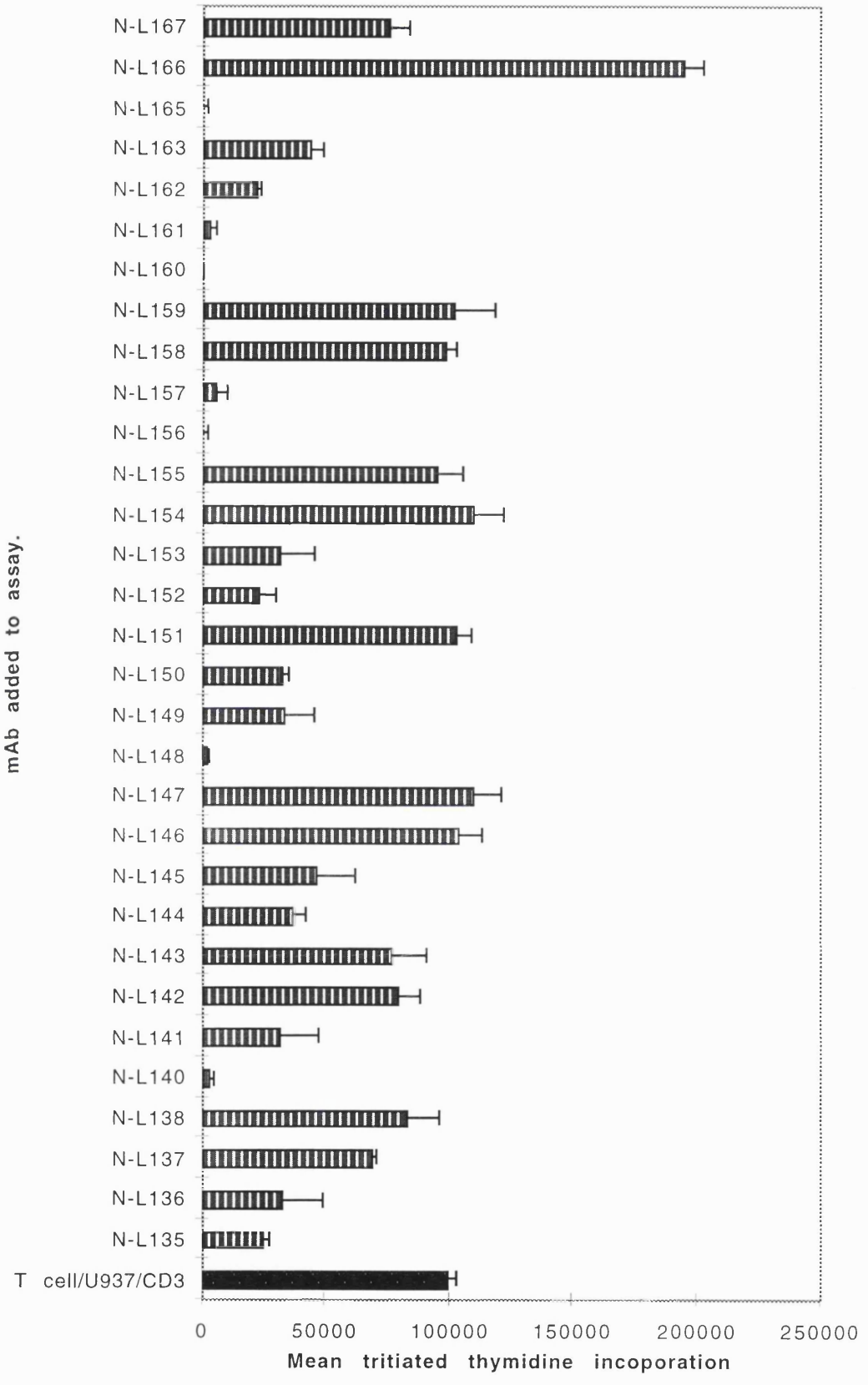

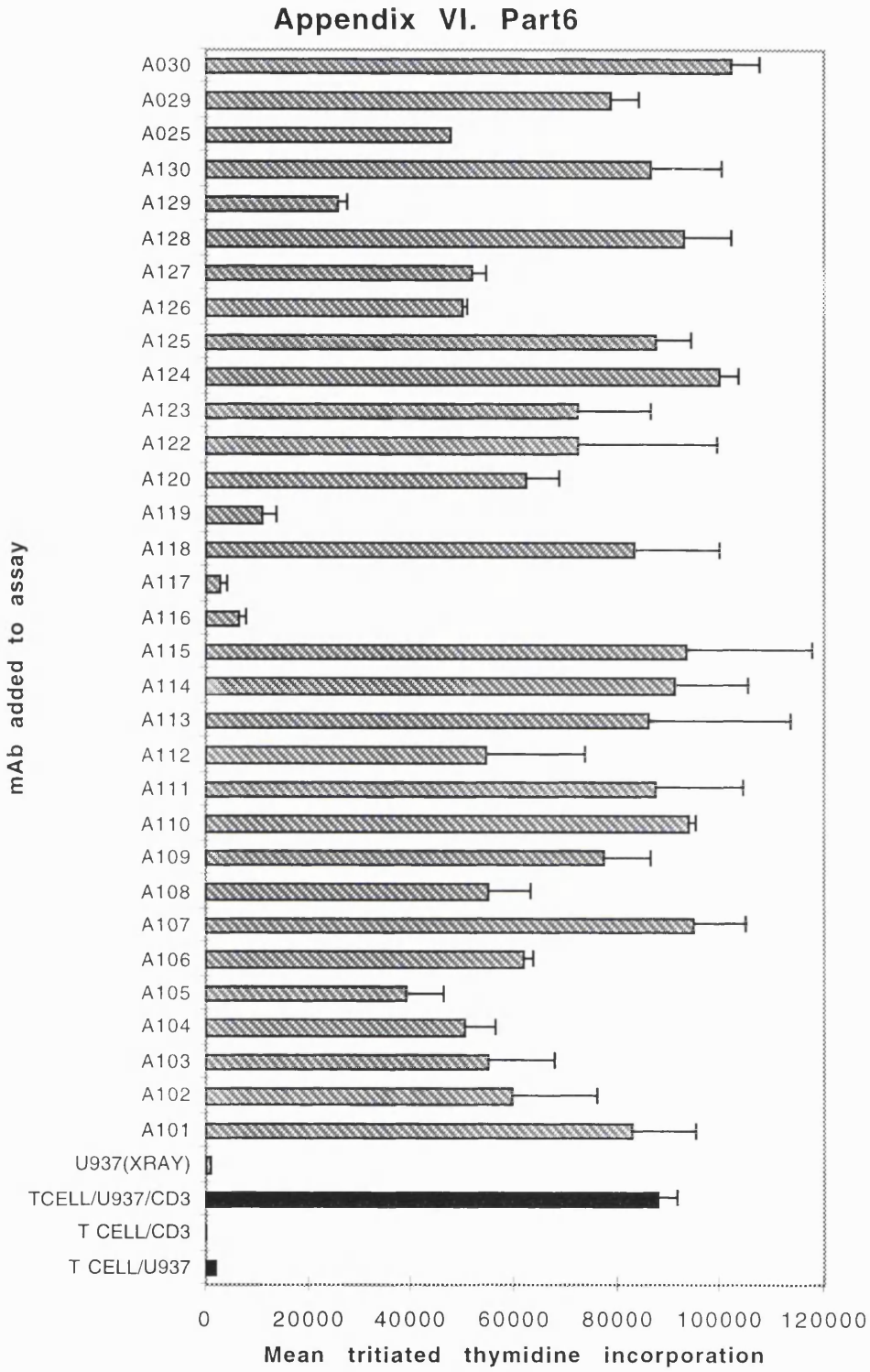

Appendix VI. Initial screen of mAbs from the 6th HLDA for effects on the U937/CD3 T-cell proliferation assay.
Assays were set up with $2x10^5$ purified tonsillar T cells, 10^4 irradiated U937 cells, and CD3 mAb (0.1μg/ml), then mAbs from the non-lineage panel (parts 1-5), and from the adhesion panel (part 6) added. In all parts the bars shown in black are the control values for T cell proliferation in the absence of any test mAb. The mAbs concentration used were suggested by the respective 6th HLDA co-ordinators. T cell proliferation was assessed by ^3H thymidine incorporation between 48 and 64 hours of culture. The values shown are the mean ^3H thymidine incorporation of triplicate wells +/- SD from one experiment.

Appendix VII

mAbs that were >70% inhibitory of T-cell proliferation on two separate occasions.

Code	Specificity	mAb Name	% Inhibition	Preliminary assay
A 116	CD18	BL5	92	4
A 116	CD18	BL5	94	5
NL 002	CD45	CBE-77	71	1
NL 002	CD45	CBE-77	91	2
NL 012	CD45	4.14	70	1
NL 012	CD45	4.14	75	2
NL 102	CD45	ICO-46	70	2
NL 102	CD45	ICO-46	75	3
NL 103	CD45	IMMU19.2	60	2
NL 103	CD45	IMMU19.2	80	3
NL 123	CD45	7E.12	81	2
NL 123	CD45	7E.12	84	3
NL 129	CD45	CF10/H5	70	2
NL 129	CD45	CF10/H5	64	3
NL 165	CD45	ML2	99	2
NL 165	CD45	ML2	70	3
NL 005	CD45RA	DBB-42	65	1
NL 005	CD45RA	DBB-42	80	2
NL 088	CD45RB	WM76	75	2
NL 088	CD45RB	WM76	87	3
NL 162	CD45RB	MT3	79	2
NL 162	CD45RB	MT3	65	3
NL 011	CD45RO	A6	68	1
NL 011	CD45RO	A6	75	2
NL 040	CD53	202-24B	91	1
NL 040	CD53	202-24B	81	2
NL 132	CD53	AC119	80	2
NL 132	CD53	AC119	63	3
NL 060	CD55	JS 11	98	1
NL 060	CD55	JS 11	95	2
NL 060	CD55	JS 11	75	3
NL 017	CD98	MEM 108	72	1
NL 017	CD98	MEM 108	89	2

Code	Specificity	mAb Name	% Inhibition	Preliminary assay
NL 042	CD98	J1-G3B	98	1
NL 042	CD98	J1-G3B	98	2
NL 044	CD98	J3-E1B	90	1
NL 044	CD98	J3-E1B	78	2
NL 124	CD98	CAF7	90	2
NL 124	CD98	CAF7	91	3
NL 140	CD98	IPO-T10	98	2
NL 140	CD98	IPO-T10	85	3
NL 148	CD98	BU89	99	2
NL 148	CD98	BU89	72	3
A 117	CD98	JI-G3B	97	4
A 117	CD98	JI-G3B	96	5
A 119	CD98	J3-E1B	88	4
A 119	CD98	J3-E1B	78	5
NL 156	CDw108	MEM-150	99	2
NL 156	CDw108	MEM-150	92	3
NL 082	CD147	UM-8D6	94	2
NL 082	CD147	UM-8D6	100	3
NL 108	CD147	HI 197	75	2
NL 108	CD147	HI 197	100	3
NL 020	Unknown	MEM 135	99	1
NL 020	Unknown	MEM 135	90	2
NL 087	Unknown	WM78	98	2
NL 087	Unknown	WM78	90	3
NL 092	Unknown	RmCB	99	2
NL 092	Unknown	RmCB	99	3
NL105	Unknown	K108	65	2
NL105	Unknown	K108	93	3

Appendix VII. mAbs that consistently inhibited T-cell proliferation.
mAbs that consistently inhibited T-cell proliferation by ~70%, over two or more assays are shown (see section 2.19.). The level of inhibition in the initial screens is shown as the mean percentage inhibition of T-cell proliferation, when test mAb was added to the assay compared to the proliferation in the absence of test mAb.

Appendix VIII

mAbs selected for further study in the U937-CD3 T-cell proliferation assay.

Specificity	mAb Name	Isotype	Species	Originator
CD45	CBE-77	G3	Mouse	Delsol G.
CD45	4.14	G1	Mouse	Aversa G.
CD45	ICO.46	G2b	Mouse	Baryshnikov A.J.
CD45	7E.12	G1	Mouse	Taskov H.
CD45	1.22	G1	Mouse	Aversa G.
CD45	IMMU19.2	G1k	Mouse	van Agthoven A.J.
CD45	CLBT200.1	G1	Mouse	Connelly M.
CD45	CF10H5	G1	Mouse	Hadam M.R.
CD45	ML2	G1	Mouse	Poppema S.
CD45 RA	DBB-42	G1	Mouse	Delsol G.
CD45 RA	BIRMA 12	G1	Mouse	McDonald D.
CD45 RA	LT45-M5	G1	Mouse	Filatov A.V.
CD45 RA	HI115	G1	Mouse	Shen D.C.
CD45 RA	OTH74D4	G1	Mouse	Hadam M.R.
CD45 RB	WM76	G1	Mouse	Henniker A.J.
CD45 RB	MT3	G1	Mouse	Poppema S.
CD45 RB	MT4	G1	Mouse	Poppema S.
CD45 RO	A6	G1	Mouse	Aversa G.
CD53	WM65	G1	Mouse	Henniker A.J.
CD53	161-2	G2a	Mouse	Vilella R.
CD53	202-24B	G1	Mouse	Vilella R.
CD53	AC119	G1k	Mouse	Buck D.W.
CD55	JS11	G	Mouse	Bensussan A.
CD55	F4-29D9	G1	Mouse	George F.
CD98	BK 19.9	G1	Mouse	van Agthoven A.J.
CD98	MEM 108	G1	Mouse	Horejsi V.
CD98	CAF 7	G1	Mouse	Taskov H.
CD98	2E12	G	Mouse	Stockbauer P.
CD98	J1-G3B	G1	Mouse	Skubitz K.M.
CD98	J1-E1B	G1	Mouse	Skubitz K.M.
CD98	IPO T10	M	Mouse	Gluzman D.F.

Specificity	mAb Name	Isotype	Species	Originator
CD98	BU53	G2a	Mouse	Hardie D.L.
CD98	BU89	G1	Mouse	Hardie D.L.
CDw108	MEM 150	M	Mouse	Horejsi V.
CD147	HI 197	G1	Mouse	Shen D.C.
CD147	HIM6	G1	Mouse	Shen D.C.
CD147	UM 8D6	G3	Mouse	Fox D.A.
CD147	H84	G2b	Mouse	Sagawa K.
Unknown	MEM 135	G1	Mouse	Horejsi V.
Unknown	WM78	G1	Mouse	Henniker A.J.
Unknown	RmCB	G1	Mouse	Finberg R.W.
Unknown	K108	M	Mouse	Kunlong B.

Appendix VIII. mAbs selected for further studies.
Antibodies that were found to be inhibitory in the initial studies along with mAbs from the panel of the same specificity were selected for further studies.

Appendix IX. Abbreviations.

αB5A	antisense RXRα-U937-derived clone
αG2S	sense RXRα-U937-derived clone
6th HLDA	6th Human Leukocyte Differentiation Workshop
A-SMase	acidic sphingomyelinases
ADCC	antibody dependent cellular cytotoxicity
AF-1.	activation function-1
AF-2.	activation function-2
Ag	antigen
AIF	apoptosis inducing factor
APC	antigen presenting cell
APL	acute promyelocytic leukaemias
BCR	B-cell receptor
BFU-E	burst forming unit-erythroid
bHLH	basic helix loop helix
BSA	bovine serum insulin
C/EBP	CCAAT enhancer-binding protein
cdk	cyclin dependent kinases
cDNA	complementary DNA
CM	RPMI 1640 complete medium
CR	complement receptor
CRABP	cellular retinoic acid binding proteins
CRBP	cellular retinol binding protein
CTE	carboxy terminal extension
Cyt c	cytochrome c
D	aspartic acid
DAG	diacylglycerol
DBD	DNA binding domain
DHCC	1,25-dihydroxycholecalciferol
DRN	direct repeat of consensus half sites separated by N base pairs

E	glutamic acid
ECL	enhanced chemiluminescence
ECM	extracellular matrix
EcR	ecdysone receptor
EGF receptor	extracellular growth factor receptor
ER	oestrogen receptor
ERK	extracellular signal regulated protein kinase
FACS	fluorescence activated cell sorting
FADD	Fas-associated death domain
FcγR	Fc-γ receptor
FcεR	Fc-ε receptor
FGF receptor	fibroblast growth factor receptor
FXR	farsenoid X activated receptor
GAP	GTPase-activating proteins
GEF	guanine nucleotide exchange factors
GEMM-CFU	granulocyte-erythrocyte-megakaryocyte-macrophage colony forming unit
GM-CFU	granulocyte-macrophage colony forming unit
GM-CSF	granulocyte-macrophage colony stimulating factor
GPI	glycosylphosphatidylinositol
GR	glucocorticoid receptor
GST-SH2	glutathione-SH2 domain fusion protein
HAT	histone acetyltransferase
HBSS	Hanks buffered saline solution
hMTIIa	human metallothionein IIa
ICAM	intracellular adhesion molecule
ICE-like	interleukin 1β-converting enzyme like
IFN	interferon
Ig	immunolglobulin
IgG	immunoglobulin G
IL-	interleukin

IP	immunoprecipitation
IP3	inositol triphosphate
IRF-1	interferon regulatory factor-1 (
ITAM	immunoreceptor tyrosine-based activation motifs
Jnk	c-Jun N-terminal kinase
kD	kilodalton
L	leucine
LBD	ligand binding domain
LFA-	leukocyte functional antigen-
LPS	lipo-polysaccheride
M-CFU	macrophage colony forming unit
M-CSF	macrophage colony stimulating factor
mAb	monoclonal antibody
MAPK	mitogen activated protein kinase
MEK	MAPK/ERK kinase
MEKK	MAPK/ERK kinase kinase
MEP	empty vector U937-derived clone
MFI	mean fluorescence intensity
MHC	major histocompatability complex
MNGC	multi-nucleated giant cells (
MTP	mitochondrial transmembrane potential
N	Asparagine
N-CoR	nuclear receptor co-repressors
N-SMase	neutral sphingomyelinases
NGF receptor	nerve growth factor receptor
NK-cells	natural killer-cells
NO	nitric oxide
NRS	normal rabbit serum
op-SRBC	opsonised-sheep red blood cell
P	proline
p-Tyr	phosphotyrosine

PAK	p21 activated protein kinase
PBDC	peripheral blood dendritic cell
PBS	phosphate buffered saline
PDGF receptor	platelet derived growth factor receptor
PH	pleckstrin homology domain
PI3-K	phosphatidylinositol 3-kinase
PKC-	protein kinase C
PLC-γ	phospholipase C-γ
PLC-D	phospholipase D
PMA	phorbol 12-myristate 13-acetate
POD	PML oncogenic domains
PPAR	peroxisome proliferator activated factor receptor
PTB	p-Tyr-binding domain
PtdIns	phosphatidylinositol
PTPase	protein tyrosine phosphatase
RA	retinoic acid
RAR	retinoic acid receptor
RE	response element (eg. RARE)
ROS	reactive oxygen species
RXR	retinoid X receptor
SD	standard deviation
SDS	sodium dodecyl sulphate
SH2	Src-homology 2 domain
SH3	Src-homology 3 domain
SM	sphingomyelin
SMRT	silencing mediator for RAR and TR
SPP	sphingosine-1-phosphate
STAT	signal transducers and activator of transcription
TAK	TGF-β-activated kinase
TAO	thousand and one amino acid kinase
TCR	T-cell receptor

TGF	tissue growth factor
TNFα	tumour necrosis factor-α
TR	thyroid hormone receptor
TRADD	TNF receptor-associated death domain
VAD	vitamin A defiency
VDR	vitamin D receptor
Y	tyrosine
ZAP-70	ζ activated protein-70

Appendix X. Solutions.

10x PBS

1.3M NaCl, 70mM Na_2HPO_4, 30mM KH_2PO_4 pH to 7.4

1x Electrode running buffer

Tris, Glycine, SDS pH to 8.3

1x Transfer Buffer

Tris, Glycine, 20% Methanol

1% NP40 lysis buffer

1% (v/v) NP40 lysis buffer, comprising 150mM NaCl, 1% NP40, 50mM Tris-HCl pH8.0, 1mM sodium orthovanadate, 2mM hydrogen peroxide, 1mM PMSF, 10μg/ml Aprotinin

1% Triton X-100 lysis buffer

50mM Hepes pH 7.5, 150mM NaCl, 10% (v/v) glycerol, 1% (v/v) Triton X-100, 1.5mM magnesium chloride, 1mM EGTA, 100mM sodium fluoride, 10mM sodium pyrophosphate, 1mM sodium orthovanadate, 1mM PMSF, 1mM benzamidine, 10μg/ml Aprotinin

2x SDS denaturing loading buffer

2% (w/v) SDS lysis buffer, comprising, 50mM Tris pH 6.8, 20% (v/v) glycerol, 10% (w/v) SDS, 10% (v/v) β-mercaptoethanol, 0.05% (w/v) bromophenol blue

Immunoblot blocking solution

PBS containing 3% (w/v) BSA

Immunoblot blocking/washing solution

PBS containing 3% (w/v) BSA and 0.1% (v/v) Tween 20

Immunoblot washing solution

PBS containing 0.1% (v/v) Tween 20.

Immunoblot stripping solution

62.5mM Tris-HCl pH 6.7, 2% (w/v) SDS and 0.7% 2-mercaptoethanol

10% SDS-polyacrylamide gels

Make 40ml of Separating Gel from the following constituents

H_2O	15.9ml
30% Acrylamide/bis-acrylamide (Protogel-National Diagnostics)	13.3ml
1.5M Tris-HCL pH8.8	10.0ml
10% SDS	0.4ml
10% Ammonium persulfate (APS)	0.3ml
TEMED	0.03ml

Make 10ml of Stacking Gel from the following constituents

H_2O	6.8ml
30% Acrylamide/bis-acrylamide	1.7ml
1M Tris-HCL pH6.8	1.25ml
10% SDS	0.1ml
10% Ammonium persulfate (APS)	0.05ml
TEMED	0.01ml

Appendix XI. Publications arising from this thesis.

PUBLICATIONS IN REFEREED JOURNALS

Brown T.R.P., **T.J. Stonehouse**, J.S. Branch, P.M. Brickell and D.R. Katz. Stable transfection of U937 cells with sense or antisense RXR-α cDNA suggests a role for RXR-α in the control of monoblastic differentiation induced by retinoic acid and vitamin D. *Experimental Cell Research* 236 (1997) 94-102.

Stonehouse T.J., V.E. Woodhead, P.S. Herridge, H. Ashrafian, M. George, B.M. Chain and D.R. Katz. Molecular characterisation of T-cell co-stimulation by the monoblastoid cell line U937. *Immunology*. in press.

Woodhead V.E., **T.J. Stonehouse,** M.H. Binks, D.A. Fox, A. Gaya, D. Hardie, A.J. Henniker, V. Horejsi, K. Sagawa, K.M. Skubitz, H. Taskov, R.S. Todd III, A. van Agthoven, D.R. Katz and B.M. Chain. Novel molecular mechanisms of T-cell activation induced by dendritic cells. *Submitted.*

PROCEEDINGS FROM MEETINGS.

Stonehouse T.J., P.S. Herridge, B.M. Chain and D.R. Katz. Adhesion structures blind panel functional studies: Role of novel adhesion molecules as co-stimulatory molecules. *Leucocyte Typing VI*, pub Garland, ed Kishimoto T et al, p438 (1997).

Stonehouse T.J., B.M. Chain and D.R. Katz. Non lineage antigens and monoblastoid cell functional studies: Role of non-lineage molecules in co-stimulation. *Leucocyte Typing VI*, pub Garland, ed Kishimoto T et al, p611 (1997).

Stonehouse T.J., J.S. Branch, T.R.P. Brown, P.M. Brickell and D.R. Katz. Myeloid antigens functional studies: Expression and function of myeloid antigens on retinoid X receptor α U937 transfectants. *Leucocyte Typing VI*, pub Garland, ed Kishimoto T et al, p1098 (1997).

References.

Adamczewski, M., Numerof, R. P., Koretzky, G. A., and Kinet, J. P. (1995). Regulation by CD45 of the tyrosine phosphorylation of high affinity IgE receptor beta- and gamma-chains. J-Immunol *154*, 3047-55.

Agarwal, A., Salem, P., and Robbins, K. C. (1993). Involvement of p72syk, a protein-tyrosine kinase, in Fc gamma receptor signaling. J-Biol-Chem *268*, 15900-5.

Aldinucci, D., Gattei, V., Zagonel, V., Improta, S., and Pinto, A. (1997). Effects of PML/RARa gene product on the regulation of members of the ICAM family (CD54, CD102, CD50) in acute promyelocytic leukemia cells. Leukocyte typing VI, 412-414.

Alland, L., Muhle, R., Hou, H., Jr., Potes, J., Chin, L., Schreiber Agus, N., and DePinho, R. A. (1997). Role for N-CoR and histone deacetylase in Sin3-mediated transcriptional repression [see comments]. Nature *387*, 49-55.

Allenby, G., Bocquel, M. T., Saunders, M., Kazmer, S., Speck, J., Rosenberger, M., Lovey, A., Kastner, P., Grippo, J. F., Chambon, P., and et al. (1993). Retinoic acid receptors and retinoid X receptors: interactions with endogenous retinoic acids. Proc-Natl-Acad-Sci-U-S-A *90*, 30-4.

Alric, S., Froeschle, A., Piquemal, D., Carnac, G., and Bonnieu, A. (1997). Functional specificity of the two retinoic acid receptor RAR and RXR families in myogenesis. Oncogene *16*, 273-82.

Altin, J. G., and Sloan, E. K. (1997). The role of CD45 and CD45-associated molecules in T-cell activation. Immunol-Cell-Biol *75*, 430-445.

Amento, E. P., Bhalla, A. K., Kurnick, J. T., Kradin, R. L., Clemens, T. L., Holick, S. A., Holick, M. F., and Krane, S. M. (1984). 1 alpha,25-dihydroxyvitamin D3 induces maturation of the human monocyte cell line U937, and, in association with a factor from human T lymphocytes, augments production of the monokine, mononuclear cell factor. J-Clin-Invest *73*, 731-9.

Andreesen, R., Brugger, W., Scheibenbogen, C., Kreutz, M., Leser, H. G., Rehm, A., and Lohr, G. W. (1990). Surface phenotype analysis of human monocyte to macrophage maturation. J-Leukoc-Biol *47*, 490-7.

Angelisova, P., Hilgert, I., and Horejsi, V. (1994). Association of four antigens of the tetraspans family (CD37, CD53, TAPA-1, and R2/C33) with MHC class II glycoproteins. Immunogenetics *39*, 249-56.

Arnaout, M. A., Todd, R. F. d., Dana, N., Melamed, J., Schlossman, S. F., and Colten, H. R. (1983). Inhibition of phagocytosis of complement C3- or immunoglobulin G-coated particles and of C3bi binding by monoclonal antibodies to a monocyte-granulocyte membrane glycoprotein (Mol). J-Clin-Invest *72*, 171-9.

Asiedu, C., Biggs, J., and Kraft, A. S. (1997). Complex regulation of CDK2 during phorbol ester-induced hematopoietic differentiation. Blood *90*, 3430-7.

August, A., Gibson, S., Kawakami, Y., Kawakami, T., Mills, G. B., and Dupont, B. (1994). CD28 is associated with and induces the immediate tyrosine phosphorylation and activation of the Tec family kinase ITK/EMT in the human Jurkat leukemic T-cell line. Proc-Natl-Acad-Sci-U-S-A *91*, 9347-51.

Ayer, D. E., and Eisenman, R. N. (1993). A switch from Myc:Max to Mad:Max heterocomplexes accompanies monocyte/macrophage differentiation. Genes-Dev *7*, 2110-9.

Azzoni, L., Kamoun, M., Salcedo, T. W., Kanakaraj, P., and Perussia, B. (1992). Stimulation of Fc gamma RIIIA results in phospholipase C-gamma 1 tyrosine phosphorylation and p56lck activation. J-Exp-Med *176*, 1745-50.

Baeuerle, P. A., and Baltimore, D. (1988). IkB: A specific inhibitor of NF-kB transcription factor. Science *242*, 540-546.

Bannister, A. J., and Kouzarides, T. (1996). The CBP co-activator is a histone acetyltransferase. Nature *384*, 641-3.

Barber, E. K., Dasgupta, J. D., Schlossman, S. F., Trevillyan, J. M., and Rudd, C. E. (1989). The CD4 and CD8 antigens are coupled to a protein-tyrosine kinase (p56lck) that phosphorylates the CD3 complex. Proc-Natl-Acad-Sci-U-S-A *86*, 3277-81.

Basu, T., Warne, P. H., and Downward, J. (1994). Role of Shc in the activation of ras in response to epidermal growth factor and nerve growth factor. Oncogene *9*, 3483-3491.

Baudino, T. A., Kraichely, D. M., Jefcoat, S. C., Jr., Winchester, S. K., Partridge, N. C., and MacDonald, P. N. (1998). Isolation and characterization of a novel coactivator protein, NCoA-62, involved in vitamin D-mediated transcription. J-Biol-Chem *273*, 16434-41.

Bergman, M., Mustelin, T., Oetken, C., Partanen, J., Flint, N. A., Amrein, K. E., Autero, M., Burn, P., and Alitalo, K. (1992). The human p50csk tyrosine kinase phosphorylates p56lck at Tyr-505 and down regulates its catalytic activity. EMBO-J *11*, 2919-24.

Berkenstam, A., Ruiz, M. M., Barettino, D., Horikoshi, M., and Stunnenberg, H. G. (1992). Cooperativity in transactivation between retinoic acid receptor and TFIID requires an activity analogous to E1A. Cell *69*, 401-12.

Beyers, A. D., Spruyt, L. L., and Williams, A. F. (1992). Molecular associations between the T-lymphocyte antigen receptor complex and the surface antigens CD2, CD4, or CD8 and CD5. Proc-Natl-Acad-Sci-U-S-A *89*, 2945-9.

Black, C. M., Catterall, J. R., and Remington, J. S. (1987). In vivo and in vitro activation of alveolar macrophages by recombinant interferon-gamma. J-Immunol *138*, 491-5.

Blomhoff, R. B. (1994). Vitamin A in health and disease, R. B. Ed., ed. (New York, USA.: Marcel Dekker).

Bodwell, J. E., Webster, J. C., Jewell, C. M., Cidlowski, J. A., Hu, J. M., and Munck, A. (1998). Glucocorticoid receptor phosphorylation: overview, function and cell cycle-dependence. J-Steroid-Biochem-Mol-Biol *65*, 91-9.

Bolen, J. B. (1991). Signal transduction by the SRC family of tyrosine protein kinases in hemopoietic cells. Cell-Growth-Differ *2*, 409-14.

Bolscher, B. G. J. M., van Zwieten, R., Kramer, I. J. M., Weening, R. S., Verhoeven, A. J., and Roos, D. (1989). A phosphoprotein of Mr 47,000, defective in autosomal chronic granulomatous disease, copurifies with one of two soluble components required for NADPH: O2 oxidoreductase activity in human neutrophils. J-Clin-Invest *83*, 757-762.

Booker, G. W., Gout, I., Downing, A. K., Driscoll, P. C., Boyd, J., Waterfield, M. D., and Campbell, I. D. (1993). Solution structure and ligand-binding site of the SH3 domain of the p85 alpha subunit of phosphatidylinositol 3-kinase. Cell *73*, 813-22.

Bosca, L., and Lazo, P. A. (1994). Induction of nitric oxide release by MRC OX-44 (anti-CD53) through a protein kinase C-dependent pathway in rat macrophages. J-Exp-Med *179*, 1119-26.

Bossy Wetzel, E., Bakiri, L., and Yaniv, M. (1997). Induction of apoptosis by the transcription factor c-Jun. EMBO-J *16*, 1695-709.

Boumsell, L., Hall, K. T., Freeman, G. J., and Bensussan, A. (1997). CD101 workshop panel report. Leukocyte typing VI, 1033-1034.

Bourette, R. P., Myles, G. M., Choi, J. L., and Rohrschneider, L. R. (1997). Sequential activation of phoshatidylinositol 3-kinase and phospholipase C-gamma2 by the M-CSF receptor is necessary for differentiation signaling. EMBO-J *16*, 5880-93.

Bourguet, W., Ruff, M., Chambon, P., Gronemeyer, H., and Moras, D. (1995). Crystal structure of the ligand-binding domain of the human nuclear receptor RXR-alpha [see comments]. Nature *375*, 377-82.

Boussiotis, V. A., Freeman, G. J., Gribben, J. G., and Nadler, L. M. (1995). The critical role of CD28 signalling in the prevention of human T-cell anergy. Res-Immunol *146*, 140-9.

Boussiotis, V. A., Freeman, G. J., Gribben, J. G., and Nadler, L. M. (1996). The role of B7-1/B7-2:CD28/CLTA-4 pathways in the prevention of anergy, induction of productive immunity and down-regulation of the immune response. Immunol Rev *153*, 5-26.

Boussiotis, V. A., Gribben, J. G., Freeman, G. J., and Nadler, L. M. (1994). Blockade of the CD28 co-stimulatory pathway: a means to induce tolerance. Curr-Opin-Immunol *6*, 797-807.

Boylan, J. F., and Gudas, L. J. (1991). Overexpression of the cellular retinoic acid binding protein-I (CRABP-I) results in a reduction in differentiation-specific gene expression in F9 teratocarcinoma cells. J-Cell-Biol *112*, 965-79.

Brent, G. A., Williams, G. R., Harney, J. W., Forman, B. M., Samuels, H. H., Moore, D. D., and Larsen, P. R. (1992). Capacity for cooperative binding of thyroid hormone (T3) receptor dimers defines wild type T3 response elements. Mol-Endocrinol *6*, 502-14.

Brooks, D., and Ravetch, J. V. (1994). Fc receptor signaling. Adv Exp Med Biol *365*, 185-95.

Brown, E. J. (1995). Phagocytosis. Bioessays *17*, 109-17.

Brown, E. J., Bohnsack, J. F., and Gresham, H. D. (1988). Mechanism of inhibition of immunoglobulin G-mediated phagocytosis by monoclonal antibodies that recognize the Mac-1 antigen. J-Clin-Invest *81*, 365-75.

Brown, G., Bunce, C. M., Rowlands, D. C., and Williams, G. R. (1994). All-trans retinoic acid and 1 alpha,25-dihydroxyvitamin D3 co-operate to promote differentiation of the human promyeloid leukemia cell line HL60 to monocytes. Leukemia *8*, 806-15.

Brown, G. R., Meek, K., Nishioka, Y., and Thiele, D. L. (1995). CD27-CD27 ligand/CD70 interactions enhance alloantigen-induced proliferation and cytolytic activity in CD8+ T lymphocytes. J-Immunol *154*, 3686-95.

Brown, T. R., Stonehouse, T. J., Branch, J. S., Brickell, P. M., and Katz, D. R. (1997). Stable transfection of U937 cells with sense or antisense RXR-alpha cDNA suggests a role for RXR-alpha in the control of monoblastic differentiation induced by retinoic acid and vitamin D. Exp-Cell-Res *236*, 94-102.

Brown, T. R. P. (1995). The regulation of gene expression during differentiation of the human monoblastic cell line U937. In Dept. of Immunology (London: Unversity of London).

Brunner, T., Mogil, R. J., LaFace, D., Yoo, N. J., Mahboubi, A., Echeverri, F., Martin, S. J., Force, W. R., Lynch, D. H., Ware, C. F., and et al. (1995). Cell-autonomous Fas (CD95)/Fas-ligand interaction mediates activation-induced apoptosis in T-cell hybridomas [see comments]. Nature *373*, 441-4.

Buday, L., and Downward, J. (1993). Epidermal growth factor regulates p21ras through the formation of a complex of receptor, Grb2 adapter protein, and Sos nucleotide exchange factor. Cell *73*, 611-20.

Buss, J. E., Kamps, M. P., Gould, K., and Sefton, B. M. (1986). The absence of myristic acid decreases membrane binding of p60src but does not affect tyrosine protein kinase activity. J-Virol *58*, 468-74.

Butterfield, L., Storey, B., Maas, L., and Heasley, L. E. (1997). c-Jun NH2-terminal kinase regulation of the apoptotic response of small cell lung cancer cells to ultraviolet radiation. J-Biol-Chem *272*, 10110-6.

Byrne, J. A., Butler, J. L., and Cooper, M. D. (1988). Differential activation requirements for virgin and memory T cells. J-Immunol *141*, 3249-57.

Cao, X., Teitelbaum, S. L., Zhu, H. J., Zhang, L., Feng, X., and Ross, F. P. (1996). Competition for a unique response element mediates retinoic acid inhibition of vitamin D3-stimulated transcription. J-Biol-Chem *271*, 20650-4.

Carlberg, C., Bendik, I., Wyss, A., Meier, E., Sturzenbecker, L. J., Grippo, J. F., and Hunziker, W. (1993). Two nuclear signalling pathways for vitamin D. Nature *361*, 657-60.

Carmo, A. M., Mason, D. W., and Beyers, A. D. (1993). Physical association of the cytoplasmic domain of CD2 with the tyrosine kinases p56lck and p59fyn. Eur-J-Immunol *23*, 2196-201.

Carmo, A. M., and Wright, M. D. (1995). Association of the transmembrane 4 superfamily molecule CD53 with a tyrosine phosphatase activity. Eur-J-Immunol *25*, 2090-5.

Carpenter, C. L., and Cantley, L. C. (1996). Phosphoinositide kinases. Curr-Opin-Cell-Biol *8*, 153-8.

Castano, E., Chen, C. W., Vorojeikina, D. P., and Notides, A. C. (1998). The role of phosphorylation in human estrogen receptor function. J-Steroid-Biochem-Mol-Biol *65*, 101-10.

Cavailles, V., Dauvois, S., L'Horset, F., Lopez, G., Hoare, S., Kushner, P. J., and Parker, M. G. (1995). Nuclear factor RIP140 modulates transcriptional activation by the estrogen receptor. EMBO-J *14*, 3741-51.

Cerny, J., Stockinger, H., and Horejsi, V. (1996). Noncovalent associations of T lymphocyte surface proteins. Eur-J-Immunol *26*, 2335-43.

Chen, H., Lin, R. J., Schiltz, R. L., Chakravarti, D., Nash, A., Nagy, L., Privalsky, M. L., Nakatani, Y., and Evans, R. M. (1997). Nuclear receptor coactivator ACTR is a novel histone acetyltransferase and forms a multimeric activation complex with P/CAF and CBP/p300. Cell *90*, 569-80.

Chen, J. D., and Evans, R. M. (1995). A transcriptional co-repressor that interacts with nuclear hormone receptors [see comments]. Nature *377*, 454-7.

Chen, J. Y., Clifford, J., Zusi, C., Starrett, J., Tortolani, D., Ostrowski, J., Reczek, P. R., Chambon, P., and Gronemeyer, H. (1996). Two distinct actions of retinoid-receptor ligands. Nature *382*, 819-22.

Chen, L. (1997). Manipulation of T cell response to tumors by targeting on costimulatory pathway. Leukemia *3*, 567-9.

Chiocca, E. A., Davies, P. J., and Stein, J. P. (1989). Regulation of tissue transglutaminase gene expression as a molecular model for retinoid effects on proliferation and differentiation. J-Cell-Biochem *39*, 293-304.

Chow, L. M. L., Fournel, M., Davidson, D., and Veilette, A. (1993). Negative regulation of T-cell receptor signalling by tyrosine protein kinase p50csk. Nature *365*, 156-160.

Collins, S. J., Robertson, K. A., and Mueller, L. (1990). Retinoic acid-induced granulocytic differentiation of HL-60 myeloid leukemia cells is mediated directly through the retinoic acid receptor (RAR-alpha). Mol-Cell-Biol *10*, 2154-63.

Conjeaud, H., Rubinstein, E., and Horejsi, V. (1997). CD53 workshop panel report. Leukocyte typing VI, 517-519.

Cooper, J. A., and Howell, B. (1993). The when and how of Src regulation. Cell *73*, 1051-4.

Costello, R., Cerdan, C., Pavon, C., Brailly, H., Hurpin, C., Mawas, C., and Olive, D. (1993). The CD2 and CD28 adhesion molecules induce long-term autocrine proliferation of CD4+ T cells. Eur-J-Immunol *23*, 608-13.

Cox, D., Chang, P., Kurosaki, T., and Greenberg, S. (1996). Syk tyrosine kinase is required for immunoreceptor tyrosine activation motif-dependent actin assembly. J-Biol-Chem *271*, 16597-602.

Damle, N. K., Klussman, K., and Aruffo, A. (1992a). Intercellular adhesion molecule-2, a second counter-receptor for CD11a/CD18 (leukocyte function-associated antigen-1), provides a costimulatory signal for T-cell receptor-initiated activation of human T cells. J-Immunol *148*, 665-71.

Damle, N. K., Klussman, K., Linsley, P. S., and Aruffo, A. (1992b). Differential costimulatory effects of adhesion molecules B7, ICAM-1, LFA-3, and VCAM-1 on resting and antigen-primed CD4+ T lymphocytes. J-Immunol *148*, 1985-92.

Darby, C., Geahlen, R. L., and Schreiber, A. D. (1994). Stimulation of macrophage Fc gamma RIIIA activates the receptor-associated protein tyrosine kinase Syk and induces phosphorylation of multiple proteins including p95Vav and p62/GAP-associated protein. J-Immunol *152*, 5429-37.

Davis, S. J., and van der Merwe, P. A. (1996). The structure and ligand interactions of CD2: implications for T-cell function. Immunol-Today *17*, 177-87.

Dawson, M. I., Elstner, E., Kizaki, M., Chen, D. L., Pakkala, S., Kerner, B., and Koeffler, H. P. (1994). Myeloid differentiation mediated through retinoic acid receptor/retinoic X receptor (RXR) not RXR/RXR pathway. Blood *84*, 446-52.

de Fougerolles, A. R., and Springer, T. A. (1992). Intercellular adhesion molecule 3, a third adhesion counter-receptor for lymphocyte function-associated molecule 1 on resting lymphocytes. J-Exp-Med *175*, 185-90.

de Fougerolles, A. R., Stacker, S. A., Schwarting, R., and Springer, T. A. (1991). Characterization of ICAM-2 and evidence for a third counter-receptor for LFA-1. J-Exp-Med *174*, 253-67.

De Haas, M., Huijboom, K., and Von Dem Borne, A. E. G. (1997). CD63 workshop panel report. Leukocyte typing VI, 664-667.

De Haas, M., and Von Dem Borne, A. E. G. (1997). CD36 workshop report. Leukocyte typing VI, 636-637.

De Titto, E. H., Catterall, J. R., and Remington, J. S. (1986). Activity of recombinant tumor necrosis factor on Toxoplasma Gondii and Trypanosoma Cruzi. J-Immunol *137*, 1342-1345.

Defacque, H., Commes, T., Sevilla, C., Rochette Egly, C., and Marti, J. (1994). Synergistic differentiation of U937 cells by all-trans retinoic acid and 1 alpha, 25-dihydroxyvitamin D3 is associated with the expression of retinoid X receptor alpha. Biochem-Biophys-Res-Commun *203*, 272-80.

Defacque, H., Sevilla, C., Piquemal, D., Rochette Egly, C., Marti, J., and Commes, T. (1997). Potentiation of VD-induced monocytic leukemia cell differentiation by retinoids involves both RAR and RXR signaling pathways. Leukemia *11*, 221-7.

Devary, Y., Gottlieb, R. A., Smeal, T., and Karin, M. (1992). The mammalian ultraviolet response is triggered by activation of Src tyrosine kinases. Cell *71*, 1081-91.

Diaz, L. A., Jr., Antony, P. A., Endres, J., and Fox, D. A. (1997a). CD98 workshop panel report. Leukocyte typing VI, 531-534.

Diaz, L. A., Jr., Friedman, A. W., He, X., Kuick, R. D., Hanash, S. M., and Fox, D. A. (1997b). Monocyte-dependent regulation of T lymphocyte activation through CD98. Int-Immunol *9*, 1221-31.

DiRenzo, J., Soderstrom, M., Kurokawa, R., Ogliastro, M. H., Ricote, M., Ingrey, S., Horlein, A. J., Rosenfeld, M. G., and Glass, C. K. (1997). Peroxisome proliferator-activated receptors and retinoic acid receptors differentially control the interactions of retinoid-X-receptor heterodimers with ligands, coactivators and corepressors. Mol-Cell-Biol *17*, 2166-2176.

Dolle, P., Fraulob, V., Kastner, P., and Chambon, P. (1994). Developmental expression of murine retinoid X receptor (RXR) genes. Mech-Dev *45*, 91-104.

Dong, S., and Hughes, R. C. (1997). Macrophage surface glycoproteins binding to galectin-3 (Mac-2-antigen). Glycoconj-J *14*, 267-74.

Driscoll, J. E., Seachord, C. L., Lupisella, J. A., Darveau, R. P., and Reczek, P. R. (1996). Ligand-induced conformational changes in the human retinoic acid receptor detected using monoclonal antibodies. J-Biol-Chem *271*, 22969-75.

Dubey, C., Croft, M., and Swain, S. L. (1995). Co-stimulatory requirements of naive CD4+ T-cells. J-Immunol *155*, 45-57.

Dusi, S., and Rossi, F. (1993). Activation of NADPH oxidase of human neutrophils involves the phosphorylation and translocation of cytosolic P67-phox. Biochem-J *296*, 367-375.

Dyck, J. A., Maul, G. G., Miller, W. H., Jr., Chen, J. D., Kakizuka, A., and Evans, R. M. (1994). A novel macromolecular structure is a target of the promyelocyte-retinoic acid receptor oncoprotein. Cell *76*, 333-43.

Edberg, J. C., Lin, C. T., Lau, D., Unkeless, J. C., and Kimberly, R. P. (1995). The Ca2+ dependence of human Fc gamma receptor-initiated phagocytosis. J-Biol-Chem *270*, 22301-7.

Ehlenberger, A. G., and Nussenzweig, V. (1977). The role of membrane receptors for C3b and C3d in phagocytosis. J-Exp-Med *145*, 357-71.

Emoto, Y., Manome, Y., Meinhardt, G., Kisaki, H., Kharbanda, S., Robertson, M., Ghayur, T., Wong, W. W., Kamen, R., Weichselbaum, R., and et al. (1995). Proteolytic activation of protein kinase C delta by an ICE-like protease in apoptotic cells. EMBO-J *14*, 6148-56.

Erpel, T., and Courtneidge, S. A. (1995). Src family protein tyrosine kinases and cellular signal transduction pathways. Curr-Opin-Cell-Biol *7*, 176-82.

Evans, R. M. (1988). The steroid and thyroid hormone receptor superfamily. Science *240*, 889-95.

Faulkner, L., Aruoma, O. I., Brickell, P. M., Davies, M. J., Halliwell, B., Woolf, N., and Katz, D. R. (1993). Effects of the synthetic anti-oxidant, probucol, on the U937 monoblastoid cell line. Atherosclerosis *99*, 1-13.

Fenczik, C. A., Sethi, T., Ramos, J. W., Hughes, P. E., and Ginsberg, M. H. (1997). Complementation of dominant suppression implicates CD98 in integrin activation [see comments]. Nature *390*, 81-5.

Ferguson, S. E., Han, S., Kelsoe, G., and Thompson, C. B. (1996). CD28 is required for germinal center formation. J-Immunol *156*, 4576-81.

Forman, B. M., and Samuels, H. H. (1990). Interactions among a subfamily of nuclear hormone receptors: the regulatory zipper model. Mol-Endocrinol *4*, 1293-301.

Forman, B. M., Umesono, K., Chen, J., and Evans, R. M. (1995). Unique response pathways are established by allosteric interactions among nuclear hormone receptors. Cell *81*, 541-50.

Forsbeck, K., Nilsson, K., Hansson, A., Skoglund, G., and Ingelman Sundberg, M. (1985). Phorbol ester-induced alteration of differentiation and proliferation in human hematopoietic tumor cell lines: relationship to the presence and subcellular distribution of protein kinase C. Cancer-Res *45*, 6194-9.

Fraser, A., and Evan, G. (1996). A license to kill. Cell *85*, 781-4.

Galandrini, R., Palmieri, G., Piccoli, M., Frati, L., and Santoni, A. (1996). CD16-mediated p21ras activation is associated with Shc and p36 tyrosine phosphorylation and their binding with Grb2 in human natural killer cells. J-Exp-Med *183*, 179-86.

Germain, R. N., and Margulies, D. H. (1993). The biochemistry and cell biology of antigen processing and presentation. Annu Rev Immunol *11*, 403-50.

Gessl, A., Willheim, M., Spittler, A., Agis, H., Krugluger, W., and Boltz Nitulescu, G. (1994). Influence of tumour necrosis factor-alpha on the expression of Fc IgG and IgA receptors, and other markers by cultured human blood monocytes and U937 cells. Scand-J-Immunol *39*, 151-6.

Ghazizadeh, S., Bolen, J. B., and Fleit, H. B. (1994). Physical and functional association of Src-related protein tyrosine kinases with Fc gamma RII in monocytic THP-1 cells. J-Biol-Chem *269*, 8878-84.

Ghiotto-Rageneau, M., Battifora, M., Truneh, A., Waterfield, M. D., and Olive, D. (1996). Comparison of CD28-B7.1 and B7.2 functional interaction in resting human T-cells: phosphatidylinositol 3-kinase association to CD28 and cytokine production. Eur-J-Immunol *26*, 34-41.

Giguere, V., Ong, E. S., Segui, P., and Evans, R. M. (1987). Identification of a receptor for the morphogen retinoic acid. Nature *330*, 624-9.

Glass, C. K., Rose, D. W., and Rosenfeld, M. G. (1997). Nuclear receptor coactivators. Curr-Opin-Cell-Biol *9*, 222-32.

Goyert, S. M. (1997a). CD13 workshop panel report. Leukocyte typing VI, 962-963.

Goyert, S. M. (1997b). CDw92 workshop report. Leukocyte typing VI, 1031-1032.

Goyert, S. M. (1997c). CDw93 workshop panel report. Leukocyte typing VI, 1032.

Goyert, S. M., Cohen, L., Gangloff, S. C., Ashmun, R., and Haeffner-Cavaillon, N. (1997d). CD14 workshop panel report. Leukocyte typing VI, 963-965.

Graham, I. L., Anderson, D. C., Holers, V. M., and Brown, E. J. (1994). Complement receptor 3 (CR3, Mac-1, integrin alpha M beta 2, CD11b/CD18) is required for tyrosine phosphorylation of paxillin in adherent and nonadherent neutrophils. J-Cell-Biol *127*, 1139-47.

Green, J. M., Noel, P. J., Sperling, A. I., Walunas, T. L., Gray, G. S., Bluestone, J. A., and Thompson, C. B. (1994). Absence of B7-dependent responses in CD28-deficient mice. Immunity *1*, 501-8.

Greenberg, S., Chang, P., and Silverstein, S. C. (1994). Tyrosine phosphorylation of the gamma subunit of Fc gamma receptors, p72syk, and paxillin during Fc receptor-mediated phagocytosis in macrophages. J-Biol-Chem *269*, 3897-902.

Greenberg, S., el Khoury, J., di Virgilio, F., Kaplan, E. M., and Silverstein, S. C. (1991). Ca(2+)-independent F-actin assembly and disassembly during Fc receptor-mediated phagocytosis in mouse macrophages. J-Cell-Biol *113*, 757-67.

Gresham, H. D., Graham, I. L., Anderson, D. C., and Brown, E. J. (1991). Leukocyte adhesion-deficient neutrophils fail to amplify phagocytic function in response to stimulation. Evidence for CD11b/CD18-dependent and -independent mechanisms of phagocytosis. J-Clin-Invest *88*, 588-97.

Grignani, F., Fagioli, M., Alcalay, M., Longo, L., Pandolfi, P. P., Donti, E., Biondi, A., Lo Coco, F., Grignani, F., and Pelicci, P. G. (1994). Acute promyelocytic leukemia: from genetics to treatment. Blood *83*, 10-25.

Groger, R. K., Morrow, D. M., and Tykocinski, M. L. (1989). Directional antisense and sense cDNA cloning using Epstein-Barr virus episomal expression vectors [published erratum appears in Gene 1989 Nov 30;83(2):395]. Gene *81*, 285-94.

Gronemeyer, H. (1991). Transcription activation by estrogen and progesterone receptors. Annu Rev Genet *25*, 89-123.

Groopman, J. E., and Golde, D. W. (1981). The histiocytic disorders: a pathophysiologic analysis. Ann-Intern-Med *94*, 95-107.

Guinan, E. C., Gribben, J. G., Boussiotis, V. A., Freeman, G. J., and Nadler, L. M. (1994). Pivotal role of the B7:CD28 pathway in transplantation tolerance and tumor immunity. Blood *84*, 3261-82.

Guttinger, M., Gassmann, M., Amrein, K. E., and Burn, P. (1992). CD45 phosphotyrosine phosphatase and p56lck protein tyrosine kinase: a functional complex crucial in T cell signal transduction. Int-Immunol *4*, 1325-30.

Harris, P., and Ralph, P. (1985). Human leukemic models of myelomonocytic development: a review of the HL-60 and U937 cell lines. J-Leukoc-Biol *37*, 407-22.

Harris, P. E., Ralph, P., Litcofsky, P., and Moore, M. A. S. (1985). Distinct activities of Interferon-g, Lymphokine and Cytokine differentiation-inducing factors acting on the human monoblastic leukemia cell line U937. Cancer-Res *45*, 9-13.

Hathcock, K. S., Laszlo, G., Pucillo, C., Linsley, P., and Hodes, R. J. (1994). Comparative analysis of B7-1 and B7-2 costimulatory ligands: expression and function. J-Exp-Med *180*, 631-40.

Hemler, M. E., and Strominger, J. L. (1982). Characterization of antigen recognized by the monoclonal antibody (4F2): different molecular forms on human T and B lymphoblastoid cell lines. J-Immunol *129*, 623-8.

Hewison, M., Barker, S., Brennan, A., Katz, D. R., and O'Riordan, J. L. H. (1989). Modulation of myelomonocytic U937 cells by vitamin D metabloits. Bone-Mineral *5*, 323-333.

Hewison, M., Dabrowski, M., Faulkner, L., Hughson, E., Vadher, S., Rut, A., Brickell, P. M., O'Riordan, J. L., and Katz, D. R. (1994). Transfection of vitamin D receptor cDNA into the monoblastoid cell line U937. The role of vitamin D3 in homotypic macrophage adhesion. J-Immunol *153*, 5709-19.

Hewison, M., Dabrowski, M., Vadher, S., Faulkner, L., Cockerill, F. J., Brickell, P. M., O'Riordan, J. L., and Katz, D. R. (1996). Antisense inhibition of vitamin D receptor expression induces apoptosis in monoblastoid U937 cells. J-Immunol *156*, 4391-400.

Heyman, R. A., Mangelsdorf, D. J., Dyck, J. A., Stein, R. B., Eichele, G., Evans, R. M., and Thaller, C. (1992). 9-cis retinoic acid is a high affinity ligand for the retinoid X receptor. Cell *68*, 397-406.

Higuchi, Y., Kataoka, M., Matsuura, K., and Yamamoto, S. (1997). CD156 (ADAM 8) workshop panel report. Leukocyte typing VI, 1083-1085.

Hintzen, R. Q., Lens, S. M., Lammers, K., Kuiper, H., Beckmann, M. P., and van Lier, R. A. (1995). Engagement of CD27 with its ligand CD70 provides a second signal for T cell activation. J-Immunol *154*, 2612-23.

Hirasawa, N., Scharenberg, A., Yamamura, H., Beaven, M. A., and Kinet, J. P. (1995). A requirement for Syk in the activation of the microtubule-associated protein kinase/phospholipase A2 pathway by Fc epsilon R1 is not shared by a G protein-coupled receptor. J-Biol-Chem *270*, 10960-7.

Hogg, N. (1997). CD11a Workshop panel report. Leukocyte typing VI, 343-345.

Horlein, A. J., Naar, A. M., Heinzel, T., Torchia, J., Gloss, B., Kurokawa, R., Ryan, A., Kamei, Y., Soderstrom, M., Glass, C. K., and et al. (1995). Ligand-independent repression by the thyroid hormone receptor mediated by a nuclear receptor co-repressor [see comments]. Nature *377*, 397-404.

Howe, A., Aplin, A. E., Alahari, S. K., and Juliano, R. L. (1998). Integrin signaling and cell growth control. Curr-Opin-Cell-Biol *10*, 220-31.

Huang, N., vom Baur, E., Garnier, J. M., Lerouge, T., Vonesch, J. L., Lutz, Y., Chambon, P., and Losson, R. (1998). Two distinct nuclear receptor interaction domains in NSD1, a novel SET protein that exhibits characteristics of both corepressors and coactivators. EMBO-J *17*, 3398-412.

Hutchcroft, J. E., and Bierer, B. E. (1996). Signaling through CD28/CTLA-4 family receptors: puzzling participation of phosphatidylinositol-3 kinase. J-Immunol *156*, 4071-4.

Igakura, T., Kadomatsu, K., Taguchi, O., Muramatsu, H., Kaname, T., Miyauchi, T., Yamamura, K., Arimura, K., and Muramatsu, T. (1996). Roles of basigin, a member of the immunoglobulin superfamily, in behavior as to an irritating odor, lymphocyte response, and blood-brain barrier. Biochem-Biophys-Res-Commun *224*, 33-6.

Ijpenberg, A., Jeannin, E., Wahli, W., and Desvergne, B. (1997). Polarity and specific sequence requirements of peroxisome proliferator-activated receptor (PPAR)/retinoid X receptor heterodimer binding to DNA. A functional analysis of the malic enzyme gene PPAR response element. J-Biol-Chem *272*, 20108-17.

Ikewaki, N., Tamauchi, H., and Inoko, H. (1993). Modulation of cell surface antigens and regulation of phagocytic activity mediated by CD11b in the monocyte-like cell line U937 in response to lipopolysaccharide. Tissue-Antigens *42*, 125-32.

Indik, Z., Chien, P., Levinson, A. I., and Schreiber, A. D. (1992). Calcium signalling by the high affinity macrophage Fc gamma receptor requires the cytosolic domain. Immunobiology *185*, 183-92.

Indik, Z., Chien, P., Levinson, A. I., and Schreiber, A. D. (1991a). The high affinity macrophage Fcγ receptor: structural requirements for the binding of IgG-sensitised cells, phagocytosis and signal transduction. Clin-Res *39*, 209A.

Indik, Z., Kelly, C., Chien, P., Levinson, A. I., and Schreiber, A. D. (1991b). Human Fc gamma RII, in the absence of other Fc gamma receptors, mediates a phagocytic signal. J-Clin-Invest *88*, 1766-71.

Indik, Z. K., Park, J. G., Hunter, S., and Schreiber, A. D. (1995). The molecular dissection of Fc gamma receptor mediated phagocytosis. Blood *86*, 4389-99.

Indoh, T., Shirakawa, S., Kubota, T., Yashiki, T., Isogai, E., and Fujii, N. (1996). Augmentation of interferon production after cell-differentiation of U937 cells by TPA. Microbiol Immunol *40*, 675-9.

Isakov, N. (1997). Immunoreceptor tyrosine-based activation motif (ITAM), a unique module linking antigen and Fc receptors to their signaling cascades. J-Leukoc-Biol *61*, 6-16.

Ishihara, K., Okuyama, Y., Lee, B. O. K., Itoh, M., Nishikawa, K., and Hirano, T. (1997). CD157 (BST-1) workshop panel report. Leukocyte typing VI, 1086-1089.

Iwashima, M., Irving, B. A., van Oers, N. S., Chan, A. C., and Weiss, A. (1994). Sequential interactions of the TCR with two distinct cytoplasmic tyrosine kinases. Science *263*, 1136-9.

Jabril Cuenod, B., Zhang, C., Scharenberg, A. M., Paolini, R., Numerof, R., Beaven, M. A., and Kinet, J. P. (1996). Syk-dependent phosphorylation of Shc. A potential link between FcepsilonRI and the Ras/mitogen-activated protein kinase signaling pathway through SOS and Grb2. J-Biol-Chem *271*, 16268-72.

James, S. Y., Williams, M. A., Kelsey, S. M., Newland, A. C., and Colston, K. W. (1997a). Interaction of vitamin D derivatives and granulocyte-macrophage colony-stimulating factor in leukaemic cell differentiation. Leukemia *11*, 1017-25.

James, S. Y., Williams, M. A., Kelsey, S. M., Newland, A. C., and Colston, K. W. (1997b). The role of vitamin D derivatives and retinoids in the differentiation of human leukaemia cells. Biochem-Pharmacol *54*, 625-34.

Jenkins, M. K., and Johnson, J. G. (1993). Molecules involved in T-cell costimulation. Curr-Opin-Immunol *5*, 361-7.

Jenkins, M. K., Mueller, D., Schwartz, R. H., Carding, S., Bottomley, K., Stadecker, M. J., Urdahl, K. B., and Norton, S. D. (1991a). Induction and maintenance of anergy in mature T cells. Adv Exp Med Biol *292*, 167-76.

Jenkins, M. K., Taylor, P. S., Norton, S. D., and Urdahl, K. B. (1991b). CD28 delivers a costimulatory signal involved in antigen-specific IL-2 production by human T cells. J-Immunol *147*, 2461-6.

Johnson, J. G., and Jenkins, M. K. (1993). Accessory cell-derived signals required for T cell activation. Immunol Res *12*, 48-64.

Johnson, J. G., and Jenkins, M. K. (1994). Monocytes provide a novel costimulatory signal to T cells that is not mediated by the CD28/B7 interaction. J-Immunol *152*, 429-37.

Johnston, R. B., Jr. (1988). Current concepts: immunology. Monocytes and macrophages. N-Engl-J-Med *318*, 747-52.

Jones, S. L., and Brown, E. J. (1996). FcgammaRII-mediated adhesion and phagocytosis induce L-plastin phosphorylation in human neutrophils. J-Biol-Chem *271*, 14623-30.

Kakizuka, A., Miller, W. H., Jr., Umesono, K., Warrell, R. P., Jr., Frankel, S. R., Murty, V. V., Dmitrovsky, E., and Evans, R. M. (1991). Chromosomal translocation t(15;17) in human acute promyelocytic leukemia fuses RAR alpha with a novel putative transcription factor, PML. Cell *66*, 663-74.

Kalkhoven, E., Valentine, J. E., Heery, D. M., and Parker, M. G. (1998). Isoforms of steroid receptor co-activator 1 differ in their ablity to potentiate transcription by the oestrogen receptor. EMBO-J *17*, 232-243.

Kamps, M. P., Buss, J. E., and Sefton, B. M. (1985). Mutation of NH2-terminal glycine of p60src prevents both myristoylation and morphological transformation. Proc-Natl-Acad-Sci-U-S-A *82*, 4625-8.

Kanai, Y., Segawa, H., Miyamoto, K., Uchino, H., Takeda, E., and Endou, H. (1998). Expression cloning and characterisation of a transporter for large neutral amino acids activated by the heavy chain of 4F2 antigen (CD98). J-Biol-Chem *273*, 23629-23632.

Kannagi, R. (1997). CD15 workshop pane lreport. Leukocyte typing VI, 348-355.

Kasinrerk, W., Fiebiger, E., Stefanova, I., Baumruker, T., Knapp, W., and Stockinger, H. (1992). Human leukocyte activation antigen M6, a member of the Ig superfamily, is the species homologue of rat OX-47, mouse basigin, and chicken HT7 molecule. J-Immunol *149*, 847-54.

Kastner, P., Grondona, J. M., Mark, M., Gansmuller, A., LeMeur, M., Decimo, D., Vonesch, J. L., Dolle, P., and Chambon, P. (1994). Genetic analysis of RXR alpha

developmental function: convergence of RXR and RAR signaling pathways in heart and eye morphogenesis. Cell *78*, 987-1003.

Katz, R. W., Subauste, J. S., and Koenig, R. J. (1995). The interplay of half-site sequence and spacing on the activity of direct repeat thyroid hormone response elements. J-Biol-Chem *270*, 5238-42.

Kiener, P. A., and Mittler, R. S. (1989). CD45-protein tyrosine phosphatase cross-linking inhibits T cell receptor CD3-mediated activation in human T cells. J-Immunol *143*, 23-8.

King, P. D., Batchelor, A. H., Lawlor, P., and Katz, D. R. (1990). The role of CD44, CD45, CD45RO, CD46 and CD55 as potential anti-adhesion molecules involved in the binding of human tonsillar T cells to phorbol 12-myristate 13-acetate-differentiated U-937 cells. Eur-J-Immunol *20*, 363-8.

Kluck, R. M., Bossy Wetzel, E., Green, D. R., and Newmeyer, D. D. (1997). The release of cytochrome c from mitochondria: a primary site for Bcl-2 regulation of apoptosis [see comments]. Science *275*, 1132-6.

Kniep, B., Peter-Katalinic, J., Muthing, J., Majdic, O., Pickl, W. F., and Knapp, W. (1997). CD65/CD65s workshop panel report. Leukocyte typing VI, 990-992.

Knudsen, P. J., Dinarello, C. A., and Strom, T. B. (1986). Purification and characterization of a unique human interleukin 1 from the tumor cell line U937. J-Immunol *136*, 3311-6.

Kobata, T., Agematsu, K., Kameoka, J., Schlossman, S. F., and Morimoto, C. (1994). CD27 is a signal-transducing molecule involved in CD45RA+ naive T cell costimulation. J-Immunol *153*, 5422-32.

Kochar, D. M. (1973). Limb development in mouse embryos. I. Analysis of teratogenic effects of retinoic acid. Teratology *7*, 289-295.

Kolanus, W., Nagel, W., Schiller, B., Zeitlmann, L., Godar, S., Stockinger, H., and Seed, B. (1996). Alpha L beta 2 integrin/LFA-1 binding to ICAM-1 induced by cytohesin-1, a cytoplasmic regulatory molecule. Cell *86*, 233-42.

Kolesnick, R. N., and Kronke, M. (1998). Regulation of ceramide production and apoptosis. Annu Rev Physiol *60*, 643-65.

Kong, G., Dalton, M., Wardenburg, J. B., Straus, D., Kurosaki, T., and Chan, A. C. (1996). Distinct tyrosine phosphorylation sites in ZAP-70 mediate activation and negative regulation of antigen receptor function. Mol-Cell-Biol *16*, 5026-35.

Koyama, S., Yu, H., Dalgarno, D. C., Shin, T. B., Zydowsky, L. D., and Schreiber, S. L. (1993). Structure of the PI3K SH3 domain and analysis of the SH3 family. Cell *72*, 945-52.

Kraft, A. L., Wang, S. S., Xiang, J., Pouncey, L., and Kidd, V. J. (1992). Regulation of the p58GTA cell division control-related protein kinase during phorbol 12-myristate 13-acetate-induced differentiation of U937 cells. Oncogene *7*, 501-506.

Kreutz, M., and Andreesen, R. (1990). Induction of human monocyte to macrophage maturation in vitro by 1,25-dihydroxyvitamin D3. Blood *76*, 2457-61.

Kreutz, M., Andreesen, R., Krause, S. W., Szabo, A., Ritz, E., and Reichel, H. (1993). 1,25-dihydroxyvitamin D3 production and vitamin D3 receptor expression are developmentally regulated during differentiation of human monocytes into macrophages. Blood *82*, 1300-7.

Krummel, M. F., and Allison, J. P. (1995). CD28 and CTLA-4 have opposing effects on the response of T cells to stimulation [see comments]. J-Exp-Med *182*, 459-65.

Krummel, M. F., and Allison, J. P. (1996). CTLA-4 engagement inhibits IL-2 accumulation and cell cycle progression upon activation of resting T cells. J-Exp-Med *183*, 2533-40.

Kubagawa, H., Shimada, T., Shimo, K., Lassoued, K., Monteiro, R. C., and Cooper, M. D. (1997). CD89 workshop panel report. Leukocyte typing VI, 1028-1029.

Kurokawa, R., DiRenzo, J., Boehm, M., Sugarman, J., Gloss, B., Rosenfeld, M. G., Heyman, R. A., and Glass, C. K. (1994). Regulation of retinoid signalling by receptor polarity and allosteric control of ligand binding. Nature *371*, 528-31.

Kurokawa, R., Yu, V. C., Naar, A., Kyakumoto, S., Han, Z., Silverman, S., Rosenfeld, M. G., and Glass, C. K. (1993). Differential orientations of the DNA-binding

domain and carboxy-terminal dimerization interface regulate binding site selection by nuclear receptor heterodimers. Genes-Dev *7*, 1423-35.

Larsen, S. L., Pedersen, L. O., Buus, S., and Stryhn, A. (1996). T cell responses affected by aminopeptidase N (CD13)-mediated trimming of major histocompatibility complex class II-bound peptides [published erratum appears in J Exp Med 1996 Nov 1;184(5):2073]. J-Exp-Med *184*, 183-9.

Laudanna, C., Campbell, J. J., and Butcher, E. C. (1996). Role of Rho in chemoattractant-activated leukocyte adhesion through integrins. Science *271*, 981-3.

Ledbetter, J. A., Deans, J. P., Aruffo, A., Grosmaire, L. S., Kanner, S. B., Bolen, J. B., and Schieven, G. L. (1993). CD4, CD8 and the role of CD45 in T-cell activation. Curr-Opin-Immunol *5*, 334-40.

LeDouarin, B., Zechel, C., Garnier, J. M., Lutz, Y., Tora, L., Pierrat, P., Heery, D., Gronemeyer, H., Chambon, P., and Losson, R. (1995). The N-terminal part of TIF1, a putative mediator of the ligand-dependent activation function (AF-2) of nuclear receptors, is fused to B-raf in the oncogenic protein T18. EMBO-J *14*, 2020-33.

Lee, H. Y., Walsh, G. L., Dawson, M. I., Hong, W. K., and Kurie, J. M. (1998). All-trans-retinoic acid inhibits Jun N-terminal kinase-dependent signaling pathways. J-Biol-Chem *273*, 7066-71.

Lee, J. W., Ryan, F., Swaffield, J. C., Johnston, S. A., and Moore, D. D. (1995). Interaction of thyroid-hormone receptor with a conserved transcriptional mediator. Nature *374*, 91-4.

Lee, M. S., Kliewer, S. A., Provencal, J., Wright, P. E., and Evans, R. M. (1993). Structure of the retinoid X receptor alpha DNA binding domain: a helix required for homodimeric DNA binding. Science *260*, 1117-21.

Lee, S. L., Wang, Y., and Milbrandt, J. (1996). Unimpaired macrophage differentiation and activation in mice lacking the zinc finger transplantation factor NGFI-A (EGR1). Mol-Cell-Biol *16*, 4566-72.

Lee, Y. F., Young, W. J., Burbach, J. P., and Chang, C. (1998). Negative feedback control of the retinoid-retinoic acid/retinoid X receptor pathway by the human TR4 orphan receptor, a member of the steroid receptor superfamily. J-Biol-Chem *273*, 13437-43.

Lee, Y. H., Lee, H. J., Lee, S. J., Min, D. S., Baek, S. H., Kim, Y. S., Ryu, S. H., and Suh, P. G. (1995). Down-regulation of phospholipase C-gamma 1 during the differentiation of U937 cells. FEBS-Lett *358*, 105-8.

Lefebvre, P., Gaub, M. P., Tahayato, A., Rochette Egly, C., and Formstecher, P. (1995). Protein phosphatases 1 and 2A regulate the transcriptional and DNA binding activities of retinoic acid receptors. J-Biol-Chem *270*, 10806-16.

Lefebvre, P., Mouchon, A., Lefebvre, B., and Formstecher, P. (1998). Binding of retinoic acid receptor heterodimers to DNA. A role for histones NH2 termini. J-Biol-Chem *273*, 12288-95.

Leid, M., Kastner, P., Lyons, R., Nakshatri, H., Saunders, M., Zacharewski, T., Chen, J. Y., Staub, A., Garnier, J. M., Mader, S., and et al. (1992). Purification, cloning, and RXR identity of the HeLa cell factor with which RAR or TR heterodimerizes to bind target sequences efficiently [published erratum appears in Cell 1992 Nov 27;71(5):following 886]. Cell *68*, 377-95.

Lenschow, D. J., Sperling, A. I., Cooke, M. P., Freeman, G., Rhee, L., Decker, D. C., Gray, G., Nadler, L. M., Goodnow, C. C., and Bluestone, J. A. (1994). Differential up-regulation of the B7-1 and B7-2 costimulatory molecules after Ig receptor engagement by antigen. J-Immunol *153*, 1990-7.

Leung, H. T., Bradshaw, J., Cleaveland, J. S., and Linsley, P. S. (1995). Cytotoxic T lymphocyte-associated molecule-4, a high-avidity receptor for CD80 and CD86, contains an intracellular localization motif in its cytoplasmic tail. J-Biol-Chem *270*, 25107-14.

Levin, A. A., Sturzenbecker, L. J., Kazmer, S., Bosakowski, T., Huselton, C., Allenby, G., Speck, J., Kratzeisen, C., Rosenberger, M., Lovey, A., and et al. (1992). 9-cis retinoic acid stereoisomer binds and activates the nuclear receptor RXR alpha. Nature *355*, 359-61.

Li, H., Gomes, P. J., and Chen, J. D. (1997). RAC3, a steroid/nuclear receptor-associated coactivator that is related to SRC-1 and TIF2. Proc-Natl-Acad-Sci-U-S-A *94*, 8479-84.

Li, Y. P., Said, F., and Gallagher, R. E. (1994). Retinoic acid-resistant HL-60 cells exclusively contain mutant retinoic acid receptor-alpha. Blood *83*, 3298-302.

Liebermann, D. A., and Hoffman, B. (1994). Differentiation primary response genes and proto-oncogenes as positive and negative regulators of terminal hematopoietic cell differentiation. Stem-Cells-Dayt *12*, 352-69.

Lin, R. H., Hwang, Y. W., Yang, B. C., and Lin, C. S. (1997). TNF receptor-2-triggered apoptosis is associated with the down-regulation of Bcl-xL on activated T cells and can be prevented by CD28 costimulation. J-Immunol *158*, 598-603.

Linsley, P. S., Bradshaw, J., Greene, J., Peach, R., Bennett, K. L., and Mittler, R. S. (1996). Intracellular trafficking of CTLA-4 and focal localization towards sites of TCR engagement. Immunity *4*, 535-43.

Linsley, P. S., Brady, W., Grosmaire, L., Aruffo, A., Damle, N. K., and Ledbetter, J. A. (1991a). Binding of the B cell activation antigen B7 to CD28 costimulates T cell proliferation and interleukin 2 mRNA accumulation. J-Exp-Med *173*, 721-30.

Linsley, P. S., Brady, W., Urnes, M., Grosmaire, L. S., Damle, N. K., and Ledbetter, J. A. (1991b). CTLA-4 is a second receptor for the B cell activation antigen B7. J-Exp-Med *174*, 561-9.

Linsley, P. S., Greene, J. L., Brady, W., Bajorath, J., Ledbetter, J. A., and Peach, R. (1994). Human B7-1 (CD80) and B7-2 (CD86) bind with similar avidities but distinct kinetics to CD28 and CTLA-4 receptors [published erratum appears in Immunity 1995 Feb;2(2):following 203]. Immunity *1*, 793-801.

Liszewski, M. K., Farries, T. C., Lublin, D. M., Rooney, I. A., and Atkinson, J. P. (1996). Control of the complement system. Adv Immunol *61*, 201-83.

Liu, M., and Freedman, L. P. (1994). Transcriptional synergism between the vitamin D3 receptor and other nonreceptor transcription factors. Mol-Endocrinol *8*, 1593-604.

Liu, M., Iavarone, A., and Freedman, L. P. (1996a). Transcriptional activation of the human p21(WAF1/CIP1) gene by retinoic acid receptor. Correlation with retinoid induction of U937 cell differentiation. J-Biol-Chem *271*, 31723-8.

Liu, M., Lee, M. H., Cohen, M., Bommakanti, M., and Freedman, L. P. (1996b). Transcriptional activation of the Cdk inhibitor p21 by vitamin D3 leads to the induced differentiation of the myelomonocytic cell line U937. Genes-Dev *10*, 142-53.

Liu, M., and Wu, M. (1992). Induction of human monocyte cell line U937 differentiation and CSF-1 production by phorbol ester. Exp-Hematol *20*, 974-979.

Liu, R., Takayama, S., Zheng, Y., Froesch, B., Chen, G. Q., Zhang, X., Reed, J. C., and Zhang, X. K. (1998). Interaction of BAG-1 with retinoic acid receptor and its inhibition of retinoic acid-induced apoptosis in cancer cells. J-Biol-Chem *273*, 16985-92.

Liversidge, J., Dawson, R., Hoey, S., McKay, D., Grabowski, P., and Forrester, J. V. (1996). CD59 and CD48 expressed by rat retinal pigment epithelial cells are major ligands for the CD2-mediated alternative pathway of T cell activation. J-Immunol *156*, 3696-703.

Loveland, B. E., and Szokolai, K. (1997). CD55 workshop panel report. Leukocyte typing VI, 519-520.

Lucas, P. J., Negishi, I., Nakayama, K., Fields, L. E., and Loh, D. Y. (1995). Naive CD28-deficient T cells can initiate but not sustain an in vitro antigen-specific immune response. J-Immunol *154*, 5757-68.

Lustgarten, J., Waks, T., and Eshhar, Z. (1991). CD4 and CD8 accessory molecules function through interactions with major histocompatibility complex molecules which are not directly associated with the T cell receptor-antigen complex. Eur-J-Immunol *21*, 2507-15.

MacDonald, P. N., Sherman, D. R., Dowd, D. R., Jefcoat, S. C., Jr., and DeLisle, R. K. (1995). The vitamin D receptor interacts with general transcription factor IIB. J-Biol-Chem *270*, 4748-52.

Mader, S., Chen, J. Y., Chen, Z., White, J., Chambon, P., and Gronemeyer, H. (1993). The patterns of binding of RAR, RXR and TR homo- and heterodimers to direct repeats are dictated by the binding specificites of the DNA binding domains. EMBO-J *12*, 5029-41.

Mangelsdorf, D. J., Borgmeyer, U., Heyman, R. A., Zhou, J. Y., Ong, E. S., Oro, A. E., Kakizuka, A., and Evans, R. M. (1992). Characterization of three RXR genes that mediate the action of 9-cis retinoic acid. Genes-Dev *6*, 329-44.

Mangelsdorf, D. J., Ong, E. S., Dyck, J. A., and Evans, R. M. (1990). Nuclear receptor that identifies a novel retinoic acid response pathway. Nature *345*, 224-9.

Mangelsdorf, D. J., Thummel, C., Beato, M., Herrlich, P., Schutz, G., Umesono, K., Blumberg, B., Kastner, P., Mark, M., Chambon, P., and Evans, R. M. (1995). The nuclear receptor superfamily: the second decade. Cell *83*, 835-839.

Marcu, K. B., Bossone, R. N., and Patel, A. J. (1992). *myc* function and regulation. Annu-rev-Biochem. *61*.

Marengere, L. E., Waterhouse, P., Duncan, G. S., Mittrucker, H. W., Feng, G. S., and Mak, T. W. (1996). Regulation of T cell receptor signaling by tyrosine phosphatase SYP association with CTLA-4 [published errata appear in Science 1996 Dec 6;274(5293)1597 and 1997 Apr 4;276(5309):21]. Science *272*, 1170-3.

Marshall, C. J. (1996). Ras effectors. Curr-Opin-Cell-Biol *8*, 197-204.

Mastroberardino, L., Spindler, B., Skelly, P. J., Loffing, J., Shoemaker, C. B., and Verrey, F. (1998). Amino-acid transport by heterodimers of 4F2hc/CD98 and members of the permease family. Nature *395*, 288-291.

Matikainen, S., Ronni, T., Hurme, M., Pine, R., and Julkunen, I. (1996). Retinoic acid activates Interferon Regulatory Factor-1 gene expression in myeloid cells. Blood *88*, 114-123.

Matkovits, T., and Christakos, S. (1995). Ligand occupancy is not required for vitamin D receptor and retinoid receptor-mediated transcriptional activation. Mol-Endocrinol *9*, 232-42.

McTernan, P. G., Sheppard, M. C., and Williams, G. R. (1998). Hormone-induced changes in nuclear receptor stoichiometry in HL60 cells correlate with induction of monocyte or neutrophil differentiation. J-Endocrinol *156*, 135-48.

Meighan Mantha, R. L., Wellstein, A., and Riegel, A. T. (1997). Differential regulation of extracellular signal-regulated kinase 1 and 2 activity during 12-O-tetradecanoylphorbol 13-acetate-induced differentiation of HL-60 cells. Exp-Cell-Res *234*, 321-8.

Meinke, A., Barahmand Pour, F., Wohrl, S., Stoiber, D., and Decker, T. (1996). Activation of different Stat5 isoforms contributes to cell-type-restricted signaling in response to interferons. Mol-Cell-Biol *16*, 6937-44.

Menu, E., Tsai, B. C., Bothwell, A. L., Sims, P. J., and Bierer, B. E. (1994). CD59 costimulation of T cell activation. CD58 dependence and requirement for glycosylation. J-Immunol *153*, 2444-56.

Metzger, H., and Kinet, J. P. (1988). How antibodies work: focus on Fc receptors. FASEB-J *2*, 3-11.

Micouin, A., Rouillard, D., and Bauvois, B. (1997). Induction of macrophagic differentiation and cytokine secretion by IgG1 molecules in human normal monocytes and myelogenous leukemia cells. Leukemia *11*, 552-60.

Miller, G. T., Hochman, P. S., Meier, W., Tizard, R., Bixler, S. A., Rosa, M. D., and Wallner, B. P. (1993). Specific interaction of lymphocyte function-associated antigen 3 with CD2 can inhibit T cell responses. J-Exp-Med *178*, 211-22.

Minucci, S., Leid, M., Toyama, R., Saint Jeannet, J. P., Peterson, V. J., Horn, V., Ishmael, J. E., Bhattacharyya, N., Dey, A., Dawid, I. B., and Ozato, K. (1997). Retinoid X receptor (RXR) within the RXR-retinoic acid receptor heterodimer binds its ligand and enhances retinoid-dependent gene expression. Mol-Cell-Biol *17*, 644-55.

Mitchell, M. A., Huang, M. M., Chien, P., Indik, Z. K., Pan, X. Q., and Schreiber, A. D. (1994). Substitutions and deletions in the cytoplasmic domain of the phagocytic receptor Fc gamma RIIA: effect on receptor tyrosine phosphorylation and phagocytosis [published erratum appears in Blood 1994 Nov 1;84(9):3252]. Blood *84*, 1753-9.

Mondino, A., and Jenkins, M. K. (1994). Surface proteins involved in T cell costimulation. J-Leukoc-Biol *55*, 805-15.

Morrison, D. K., and Cutler, R. E. (1997). The complexity of Raf-1 regulation. Curr-Opin-Cell-Biol *9*, 174-9.

Moudgil, K. D., and Sercarz, E. E. (1993). Dominant determinants in hen eggwhite lysozyme correspond to the cryptic determinants within its self-homologue, mouse lysozyme: implications in shaping of the T cell repertoire and autoimmunity. J-Exp-Med *178*, 2131-8.

Mudad, R., Rao, N., Angelisova, P., Horejsi, V., and Telen, M. J. (1995). Evidence that CDw108 membrane protein bears the JMH blood group antigen. Transfusion *35*, 566-70.

Nada, S., Okada, M., MacAuley, A., Cooper, J. A., and Nakagawa, H. (1991). Cloning of a complementary DNA for a protein-tyrosine kinase that specifically phosphorylates a negative regulatory site of p60c-src. Nature *351*, 69-72.

Nagpal, S., Friant, S., Nakshatri, H., and Chambon, P. (1993). RARs and RXRs: evidence for two autonomous transactivation functions (AF-1 and AF-2) and heterodimerization in vivo. EMBO-J *12*, 2349-60.

Nagpal, S., Saunders, M., Kastner, P., Durand, B., Nakshatri, H., and Chambon, P. (1992). Promoter context- and response element-dependent specificity of the transcriptional activation and modulating functions of retinoic acid receptors. Cell *70*, 1007-19.

Nagy, L., Kao, H. Y., Chakravarti, D., Lin, R. J., Hassig, C. A., Ayer, D. E., Schreiber, S. L., and Evans, R. M. (1997). Nuclear receptor repression mediated by a complex containing SMRT, mSin3A, and histone deacetylase. Cell *89*, 373-80.

Nagy, L., Thomazy, V. A., Shipley, G. L., Fesus, L., Lamph, W., Heyman, R. A., Chandraratna, R. A., and Davies, P. J. (1995). Activation of retinoid X receptors induces apoptosis in HL-60 cell lines. Mol-Cell-Biol *15*, 3540-51.

Nakajima, H., Kizaki, M., Ueno, H., Muto, A., Takayama, N., Matsushita, H., Sonoda, A., and Ikeda, Y. (1996). All-trans and 9-cis retinoic acid enhance 1,25-dihydroxyvitamin D3-induced monocytic differentiation of U937 cells [see comments]. Leuk-Res *20*, 665-76.

Nakajima, T., Uchida, C., Anderson, S. F., Lee, C. G., Hurwitz, J., Parvin, J. D., and Montminy, M. (1997). RNA helicase A mediates association of CBP with RNA polymerase II. Cell *90*, 1107-12.

Nelms, K., Snow, A. L., Hu-Li, J., and Paul, W. E. (1998). FRIP, a hematopoietic cell-specific rasGAP-interacting protein phosphorylated in response to cytokine stimulation. Immunity *9*, 13-24.

Nguyen, H. Q., Hoffman Liebermann, B., and Liebermann, D. A. (1993). The zinc finger transcription factor Egr-1 is essential for and restricts differentiation along the macrophage lineage. Cell *72*, 197-209.

Nickells, M. W., Marsh JR, H. C., and Atkinson, J. P. (1997). CD35 workshop panel report. Leukocyte typing VI, 984-988.

Ninomiya, N., Hazeki, K., Fukui, Y., Seya, T., Okada, T., Hazeki, O., and Ui, M. (1994). Involvement of phosphatidylinositol 3-kinase in Fc gamma receptor signaling. J-Biol-Chem *269*, 22732-7.

Nishio, H., Tada, J., Hashiyama, M., Hirn, J., Ingles-Esteve, J., and Suda, T. (1997). CD34 workshop panel report. Leukocyte typing VI, 974-976.

Noel, P. J., Boise, L. H., Green, J. M., and Thompson, C. B. (1996). CD28 costimulation prevents cell death during primary T cell activation. J-Immunol *157*, 636-42.

Norton, S. D., Zuckerman, L., Urdahl, K. B., Shefner, R., Miller, J., and Jenkins, M. K. (1992). The CD28 ligand, B7, enhances IL-2 production by providing a costimulatory signal to T cells. J-Immunol *149*, 1556-61.

Oberg, F., Botling, J., and Nilsson, K. (1993). Functional antagonism between vitamin D3 and retinoic acid in the regulation of CD14 and CD23 expression during monocytic differentiation of U-937 cells. J-Immunol *150*, 3487-95.

Ogawa, M. (1993). Differentiation and proliferation of hematopoietic stem cells. Blood *81*, 2844-53.

Ogryzko, V. V., Schiltz, R. L., Russanova, V., Howard, B. H., and Nakatani, Y. (1996). The transcriptional coactivators p300 and CBP are histone acetyltransferases. Cell *87*, 953-9.

Ohgimoto, S., Tabata, N., Suga, S., Nishio, M., Ohta, H., Tsurudome, M., Komada, H., Kawano, M., Watanabe, N., and Ito, Y. (1995). Molecular characterization of fusion regulatory protein-1 (FRP-1) that induces multinucleated giant cell formation of monocytes and HIV gp160-mediated cell fusion. FRP-1 and 4F2/CD98 are identical molecules. J-Immunol *155*, 3585-92.

Olsson, I. L., and Breitman, T. R. (1982). Induction of differentiation of the human histiocytic lymphoma cell line U-937 by retinoic acid and cyclic adenosine 3':5'-monophosphate-inducing agents. Cancer-Res *42*, 3924-7.

Onate, S. A., Tsai, S. Y., Tsai, M. J., and O'Malley, B. W. (1995). Sequence and characterization of a coactivator for the steroid hormone receptor superfamily. Science *270*, 1354-7.

Palmer, E. M., and van Seventer, G. A. (1997). Human T helper cell differentiation is regulated by the combined action of cytokines and accessory cell-dependent costimulatory signals. J-Immunol *158*, 2654-62.

Park, J. G., Isaacs, R. E., Chien, P., and Schreiber, A. D. (1993a). In the absence of other Fc receptors, Fc gamma RIIIA transmits a phagocytic signal that requires the cytoplasmic domain of its gamma subunit. J-Clin-Invest *92*, 1967-73.

Park, J. G., Murray, R. K., Chien, P., Darby, C., and Schreiber, A. D. (1993b). Conserved cytoplasmic tyrosine residues of the gamma subunit are required for a phagocytic signal mediated by Fc gamma RIIIA. J-Clin-Invest *92*, 2073-9.

Parsons, J. T., and Parsons, S. J. (1997). Src family protein tyrosine kinases: cooperating with growth factor and adhesion signaling pathways. Curr-Opin-Cell-Biol *9*, 187-92.

Pastorino, J. G., Simbula, G., Yamamoto, K., Glascott, P. A., Jr., Rothman, R. J., and Farber, J. L. (1996). The cytotoxicity of tumor necrosis factor depends on induction of the mitochondrial permeability transition. J-Biol-Chem *271*, 29792-8.

Pawlowski, N. A., Abraham, E. L., Pontier, S., Scott, W. A., and Cohn, Z. A. (1985). Human monocyte-endothelial cell interaction in vitro. Proc-Natl-Acad-Sci-U-S-A *82*, 8208-12.

Pawlowski, N. A., Kaplan, G., Abraham, E., and Cohn, Z. A. (1988). The selective binding and transmigration of monocytes through the junctional complexes of human endothelium. J-Exp-Med *168*, 1865-82.

Pawson, T. (1997). New impressions of Src and Hck [news; comment]. Nature *385*, 582-3,.

Pawson, T., and Scott, J. D. (1997). Signaling through scaffold, anchoring, and adaptor proteins. Science *278*, 2075-80.

Pazin, M. J., and Kadonaga, J. T. (1997). What's up and down with histone deacetylation and transcription? Cell *89*, 325-8.

Peach, R. J., Bajorath, J., Brady, W., Leytze, G., Greene, J., Naemura, J., and Linsley, P. S. (1994). Complementarity determining region 1 (CDR1)- and CDR3-analogous regions in CTLA-4 and CD28 determine the binding to B7-1. J-Exp-Med *180*, 2049-58.

Peiper, S. C., and Guo, H.-H. (1997). CD33 workshop panel report. Leukocyte typing VI, 972-974.

Perez, A., Kastner, P., Sethi, S., Lutz, Y., Reibel, C., and Chambon, P. (1993). PMLRAR homodimers: distinct DNA binding properties and heteromeric interactions with RXR. EMBO-J *12*, 3171-82.

Perlmann, T., and Evans, R. M. (1997). Nuclear receptors in Sicily: all in the famiglia. Cell *90*, 391-7.

Petkovich, M., Brand, N. J., Krust, A., and Chambon, P. (1987). A human retinoic acid receptor which belongs to the family of nuclear receptors. Nature *330*, 444-50.

Pickl, W. F., Majdic, O., Kohl, P., Stockl, J., Riedl, E., Scheinecker, C., Bello Fernandez, C., and Knapp, W. (1996). Molecular and functional characteristics of dendritic cells generated from highly purified CD14+ peripheral blood monocytes. J-Immunol *157*, 3850-9.

Pieters, R. H., Bol, M., Ariens, T., Punt, P., Seinen, W., Bloksma, N., and Penninks, A. H. (1994). Selective inhibition of immature CD4-CD8+ thymocyte proliferation, but not differentiation, by the thymus atrophy-inducing compound di-n-butyltin dichloride. Immunology *81*, 261-7.

Piwnica Worms, H., Saunders, K. B., Roberts, T. M., Smith, A. E., and Cheng, S. H. (1987). Tyrosine phosphorylation regulates the biochemical and biological properties of pp60c-src. Cell *49*, 75-82.

Prieto, J., Eklund, A., and Patarroyo, M. (1994). Regulated expression of integrins and other adhesion molecules during differentiation of monocytes into macrophages. Cell-Immunol *156*, 191-211.

Pronk, G. J., de Vries-Smits, A. M. M., Buday, L., Downward, J., Maassen, J. A., Madema, R., and Bos, J. L. (1994). Involvemant of Shc in insulin- and epidermal growth factor-induced activation of p21-Ras. Mol-Cell-Biol *14*, 1575-1581.

Pulford, K., Micklem, K., Law, S. K. A., and Mason, D. (1997). CD163 (M130 antigen) workshop panel report. Leukocyte typing VI, 1089-1091.

Pulverer, B. J., Hughes, K., Franklin, C. C., Kraft, A. S., Leevers, S. J., and Woodget, J. R. (1993). Co-purification of mitogen-activated protein kinases with phorbol ester-induced c-Jun kinase activity U937 leukaemic cells. Oncogene *8*, 407-415.

Qian, D., and Weiss, A. (1997). T cell antigen receptor signal transduction. Curr-Opin-Cell-Biol *9*, 205-12.

Rastinejad, F., Perlmann, T., Evans, R. M., and Sigler, P. B. (1995). Structural determinants of nuclear receptor assembly on DNA direct repeats [see comments]. Nature *375*, 203-11.

Ravetch, J. V., and Kinet, J. P. (1991). Fc receptors. Annu Rev Immunol *9*, 457-92.

Reed, S. G., Nathan, C. F., Pihl, D. L., Rodricks, P., Shanebeck, K., Conlon, P. J., and Grabstein, K. H. (1987). Recombinant granulocyte/macrophage colony-stimulating factor activates macrophages to inhibit Trypanosoma cruzi and release hydrogen peroxide. Comparison with interferon gamma. J-Exp-Med *166*, 1734-46.

Reif, K., and Cantrell, D. A. (1998). Networking Rho family GTPases in lymphocytes. Immunity *8*, 395-401.

Resh, M. D. (1994). Myristylation and palmitylation of Src family members: the fats of the matter. Cell *76*, 411-3.

Reth, M. (1989). Antigen receptor tail clue [letter]. Nature *338*, 383-4.

Robinson, M. J., and Cobb, M. H. (1997). Mitogen-activated protein kinase pathways. Curr-Opin-Cell-Biol *9*, 180-6.

Roos, D., de Boer, M., Kuribayashi, F., Meischl, C., Weening, R. S., Segal, A. W., Ahlin, A., Nemet, K., Hossle, J. P., Bernatowska-Matuszkiewicz, E., and Middleton-

Price, H. (1996). Mutations in the X-linked and autosomal recessive forms of chronic granulomatous disease. Blood *87*, 1663-1681.

Rosales, C., and Brown, E. J. (1991). Two mechanisms for IgG Fc-receptor-mediated phagocytosis by human neutrophils. J-Immunol *146*, 3937-44.

Rosales, C., Jones, S. L., McCourt, D., and Brown, E. J. (1994). Bromophenacyl bromide binding to the actin-bundling protein l-plastin inhibits inositol trisphosphate-independent increase in Ca2+ in human neutrophils. Proc-Natl-Acad-Sci-U-S-A *91*, 3534-8.

Rosen, E. D., Beninghof, E. G., and Koenig, R. J. (1993). Dimerization interfaces of thyroid hormone, retinoic acid, vitamin D, and retinoid X receptors. J-Biol-Chem *268*, 11534-41.

Rowe, A., and Brickell, P. M. (1993). The nuclear retinoid receptors. Int-J-Exp-Pathol *74*, 117-26.

Rusten, L. S., Dybedal, I., Blomhoff, H. K., Blomhoff, R., Smeland, E. B., and Jacobsen, S. E. (1996). The RAR-RXR as well as the RXR-RXR pathway is involved in signaling growth inhibition of human CD34+ erythroid progenitor cells. Blood *87*, 1728-36.

Saitou, M., Sugai, S., Tanaka, T., Shimouchi, K., Fuchs, E., Narumiya, S., and Kakizuka, A. (1995). Inhibition of skin development by targeted expression of a dominant-negative retinoic acid receptor [see comments]. Nature *374*, 159-62.

Sakashita, A., Kizaki, M., Pakkala, S., Schiller, G., Tsuruoka, N., Tomosaki, R., Cameron, J. F., Dawson, M. I., and Koeffler, H. P. (1993). 9-cis-retinoic acid: effects on normal and leukemic hematopoiesis in vitro. Blood *81*, 1009-16.

Salbert, G., Fanjul, A., Piedrafita, F. J., Lu, X. P., Kim, S. J., Tran, P., and Pfahl, M. (1993). Retinoic acid receptors and retinoid X receptor-alpha down-regulate the transforming growth factor-beta 1 promoter by antagonizing AP-1 activity. Mol-Endocrinol *7*, 1347-56.

Sambrook, J., Fritsch, E.F. and Maniatis, T. (1989). Molecular Cloning: A laboratory manual, 2nd Edition: Cold Spring Harbour).

Sanchez Mejorada, G., and Rosales, C. (1998). Signal transduction by immunoglobulin Fc receptors. J-Leukoc-Biol *63*, 521-33.

Santana, C., Noris, G., Espinoza, B., and Ortega, E. (1996). Protein tyrosine phosphorylation in leukocyte activation through receptors for IgG. J-Leukoc-Biol *60*, 433-40.

Santana, P., Pena, L. A., Haimovitz Friedman, A., Martin, S., Green, D., McLoughlin, M., Cordon Cardo, C., Schuchman, E. H., Fuks, Z., and Kolesnick, R. (1996). Acid sphingomyelinase-deficient human lymphoblasts and mice are defective in radiation-induced apoptosis. Cell *86*, 189-99.

Santini, F., and Beaven, M. A. (1993). Tyrosine phosphorylation of a mitogen-activated protein kinase-like protein occurs at a late step in exocytosis. Studies with tyrosine phosphatase inhibitors and various secretagogues in rat RBL-2H3 cells. J-Biol-Chem *268*, 22716-22.

Sawyer, D. W., Sullivan, J. A., and Mandell, G. L. (1985). Intracellular free calcium localization in neutrophils during phagocytosis. Science *230*, 663-6.

Schlosshauer, B. (1991). Neurothelin: molecular characteristics and developmental regulation in the chick CNS. Development *113*, 129-40.

Schlosshauer, B., Bauch, H., and Frank, R. (1995). Neurothelin: amino acid sequence, cell surface dynamics and actin colocalization. Eur-J-Cell-Biol *68*, 159-66.

Schrader, M., Muller, K. M., Nayeri, S., Kahlen, J. P., and Carlberg, C. (1994). Vitamin D3-thyroid hormone receptor heterodimer polarity directs ligand sensitivity of transactivation [see comments]. Nature *370*, 382-6.

Schraven, B., Hegen, M., Autschbach, F., Gaya, A., Schwarz, C., and Meuer, S. C. (1997). CD148 (p260 phosphatase) workshop panel report. Leukocyte typing VI, 576-580.

Schule, R., Rangarajan, P., Yang, N., Kliewer, S., Ransone, L. J., Bolado, J., Verma, I. M., and Evans, R. M. (1991). Retinoic acid is a negative regulator of AP-1-responsive genes. Proc-Natl-Acad-Sci-U-S-A *88*, 6092-6.

Schwartz, R. H. (1992). Costimulation of T lymphocytes: the role of CD28, CTLA-4, and B7/BB1 in interleukin-2 production and immunotherapy. Cell *71*, 1065-8.

Schwartz, R. H. (1985). T-lymphocyte recognition of antigen in association with gene products of the major histocompatibility complex. Annu Rev Immunol *3*, 237-61.

Sellmayer, A., Goessl, C., Obermeier, H., Volk, R., Reder, E., Weber, C., and Weber, P. C. (1994). Differential induction of eicosanoid synthesis in monocytic cells treated with retinoic acid and 1,25-dihydroxy-vitamin D3. Prostaglandins *47*, 203-20.

Seulberger, H., Unger, C. M., and Risau, W. (1992). HT7, Neurothelin, Basigin, gp42 and OX-47--many names for one developmentally regulated immuno-globulin-like surface glycoprotein on blood-brain barrier endothelium, epithelial tissue barriers and neurons. Neurosci-Lett *140*, 93-7.

Shaw, A. S., Amrein, K. E., Hammond, C., Stern, D. F., Sefton, B. M., and Rose, J. K. (1989). The lck tyrosine protein kinase interacts with the cytoplasmic tail of the CD4 glycoprotein through its unique amino-terminal domain. Cell *59*, 627-36.

Shiroo, M., Goff, L., Biffen, M., Shivnan, E., and Alexander, D. (1992). CD45 tyrosine phosphatase-activated p59fyn couples the T cell antigen receptor to pathways of diacylglycerol production, protein kinase C activation and calcium influx. EMBO-J *11*, 4887-97.

Shivnan, E., Clayton, L., Allridge, L., Keating, K. E., Gullberg, M., and Alexander, D. R. (1996). CD45 monoclonal antibodies inhibit TCR-mediated calcium signals, calmodulin-kinase IV/Gr activation, and oncoprotein 18 phosphorylation. J-Immunol *157*, 101-9.

Skubitz, K. M., Grunnert, F., Jantscheff, P., Kuroki, M., and Skubitz, P. N. (1997). CD66 family workshop panel report. Leukocyte typing VI, 992-1000.

Spiegel, S., Foster, D., and Kolesnick, R. (1996). Signal transduction through lipid second messengers. Curr-Opin-Cell-Biol *8*, 159-67.

Springer, T. A. (1990). Adhesion receptors of the immune system. Nature *346*, 425-34.

Stefanova, I., Corcoran, M. L., Horak, E. M., Wahl, L. M., Bolen, J. B., and Horak, I. D. (1993). Lipopolysaccharide induces activation of CD14-associated protein tyrosine kinase p53/56lyn. J-Biol-Chem *268*, 20725-8.

Su, B., Jacinto, E., Hibi, M., Kallunki, T., Karin, M., and Ben Neriah, Y. (1994). JNK is involved in signal integration during costimulation of T lymphocytes. Cell *77*, 727-36.

Sucov, H. M., Dyson, E., Gumeringer, C. L., Price, J., Chien, K. R., and Evans, R. M. (1994). RXR alpha mutant mice establish a genetic basis for vitamin A signaling in heart morphogenesis. Genes-Dev *8*, 1007-18.

Suga, S., Tsurudome, M., Ito, M., Ohgimoto, S., Tabata, N., Nishio, M., Kawano, M., Komada, H., Ito, M., Sakurai, M., and Ito, Y. (1997). Human immunodeficiency virus type-1 envelope glycoprotein gp120 induces expression of fusion regulatory protein (FRP)-1/CD98 on CD4+ T cells: a possible regulatory mechanism of HIV-induced syncytium formation. Med-Microbiol-Immunol-Berl *185*, 237-43.

Sumimoto, H., Hata, K., Mizuki, K., Ito, T., Kage, Y., Sakaki, Y., Fukumaki, Y., Nakamura, M., and Takeshige, K. (1996). Assembly and activation of the phagocyte NADPH oxidase. Specific interaction of the N-terminal Src homology 3 domain of p47phox with p22phox is required for activation of the NADPH oxidase. J-Biol-Chem *271*, 22152-8.

Sun, W., O'Shea, J. K., and Guyre, P. M. (1997). CD64 workshop panel report. Leukocyte typing VI, 988-990.

Sundstrom, C., and Nillson, K. (1976). Establishment and characterisation of a human histiocytic lymphoma cell line (U-937). Int-J-Cancer *17*, 565-577.

Susin, S. A., Zamzami, N., Castedo, M., Daugas, E., Wang, H. G., Geley, S., Fassy, F., Reed, J. C., and Kroemer, G. (1997). The central executioner of apoptosis: multiple connections between protease activation and mitochondria in Fas/APO-1/CD95- and ceramide-induced apoptosis. J-Exp-Med *186*, 25-37.

Szondy, Z., Reichert, U., Bernardon, J. M., Michel, S., Toth, R., Ancian, P., Ajzner, E., and Fesus, L. (1997). Induction of apoptosis by retinoids and retinoic acid receptor gamma-selective compounds in mouse thymocytes through a novel apoptosis pathway. Mol-Pharmacol *51*, 972-82.

Taga, K., Kasahara, Y., Yachie, A., Miyawaki, T., and Taniguchi, N. (1991). Preferential expression of IL-2 receptor subunits on memory populations within CD4+ and CD8+ T cells. Immunology *72*, 15-9.

Taimi, M., Defacque, H., Commes, T., Favero, J., Caron, E., Marti, J., and Dornand, J. (1993). Effect of retinoic acid and vitamin D on the expression of interleukin-1 beta, tumour necrosis factor-alpha and interleukin-6 in the human monocytic cell line U937. Immunology *79*, 229-35.

Testa, U., Masciulli, R., Tritarelli, E., Pustorino, R., Mariani, G., Martucci, R., Barberi, T., Camagna, A., Valtieri, M., and Peschle, C. (1993). Transforming growth factor-beta potentiates vitamin D3-induced terminal monocytic differentiation of human leukemic cell lines. J-Immunol *150*, 2418-30.

Teunissen, M. B., Koomen, C. W., and Bos, J. D. (1995). Intercellular adhesion molecule-3 (CD50) on human epidermal Langerhans cells participates in T-cell activation. J-Invest-Dermatol *104*, 995-8.

Thomas, R., Davis, L. S., and Lipsky, P. E. (1993). Comparative accessory cell function of human peripheral blood dendritic cells and monocytes. J-Immunol *151*, 6840-52.

Tickle, C., Alberts, B., Wolpert, L., and Lee, J. (1982). Local application of retinoic acid to the limb bud mimics the action of the polarising region. Nature *296*, 564-466.

Ting, A. T., Karnitz, L. M., Schoon, R. A., Abraham, R. T., and Leibson, P. J. (1992). Fc gamma receptor activation induces the tyrosine phosphorylation of both phospholipase C (PLC)-gamma 1 and PLC-gamma 2 in natural killer cells. J-Exp-Med *176*, 1751-5.

Tivol, E. A., Borriello, F., Schweitzer, A. N., Lynch, W. P., Bluestone, J. A., and Sharpe, A. H. (1995). Loss of CTLA-4 leads to massive lymphoproliferation and fatal multiorgan tissue destruction, revealing a critical negative regulatory role of CTLA-4. Immunity *3*, 541-7.

Todd, R., Magdolen, V., Cines, D., Kramer, M., Mizukami, I., Mazar, A., WAng, J., Schaefer, B., and Luther, T. (1997). CD87 workshop panel report. Leukocyte typing VI, 1016-1020.

Toker, A. (1998). The synthesis and cellular roles of phosphatidylinositol 4,5-bisphosphate. Curr-Opin-Cell-Biol *10*, 254-61.

Totpal, K., Chaturvedi, M. M., LaPushin, R., and Aggarwal, B. B. (1995). Retinoids downregulate both p60 and p80 forms of tumor necrosis factor receptors in human histiocytic lymphoma U-937 cells. Blood *85*, 3547-55.

Treisman, R. (1996). Regulation of transcription by MAP kinase cascades. Curr-Opin-Cell-Biol *8*, 205-15.

Tsai, S., Bartelmez, S., Heyman, R., Damm, K., Evans, R., and Collins, S. J. (1992). A mutated retinoic acid receptor-alpha exhibiting dominant-negative activity alters the lineage development of a multipotent hematopoietic cell line. Genes-Dev *6*, 2258-69.

Turcovski Corrales, S. M., Fenton, R. G., Peltz, G., and Taub, D. D. (1995). CD28:B7 interactions promote T cell adhesion. Eur-J-Immunol *25*, 3087-93.

Turner, C. E., Glenney, J. R., Jr., and Burridge, K. (1990). Paxillin: a new vinculin-binding protein present in focal adhesions. J-Cell-Biol *111*, 1059-68.

Turner, H., Reif, K., Rivera, J., and Cantrell, D. A. (1995). Regulation of the adapter molecule Grb2 by the Fc epsilon R1 in the mast cell line RBL2H3. J-Biol-Chem *270*, 9500-6.

Turner, J. M., Brodsky, M. H., Irving, B. A., Levin, S. D., Perlmutter, R. M., and Littman, D. R. (1990). Interaction of the unique N-terminal region of tyrosine kinase p56lck with cytoplasmic domains of CD4 and CD8 is mediated by cysteine motifs. Cell *60*, 755-65.

Umesono, K., Murakami, K. K., Thompson, C. C., and Evans, R. M. (1991). Direct repeats as selective response elements for the thyroid hormone, retinoic acid, and vitamin D3 receptors. Cell *65*, 1255-66.

Valledor, A. F., Borras, F. E., Cullell Young, M., and Celada, A. (1998). Transcription factors that regulate monocyte/macrophage differentiation. J-Leukoc-Biol *63*, 405-17.

van der Merwe, P. A., Barclay, A. N., Mason, D. W., Davies, E. A., Morgan, B. P., Tone, M., Krishnam, A. K., Ianelli, C., and Davis, S. J. (1994). Human cell-adhesion

molecule CD2 binds CD58 (LFA-3) with a very low affinity and an extremely fast dissociation rate but does not bind CD48 or CD59. Biochemistry *33*, 10149-60.

Van der Merwe, P. A., Bodian, D. L., Daenke, S., Linsley, P., and Davis, S. J. (1997). CD80 (B7-1) binds both CD28 and CTLA-4 with low affinity and very fast kinetics. J-Exp-Med *185*.

van Oers, N. S., Killeen, N., and Weiss, A. (1996a). Lck regulates the tyrosine phosphorylation of the T cell receptor subunits and ZAP-70 in murine thymocytes. J-Exp-Med *183*, 1053-62.

van Oers, N. S., Lowin Kropf, B., Finlay, D., Connolly, K., and Weiss, A. (1996b). alpha beta T cell development is abolished in mice lacking both Lck and Fyn protein tyrosine kinases. Immunity *5*, 429-36.

Van Seventer, G. A., Bonvini, E., Yamada, H., Conti, A., Stringfellow, S., June, C. H., and Shaw, S. (1992). Costimulation of T cell receptor/CD3-mediated activation of resting human CD4+ T cells by leukocyte function-associated antigen-1 ligand intercellular cell adhesion molecule-1 involves prolonged inositol phospholipid hydrolysis and sustained increase of intracellular Ca2+ levels. J-Immunol *149*, 3872-80.

Van Seventer, G. A., Shimizu, Y., Horgan, K. J., Luce, G. E., Webb, D., and Shaw, S. (1991). Remote T cell co-stimulation via LFA-1/ICAM-1 and CD2/LFA-3: demonstration with immobilized ligand/mAb and implication in monocyte-mediated co-stimulation. Eur-J-Immunol *21*, 1711-8.

Van Seventer, G. A., Shimizu, Y., Horgan, K. J., and Shaw, S. (1990). The LFA-1 ligand ICAM-1 provides an important costimulatory signal for T cell receptor-mediated activation of resting T cells. J-Immunol *144*, 4579-86.

Verheij, M., Bose, R., Lin, X. H., Yao, B., Jarvis, W. D., Grant, S., Birrer, M. J., Szabo, E., Zon, L. I., Kyriakis, J. M., Haimovitz Friedman, A., Fuks, Z., and Kolesnick, R. N. (1996). Requirement for ceramide-initiated SAPK/JNK signalling in stress-induced apoptosis. Nature *380*, 75-9.

Vivanco Ruiz, M. D. M., Bugge, T. H., Hirschmann, P., and H.G., S. (1991). Functional characterisation of a natural retinoic acid responsive element. EMBO-J *10*, 3829-3838.

Voegel, J. J., Heine, M. J., Tini, M., Vivat, V., Chambon, P., and Gronemeyer, H. (1998). The coactivator TIF2 contains three nuclear receptor-binding motifs and mediates transactivation through CBP binding-dependent and -independent pathways. EMBO-J *17*, 507-19.

Vyth Dreese, F. A., Dellemijn, T. A., Frijhoff, A., van Kooyk, Y., and Figdor, C. G. (1993). Role of LFA-1/ICAM-1 in interleukin-2-stimulated lymphocyte proliferation. Eur-J-Immunol *23*, 3292-9.

Vyth Dreese, F. A., Dellemijn, T. A., Majoor, D., and de Jong, D. (1995). Localization in situ of the co-stimulatory molecules B7.1, B7.2, CD40 and their ligands in normal human lymphoid tissue. Eur-J-Immunol *25*, 3023-9.

Waksman, G., Kominos, D., Robertson, S. C., Pant, N., Baltimore, D., Birge, R. B., Cowburn, D., Hanafusa, H., Mayer, B. J., Overduin, M., and et al. (1992). Crystal structure of the phosphotyrosine recognition domain SH2 of v-src complexed with tyrosine-phosphorylated peptides [see comments]. Nature *358*, 646-53.

Walunas, T. L., Lenschow, D. J., Bakker, C. Y., Linsley, P. S., Freeman, G. J., Green, J. M., Thompson, C. B., and Bluestone, J. A. (1994). CTLA-4 can function as a negative regulator of T cell activation. Immunity *1*, 405-13.

Wange, R. L., and Samelson, L. E. (1996). Complex complexes: signaling at the TCR. Immunity *5*, 197-205.

Warrell, R. P., de The, H., Wang, Z. Y., and Degos, L. (1993). Acute promyelocytic leukemia. New-Engl-J-Med *329*, 177-189.

Warren, A. P., Patel, K., McConkey, D. J., and Palacios, R. (1996). CD98: a type II transmembrane glycoprotein expressed from the beginning of primitive and definitive hematopoiesis may play a critical role in the development of hematopoietic cells. Blood *87*, 3676-87.

Weber, M., Uguccioni, M., Baggiolini, M., Clark Lewis, I., and Dahinden, C. A. (1996). Deletion of the NH2-terminal residue converts monocyte chemotactic protein 1 from an activator of basophil mediator release to an eosinophil chemoattractant. J-Exp-Med *183*, 681-5.

Weinberg, J. B., Hobbs, M. M., and Misukonis, M. A. (1984). Recombinant human gamma-interferon induces human monocyte polykaryon formation. Proc-Natl-Acad-Sci-U-S-A *81*, 4554-7.

Weis, K., Rambaud, S., Lavau, C., Jansen, J., Carvalho, T., Carmo Fonseca, M., Lamond, A., and Dejean, A. (1994). Retinoic acid regulates aberrant nuclear localization of PML-RAR alpha in acute promyelocytic leukemia cells. Cell *76*, 345-56.

Weiss, A., and Littman, D. R. (1994). Signal transduction by lymphocyte antigen receptors. Cell *76*, 263-74.

Willy, P. J., and Mangelsdorf, D. J. (1997). Unique requirements for retinoid-dependent transcriptional activation by the orphan receptor LXR. Genes-Dev *11*, 289-98.

Willy, P. J., Umesono, K., Ong, E. S., Evans, R. M., Heyman, R. A., and Mangelsdorf, D. J. (1995). LXR, a nuclear receptor that defines a distinct retinoid response pathway. Genes-Dev *9*, 1033-45.

Windebank, K. P., Abraham, R. T., Powis, G., Olsen, R. A., Barna, T. J., and Leibson, P. J. (1988). Signal transduction during human natural killer cell activation: inositol phosphate generation and regulation by cyclic AMP. J-Immunol *141*, 3951.

Winkelstein, A., Weaver, L. D., Salva, N., and Machen, L. L. (1990). Interleukin-2-induced lymphoproliferative responses. Cancer Immunol Immunother *32*, 110-6.

Woldman, I., Mellitzer, G., Kieslinger, M., Buchhart, D., Meinke, A., Beug, H., and Decker, T. (1997). STAT5 involvement in the differentiation response of primary chicken myeloid progenitor cells to chicken myelomonocytic growth factor. J-Immunol *159*, 877-86.

Wolffe, A. P. (1997). Transcriptional control. Sinful repression [news; comment]. Nature *387*, 16-7.

Woodhead, V. E., Stonehouse, T. J., Binks, M. H., Fox, D. A., Gaya, A., Hardie, D., Henniker, A. J., Horejsi, V., Sagawa, K., Skubitz, K. M., Taskov, H., Todd III, R. S., van Agthoven, A., Katz, D. R., and Chain, B. M. (1998). Novel molecular mechanisms of T-cell activation induced by dendritic cells. submitted.

Woods, C., Domenget, C., Solari, F., Gandrillon, O., Lazarides, E., and Jurdic, P. (1995). Antagonistic role of vitamin D3 and retinoic acid on the differentiation of chicken hematopoietic macrophages into osteoclast precursor cells. Endocrinology *136*, 85-95.

Wurtz, J. M., Bourguet, W., Renaud, J. P., Vivat, V., Chambon, P., Moras, D., and Gronemeyer, H. (1996). A canonical structure for the ligand-binding domain of nuclear receptors [see comments] [published erratum appears in Nat Struct Biol 1996 Feb;3(2):206]. Nat-Struct-Biol *3*, 87-94.

Xia, Z., Dickens, M., Raingeaud, J., Davis, R. J., and Greenberg, M. E. (1995). Opposing effects of ERK and JNK-p38 MAP kinases on apoptosis. Science *270*, 1326-31.

Xu, H., Kramer, M., Spengler, H. P., and Peters, J. H. (1995). Dendritic cells differentiated from human monocytes through a combination of IL-4, GM-CSF and IFN-gamma exhibit phenotype and function of blood dendritic cells. Adv Exp Med Biol *378*, 75-8.

Yamanashi, Y., Fukui, Y., Wongsasant, B., Kinoshita, Y., Ichimori, Y., Toyoshima, K., and Yamamoto, T. (1992). Activation of Src-like protein tyrosine kinase Lyn and its association with phospahtidylinositol 3-kinase upon B-cell antigen receptor -mediated signaling. Proc-Natl-Acad-Sci-U-S-A *89*, 1118-1122.

Yao, T. P., Forman, B. M., Jiang, Z., Cherbas, L., Chen, J. D., McKeown, M., Cherbas, P., and Evans, R. M. (1993). Functional ecdysone receptor is the product of EcR and Ultraspiracle genes. Nature *366*, 476-9.

Yen, P. M., Liu, Y., Sugawara, A., and Chin, W. W. (1996). Vitamin D receptors repress basal transcription and exert dominant negative activity on triiodothyronine-mediated transcriptional activity. J-Biol-Chem *271*, 10910-6.

Yu, H., Chen, J. K., Feng, S., Dalgarno, D. C., Brauer, A. W., and Schreiber, S. L. (1994). Structural basis for the binding of proline-rich peptides to SH3 domains. Cell *76*, 933-45.

Yu, V. C., Delsert, C., Andersen, B., Holloway, J. M., Devary, O. V., Naar, A. M., Kim, S. Y., Boutin, J. M., Glass, C. K., and Rosenfeld, M. G. (1991). RXR beta: a coregulator that enhances binding of retinoic acid, thyroid hormone, and vitamin D receptors to their cognate response elements. Cell *67*, 1251-66.

Zechel, C., Shen, X. Q., Chambon, P., and Gronemeyer, H. (1994a). Dimerization interfaces formed between the DNA binding domains determine the cooperative binding of RXR/RAR and RXR/TR heterodimers to DR5 and DR4 elements. EMBO-J *13*, 1414-24.

Zechel, C., Shen, X. Q., Chen, J. Y., Chen, Z. P., Chambon, P., and Gronemeyer, H. (1994b). The dimerization interfaces formed between the DNA binding domains of RXR, RAR and TR determine the binding specificity and polarity of the full-length receptors to direct repeats. EMBO-J *13*, 1425-33.

Zhang, D. E., Hetherington, C. J., Gonzalez, D. A., Chen, H. M., and Tenen, D. G. (1994). Regulation of CD14 expression during monocytic differentiation induced with 1 alpha,25-dihydroxyvitamin D3. J-Immunol *153*, 3276-84.

Zhang, J., Alter, N., Reed, J. C., Borner, C., Obeid, L. M., and Hannun, Y. A. (1996). Bcl-2 interrupts the ceramide-mediated pathway of cell death. Proc-Natl-Acad-Sci-U-S-A *93*, 5325-8.

Zhang, X. K., Lehmann, J., Hoffmann, B., Dawson, M. I., Cameron, J., Graupner, G., Hermann, T., Tran, P., and Pfahl, M. (1992). Homodimer formation of retinoid X receptor induced by 9-cis retinoic acid. Nature *358*, 587-91.

Zhou, M., Todd, R. F. d., van de Winkel, J. G., and Petty, H. R. (1993). Cocapping of the leukoadhesin molecules complement receptor type 3 and lymphocyte function-associated antigen-1 with Fc gamma receptor III on human neutrophils. Possible role of lectin-like interactions. J-Immunol *150*, 3030-41.

Zoller, K. E., MacNeil, I. A., and Brugge, J. S. (1997). Protein tyrosine kinases Syk and ZAP-70 display distinct requirements for Src family kinases in immune response receptor signal transduction. J-Immunol *158*, 1650-9.

Zou, A., Elgort, M. G., and Allegretto, E. A. (1997). Retinoid X receptor (RXR) ligands activate the human 25-hydroxyvitamin D3-24-hydroxylase promoter via RXR heterodimer binding to two vitamin D-responsive elements and elicit additive effects with 1,25-dihydroxyvitamin D3. J-Biol-Chem *272*, 19027-34.

Zuckerman, S. H., Surprenant, Y. M., and Tang, J. (1988). Synergistic effect of granulocyte-macrophage colony-stimulating factor and 1,25-dihydroxyvitamin D3 on the differentiation of the human monocytic cell line U937. Blood *71*, 619-24.